Identifying signalling molecules controlling T cell antigen sensitivity and discrimination



Violaine André

Sir William Dunn School of Pathology

University of Oxford

Supervisor: Pr. Omer Dushek

This thesis is submitted for the degree of *Doctor of Philosophy*

Lincoln College Trinity Term 2022

Acknowledgement

This work is the result of four years of research, four years of learning and development that I have enjoyed and found particularly rewarding because of the excellent supervision and the supportive environment I was provided with.

First, I would like to thank my supervisor, Omer Dushek, for his constant availability and support, his door always open to scientific discussion or feedback. His patient but efficient guidance made my PhD a very enjoyable experience.

I would also like to thank my examiners through the years, I am grateful to Simon Davis, Graham Ogg and Ricardo Fernandes for their interesting scientific discussions and useful feedback during my transfer and confirmation. I am also grateful to Mike Dustin and Arianne Richard for agreeing to examine this thesis.

I am grateful to have been able to carry out this work in the Dunn School of Pathology, a department that perfectly combines supportive environment with scientific excellence. I am grateful for the continuous support I received, from the availability and informative guidance of Lucinda Risius and Anton van der Merwe, to the special effort carried out by the entire department during the Coronavirus pandemic. The efficient policy lead by the Dunn School, from its head Matthew Freeman, to the administration and facilities allowed our work, as PhD students, to be minimally disturbed. I would like to thank specifically Robert Henley, Michal Maj, Vasiliki Tsioligka and Line Eriksen from the flow facility and Alan Wainman from the light microscopy facility for their help and support. I am also grateful to Salvatore Valvo from the Dustin laboratory in the Kennedy institute for his help setting up the bilayer system and to Caitlyn O'Brien from the Davis laboratory in the Weatherall Institute for Molecule Medicine for her advice regarding work with Jurkat cells.

I am grateful for the lab environment, thank you to the "senior PhD students" who are now Postdoc or beyond academia. Thank you to John Nguyen for his guidance during my first weeks in the lab, to Johannes Pettmann and Jesus Siller-Farfán for their constant help, availability

and patience. And to the "junior PhD students" who are not so junior anymore. Thank you to Jake and Ashna for endless support, help and encouragements. Thank you to Anna, Jose and Sophie for interesting discussions and advice. I am also grateful to Mikhail Kutuzov, for his help with biochemistry and regular delivery of rhubarb. I would also like to thank everyone in the Molecular Immunology Group, Anton van der Merwe and Marion Brown for the many advice, feedback and discussions through the years. Thank you to Mike Barton for his great work as lab manager and constant guidance when I tried to be a decent one. Thank you also to all the members who have come and gone during my time, with special thank you to Eleanor Denham and to my graduate adviser Enas Abu-Shah for all the help and advice through the years.

I am also grateful for the support I received from so many in Oxford. Starting with Mike Barnkob who convince me to stay and embark on a PhD, I am grateful for his support from the application to the submission stage. Thank you to the many roommates who patiently listened to many T cell stories, to Ricky, Will, Jack, Emily, Emile, Lucrezia and Bertie who were extraordinary support before, during and after the pandemic. I am also grateful for the environment that Lincoln College offered me and the many interesting people I met there. And a special thank you to LCBC who provided me with daily distraction and outlet for the lab challenges, the discipline and team spirit I encountered there contributed directly to my resilience in the lab.

Finally, I would like to thank my friends in Belgium who sent me constant support across the Channel, despite pandemic-imposed years of only skype calls, I was always welcomed with supportive friendship; thank you especially to Loralie, Cyril, Sophie and Anna for not giving up on a long-distance friendship. Most importantly thank you to my family, my parents, Marie-Christine Dewez and Philippe André, who gave me roots and wings, my sister, Eléonore, who provided constant inspiration but also distraction and my brother, Corentin, who taught me to question and investigate everything; and thank you to my partner Arnau Bertran-Inglada, for his incredible support, encouragements and motivation.

Contributions

This work is not an isolated project but rather a contribution to the research carried out in the Dushek lab, it contains therefore the work of others.

The mathematical model I used to predict the impact of modulation of signalling molecules was established by my supervisor, Omer Dushek. I used it as basic model on which I simulated the impact of inhibition of signalling molecules.

The ICAM-1 knocked-out U87 cell line we used to study the impact of Calcineurin was generated by Johannes Pettmann.

The research strategy we chose to study the impact of the SHP1 phosphatase was based on previous observations and experimental data generated by a previous PhD student in the lab, John Nguyen. These data are present in the appendix. The Jurkat cell line we used for the SHP1 KO experiments were provided by the Enfu Hui's lab (UCSD). The validation of the knock-out of SHP1, as well as the confirmation of successful SHP1 electroporation in this jurkat cell line was performed by Western Blot, by Mikhail Kutuzov.

The short-length versions of CD166 WT and mutant were produced by Marion Brown.

Abstract

T cells are critical checkpoints in adaptive immunity and they are activated when their T cell surface receptor (TCR) recognises antigens presented on major histocompatibility complex (pMHC). It is well established that T cells have high sensitivity able to recognise even a single pMHC ligand and high discrimination able to respond to higher-affinity foreign pMHC but not to lower-affinity self pMHC. The mechanism(s) of antigen sensitivity and discrimination have been proposed to be dependent on a large number of molecules. These molecules are often identified by their association with TCR-proximal signalling events using different experimental assays. As a result, these conclusions rely on inference. Here, we directly quantified antigen sensitivity and discrimination in systematic experiments where different T cell molecules were modulated. Using chemical inhibitors, we identified the tyrosine kinase Lck as controlling antigen discrimination, Lck and Phospholipase Cγ (PLCγ) as controlling antigen sensitivity, and Lck, PLCγ, Calcineurin, Phosphoinisitide-3-kinase (PI3K), Protein kinase Cθ (PKCθ), Mitogen-activated protein kinase (MEK) and mammalian Target of rapamycin (mTorc) as controlling antigen efficacy (maximum response). We found no evidence that molecules Calcineurin, PI3K, PKCθ, MEK or mTorc impact antigen sensitivity or discrimination. These basic insights can improve T cell-based therapies, especially cell therapies where increasing antigen sensitivity and discrimination can improve efficacy and safety.

Contents

1 Introduction **21**

1.1 The two sides of the immune system 21

1.1.1 Natural barriers and innate immune system 21

1.1.2 The adaptive immune system 22

1.2 An essential actor of the adaptive immunity, the $CD8^+$ T cell 24

1.3 Mechanisms of TCR triggering 26

1.4 From recognition to response, the T cell signalling pathway 28

1.4.1 Cytokine and surface marker regulation by transcription factors 32

1.4.2 T cell interaction with Antigen Presenting Cells relies on cytoskeletal remodelling 33

1.5 How T cells mediate antigen sensitivity 37

1.5.1 Impact of co-receptors on antigen sensitivity 38

1.5.2 Impact of accessory receptors on antigen sensitivity 39

1.5.3 Impact of soluble factors on antigen sensitivity 41

1.5.4 Impact of intracellular molecules on antigen sensitivity 41

1.6 How T cells mediate antigen discrimination 41

1.7 Aim of this thesis 44

2 How T cells control antigen sensitivity and discrimination **46**

2.1 Introduction 46

2.1.1 Mechanisms of antigen sensitivity and discrimination 47

2.1.2 Molecules controlling antigen sensitivity and discrimination 49

2.2 Results 54

2.2.1 A mathematical model can localise a signalling molecule based on its impact on antigen sensitivity 54

2.2.2 Systematic identification of signalling molecules impacting antigen sensitivity 57

2.2.3 Systematic identification of signalling molecules impacting antigen discrimination 66

2.3 Discussion 72

3 Application of the system to intracellular molecules 81

3.1 Introduction 81

3.1.1 Calcineurin 81

3.1.2 Nck 82

3.1.3 SHP1 83

3.2 Results 84

3.2.1 Inhibition of Calcineurin does not impact antigen sensitivity independent of ligation of LFA-1 84

3.2.2 The compound AX-024 increases T cell antigen sensitivity and decreases cytokine secretion 90

3.2.3 SHP1 reconstitution in jurkat cells 97

3.3 Discussion 98

4 Application of the system to surface molecules 105

4.1 Introduction 105

4.1.1 The PD-1 inhibitory receptor 105

4.1.2 The CD6 receptor . . . 106

4.2 Results . . . 109

4.2.1 Purified PD-L1 does not impact T cell responses in a solid-phase stimulation system . . . 109

4.2.2 Purified CD166 does not impact T cell responses in a solid-phase stimulation system . . . 112

4.2.3 Establishment of a lipid bilayer-based assay system to study the impact of surface molecule on T cell antigen sensitivity . . . 117

4.3 Discussion . . . 119

5 Discussion and future directions **123**

5.1 Strengths and limitations of our set up . . . 123

5.2 Future directions and applications . . . 125

6 Material and methods **128**

6.1 Methods . . . 128

6.1.1 Cell lines and maintenance . . . 128

6.1.2 Lentivirus production . . . 128

6.1.3 Isolation of $CD8^+$ T cells . . . 128

6.1.4 pMHC tetramer . . . 129

6.1.5 Peptides . . . 129

6.1.6 Functional assay : incubation of T cells on plate . . . 130

6.1.7 Functional assay : co-culture of T cells with U87 . . . 130

6.1.8 Inhibition by small-molecule chemical inhibitor . . . 131

6.1.9 Flow cytometry 131
6.1.10 Surface staining of TNFα 132
6.1.11 Enzyme-linked immuno-assays 132
6.1.12 Re-constitution of SHP-1 KO jurkats cells by protein electroporation . . . 132
6.1.13 Preparation of the bilayer-based stimulation platform 133
6.1.14 Fluorescence Recover After Photo bleaching (FRAP) on bilayers 133
6.1.15 Concentrations tables 134
6.2 Modeling 136
6.2.1 Model parameters and ODE 136
6.2.2 Fitting dose-response curves 140
6.3 Reagents 141

7 Appendix **145**

List of Figures

1 TCR complex 25

2 T cell signalling 32

3 Immunological synapse 34

4 Cytoskeleton regulation 37

5 Phenotypic model of T cell signalling. 55

6 Phenotypic model predicts that only molecules upstream of the intracellular switch will impact antigen sensitivity. 57

7 $CD8^+$ T cells isolation and transduction. 58

8 Studying sensitivity on pMHC coated plate: experimental set up. 59

9 Impact of the inhibition of signalling molecules on antigen sensitivity as measured by cytokine production in the plate-based assay. 60

10 Studying sensitivity on pulsed APC: experimental set up. 61

11 Impact of the inhibition of signalling molecules on antigen sensitivity measured by cytokine production in an APC co-culture assay. 63

12 Impact of the inhibition of signalling molecules on antigen sensitivity measured by cytokine production in an APC co-culture assay. 65

13 Studying antigen discrimination on pulsed APC: experimental set up. 66

14 Impact of inhibition of signalling molecules on T cell discrimination. 68

15 Impact of inhibition of actin-modulatory molecules on T cell discrimination. . . . 69

16 Impact of titrating doses of inhibitor on the T cell discriminatory power. 71

17 Lck controls T cell antigen discrimination. 72

18 Experimental protocol for assessing the impact of small-molecule inhibition on antigen sensitivity to a titration of purified pMHC alone or in combination with purified ICAM-1. 85

19 Lck, but not Calcineurin, controls the sensitivity of T cells to purified antigen in the presence of purified ICAM-1. 87

20 Experimental protocol for assessing the impact of small-molecule inhibition on antigen sensitivity to a titration of peptide on APCs with and without ICAM-1. 88

21 Lck, but not Calcineurin, controls the sensitivity of T cells to antigens on APCs presenting or no surface ICAM-1. 89

22 Lck, but not Calcineurin, impacts antigen sensitivity. 90

23 Inhibition of Nck using the compound AX-024 increases antigen sensitivity. . . . 92

24 Impact of inhibition of actin-modulatory molecules on the magnitude of T cell response. 94

25 Inhibition of Nck and actin polymerization can increase supernatant cytokine levels. 95

26 Inhibition of Nck and actin polymerisation reduces cytokine production at the single cell level. 96

27 Impact of titrating re-constitutive concentrations of SHP1 protein on Jurkat functions. 98

28 PD-L1 does not impact T cell activation to different concentrations of pMHC in the presence or absence of CD86. 110

29 Pre-stimulated T cells with increased PD-1 expression remain inert to PD-L1 inhibition. 111

30 CD166 reduces T cell antigen sensitivity independently of its ability to bind CD6. 114

31 The short-length version of CD166 has no impact on antigen sensitivity to a titration of purified antigen in a plate-based system. 116

32 Lipid bilayer-based assay to study the impact of surface molecules on antigen sensitivity. 118

33 Phenotypic model as described in figure 6. 145

34 Independent repeat as described in figure 9. 146

35 Independent repeat as described in figure 11. 147

36 Independent repeat as described in figure 11. 148

37 Optimisation of the CK666 (Arp2/3 inhibitor) concentrations range measured by impact on cytokine production and surface marker expression in an APC co-culture assay. 149

38 Independent repeat as described in figure 12. 149

39 Independent repeat as described in figure 12. 150

40 Impact of inhibition of signalling molecules on T cell discrimination - surface markers output 151

41 Independent dataset as described in figure 16. 152

42 Independent dataset as described in figure 16. 153

43 Impact of inhibitor treatment on cell viability. 154

44 Independent repeat as described in figure 19. 155

45 Independent repeat as described in figure 21. 156

46 Independent repeat as described in figure 24. 157

47 Independent repeat as described in figure 24. 158

48 Independent repeats as described in figure 25. 158

49 Constitutive knock-down of SHP1 in Jurkat cells. 159

50 Induced knock-down of SHP1 in Jurkat cells. 160

51 Validation of SHP1 KO in jurkat. 160

52 Lck, but not Calcineurin, controls the sensitivity to purified antigen in jurkat cells.161

53 Independent repeat as described in figure 28. 161

54 Independent repeat as described in figure 29. 161

55 Independent repeat as described in figure 30. 162

56 Independent repeat as described in figure 30. 163

57 Independent repeat as described in figure 31. 164

List of Tables

1 Affinities of the NYE-ESO peptides variants for the 1G4 TCR 130

2 Inhibitor concentrations used in sensitivity experiments on plate 134

3 Inhibitor concentrations used in sensitivity experiments by co-culture 134

4 Inhibitor concentrations used in sensitivity experiments by co-culture 135

5 Peptide concentrations used in experiments 135

6 Concentrations of accessory proteins used 135

7 Concentrations of proteins used on bilayer experiments 136

8 Concentrations of proteins used in electroporation experiments 136

9 Definition of the parameters used in the model 138

10 Cell lines 141

11 Antibodies and cell staining reagents 142

12 Chemical inhibition reagents 142

13 Functional assay reagents 142

14 Cell culture reagents 143

15 Buffers and media 143

16 Transfection mix 144

17 Lipid bilayer reagents 144

18 Consumables 144

19 Equipment 145

20 Softwares and packages 145

Abbreviations

3MB-PP1	(3-methylbenzyl)pyrazolo[3,4-d]pyrimidine
4-1BB	Also known as CD137
5-LOX	5-LipOXygenase
ADAM17	A Disintegrin And Metalloprotease 17
ADCC	Antibody-Dependent Cell Cytotoxicity
AP-1	Activator protein 1
APC	Antigen Presenting Cell
Arp2/3	Actin-related protein 2/3
ATP	Adenosine TriPhosphate
Bcl10	B cell leukemia 10
BSA	Bovine Serum Albumin
BTLA	B- and T-Lymphocyte Attenuator
cAMP	cyclic Adenosine MonoPhosphate
CAR	Chimeric Antigen Receptor
CARMA1	CARD-containing MAGUK protein 1
CD2	Cluster of Differentiation 2
CD3	Cluster of Differentiation 3
CD4	Cluster of differentiation 4
CD6	Cluster of Differentiation 6
CD8	Cluster of Differentiation 8
CD27	Cluster of Differentiation 27
CD28	Cluster of Differentiation 28
CD43	Cluster of Differentiation 43
CD45	Cluster of Differentiation 45
CD48	Cluster of Differentiation 48
CD49d	Cluster of Differentiation 49d
CD58	Cluster of Differentiation 58
CD69	Cluster of Differentiation 69
CD70	Cluster of Differentiation 70
CD80	Cluster of Differentiation 80
CD86	Cluster of Differentiation 86
CD137	Cluster of Differentiation 137
CD166	Cluster of Differentiation 166
CD247	Cluster of Differentiation 247, also known as zeta chain
CDR	Complementarity-Determining Region
CFP	Cyan Fluorescent Protein
CIA	Collagen-Induced Arthritis
CO2	Carbon diOxyde
CREB	cAMP Response Element-Binding protein
Csk	C-terminal Src family Kinase
DAG	DiAcylGlycerol
DAMP	Damage-associated molecular motifs
DC	Dentritic Cell
DMEM	Dubelcco's Modified Eagle Medium
DNA	DeoxyriboNucleic Acid
DOPC	DiOleoylPhosphatidylCholine
DOPE	DiOleoylPhosphatidylEthanolamine
DPC	Distal Pole Complex

EAE	Experimental Autoimmune Encephalomyelitis
EC50	Half maximal Effective Concentration
EDTA	EthyleneDiamineTetraacetic Acid
ELISA	Enzyme-Linked ImmunoSorbent Assay
Elk1	ETS like 1
Emax	maximal Efficacy
ER	Endoplasmic Reticulum
Erk	Extracellular signal-regulated kinase
ERM	Ezrin Radixin Moesin
Ets	Erythroblast transformation specific
FBS	Fetal Bovine Serum
FRAP	Fluorescence Recovery After Photobleaching
FRB	FKBP-rapamycin-binding
Gads	Grb2-related adaptor downstream of Shc
GEF	Guanine nucleotide Exchange Factor
Grb2	Growth factor Receptor-Bound protein 2
GSK3	Glycogen Synthase Kinase 3
GTP	Guanosine TriPhosphate
hCG	human Chorionic Gonadotropin
HEK293	Human Embryonic Kidney 293
HLA	Human Leukocyte Antigen
HRP	HorseRadish Peroxidase
ICAM	Intercellular Adhesion Molecule 1
IFNγ	Type I InterFeroN gamma
IgG	Immunoglobulin G
IKK	I Kappa Kinase
IL-2	InterLeukin 2
IL-8	InterLeukin 8
IP3	Inositol triPhosphate
IR	Inhibitory Receptor
IS	Immunological Synapse
ITAM	Immunoreceptor Tyrosine-based Activation Motif
Itk	Interleukin-2-inducible T cell Kinase
JAM-A	Junctional Adhesion Molecule-A
k_{act}	Activation rate
k_{basal}	Basal downregulation rate
k_D	Dissociation constant
k_{deg}	Degradation rate
KO	Knocked-Out
k_{off}	Off-rate
k_{on}	On-rate
k_p	Proofreading rate
k_{prod}	Production rate
k_{remove}	Removal rate
k_{syn}	Synthesis rate

LAT	Linker for Activation of T cells
Lck	LymphoCyte-specific protein tyrosine Kinase
LCMV	Lymphocytic ChorioMeningitis Virus
LFA-1	Lymphocyte function-associated antigen 1
LM	Listeria Monocytogenes
LUV	Large Unilamellar Vesicules
MALT1	Mucosa-Associated Lymphoid Tissue lymphoma translocation protein 1
MAPK	Mitogen-Activated Protein Kinase
MEK	Mitogen-Activated Protein Kinase 2 (MAP2K)
mRNA	messenger RiboNucleic Acid
MTOC	MicroTubules-Organizing Center
mTorc1	mammalian Target of rapamycin 1
Nck	Non Catalytic region of tyrosine Kinase adaptor protein
NFAT	Nuclear factor of activated T-cells
NFkB	Nuclear factor kappa-light-chain B
NIK	Nck Interacting Kinase
NK	Natural Killer
NY-ESO	New-York ESOphageal squamous cell carcinoma
Oct1	Octamer transcription factor 1
OVA	OVAlbumin
PA	Phosphatidic Acid
PAMP	Pathogen-associated molecular motifs
PBS	Phosphate-Buffered Saline
PD-1	Programmed cell Death 1
PD-L1	Programmed cell Death Ligand 1
PD-L1	Programmed cell Death Ligand 2
Pen	Penicillin
PI3K	Phosphoinisitide 3-kinase
PiP2	Phosphatidylinositol 4,5-bisphosphate
PKCθ	Protein Kinase C theta
PLCγ	PhosphoLipase C gamma
PLD	Phospholipase D
PMA	Phorbol Myristate Acetate
(p)MHC	(peptide) Major HistoCompatibility Complex
PRR	Pattern Recognition Receptor
PRS	Proline-Rich Sequence
qPCR	quantitative Polymerase Chain Reaction
RAG	Recombinant ActivatinG protein
Ras	Rat sarcoma virus
RIPR	Receptor Inhibition by Phosphatase Recruitment
RPMI	Roswell Park Memorial Institute

SH2	Src Homology 2
SH3	Src Homology 3
SHP1	Src Homology region 2 domain-containing Phosphatase-1
SLB	Supported Lipid Bilayer
SLP-76	SH2 domain-containing Leucocyte Protein of 76kd
SMAC	SupraMolecular Activation Complex
SNP	Single-Nucleotide Polymorphism
Sos	Son of sevenless
Sp1	Specificity protein 1
SPR	Surface Plasmon Resonance
Src	Sarcoma
STAT4	Signal Transducer and Activator of Transcription 4
STIM	STromal Interaction Molecule
Strep	Streptomycin
TACE	TNFa Converting Enzyme
TAP	Transporter-associated with Antigen Processing
TCR	T Cell Receptor
TIL	Tumour Infiltrating Lymphocyte
TMB	TetraMethylBenzidine
TNFα	Tumor Necrosis Factor alpha
TRAF6	TNF Receptor-Associated Factor 6
WASp	Wiskott-Aldrich Syndrome Protein
Wave2	WASP family verprolin homologous protein 2
WB	Western Blot
WT	Wild-Type
ZAP70	Zeta-chain-Associated Protein kinase 70
ZEB1	Zinc finger E-box-Binding homeobox 1
Zn	Zinc

Do you believe in miracles? Well you should. In fact, life itself is a big miracle. There are so many things that are beyond our understanding. There are two ways to live: you can live as if nothing is a miracle; you can live as if everything is a miracle.

- A. Einstein

Chapter 1

Introduction

1 Introduction

1.1 The two sides of the immune system

1.1.1 Natural barriers and innate immune system

The role of the immune system is to recognise and eliminate pathogens. Such surveillance relies on two cooperative branches: the innate and adaptive immune systems.

In order to enter the body, pathogens must first cross the physical barrier produced by epithelial cells. The epithelial barrier, whether external (skin) or internal (airways, digestive tract, genital tract), plays the essential role of the first line of defence [1][2]. The cells lining these interfaces form tight junctions, physically preventing the incursion of pathogens. Moreover, they can be covered in mucus preventing pathogen adhesion and ensuring protection from chemicals; some epithelial cells also have cilia which allow mechanical clearance of pathogens [3].

Once the physical barrier is breached, the component of the innate immune system come into play; although they cannot carry out specific recognition, they have the advantage of speed, ensuring an effective response to pathogen entry. The innate immune system relies on the recognition of patterns called pathogen-associated molecular patterns (PAMPs) or endogenous defects damage-associated molecular patterns (DAMPs). Neutrophils can also recognise bacterial peptides and distinguish a formylated methionine, typical in bacteria, from the unmodified methionine in eukaryotes. Many of these pathogenic motifs are recognised by Pattern Recognition Receptor (PRR). Several innate cell types such as neutrophils and macrophages express these receptors [4]. Upon detection of these pathogenic motifs, they deploy direct elimination mechanisms such as phagocytosis and secrete mediator molecules that lead to the recruitment of adaptive immune cells [3].

These mediator molecules can be lipid-derived, such as prostaglandines or protein-based such as cytokines and chemokines. Cytokines play diverse roles such as inducing fever which hinders bacterial and viral growth, but promotes the action of the adaptive immune system [5][6]. Chemokines are responsible

for attracting cells to the infectious site [6]. They first attract neutrophils then monocytes and dendritic cells. The latter phagocytose material that they break down and present in the form of antigenic peptides on their surface [3]. In combination with this process, inflammatory cytokines such as interferon (IFN) induce expression of the Major Histocompatibility Complex (MHC) molecules on the surface of antigen presenting cells (APCs). Through these roles, they bridge over to the adaptive immune system and trigger a specific response [7]. However, virus-infected and stressed cells can repress expression of the MHC molecules to shield from the adaptive system. Therefore, innate effectors such as the natural killer cells (NK cells) are able to detect cells lacking MHC and induce their lysis [4].

These interactions and collaborations between the two sides of the immune system are essential. The innate immune system on its own is not sufficient, as infants born with a deficient adaptive immune system are susceptible to a wide range of infections, such as bacterial, fungal, viral and parasitic [3]. This is because, while the innate immune system has the key advantage of speed, it lacks key properties of the adaptive immune system: specific pathogen recognition and memory.

1.1.2 The adaptive immune system

In contrast with the innate immune system, the adaptive immune system ensures specific recognition of peptides, fragments derived from endogenous or pathogens protein, or epitopes. It also provides long-lasting protection against previously encountered pathogens, termed immunological memory [4].

Molecules generating adaptive immune responses are termed antigens, from ANTIbody GENerators. They are specifically recognised by lymphocytes of two types: B and T cells, through their B cell receptor (BCR) and T cell receptor (TCR) respectively. The first category, B lymphocytes, provides antibody-mediated response, while the second class, T lymphocytes, provide the cell-mediated response.

B lymphocytes produce antibodies that specifically bind to epitopes on pathogens. Antibodies have different roles: neutralisation of toxins, prevention of pathogen adhesion, induction of the complement activation, antibody-dependent cell cytotoxicity (ADCC) and opsonization. The latter leading to endocytosis by phagocytic cells carrying Fc receptors (receptors to the Fragment crystallizable region of the

antibody) such as macrophages and neutrophils [8].

T lymphocytes are classified in 2 main groups according to the co-receptor they express: CD4 or CD8. Both T cell groups are able to specifically recognise peptides presented on the MHC complex (pMHC). The two groups work in collaboration to ensure specific lysis, with each type exerting specialised functions.

$CD4^+$ lymphocytes express the CD4 co-receptor that recognise class II MHC on professional APCs. They recognise exogenous peptides derived from antigens that are internalized and processed to be presented on MHC II [9][10]. $CD4^+$ T cells are called helper T cells as their role is to help other cell types perform their functions. They support B cells maturation and clonal selection. They also participate in establishing the long term memory response of $CD8^+$ T cells [11].

$CD8^+$ lymphocytes express the CD8 co-receptor that recognises class I MHC, expressed on all nucleated cells [12]. MHC I is a dimer composed of a heavy chain, encoded by the Human Leucocyte Antigen (HLA) A, B and C genes in humans, that couples with an invariable chain called beta-2-microglobulin (β-2M). This dimer forms a structure that bears a groove for a 8 to 10-amino acid peptide [13]. Peptides loaded on the class I MHC molecules are most commonly endogenous peptides, digested by the proteosome and transported into the endoplasmic reticulum (ER) by the Transporter-associated with Antigen Processing (TAP). In the ER, the peptides presenting the right length and anchor residues are loaded onto MHC I molecules. Only higher-affinity peptides that produce a stable complex with the MHC I can be released from the ER to the cell surface [13]. In addition to intracellular peptides, $CD8^+$ lymphocytes are able to respond to exogenous extracellular antigens presented by professionals APCs through peptide cross-presentation [14]. Professional APCs have the ability to perform endocytosis of extracellular pathogens such as viruses or cancerous cells and direct the presentation of peptides from these exogenous origins to the class I MHC presentation pathway [15]. Loading of these exogenous peptides onto class I MHC molecules is proposed to occur either in phagosomes via an alternative pathway [16] or via the classical pathway, in the ER, after export of the exogenous peptides from the phagosome to the cytoplasm [17]. Because APCs migrate to secondary lymphoid organs, this cross-presentation mechanism allows the cross-priming of $CD8^+$ lymphocytes to pathogens that do not infect APCs and prevents immune evasion.

1.2 An essential actor of the adaptive immunity, the CD8$^+$ T cell

CD8$^+$ T cells are responsible for the defence against viruses, intracellular bacteria and parasites as well as malignant cells in the context of cancer for example [7][12].

The T cells precursors originate from the bone marrow, but their essential development occurs in the thymus. Upon migration to the thymus, T cells enter through the cortex. At this stage, they have yet to express co-receptors (CD4 or CD8) or a T cell receptor (TCR). Through interaction with the cortical thymic cells, they start differentiating into a major (α β) and a minor (γ δ) population of T cells. These two lines differ by the antigens they target, the expression profiles of their co-receptors and their histological locations. Their differentiation is determined by the first chain to be correctly rearranged, the β chain in the majority of cases [18][19].

The β chain first associates with a substitutive α chain, which allow its expression on the surface. This leads to proliferation, co-receptor expression, and rearrangement of the final α chain. These chains are encoded by the *TRA* and *TRB* genes. The final T Cell Receptor molecule is the result of somatic recombinations of these genes in the thymus. First, the *TRB* gene is a result of the recombination of its V, D and J segments, mediated by the Recombination ActivatinG protein RAG1 and RAG2 in thymocytes. Once this recombination generates a functional β chain, the thymocytes recombine the V and J segment of the TRA gene to generate a functional α chain[18]. To increase this diversity further, the terminal deoxynucleotidyl transferase (TdT) enzyme incorporate nucleotides to the end of the V, D and J segments before they are joined and generates semi-random cleaving of the hairpin intermediate [18][20]. The recombination process, and the association of a random β chain with a random α chain could, in theory, generate up to 10^{20} different TCRs in humans. However, the human repertoire consist of approximately 10^{12} T cells, with approximately 10^8 different TCR clones [20].

These alpha and beta chains, are associated with 3 dimers at the cell surface : invariant CD3 gamma/epsilon and delta/epsilon heterodimers and an homodimer of zeta chains (CD247). These molecules contain immunotyrosine activation-based motifs (ITAMs) in their cytoplasmic tails that are responsible for transducing the signal from the alpha/beta heterodimer that recognises antigen to the

intracellular signalling machinery. Together, they form the TCR-CD3 complex (figure 1) [21].

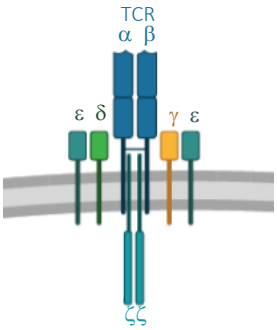


Figure 1: TCR complex. The alpha and beta chains are associated with 3 dimers, invariant CD3 gamma/epsilon and delta/epsilon heterodimers and a zeta chains homodimer (CD247).

After production of a recombined surface TCR, T cells upregulate both co-receptors (CD4/CD8) and are hence known as double positive (DP) thymocytes. At that stage, T cells are exposed to MHC molecules presented by the thymus cortical epithelial cells. These cells present class I or class II MHC. Only T cells bearing a TCR able to recognise self pMHCs with an intermediate affinity survive. Through this positive selection process, the T cells recognising class I MHC select the CD8 co-receptor and lose expression of the CD4 receptor; while T cell interacting with class II MHC select expression of the CD4 co-receptor. These developing, single-positive T cells are also exposed to self-antigen in the thymus. Cells carrying a receptor binding to these self-antigens are eliminated through the negative selection process [22]. These processes should ensure that no T cells leaving the thymus are self-reactive. However the system is imperfect [23] so the requirement for T cells activation in the periphery are more stringent than in the thymus.

In the periphery, the antigen dose and affinity necessary to activate T cells are higher than those in the thymus and naive T cells can only be activated by mature APCs which have been stimulated themselves [24]. To increase the chance of encountering mature APCs carrying their cognate antigens, naive T cells are in constant circulation through the bloodstream and lymphatic system. Upon recognition of their target peptide, $CD8^+$ T cells expand, differentiate into effector and memory types and induce lysis of their target. Because the $CD8^+$ T cell response is so efficient and destructive, it is essential for it to only arise against non-self, pathogenic molecules. $CD8^+$ T cells have evolved remarkable discrimination

abilities, able to be highly sensitive to the affinity and/or off-rate of the TCR/pMHC interaction [3].

1.3 Mechanisms of TCR triggering

$CD8^+$ T cells continuously migrate throughout the body scanning the surface of nearly all cells for antigens derived from pathogens. The scanning of individual cells is a rapid process mediated by actin-rich protrusions termed microvilli [25]. Using this method, it has been shown that the T cell can scan the APC surface within about 60 seconds [25].

The TCR dimer itself, composed of an α and β chain, does not have intrinsic signalling function. For signal transmission, it relies on the complex it forms with the transmembrane chains dimers CD3$\delta\epsilon$, $\gamma\epsilon$ and $\zeta\zeta$. The TCR complex carries a total of 10 ITAMs distributed on the CD3 chains. This is the largest number of ITAMs found on any receptor. These motifs include two tyrosine residues, each of which is a target for phosphorylation by the Lymphocyte-specific protein tyrosine Kinase (Lck) and dephosphorylation by the phosphatase CD45. Precisely how pMHC binding to the TCR leads to phosphorylation of ITAMs, a process termed TCR triggering, remains controversial.

Several models have been proposed to describe how TCR triggering occurs.

The heterodimerisation model proposes a central role of the co-receptor CD8. It suggests that the T cell triggering is a result of the TCR and the CD8 co-receptor binding to the same pMHC forming an heterodimer. Upon TCR binding, CD8, that carries the Lck kinase bound to its intracellular tail, is brought into close proximity of the TCR intracellular chains. This leads to TCR chains phosphorylation by Lck [26] . However, this model has limits as TCR triggering has been shown to occur in the absence of CD8. Moreover, this model relies on Lck-bound CD8 as sole responsible for TCR phosphorylation when free diffusing Lck has been shown to be able to induce T cell activation [27][28] .

The conformational change model proposes that initiation of signal transduction is due to a change in the TCR structure. Many receptors convert ligand binding into intracellular response through conformational change, that is the case of the G protein-coupled receptor family for example [29]. Therefore

a similar model was proposed in the case of the TCR. The conformational hypothesis was proposed on the observation of conformational change in the structure of the Complementarity-Determining Region 1 alpha (CDR1α), CDR3α, and slight modification of CDR3β (located in the variable domains of the α β chains) upon pMHC binding [30][31]. This model is supported by thermodynamics observations demonstrating changes in heat capacity indicative of conformational modifications [32]. However, crystallography of the TCR failed to demonstrate that the α β chains of the TCR acquire different structures when exposed to stimulatory or non-stimulatory antigens [30][33]. To explain that, some groups suggest that the conformational change occurs on the CD3 chains, as Gil *et al.* showed that the CD3ζ chain can convert from a helical structure to a beta-sheet pattern upon phosphorylation in cell-free systems [34]. According to this hypothesis, conformational change in the CD3 chains would result in the exposure of a proline-rich sequence (PRS) of the CD3ϵ chain [34]. That revealed sequence would bind to the adaptor Non Catalytic region of tyrosine Kinase adaptor protein (Nck), independently and before phosphorylation of the neighbouring ITAMs motifs. However the TCR-proximal role of Nck is not yet elucidated, and its involvement in TCR activation relies on observations that its inhibition impacts T cell functions, conjugate formation with APCs and maturation of the immunological synapse [34]. Moreover, this model fails to explain that the amplitude of response varies in different T cell subsets (naive, effector and memory). Lastly, the Cryo-EM structures of the complete TCR-CD3 complex with and without pMHC binding has been published, showing that the TCR-CD3 complex adopts the same conformation independent of ligand binding [35].

An alternative model is the kinetic segregation model proposed by Davis and Van der Merwe [36]. It relies on steric regulation of essential signalling molecules according to their size. This model propose that TCR triggering occurs at sites where T cells form close contacts with APCs. In the absence of close-contacts, molecules with tyrosine-phosphorylation motifs, such as the ITAM motifs of the TCR, are subject to phosphorylation and de-phosphorylation by kinases and phosphatases. In steady-state, the activity of phosphatases is higher than kinases which keeps the TCR in a largely dephosphorylated state. However, upon interaction with an APC, the T cells form close-contact sites through interaction of adhesion receptors such as CD2 and Lymphocyte Function-associated Antigen 1(LFA-1) on the T cells, with their ligands CD58 and InterCellular Adhesion Molecule 1 (ICAM-1) on the APC. Because

the membranes of the two cells come in close proximity at these close-contact sites, proteins with large extracellular domains such as the CD45 phosphatase are excluded from the area [37][38]. Following this phosphatase exclusion, the balance of phosphorylation and de-phosphorylation at the close-contact site changes and shifts in favour of phosphorylation by kinases. As a result, the half-life of phosphorylated molecule in the region is increased and provided the TCR is trapped in the close-contact by pMHC for a sufficient duration, it can lead to TCR triggering and downstream signalling [39]. Recent work from Chen *et al.* supports this model as holding the TCR in a phosphatase-free close contact region suffice to initiate signalling [40].

We note that the mechanism underlying antigen discrimination is kinetic proofreading, which is consistent with all models of triggering and will be discussed in section 1.6.

Once the TCR is triggered, a large signalling pathway is initiated that culminates in full T cell activation.

1.4 From recognition to response, the T cell signalling pathway

The Src-family kinase Lck is the main kinase responsible for ITAM phosphorylation in T cells. A fraction of total Lck interacts with the co-receptor CD8 through a Zinc (Zn2+) interaction [41]. Some studies propose that this interaction ensures Lck recruitment to the TCR complex and its subsequent phosphorylation when the CD8 co-receptor interacts with the MHC molecule [42]. In thymocytes, all Lck molecules are associated with a CD4 or CD8 co-receptor [43][44], this proportion decreases in mature $CD8^+$ T cells to 60% [45]. However free, co-receptor-independent, Lck is also able to induce T cell activation [27][28]. As it is the first kinase activated upon TCR engagement, the regulation of Lck activity is key in T cell activation. Lck possesses 2 tyrosines that are phosphorylation sites, at positions 394 (Y394) and 505 (Y505). The former is an activatory site, phosphorylated by Lck itself (auto-phosphorylation) and dephosphorylated by CD45 [46][47]. The later is an inhibitory site phosphorylated C-terminal Src Kinase (Csk) and dephosphorylated by CD45 [48]. Lck activity is also controlled by phosphorylation of its serine at position 59 (S59) which is phosphorylated by Extracellular signal-Regulated Kinase 1/2 (Erk1/2) [49] and dephosphorylated by calcineurin [50]. It plays a central role as its mutation to a glutamic acid

(S59E) abrogates TCR signalling in Jurkat T cells [50]. However its impact is still controversial as its phosphorylation was initially proposed to reduce Lck activity *in vitro* [51] but it has since been shown to play a protective role by preventing interaction of Small Heterodimer Partner 1 (SHP1) with Lck [52], and protecting Lck from dephosphorylation on its activatory tyrosine (Y394). Once activated, Lck is responsible for its own phosphorylation on tyrosine Y394 and tyrosine phosphorylation of the ITAM motifs.

The phosphorylated ITAM motifs forms docking sites for the Syk-family kinase Zeta chain Associated Protein kinase 70 (ZAP70)(figure 2). Once docked onto the ITAM motifs, ZAP70 is relieved from its auto-inhibition and is phosphorylated by Lck and/or ZAP70 itself to complete its activation [53][54]. This feedback activation step, relying on interaction between the Src homology 2 (SH2) domain of Lck and ZAP70, is essential as mutation of the Lck SH2 domain abrogates signalling [44]. Activated ZAP70 goes on to phosphorylate Linker for Activation of T cells (LAT) on several residues allowing binding of downstream effectors.

LAT is a scaffolding protein anchored in the membrane. LAT carries a membrane proximal, proline-rich motif that mediates interaction with the SH3 domain of Lck. Through this interaction, Lck recruits LAT to the proximity of its associated TCR, and acts to bridge it with ZAP70, favouring its phosphorylation [55]. This bridging is essential as deletion of this proline-rich region prevents LAT phosphorylation and Phospholipase Cγ (PLCγ) activation. This recruitment ensures the specificity of TCR-induced LAT phosphorylation [55]. Control of LAT localisation to the TCR is essential as its perturbation impacts antigen discrimination, especially for weak affinities antigens [56]. Proper localization of LAT in the membrane is therefore essential for its own activation by ZAP70-mediated phosphorylation, but also for the propagation of the signal as its localization places effector molecules in close proximity with membrane-bound substrates such as Phosphatidylinositol 4,5-bisphosphate (PIP2) [57].

The LAT molecule carries 9 tyrosines, 5 of which are major phosphorylation sites [58]. Because of these numerous binding site, LAT acts as an adaptor protein for many effector molecules (Growth factor receptor-bound protein 2 (Grb2), Son of Sevenless (Sos), Grb2-related adaptor downstream of Shc (Gads), SRC homology 2 (SH2)-domain-containing leukocyte protein of 76 kDa (SLP76) and Nck [59]), therefore increasing their density and facilitating cross-activation. It also forms a platform for activating

phosphorylation of PLCγ by interleukin-2-inducible T-cell kinase (Itk). Once activated, PLCγ produces Inositol-1,4,5-triphosphate (IP_3) and Diacylglycerol (DAG) from Ptdlns(4,5)P2 (PIP2). From that step, the TCR signalling diverges in 3 main signalling cascades, each leading to the activation of an essential transcription factor Nuclear factor kappa-light-chain-enhancer of activated B cells (NFκB), Nuclear factor of activated T-cells (NFAT) and Activator protein 1 (AP-1) [60] (figure 2).

IP_3 binds its receptors IP_3R which are large-conductance ion channels that mediate the release of calcium (Ca^{2+}) from the endoplasmic reticulum [61]. This intracellular calcium stimulates the clustering of STromal Interaction Molecule 1 and 2 (STIM1 and STIM2) which triggers the opening of the Orai1 channels in the cell membrane and leads to a further increase in intracellular calcium concentration. Calmodulin has the ability to bind this calcium and activate Calcineurin which is responsible for the dephosphorylation of the transcription factor Nuclear Factor of Activated T cells (NFAT). When the intracellular concentration of calcium is low, NFAT is kept outside of the nucleus through constant phosphorylation by Glycogen synthase kinase 3 (GSK3). But once dephosphorylated, NFAT translocates into the nucleus where it regulates the expression of essential genes for T cell functions [62][63][64].

The other product of the cleavage of PIP2 is DAG. Proteins that contain cysteine-rich domains such as the Protein Kinase Cθ (PKCθ) and guanine exchange factor (GEF) responsible for the activation of Rat sarcoma virus (Ras) and Ras-related proteins GTPases (Rap GTPases), can bind to DAG with high-affinity [65][66].

The guanine exchange factor induces Ras activation by promoting its transition to the active GTP-bound state and initiates the mitogen-associated protein kinase (MAPK) cascade. Once activated, Ras induces activation of Raf-1 (also known as MAPKKK). Raf-1 is responsible for the activating phosphorylation of MEK (also known as MAPKK), which in turn activates Erk1/2 (also known as MAPK)[67]. The Erk kinase induces the activation of the transcription factor ETS Like-1 protein (Elk1) which is responsible for the activity of c-Fos, member of the AP-1 dimer composed of c-Fos and c-Jun [48] [63] (figure 2). Ras can also associate with Rac and initiate a cascade leading to the activation of JNK and p38, inducing the transcription factor Jun.

In addition to these functions, DAG also serves as docking site for PKCθ. Activation of PKCθ initiates the signalling cascade leading to the activation of the NFκB transcription factor. PKCθ is responsible for Carma-1 phosphorylation, this modification induces a conformational changes in Carma-1 allowing the formation of a complex around it which recruits B-cell lymphoma/leukemia 10 (Bcl10) and Mucosa-associated lymphoid tissue lymphoma translocation protein 1 (MALT1) (CBM complex)[68]. Once this complex is formed, it recruits Tumor Necrosis Factor (TNF) receptor-associated factor 6 (TRAF6) and undergoes poly-ubiquitination [69]. This ubiquitination allows for the recruitment of the IκB kinase (IKK). The IKK kinase is composed of 3 subunits (α, β and γ). Upon association with the ubiquitination motif, IKKγ is poly-ubiquitinated and IKKβ is phosphorylated [70]. Upon phosphorylation IKKβ phosphorylates IKKα. This induces its degradation, exposing a nuclear localization motif and Deoxyribonucleic acid (DNA)-binding domains on the NFκB transcription factor, which induces its localization to the nucleus [71] (figure 2).

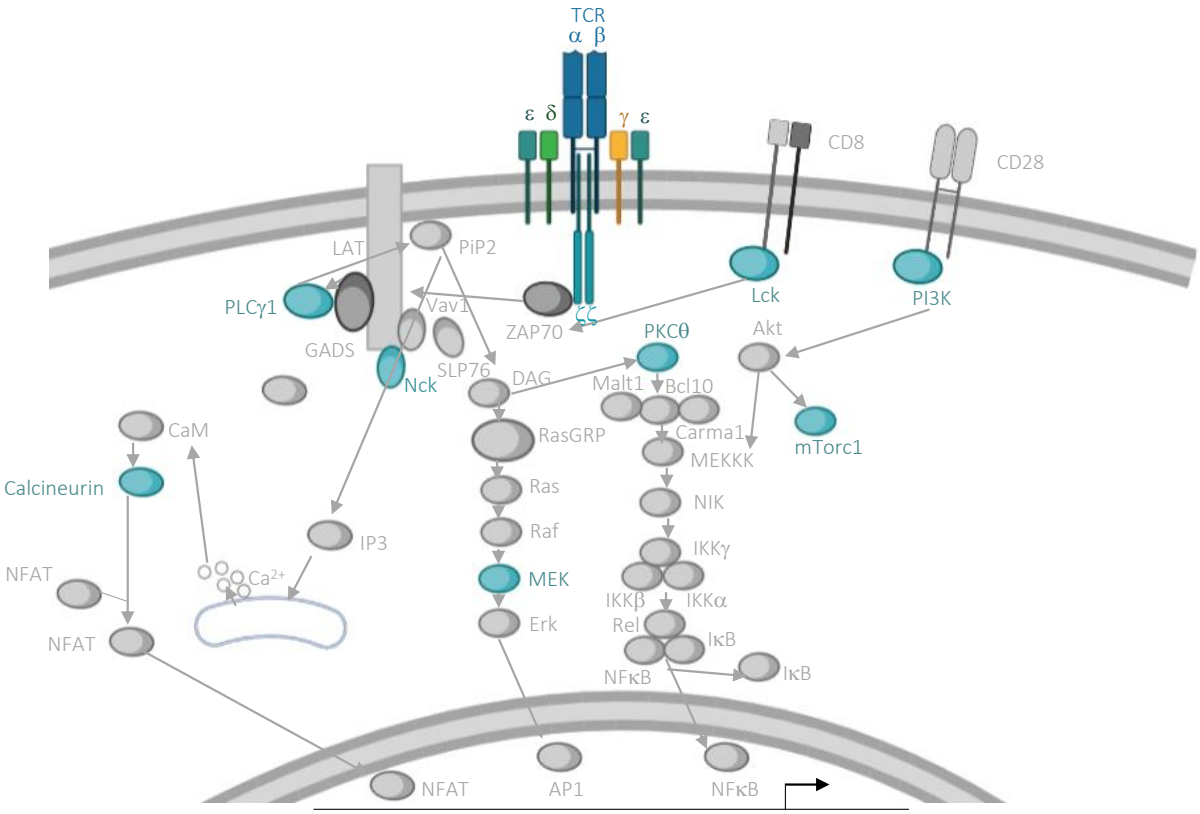


Figure 2: T cell signalling. T cell signalling occurs subsequently to TCR triggering. Triggering leads to CD3 ITAM motifs phosphorylation by Lck and ZAP70 recruitment. ZAP70 in turns phosphorylates LAT leading to the formation of the LAT signalosome and activation of the phospholipase C gamma. From there the TCR signalling diverges into three pathways, each culminating in the activation of a transcription factor. *Signalling molecules in turquoise will be studied in detail in the results chapters of this thesis.*

1.4.1 Cytokine and surface marker regulation by transcription factors

Nuclear translocation of transcription factors induces transcriptional activity that regulates the expression of a large number of genes, including cytokines and surface receptors, which have important functional implications. In the case of cytokines (e.g. IFNγ, TNFα, InterLeukin-2 (IL-2)), they allow T cells to initiate, maintain, and regulate immune responses by controlling other cells. In the case of surface receptors, they can make T cells more or less receptive to signals from other cells or control their migration (e.g. CD69).

We have described above the translocation of NFAT into the nucleus. On its own, activation of NFAT leads to T cell tolerance and anergy [72][73], but in combination with AP-1 [74], the NFAT/AP-1 complex induces the production of cytokines [62] such as IFNγ, IL2 and TNFα [75] [76][77]. NFAT is

dispensable for the induction of the surface marker expression CD69, as deletion of the NFAT binding site on the CD69 gene, does not prevent its expression [78]. NFAT has also been shown to be dispensable for induction of the 4-1BB (CD137) activation marker [79].

CD69 expression, can be however mediated by the activation of transcription factor NFκB [80] , which can also mediate expression of the activation marker 4-1BB [41]. NFκB activation also induces the production of cytokines such as IL-2 [75] and IFNγ [76].

The AP-1 trancription factor, resulting from the activation of the MAPK cascade, is also capable of inducing the expression of activation markers such as CD69 [81] and 4-1BB [82]. AP-1 can interact with the NFAT transcription factor to induce cytokine (IL-2, IFNγ), it can also interact with NFκB to induce the expression of proinflammatory genes [83].

As these three transcription factors illustrate, gene regulation is often the result of the interplay of multiple transcription factors. Also these three transcription factors are complemented by others to regulate the many aspects of T cell activation. Transcription factors such as Oct1, Specificity protein 1 (Sp1), cAMP response element-binding protein (CREB), Zinc finger E-box-binding homeobox 1 (ZEB1), Ets and Signal transducer and activator of transcription 4 (STAT4) are also involved in cytokine production for example [84][77][85].

1.4.2 T cell interaction with Antigen Presenting Cells relies on cytoskeletal remodelling

Successful interaction between a T cell and its cognate APC relies on them forming a stable interaction, which will evolve into a close contact, allowing targeted cytotoxicity and specific cell killing. At the interface between the two cells, this remodelling leads to formation of the immunological synapse (IS). The IS is an organised structure, formed of three rings. In the periphery, the distal SupraMolecular Activation Complex (dSMAC) sees the formation of the first TCR/pMHC interactions. After formation, these interacting complexes follow a centripetal movement to the peripheral SMAC (pSMAC) where are concentrated complexes of larger adhesion molecules such as LFA-1/ICAM. Finally the TCR/pMHC com-

plexes coalesce into the central SMAC (cSMAC), containing the complexes of smaller adhesion molecules such as CD2/CD58 and CD28/CD80/86 [86][87] (figure 3).

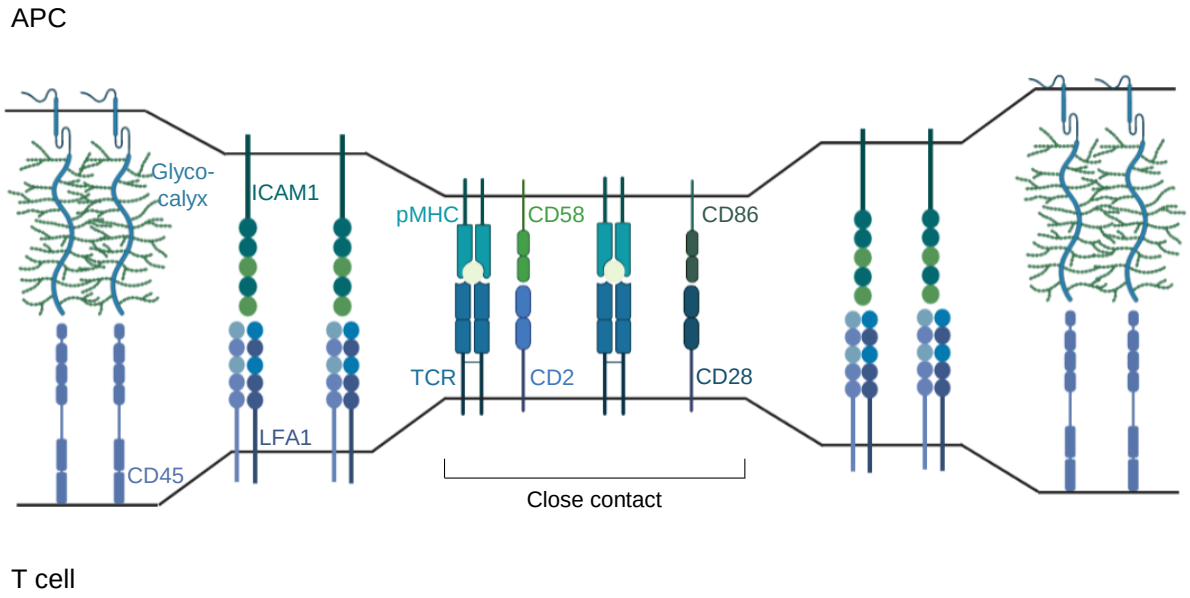


Figure 3: The immunological synapse. The immunological synapse is formed by three intercalating rings, in the periphery the dSMAC where the TCR and pMHC first interact. Inside the dSMAC, the pSMAC that contains large adhesion molecules such as ICAM1/LFA1. Within the pSMAC, the cSMAC is composed of small adhesion molecules such as CD2/CD58 and CD28/CD80/86.

The close contact formed by the immune synapse also allows release of cytotoxic factors from the T cell. In this enclosed area between cells, T cells secrete cytotoxic granules containing perforin and granzyme, which are respectively a pore-forming cytolytic protein, responsible for the formation of pores inside the membrane of the target cell; and a serine protease responsible for the activation of caspase in the target cells, leading to its apoptosis [88].

Actin remodelling is essential for immune synapse dynamics, generating this centripetal movement of TCR complexes from periphery to center. On the other side of the cell, actin-interacting cargo molecules mediate sequestration of molecules inhibitory to T cell activation, such as CD43 [89].

The microtubule network see their MicroTubules-Organizing Center (MTOC) re-localise to position

itself just beneath the cell/cell interface, from there, it ensures the directional secretion of cytokines and cytotoxic factors towards the target APC [90].

Cytoskeletal remodelling is controlled from the early steps of signalling. As described above, formation of the LAT signalosome induces recruitment of SLP76, which bears a N-terminal domain that binds the SH2 domains of Itk, Nck and Vav1 upon phosphorylation (figure 4).

Itk is responsible for phosphorylation of SLP76 at Vav1 binding site, therefore playing an essential role in Vav1 recruitment to the immunological synapse [91].

Nck activates Nck Interacting Kinase (NIK), which phosphorylates the Arp2 subunit of the Actin-related protein (Arp2/3) to allow complex activation. Once activated the Arp2/3 complex is responsible for actin nucleation [92]. Nck is also responsible, together with SLP76, for the recruitment of Wiskott-Aldrich syndrome protein (WASp) to the immunological synapse, which has a key role in actin and microtubule remodelling as it will be described below.

Vav1 is a guanine nucleotide exchange factor (GEF), it is responsible for the activation of the Rho-family GTPases Cdc42 and Rac1 which in turn activate respectively WASp and the WASp family verprolin homologous protein (Wave2) [48].

Wasp and Wave 2 are implicated in both the actin and microtubule remodelling.
WASp supports actin polymerization at active TCR signalling sites following TCR engagement. Upon TCR activation, WASp is recruited to the TCR-proximal effector ZAP70 and relieved from its inhibitory interaction with WASp-interacting protein (WIP) [93]. It then binds and activates Arp2/3 to initiate actin polarisation. Together, they allow T cell migration through the formation of podosomes that allow cellular movement through the extracellular matrix. The ability of T cells to produce podosomes is a key aspect of their mobility and defect in their formation, as observed in patients deficient for WASp, results in impaired T cell chemotaxis and leads to immunodeficiencies [87]. But WASp deficiency has wider impacts on T cell response, due to their inability to induce actin remodelling upon TCR activation, WASp-deficient T cells also show defective proliferation and IL-2 secretion.

Wave2 is responsible, together with formins, for the organisation of the meshwork of actin. They respectively allow formation of lamellipodia and filipodia that allow T cell crawling and spreading [94]

[95]. To allow the formation of these protrusions, Wave2 mainly localises at the periphery of the lamellipod where it promotes actin nucleation [96]. Wave2 is also involved in integrin clustering and affinity maturation through the activation of the Rap1 small GTPase [97].

Together, WASp and Wave2 control the actin centripetal flow that directs TCR microcluster migration [87] and ensure reorientation of the MTOC (microtubule-organising center) to the immunological synapse allowing stable interaction of the T cell with its target [87][98].

Vav1 is also responsible for the dephosphoryaltion of ERM proteins (ezrin, radixin and moesin), which abrogates their ability to link the plasma membrane to the actin cytoskeleton. Following this dephosphorylation, the ERM proteins migrate to the distal pole complex (DPC), at the opposite of the MicroTubule Organising Center (MTOC), to ensure sequestration of negative regulators of TCR activation (such as CD43) [89].

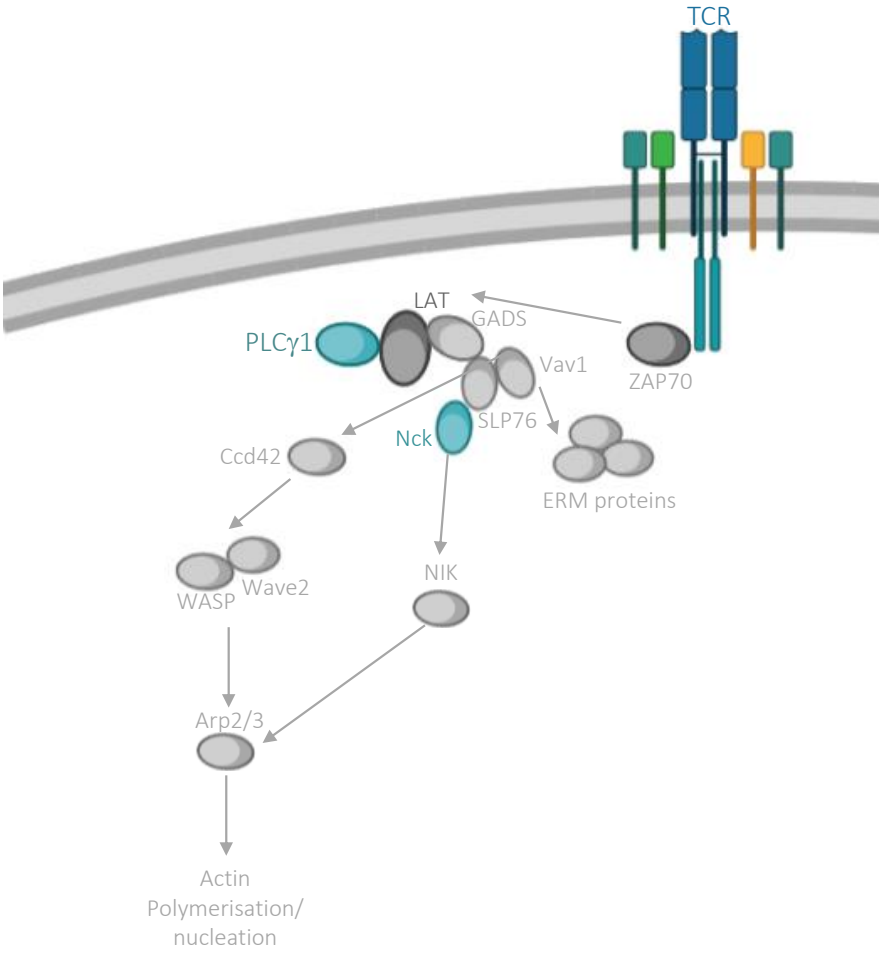


Figure 4: Cytoskeleton regulation. The LAT signalosome is the initiation point of actin and microtubules remodelling. Recruitment and activation of Vav1, Nck and Itk allow the activation of the Arp2/3 complex, WASp and Wave2. The three molecules are responsible for actin polymerisation and nucleation, MTOC and DPC organisations.

We have given here a topological description of the T cell signalling cascade. We will now describe how the components of these pathways have been proposed to contribute to the key properties of T cells, their high antigen sensitivity and effective discrimination.

1.5 How T cells mediate antigen sensitivity

T cells have the ability to recognise minute amount of non-self antigen while ignoring abundant self antigens. This high sensitivity is essential as a common strategy of cancer cells and viruses is to downregulate their pMHC expression in an attempt to avoid recognition by the immune system [99][100].

Evidence that T cells exhibit high antigen sensitivity has been provided by several studies. Using

confocal microscopy with tagged pMHC loaded on APCs at limiting concentrations, it was shown that $CD4^+$ T cells have the ability to respond to a single pMHC [101][102]. In the case of $CD8^+$ T cells, sensitivities as low as 3 pMHC or less have been reported [103]. Using DNA origami rafts on supported lipid bilayer, Hellmeier *et al.* [104] suggest that a pMHC induces T cell activation as a single unit because it allows for unbinding and rebinding of TCRs, which can subsequently cluster.

1.5.1 Impact of co-receptors on antigen sensitivity

The CD4 and CD8 co-receptors bind via their extracellular domain to the MHC complex II and I respectively, at a site that is independent from TCR binding. They exert an impact on antigen sensitivity through both their extracellular and intracellular domains.

Through their extracellular domain, both receptors have also been shown to enhance TCR avidity [105] and stabilise the interaction of the TCR with the MHC molecule [106]. While they are dispensable in the case of strong agonists or anti-TCR antibodies [107] [105], they play a central role in most interactions [108].

The intracellular domain of the co-receptor interacts with Lck. Both the extent and the role of this interaction are still matters of debate. Some studies suggest that co-receptor-bound Lck plays a role in T cell sensitivity. Artyomov *et al.* [109] propose a model of TCR triggering in two steps, where the TCR is first phosphorylated by free Lck, followed by recruitment of the co-receptor bound to Lck. At this second step, the co-receptor interacts with the MHC which ensures Lck proximity [109] to the TCR and allows enhanced TCR phosphorylation. In this scenario, the CD8 co-receptor is thought to play a role in T cell antigen sensitivity, as bringing Lck in close proximity of the TCR is essential for efficient phosphorylation of the ITAM motifs of the TCR. This model is in agreement with the scanning model described by Stepanek *et al.* [110] which proposes that a succession of co-receptors must interact with the MHC before a successful Lck-coupled co-receptor interaction occurs. In this context, they showed that stabilisation of the interaction between CD8 and Lck increases T cell response to weak affinity pMHC. However, Wei *et al.* [27] showed that co-receptor-free Lck has high mobility and kinase activity compared to receptor-bound Lck, therefore rendering the recruitment of co-receptor to the TCR redundant for ITAM phosphorylation.

1.5.2 Impact of accessory receptors on antigen sensitivity

Accessory receptors such as CD2, LFA-1, CD27 and CD28 are known to enhance T cell adhesion to targets and/or boost T cell activation. They have all been shown to increase T cell sensitivity to antigen.

The central role of CD2 in T cell functions is well established as blocking its interaction with its ligand, CD58, by monoclonal antibodies prevent killing of target cells [111]. Its importance is also highlighted by its common loss in cancer and viral infection as a mechanism of immune evasion. Indeed viruses such as Human CytoMegaloVirus (HCMV) induce downregulation of CD58 to prevent the recognition of infected cells by $CD8^+$ T cells [112] and knock-out of CD58 on cancer cells impairs recognition and T cell killing [113]. On the T cell side, loss of CD2 has been described in a model of mouse carcinoma (MC-38) where Tumor-Infiltrating Lymphocytes (TILs) display reduced CD2 expression and loss of cytotoxicity [114]. Ligation of CD2 is essential in immune response as it enhances T cell sensitivity, allowing T cell to respond to lower concentrations of antigens [115][116]. This enhancement of sensitivity happens both through increased adhesion of T cells to their target and through amplification of TCR proximal signalling.
On the one hand, CD2 plays an adhesion role as it stabilises close contacts with target cells via binding to CD58 expressed on APCs. Because of its size, similar to the one of the TCR and pMHC, the CD2/CD58 interaction helps maintain the optimal inter-membrane distance.
CD2 also plays a signalling role. It is recruited to the dSMAC of the IS, where it forms a corolla, a CD2-rich compartment [117]. There, it recruits effectors to its intracellular tail, eventually forming micro-domains in which proximal effectors such as Src kinases (e.g. Lck), LAT and PLCγ1 are recruited and activated. CD2 therefore amplifies the TCR signal of proximal effector molecules [117].
In mice too, CD2 interaction with its ligand (CD48) enhances T cells sensitivity as loss of CD2 reduces sensitivity by 3-10 fold [118].

LFA-1 is another surface molecule that increases T cell antigen sensitivity as shown by Bachmann *et al.* [119] and Pettmann *et al.*[115]. The LFA-1-mediated increase in sensitivity is though to be due to increased adhesion alone (as described in 1.4.2) as LFA-1 only caries a short intracellular tail that does not integrate into TCR signalling [120]. The adhesion process however is responsible for inducing signalling independently of the TCR. Indeed, integrins play key roles in sensing the environment. Their

interaction with their specific ligand, and the force-induced activation that results from it, is transmitted to the intracellular signalling pathways via talin and kindlin proteins. Signals perceived by the surface integrins are translated into cytoskeleton remodelling, allowing essential aspects of T cell activation such as cell migration, protrusions formation, cell/cell adhesion and synapse formation [121]. As examples, cell adhesion to fibronectin via beta 1 integrins triggers the rapid activating phosphorylation of Vav1, an essential actor of cytoskeleton remodelling as described in section 1.4.2 and figure 4 [122]. Integrins ligation also induce the recruitment of SLP76 to forms microclusters via the adaptor protein ADAP. The formation of these clusters induces increased adhesion and T cell proliferation, in a TCR-independent manner [123].

Binding of CD27 to CD70 on APC enhances T cell antigen sensitivity as it lowers the threshold for the activation of $CD8^+$ T cells, especially for low-affinity antigens [124]. Upon ligation, CD27 induces proliferation and IFNγ secretion at lower antigen concentrations. This is due to the co-stimulatory role of CD27, whose signalling integrates into the TCR signalling cascade, leading to NFκB and AP-1 activation [125].

The role of CD28 in T cell antigen sensitivity is less clear, as some groups showed that ligation of CD28 enhances T cell antigen sensitivity. Viola *et al.* [126] demonstrated that a stronger stimulus is required for IFNγ secretion and proliferation in absence of CD28 ligation in mice. In line with this, Zhang *et al.* [127] showed that loss of CD28 requires increased antigen concentration for proliferation in mice. However, in a controlled system, where the effect of each accessory receptor can be isolated, it was shown that CD2 and LFA-1 have a larger 125-fold and 20-fold increase in antigen sensitivity compared to a modest 4-fold by CD28 [128].
CD28 is described as a co-stimulatory molecule. It plays a signalling role as its intracellular domain carries several binding motifs that mediate recruitment and activation of key signalling molecules upon ligation, leading to T cell proliferation, IL-2 production and actin remodelling [129][130][131] .

1.5.3 Impact of soluble factors on antigen sensitivity

Soluble factors such as cytokines have also been shown to impact T cell sensitivity. *In vivo*, different pathogens produce different inflammatory environments. These were studied by Richter *et al.* [132] who mimicked these inflammatory conditions by stimulating T cells in presence of various inflammatory factors. They showed that T cell sensitivity to antigen was increased in the presence of bacterial or viral strains such as Listeria Monocytogenes (LM) (inducing IL-12 production and type I IFN) or Lymphocytic ChorioMeningitis Virus (LCMV) (mainly inducing type I IFN production). Both these soluble factors act by co-stimulation, enhancing activation of TCR proximal molecules such as ZAP70, although the extent of their impact varies depending on the pathogen context. The exact mechanism through which these soluble factors impact T cell sensitivity is still unknown, enhancement of TCR clustering or exclusion of negative regulators such as phosphatases are current hypothesis [132].

1.5.4 Impact of intracellular molecules on antigen sensitivity

As discussed above, both surface and soluble molecules are the object of extensive research to their role in T cell antigen sensitivity. However, little is known about the impact of intracellular molecules on this key property of T cells. Some groups approached each signalling molecule individually and/or indirectly to evaluate its impact on T cell sensitivity to antigen. While some data suggest a role for Lck [110][133][134], ZAP70 [135][136] and LAT [137], there is no comprehensive and systematic study of the impact of intracellular signalling molecule on T cell sensitivity. We will discuss in detail the available data indicating a role for these three signalling molecules on T cell sensitivity in section 2.1.2.

1.6 How T cells mediate antigen discrimination

The ability of T cells to discriminate between peptides with a single amino acid change was first explored in inbred mice recognising cytochrome C in 1983 [138]. Despite 40 years of research on the topic, the molecular mechanism behind T cell discrimination remains unsolved. Over time, several models have been proposed.

First, a simple occupancy model (or affinity model) proposed that T cell activation was proportional

to the amount of TCR interacting with pMHC [139]. This model hypothesised that the potency of an antigen was directly dependent on its dissociation constant (k_D). In this model, a high concentration of low affinity antigens would therefore trigger a similar response as would a low concentration of high affinity antigens. However, self antigens are expressed at high levels throughout the human body, so this model is not sufficient to explain physiological discrimination. Moreover, this hypothesis supposes that the maximal response is not impacted by dissociation time, which is in contradiction with experimental data [140][56] .

In light of these shortcomings, the kinetic proofreading model was proposed [141], and it is now the predominant model of antigen discrimination. The kinetic proofreading model proposes that T cell activation depends on the concentration of activated TCR, which is defined as TCRs that have bound pMHC for a sufficient duration. This duration is determined by the number of biochemical modifications needed to place the TCR in a signalling-competent state [141]. Given that TCR/pMHC off-rate (k_{off}) determines the duration of binding, the model predicts, and experiments confirm, that the off-rate can predict antigen potency.

This model of kinetic proofreading is sufficient to explain a enhanced discrimination [115], but not the near-perfect discrimination that T cells were assumed to possess [142][143][144]. Under this model, small changes in affinity (3-5 fold) were considered sufficient to abrogate T cell response despite significant increases in peptide concentration (up to 100,000 fold) [145][146][147] [148][149][150]. In attempts to explain this near-perfect discrimination ability, some proposed additions and modifications have been made to the kinetic proofreading model.

Stefanova *et al.* [52] and Altan-Bonnet *et al.* [151] proposed the introduction of a negative feedback mechanism mediated by the SHP1 phosphatase and positive feedback mediated by the Erk kinase. They proposed that under low affinity antigen activation, only the first phosphorylation steps of the TCR/pMHC complex occur and lead to the activation of SHP1 and its recruitment to Lck. In addition to Lck inactivation, the newly formed Lck/SHP1 complex could also target the CD3 chains and ZAP70 for dephosphorylation. Under higher affinity antigen interactions, and with a slight delay, the subsequent

phosphorylations of the TCR/pMHC complex lead to activation of the MAPK cascade and ultimately generate active forms of Erk that phosphorylate Lck and prevent SHP1 binding [152][151].
This model is supported by experimental data that show that naive T cells, expressing low concentrations of SHP1, demonstrate increased affinity to antigen compared to their mature form, which express higher concentration of the SHP1 phosphatase [153]. Recent experimental data however question this model, Paster *et al.* [154] showed that preventing the phosphorylation of Lck by Erk on S59 had no negative impact on T cell activation. Vogel *et al.* [155] also failed to observe a feedback effect of Erk on Lck activity. They showed that MEK inhibition did not impact MEK phosphorylation while the model by Stefanova *et al.* [52] would predict that inhibition of MEK should result in inhibition on Erk and therefore increase activity of Lck leading to an increased MEK phosphorylation.

Dushek *et al.* [143] invoked a model of induced rebinding to explain T cell near-perfect discrimination. They proposed that the initial binding of pMHC to TCR induces modifications such as triggering-induced TCR clustering to increase the concentration of TCR at the site of initial TCR/pMHC interaction and therefore increase the chances of re-binding. This is supported by the experimental observations of TCR cluster formation subsequent to TCR triggering [156][157].

However, such a heightened discrimination was not compatible with emerging data showing their ability to respond to lower-affinity self-antigens [158] and mount autoimmunity against self-antigen [159]. This near-perfect discrimination model mainly relied on early data obtained with murine transgenic TCRs. Recent improvements in Surface Plasmon Resonance (SPR) techniques allowed new measures of these interactions and demonstrated that peptides assumed to be ignored by the T cell were actually unable to bind the TCR altogether [110]. Using a new SPR protocol, Pettmann *at al.* [115] showed that T cell response was gradually lost upon decrease in affinity. These new data propose that the discrimination ability of T cell is enhanced compared to other conventional surface receptors, but remains imperfect.

In conclusion, the kinetic proofreading model can explain the enhanced but imperfect discrimination produced by the TCR and is compatible with the reported high sensitivity of the TCR [160]. Recent data from Pettmann *et al.* [115] propose that kinetic proofreading relies on a small number of steps

(2.67) and is performed in a short time (2.8 seconds). This is in agreement with experimental data showing LAT phosphorylation within 4 seconds of TCR triggering [161]. However these data are still lacking the identification of the molecules involved in these 2.67 kinetic proofreading steps. Many TCR signalling molecules have been proposed to be involved in antigen sensitivity and discrimination, from the TCR itself to molecules located distally, downstream of the signalling cascade. We discuss in detail the candidate molecules and the data supporting their implication in 2.1.1 and 2.1.2.

1.7 Aim of this thesis

The remarkable properties of T cells allow them to recognise antigens with speed, sensitivity and discrimination. Despite extensive research to identify signalling molecules in the TCR signalling cascade, we have yet to identify which molecules can impact antigen sensitivity and/or discrimination. This is important as manipulating these molecules can be a useful way to improve the efficacy and safety of T-cell based immunotherapies. In this thesis, we describe a systematic method to identify the molecules involved in T cell antigen sensitivity and discrimination.

Chapter 2

How T cells control antigen sensitivity and discrimination

2 How T cells control antigen sensitivity and discrimination

2.1 Introduction

A key property to effective adaptive immune responses is the ability of T cells to become activated when presented with only a single peptide antigen. This property is known as antigen sensitivity and it allows T cells to recognise infected or cancerous cells with high efficiency [162][163]. The ability of T cells to respond to even a single antigen is remarkable given that the TCR/pMHC interaction has a weak affinity (K_D= 1μM) and fast kinetics (k_{off} 0.1/s) [164][165][166] compared to other surface receptors (e.g. cytokine receptors recognise ligands with k_D around 10 to 100 pM) [167].

Discrimination is another key property of T cells. The ability of T cells to discriminate between self-antigen and non-self peptide is essential, as any defect of recognition can lead to pathogen escape or autoimmunity.

T cells were long assumed to possess near-perfect discrimination, by which small changes in affinity (3-5 fold) would be enough to abrogate T cell responses despite big increases in peptide concentrations (up to 100.000 fold). However, improvements in affinity measurement techniques and development of mechanistic models demonstrated that T cell discrimination ability had been overestimated.

Recent improvements in Surface Plasmon Resonance (SPR) revealed that low affinity peptides (such as the E1 peptide variant from the OVAlbumin protein) that were thought to be ignored by T cells, were actually unable to bind the TCR altogether [110]. Therefore previous conclusions based on misguiding SPR data had overestimated T cells discrimination abilities.

The kinetic proofreading model is currently the lead model to explain T cell discrimination as discussed in the introduction (1.6). As described above, this model proposes that only antigen with a long enough binding half-life would lead to T cell activation. Binding triggers a sequence of successive biochemical events leading to T cell stimulation and only ligands that remain bound until the completion of this sequence, are stimulatory. This model can explain high discrimination, but it can not explain T cells near-perfect discrimination while keeping in line with experimental observations such as T cells high sensitivity [102][168] or their ability to respond to lower-affinity self-antigens [158] and mount autoimmunity against self-antigens [159] .

Therefore recent papers concluded that while enhanced compared to other conventional surface receptors, the discrimination ability of the TCR remains imperfect [115] .

In this chapter we aim to gain a better understanding of these two key properties. For that, we need to understand the mechanisms that underlay T cell sensitivity and discrimination and identify the signalling molecules that are involved in these processes.

2.1.1 Mechanisms of antigen sensitivity and discrimination

The TCR interaction with pMHC is one of many examples of receptor-ligand interaction leading to a cascade of intracellular events. However, as discussed above, the T cell signalling cascade allows the T cell unique properties of high sensitivity and discrimination. This suggests that the TCR cascade differs from classic signalling pathways.

In many signalling cascades, the signal is passed down the cascade efficiently, because at each level, enough signalling molecules are activated to saturate activation of the molecules located downstream. An example of such a cascade has been modelled by Strickland and Loeb where binding of the human chorionic gonadotropin (hCG) to its receptor leads to activation of the adenylate cyclase receptor, responsible for the conversion of Adenosine TriPhosphate (ATP) into cyclic Adenosine MonoPhosphate (cAMP) [169]. They showed that changes in the availability of any intermediate molecule impacts both the sensitivity and the amplitude of the response.

In this study, like in ours, data were plotted as dose-response curves. This way of visualising data allows the extraction of two key parameters to measure sensitivity and magnitude of the T cell response:
- Emax, which stands for maximal response achievable.
- EC_{50}, which stands for half-maximal effective concentration. It is a measure of the concentration of ligand required to generate half of the maximal response.

Therefore, the Emax can be used as a measure of the magnitude of the response; and the EC_{50} can be used as a measure of sensitivity.

In this model by Strickland and Loeb, any change in the availability of an intermediate signalling molecule

induced both a shift of the EC_{50} of the curve and a decrease of its maximum. In such a cascade, no change in molecule availability is able to induce a decrease of the amplitude of the response independently of a shift of the EC_{50} of the curve [169]. In other words, no modulation of intermediate molecule ever impacts the Emax but not the EC_{50}.

In T cells however, modulation of many signalling molecules results in changes of the magnitude of T cell activation with no impact on the EC_{50}. This can be visualised by the activation patterns of many effector molecules [170][171][172][151][173][174], transcription factors[175][176] and outputs [102][177], which become activated at a given concentration of ligand (fixed EC_{50}) and only see their level of activation vary (variable Emax). A linear signalling cascade is not sufficient to explain these observations, therefore we need to invoke the presence of an intracellular switch.

An intracellular switch is a molecule (or set of molecules) which acts as threshold sensor, before which changes in ligand concentration directly impact T cell response and after which activation is bimodal : either the threshold has been reached and activation proceeds, or the threshold has not been achieved and activation is abrogated. Activation of all the molecules located after the switch occurs at the concentration of ligand sufficient to reach threshold activation and modulation of molecules after the switch has no impact on EC_{50}.

In presence of an intracellular switch, the TCR signalling cascade is composed of two sets of signalling effectors: a set located before the switch, and a set located downstream of it.
The activation of upstream molecules directly depend on the stimulus perceived. An increase in signalling intensity induces an increase in their activation level and number. On the other hand, the activation level of signalling molecules located downstream of the switch is unaffected by stimulus intensity; these molecules either adopt a fully activated or fully inactivated phenotype. The exact molecule(s) forming this switch are still a matter of debate.

The presence of a switch alone is not sufficient to explain the remarkable sensitivity and discrimination of T cells. As discussed above, the enhanced discrimination power of the T cell receptor can be

explained by the mechanism of kinetic proofreading [141], which proposed that ligand binding half-life is the main determinant of a successful T cell activation. A recent study by Tischer and Weiner brings experimental evidence to this model. They used an optogenetic-based method in T cells transduced with chimeric antigen receptor (CAR T cells), where binding half-life of the antigen receptor is modulated by light. The strength of their study relies in the fact that illumination induces dissociation of the intracellular moiety from the bound-receptor in seconds, its physiologic range. Their study concluded that binding half-life is the strongest determinant of activation [178]. These results are also in agreement with data from the Schamel group, which demonstrated a similar effect on calcium increase [179].

Therefore the literature supports the kinetic proofreading model as mechanism for T cells enhanced discrimination. However, which molecules are involved in kinetic proofreading remains a matter of debate. Some have proposed that the kinetic proofreading is restricted to the TCR and its co-receptor [110][180]. Because the TCR carries 10 ITAM motifs [181] - the largest amount of ITAM motifs carried by any receptor [182] - mathematical models suggested that this pattern could be sufficient to generate digital signalling with switch-like response from the level of the TCR itself [140][183][184]. However, experimental data failed to support this hypothesis [185][186] and suggests that the multiplicity of motifs acts as a first amplification step of the signal. Moreover, recent research based on optogenic systems (allowing fast and specific visualisation of TCR downstream events) suggests that the kinetic proofreading process extend downstream of the TCR [187].

2.1.2 Molecules controlling antigen sensitivity and discrimination

Identification of the molecules controlling antigen sensitivity and discrimination is essential to help us understand failures of the sensitivity or discrimination processes in the context of autoimmunity. It is also crucial in the design of therapies that rely on manipulation of T cells such as adoptive cell transfer of CAR T cells (T cells transduced with Chimeric Antigen Receptors). Deciphering which molecules are involved in T cell sensitivity and discrimination would allow their manipulation to improves these processes.

Many groups have studied TCR signalling effectors and the role they play in these key processes, however most of them rely on inference and do not demonstrate direct impact on antigen sensitivity or

discrimination. Most studies in the literature based their work on protein interactions observed through biochemical methods such as immuno-precipitation or interactomics.

Many studies rely on observed interactions with the TCR : Stefanova *et al.* [52] observed immuno-precipitation of the SHP1 phosphatase with the TCR, that prompted them to suggest a direct feedback effect of SHP1 on the TCR. They proposed that low-affinity stimuli induce SHP1 recruitment to Lck and its dephosphorylation, while only high-affinity stimuli induce activation of Erk via the MAPK cascade. Recruitment of Erk to Lck would ensure protective phosphorylation and effective TCR signalling. However, while Stefanova *et al.* [52] showed that over-expression of the SHP1 phosphatase induced a decrease of the magnitude of the T cell response (observed as reduced cytokine production), they showed no functional evidence of SHP1 impacting antigen discrimination [52]. Moreover, this SHP1/Erk feedback hypothesis has been subsequently disproved, as preventing the Lck - Erk interaction had no negative impact on T cell activation and discrimination [154]. Dutta *et al.* [50] detected Calcineurin in immuno-precipitation with the TCR, and suggested that Calcineurin is recruited to the TCR to prevent phosphorylation of Lck. This inhibition resulted in a decrease of activation of the integrin LFA-1 with drastic impact on its ability to interacts with its binding partner, ICAM, on Antigen Presenting Cells (APCs) [50]. However, the authors did not show functional data indicating an impact of Calcineurin on T cell sensitivity or discrimination. Voisinne *et al.* [188] performed an extensive interaction study of TCR proximal events. They tagged proteins (that they called bait) for affinity purification of interacting complexes before performing mass spectrometry on these purified complexes. Their study revealed 366 interactions between 277 proteins, including 117 interactions detected with Lck [188]. However, their approach did not include any validation of the functional relevance of these interactions.

T cell accessory receptors also have been suggested to impact T cells sensitivity or discrimination to antigen. The accessory receptor CD28 recruits Lck to its cytoplasmic tail, interaction that stabilises Lck in its active form. Dobbins *et al.*[189] suggested that proximity of the CD28 cytoplasmic domain with the CD3 chains of the TCR could contribute to phosphorylation of these chains by bringing Lck in proximity. They proposed that modulating CD28 signalling could therefore impact antigen sensitivity by affecting the T cell activation threshold [189]. However, the authors did not show functional evidence to support

this hypothesis. Yang *et al.* [190] showed that the increase in calcium induced by TCR activation lead to CD28 opening and signalling. Signalling through CD28 enhanced phosphorylation of PLCγ1 which augmented calcium signalling [191]. They suggested that this forms a dual-positive feedback involving calcium, TCR and CD28, amplify TCR signalling. Using mathematical modelling, the authors proposed that this feedback increases antigen sensitivity and explains the high sensitivity property of T cells [190], however they did not confirm these model predictions functionally. Therefore, in this context also, most studies only infer effects from observed interactions.

A few studies however show a functional impact of TCR proximal molecules on antigen sensitivity and/or discrimination.

Stepanek *et al.* [110] showed that increasing the proportion of active Lck coupled to the CD8 co-receptor allows T cells to respond to lower concentration of peptides. They also showed that the effect was increased upon stimulation with low affinity peptides [110]. This study suggests a role for Lck in antigen sensitivity and discrimination. However, it focuses on the co-receptor-bound form of Lck alone, while subsequent studies showed that free Lck is recruited to the TCR as well and able to induce its phosphorylation [192][27]. There is therefore a need for a study looking at the impact of total Lck on antigen sensitivity and discrimination.

Moogk *et al.* studied the impact of different amounts of Lck in effector versus memory T cells. They showed that effector T cells - bearing a higher concentration of constitutively active Lck (54%) in comparison to their memory counterparts (18%) - have a more efficient cytotoxic capacity to their specific targets. Effector T cells require lower effector/target (E/T) ratio to mediate the same efficacy of killing, as shown by the lower EC_{50} of their killing curve when compared to memory T cells [133]. Variation of the E/T ratio however is not a direct measure of sensitivity, repeating this observation with a constant ratio but titrating concentrations of peptide would be necessary for a conclusive result. This study is also missing variation of ligands affinities to evaluate the role of Lck in antigen discrimination. A wider range of proportion of active Lck would also be more informative.

Manz *et al.* [134] performed an indirect titration of Lck activity by modulating the inhibition of Csk (C-terminal Src Kinase), its primary negative regulator. By titrating the stimulus (different concentration of

αCD3 antibody) in presence and absence of Csk inhibitor, they showed that T cell activation (measured through Erk phosphorylation and proliferation) occurs at lower stimulus when Lck inhibition is lifted. Therefore, decreased Lck inhibition decreases T cell threshold of response, this is indirect evidence that Lck plays a role in antigen sensitivity. Using a panel of OVA peptides (peptide variants derived from the OVAlbumine protein) with different affinities presented on APCs, they showed that inhibition of Csk results in an increased expression of the activation marker CD69 on their surface. The impact of Csk inhibition was greater, upon stimulation by lower affinity peptides. This is indirect evidence of an implication of Lck in antigen discrimination [134].

Shen *et al.* [135] showed that regulation of ZAP70 activity plays a key role in antigen sensitivity and discrimination. Patients with a mutation (R360P) preventing ZAP70 auto-inhibition demonstrate enhanced antigen sensitivity. T cells from these patients become responsive at lower concentrations of peptides compared to unaffected controls (visualised by CD69 expression). This work also suggests an impact on antigen discrimination as the enhanced sensitivity is exacerbated on low peptide affinities and T cells become able to respond to self-peptides in an inflammatory context [135].
Katz *et al.* [136] showed that the duration of ZAP70 interaction with the TCR is optimised and modulation of this binding time, either by preventing or forcing dissociation, negatively impacts T cells functions such as calcium release. They propose that ZAP70 plays a role in antigen sensitivity as its modulation decreases T cell response upon low stimulus (low concentration of αCD3 antibody) [136].

Lo *et al.* [137] demonstrated that the phosphorylation rate of LAT has a critical impact on antigen discrimination. The tyrosine at position 132 (Y132) on LAT is phosphorylated by ZAP70 leading to the recruitment of PLCγ1. This tyrosine distinguishes itself by the speed of its phosphorylation, slower than any other tyrosines on LAT. This slow phosphorylation is due to the presence of a preceding glycine residue. Because it is neutral, this residue does not facilitate interaction with the basic residues of the ZAP70 kinase as well as its other tyrosines, located in acidic environment. A point mutation of this glycine residue to an acidic aspartate (G131D) or glutamate (G131E) residue increases the speed and magnitude of activation of PLCγ1. This results in enhanced antigen sensitivity to low affinity peptides. That gain however is at the detriment of discrimination as G131D T cells become reactive to self-peptides [137][193].

Pettmann *et al.* [115] showed that the accessory receptors CD2 and LFA-1 both improve antigen sensitivity and discrimination. By stimulating T cells using a titration of peptide concentrations, they demonstrated that binding of the receptors CD2 or LFA-1 - by presentation of their purified ligands (CD58 and ICAM-1) on plate - allows T cell to respond to lower concentrations of peptides. They also made use of a panel of different peptide affinities to show that upon ligation of CD2 or LFA-1, T cells show enhanced discriminatory abilities [115][194]. However their observations are restricted to purified proteins presented on plate, repeating these observations in a more physiological system would be interesting.

In conclusion, most data from the literature are based on molecular interactions, from which impact on antigen sensitivity and/or discrimination is only inferred. The few studies that provide functional data based on T cell functions measured upon titration of peptide concentrations and affinities only focused on a small number of TCR signalling effectors. This motivated us to generate a systematic study of antigen sensitivity and discrimination by perturbing the activity of a wide range of signalling molecules, located proximally and distally to the TCR.

In order to design this systematic strategy and guide our experimental approach, we decided to develop a mathematical model of TCR signalling. Complex models of the TCR signalling cascade can - and have been - developed in an attempt to replicate the network complexity and involve all its signalling effectors. Their complexity however prevents those models to produce useful quantitative predictions [195]. Therefore, we chose an alternative approach and developed a simplified phenotypic model. Phenotypic models are not based on highly complex molecular cascades established from the literature but focus on quantitative phenotypes generated experimentally.

2.2 Results

2.2.1 A mathematical model can localise a signalling molecule based on its impact on antigen sensitivity

In our model, we simulated the input as a titration of peptide concentrations (with known TCR recycling and ligand binding rates) and observed the impact on T cell phenotype (with cytokine secretion and surface markers expression as outputs). This approach allows us to work with a minimal number of reactions necessary to resolve the input-output relation that we observe experimentally. The model (figure 5) is based on two molecules: a ligand (L) and its unbound receptor (R). Their interaction and resulting reactions are governed by rate parameters. The binding of L and R is governed by the on-rate (k_{on}) and their unbinding is governed by their off-rate (k_{off}). Upon binding, the complex C_0 can undergo modifications (e.g. phosphorylations) with rate k_p. After N modifications, the complex can achieve a signalling competent state (C_N). This, for example, may be a state where phosphorylated ITAMs are bound by phosphorylated ZAP70 molecules. This state can induce activation of downstream signalling with an activation rate (k_{act}). This parameter governs the activation of effectors located before the switch. We postulate that the switch is a molecule, or interacting molecules, which gather signals coming from upstream molecules. Thus, once there is sufficient upstream signal (e.g. the concentration of C_N is above a threshold value) the switch is turned on. Molecules activated downstream of the switch are produced with the rate k_{prod}. These molecules include cytokines (e.g. IFNγ, TNFα, IL-2) and cell surface proteins (e.g. CD69, 4-1BB).

This model is based on the current model of kinetic proofreading [141] with the addition of a switch to explain the digital behaviour of T cells response.

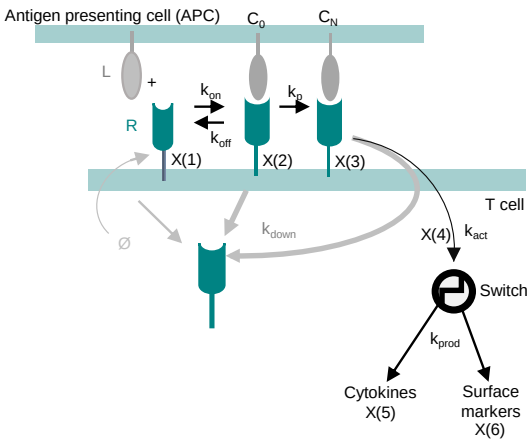


Figure 5: Phenotypic model of T cell signalling. The unbound T cell receptor is modelled as "R" with its unbound peptide-MHC ligand as "L". R can be removed from the surface (e.g. degraded, recycled, etc) and added to the surface (e.g. synthesis, recycling) with constitutive rates. Binding of L and R leads to the formation of a complex (C_0). This complex undergoes N modifications at rate k_p to generate a signalling competent complex (C_N). The bound complex can undergo ligand-induced down-regulation at any step with rate k_{down}. C_N triggers the activation of downstream effectors with rate k_{act}. Activation of effector is analogue until the activation of a "switch" module. Activation of effectors after the switch follow digital behaviour. They generate output in the form of cytokine secretion and surface marker activation at rate k_{prod}. All parameters described in 6.2.1.

We next used the mathematical model to predict the impact of modulation of signalling effector activity (e.g. inhibition of signalling molecules) on the measured T cell output (cytokine secretion or surface marker expression). For this, we plotted the output by varying antigen concentrations and then repeated this plot while inhibiting each rate. This allowed us to assess the EC50, the concentration of antigen required to elicit 50% of the maximal response. We use this EC50 parameter as a measure of antigen sensitivity, with low values of E50 indicative of a high sensitivity.

An inhibition on k_{on} represents a decrease of binding of the ligand to its receptor, and, in this scenario, the dose-response curves are shifted to the right (increased EC50) (figure 6 B). This indicates that more ligand is necessary to reach the non-inhibited response level (figure 6 A). In this condition however, the amplitude of the response (E_{max}) is not affected (figure 6 C).

Inducing an inhibition of the kinetic proofreading rate k_p results in a shift of the dose-response curves to the right (figure 6 A), generating an increase in the EC_{50} of the curves (figure 6 B) as well as a decrease in the amplitude of the response (figure 6 C).

An inhibition of the activation rate k_{act} generates the same effects: an increase of the EC50 of the curves and a decrease of the response magnitude. Modulation of these three rates (k_{on}, k_p and k_{act}) located before the switch results in change in the EC50 of the curves. This indicates that effector molecules implicated in these processes impact the stimulus (ligand concentration) required to reach a given response, these signalling molecules are therefore involved in the sensitivity process (figure 6).

Inducing an inhibition of the production rate k_{prod}, located after the switch, does not induce a shift of the dose-response curves (figure 6 A); the EC50 of each curve remains unchanged (figure 6 B). However, the inhibition results in a decrease of the maximal response (E_{max}, figure 6 C).

This model gives an accurate representation of non-saturating outputs, such as cytokines secretion that generate bell-shaped curves as dose-response curves. The decrease of the response we observe at high concentrations of ligand is due to an accelerated ligand-induced downregulation of the TCR at these high concentrations. This results in lower concentrations of receptors available on the surface, therefore limiting the cell response at these ligand concentrations.

This model suggests that molecules located upstream of the switch can influence antigen sensitivity whereas those located downstream of the switch cannot. We have also modelled the output resulting from an inhibition of the switch itself (appendix figure 33). Inhibition of the switch generates an output similar to modulation of k_p and k_{act} , with an increase of the EC50 of the curves and a decrease of the magnitude of the response. Therefore, observation of the output alone, does not allow discrimination between an impact on a reaction taking place before the switch or at the switch itself.

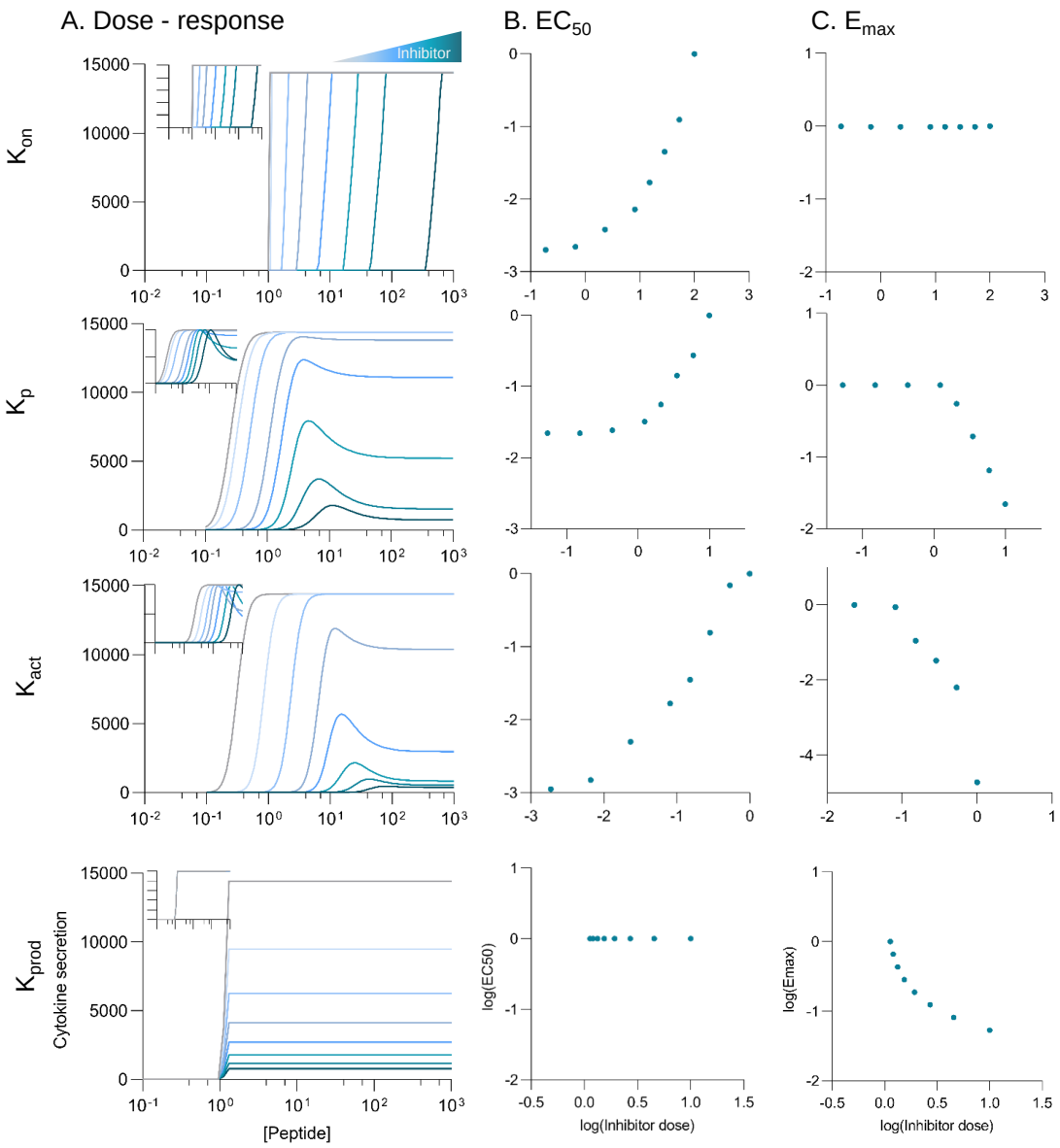


Figure 6: Phenotypic model predicts that only molecules upstream of the intracellular switch will impact antigen sensitivity. The model predicts the output produced by T cells upon stimulation with ligand titration under increasing inhibition. (A. column). Simulated degrees of inhibition on the reaction rates (k_{on}, k_p, k_{act} and k_{prod}) predict the impact on the E_{max} and EC50 of the dose-response curves. (B. column) The value of EC50 determined from the dose-response curves in (A) over the degree of inhibition of the indicated parameter. (C. column) The value of E_{max} determined from the dose-response curves in (A) over the degree of inhibition of the indicated parameter.

2.2.2 Systematic identification of signalling molecules impacting antigen sensitivity

We made the choice of a systematic approach to study individual molecules of the TCR signalling cascade. For each targets studied, we made use of commercially available, small chemical inhibitors. Most of the effectors we considered in this study had been functionally studied previously, but most approaches had looked at individual molecules in different set-ups and contexts, and made use of a diversity of targeting

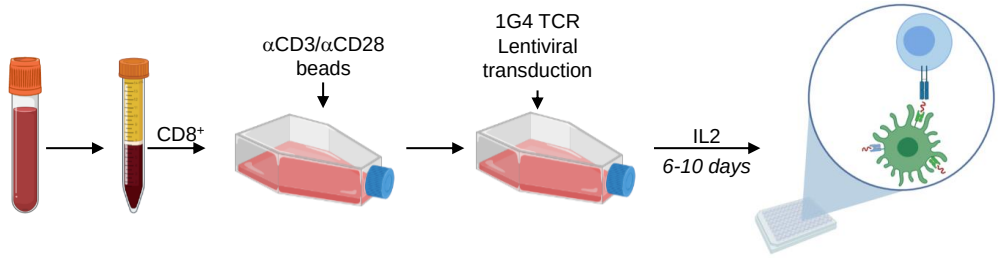


Figure 7: $CD8^+$ T cells isolation and transduction. $CD8^+$ T cells are isolated from the blood of healthy donors. The T cells are stimulated overnight by anti-CD3/CD28 coated beads then transduced to express the 1G4 TCR. The $1G4^+$ $CD8^+$ T cells are maintained for 6-10 days by addition of IL-2 every 48h before use in experiments.

approach, making general conclusion challenging.

We decided to study T cell signalling using primary $CD8^+$ T cells. In our experimental set up, parameters modulation are recapitulated by treatment of the T cell with a panel of small-molecule inhibitors, each specifically targeting an effector molecule in the signalling cascade.

The primary T cells we used were freshly isolated from healthy blood donors. After isolation, the $CD8^+$ T cells were expanded using anti-CD3/CD28 beads and transduced to express the 1G4 TCR. The well-characterised 1G4 TCR [196][197], specifically recognises the NY-ESO peptide presented on HLA-A*02:01 (figure 7).

In preliminary work, we used a reductionist system where T cells were stimulated by a titration of pMHC on plate. We coated streptavidin-coated plates with decreasing amount of biotinylated MHC presenting the 9V peptide (variant of the NY-ESO peptide) to induce titrating T cell responses and generate dose-response curves. The plates were also coated with a constant concentration of CD58, ligand for the adhesion receptor CD2. We pre-treated the T cell for one hour with titrating doses of inhibitor against each of the candidate molecule, before stimulation on the coated plates (figure 8). We used cytokine secretion (figure 9 and appendix figure 34) as measure of T cell activation (output).

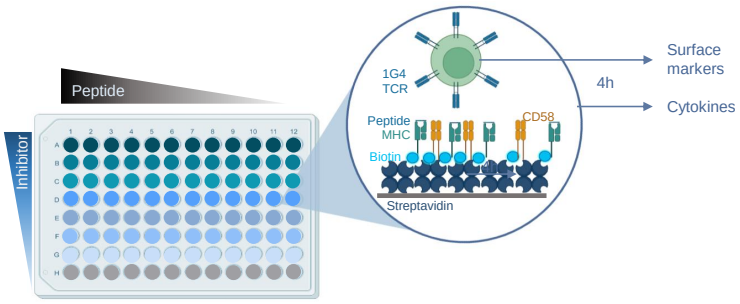


Figure 8: Studying sensitivity on pMHC coated plate: experimental set up. 1G4$^+$ T cells are incubated with a titration of inhibitor for one hour followed by activation for 4h on streptavidin-coated plate presenting a titration of the 9V peptide on biotinylated MHC with a constant concentration of CD58 (250ng/well). The impact of inhibitor on T cell functions is studied by staining of T cell for activation markers and measure of cytokine secretion.

We selected molecules that spanned the entire signalling pathway for which well-established small-molecule inhibitors were commercially available. We tested a member of the proximal pathway downstream of the TCR (Lck). But we also studied effectors involved in the different divergent signalling pathways: PI3K and PKCθ from the NFκB signalling cascade and Calcineurin, a direct regulator of the NFAT transcription factor.

Lck was targeted by the inhibitor A-770041. This small-molecule inhibitor was developed to prevent allograph rejection [198], it inhibits the Src family members with a preferential affinity to Lck. We chose the widely-used immunosupressor molecule Cyclosporin A to target Calcineurin [199]. To inhibit PI3K, we used the selective, small-molecule inhibitor Pictilisib, that was developed as anti-cancer therapeutic agent by Genentech, Inc [200]. Finally, we targeted PKCθ using Sotrastaurin, an inhibitor developed by Novartis AG to prevent rejection after transplantation [201].

Treatment with A-770041 (Lck inhibitor) induced the dose-response curves to shift to the right (highlighted in the normalised inset graphs) (figure 9 A). This translates into an increase of the EC50s of the curves (figure 9 B). Treatment with Cyclosporin A (Calcineurin inhibitor), Pictilisib (PI3K inhibitor) and Sotrastaurin (PKC inhibitor) did not induce a shift of the dose-response curve (highlighted in the normalised inset graphs in figure 9 A). The EC50s of these curves remained unchanged (figure 9 B). Each inhibitor treatment, against Lck, Calcineurin, PI3K and PKC, induced a decrease of the magnitude of the response (decrease of the E_{max}) (figure 9 C).

Because inhibition of Lck impacted the EC50 and the E_{max} of the dose-response curves, this indicates that Lck is located upstream of the switch in the signalling cascade. As inhibition of Calcineurin, PI3 kinase and PKCθ only impacts the amplitude of the response, our result indicates that all three molecules are located after the switch in the signalling cascade. These results were reproducible across multiple donors (appendix figure 34).

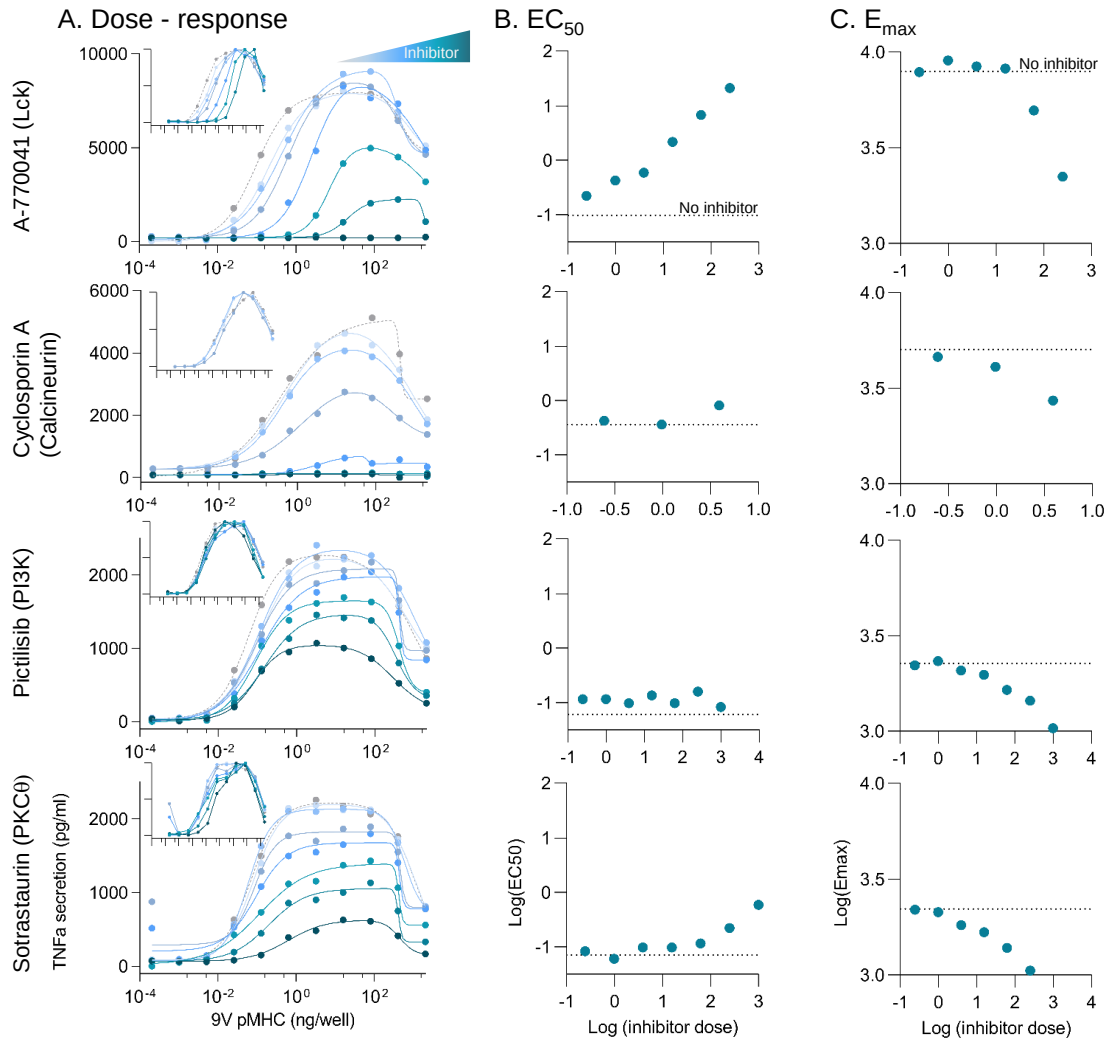


Figure 9: Impact of the inhibition of signalling molecules on antigen sensitivity as measured by cytokine production in the plate-based assay. (A. column) Cytokine secretion upon stimulation of 1G4$^+$ T cells on streptavidin-coated plates presenting a titration of biotinylated pMHC (9V of the NY-ESO antigen) under increasing concentrations of inhibitor. Inset shows curves normalised to their individual E_{max} values. One representative donor. (B. column) The EC50 values are extracted from bell-shaped curves fitted to the raw data. The EC50 of the no inhibitor condition is represented by the dotted line. (C. column) The E_{max} values are extracted from bell-shaped curves fitted to the raw data. The E_{max} of the null inhibitor dose is showed by the dotted line.

In order to test if our observations could be reproduced in a more physiological setting, we made use of the U87 glioblastoma cell line as antigen presenting cells. We co-cultured $1G4^+$ $CD8^+$ T cells with U87 cells pulsed with titrating amount of antigen to generate dose-response curves. We used the same time points as for the plate-based experiment, with a pre-incubation phase of the T cell with titrating dose of inhibitors for one hour, followed by 4 hours of activation by co-culture (figure 10).

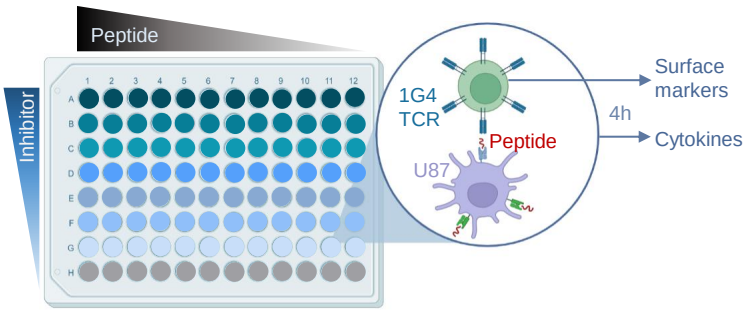


Figure 10: Studying sensitivity on pulsed APC: experimental set up. $1G4^+$ T cells are incubated with a titration of inhibitor for one hour, followed by activation for 4h by co-culture with U87 pulsed with the 9V peptide at titrating doses. The impact of inhibitor on T cell functions is studied by staining of T cell for activation markers and measure of cytokine secretion.

In this more physiological set up, we reproduced our previous observations. We confirmed that Lck is the only molecule tested inducing a shift of the dose-response curves (increase in EC50 – figure 11 B) as highlighted on the normalised inset graphs (figure 11 A). In this setting, again, we observed that inhibition of Lck (using the A-770041 molecule) induced an increase of the EC50 and a decrease of the E_{max}. This confirms that, in a more physiological set up too, inhibition of Lck impacts T cell antigen sensitivity. Inhibition of Calcineurin (Cyclosporin A), PI3K (Pictilisib) and PKCθ (Sotrastaurin) only impacts the maximal responses, but does not affect the EC50 of the curves. Therefore, using this co-culture system, we can confirm that Calcineurin, PI3K and PKC do not affect antigen sensitivity and are located downstream of the switch.

We interrogated more candidate molecules from the TCR signalling cascade. We tested the impact of inhibition of PLCγ1, which is the last effector before pathway branching. Indeed, after PLCγ1 hydrolyses PiP2 (PhosphatidylInositol 4,5-bisPhosphate) to form IP_3 (Inositol trisPhosphate) and DAG (DiAcyl-Glycerol), the signalling pathway diverges into three cascades leading to the activation of three different

transcription factors. We have previously studied the impact of inhibiting Calcineurin located in the NFAT cascade and PI3 kinase and PKCθ in the NFκB cascade. We decided to interrogate the impact of inhibition of mTorc, another effector of the NFκB pathway and to study the impact of inhibition of MEK, which is part of the MAPK cascade leading to the activation of AP-1. We chose the widely-used U-73122 small pharmacological molecule inhibitor against PLCγ [202][203]. To target the MEK kinase, we made use of the Trametinib molecule, specific MEK1/2 inhibitor that has been validated against a panel of 180 kinases [204] [205]. We chose the widely-used Rapamycin inhibitor against mTorc1, which interaction with the FRB domain of mTorc1 ensures its specificity [185].

Inhibition of PLCγ1 by U-73122 induced a shift of the dose-response curves (highlighted in normalised inset graph in figure 11 A), which results in an increase of the EC50 of the curves (figure 11 B.). Increasing concentrations of U-73122 (PLCγ inhibitor) induced a decrease of the maximal response (figure 11 C). Titrating concentrations of Trametinib, the MEK inhibitor, induced no shift of the dose-response curves and had therefore no impact on the EC50 (figure 11 A and B), but titrating concentrations of the inhibitor induced a decrease of the maximal T cell response (Figure 11 C). Inhibition of mTorc1 using Rapamycin did not induce a shift of the dose-response curve, leaving the EC50 unaffected (figure 11 A and B) but induced a decrease of the E_{max} (figure 11 C). These results were reproducible across multiple donors (appendix figures 35 and 36).

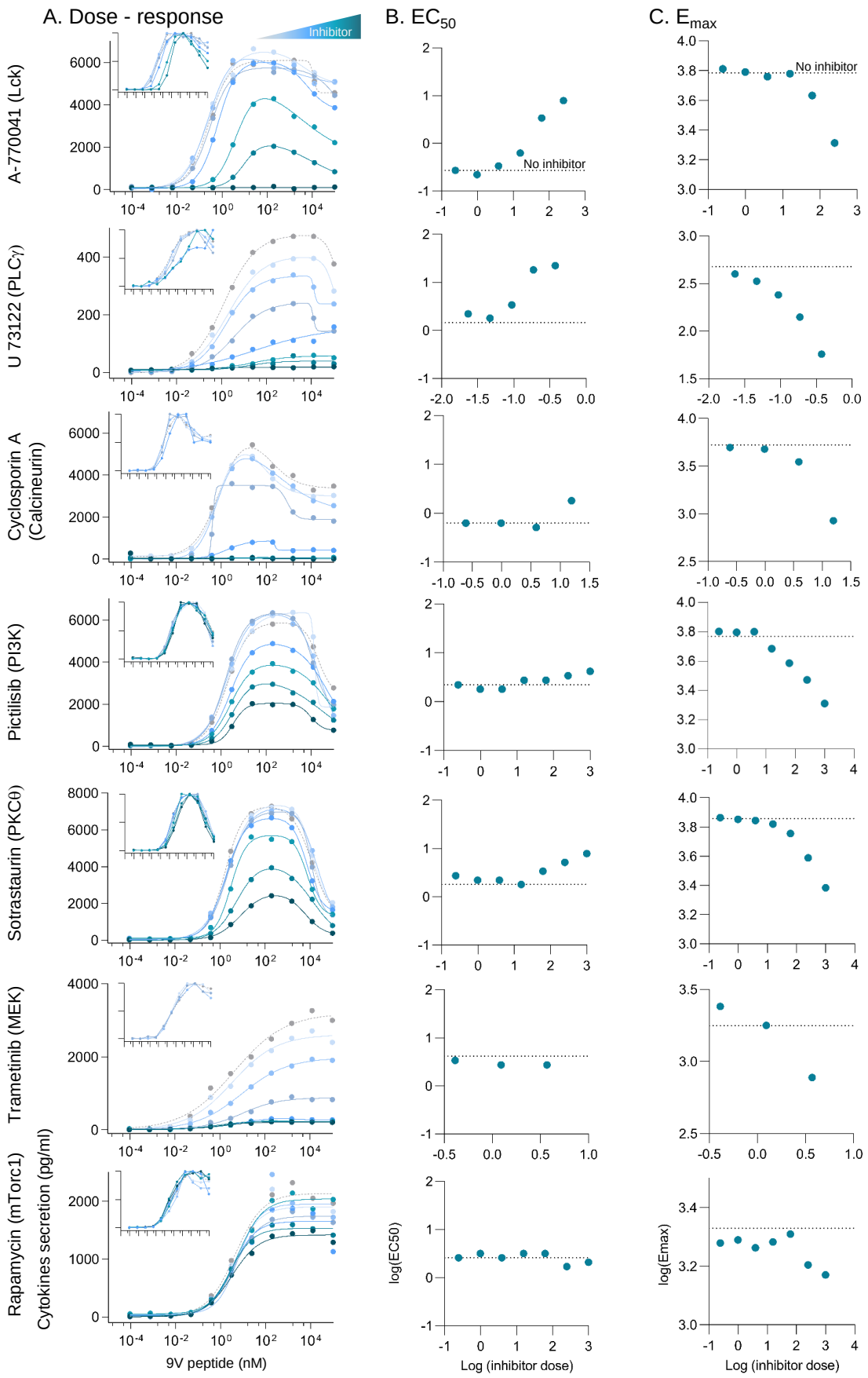

A. Dose - response
B. EC50
C. Emax
Inhibitor
No inhibitor
A-770041 (Lck)
U 73122 (PLCγ)
Cyclosporin A (Calcineurin)
Pictilisib (PI3K)
Sotrastaurin (PKCθ)
Trametinib (MEK)
Rapamycin (mTorc1)
Cytokines secretion (pg/ml)
9V peptide (nM)
log(EC50)
log(Emax)
Log (inhibitor dose)

Figure 11

Figure 11: Impact of the inhibition of signalling molecules on antigen sensitivity measured by cytokine production in an APC co-culture assay. (A. column) Dose-response curves and their normalisation (inset graph) under titrating concentrations of inhibitors, one representative donor. (B. column) Impact of titrating concentrations of inhibitors on the EC50 of the curves. (C. column) Impact of titrating concentrations of inhibitors on the maximum of the curves (E_{max}). The EC50 and E_{max} values are extracted from sigmoid or bell-shaped curves (best fit) fitted to the raw data. The EC50 and E_{max} of the no inhibitor concentration are represented by the dotted lines.

As discussed in the introduction (1.4.2), actin and its regulation play a key role in all the essential functions of T cells, from their mobility to antigen recognition via cell-to-cell interaction [48]. It also mediates the key events of T cell activation: proliferation, synapse formation and cytotoxicity [206]. Because actin plays such a central role in T cell functions, we set out to elucidate the implication of its regulation in T cell sensitivity.

The molecules responsible for the regulation of the actin pathway branch out of the LAT signalosome, with binding of Vav1 and Nck to LAT-recruited SLP76. We used inhibitors of multiple effectors along the actin pathway, from the first actor Nck and its direct partner the Arp2/3 complex, to direct inhibition of actin polymerisation. We inhibited actin polymerisation through both sequestration of its monomers (Latrunculin A) and inhibition of the extension of its filaments (Cytochalasin D).

We made use of the small inhibitor molecule AX-024 to target Nck [207][208]. Treatment with this small-molecule inhibitor resulted in a surprising phenotype: increasing concentration of the inhibitor induced a shift to the left of the dose-response curves (figure 12 B.), allowing T cell to respond at lower doses of peptides (figure 12 A.). However, the addition of the inhibitor did not impact the magnitude of the response (figure 12C.). This surprising observation lead us to perform a more in-depth characterisation of the inhibitor effects, we detail this in chapter 3.

Inhibition of the Arp2/3 complex only had a small impact on the magnitude of the response at high doses (figure 12 C.), but did not impact the EC50 (figure 12 B.) of the dose-response curves (figure 12 A.). The direct inhibitors of actin polymerisation however both induced a shift of the dose-response curves to the right (figure 12 A.) highlighted by the normalised inset graphs and the increase in the EC50s of the curves (figure 12 B.). They also both affected the magnitude of the response. The regulation of actin

polymerisation therefore plays a role in T cell sensitivity to antigen, however Arp2/3 inhibition does not impact the sensitivity process. This could be reproduced across several donors (appendix figures 38 and 39).

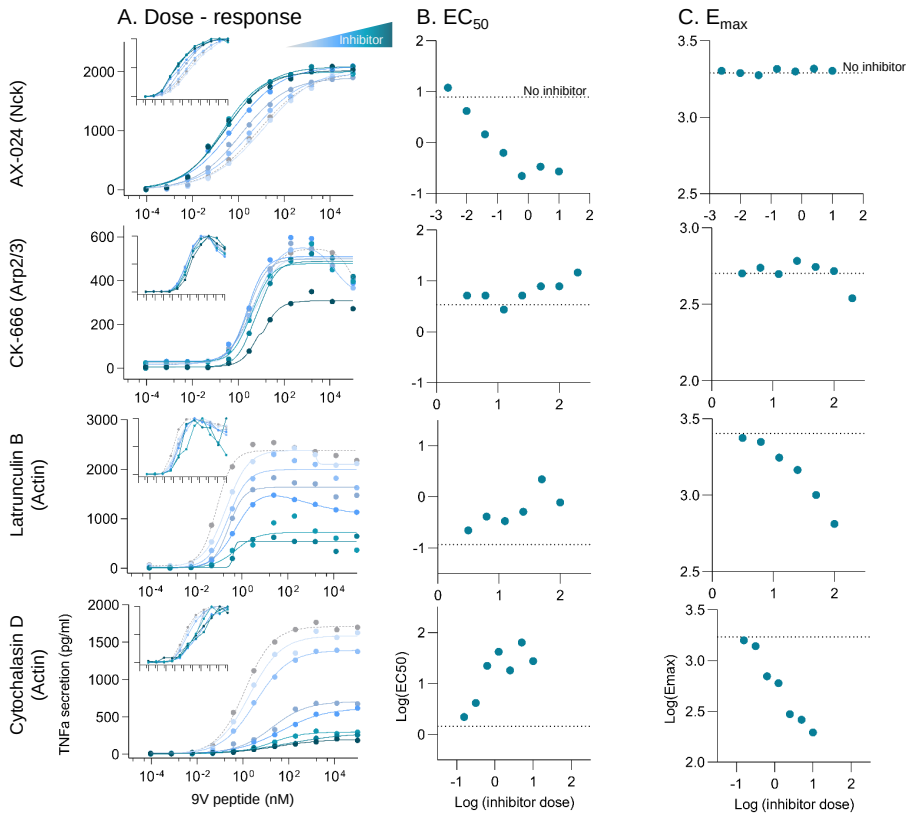


Figure 12: Impact of the inhibition of signalling molecules on antigen sensitivity measured by cytokine production in an APC co-culture assay. (A. column) Dose-response curves and their normalisation (inset graph) under titrating concentrations of inhibitors, one representative donor. (B. column) Impact of titrating concentrations of inhibitors on the EC50 of the curves. (C. column) Impact of titrating concentrations of inhibitors on the maximum of the curves (E_{max}). The EC50 and E_{max} values are extracted from sigmoid or bell-shaped curves (best fit) fitted to the raw data. The EC50 and E_{max} of the no inhibitor concentration are represented by the dotted lines.

Practically, the study of antigen discrimination by T cell is often performed by studying the response of T cell expressing a monoclonal TCR against a set of altered peptide ligands. In this work, we have chosen the systematic approach of studying the impact of each individual molecule on antigen discrimination. We have targeted signalling molecules located early in the signalling cascade as well as downstream effectors; as we mentioned in the introduction to this chapter that we found arguments in the literature implicating a wide range of effectors.

2.2.3 Systematic identification of signalling molecules impacting antigen discrimination

As described in the context of the study of T cells sensitivity, we made use of 1G4 expressing T cells (isolated as described in 2.2.2) stimulated by peptide-loaded U87 glioblastoma cells. We followed a similar approach as the one used to study sensitivity (2.2.2). T cells were pre-treated for one hour with titrating doses of a small-molecule inhibitor, followed by incubation on U87 loaded antigen presented cells. In this discrimination study, we chose to stimulate the cells for longer (6h) in order to measure the up-regulation of the surface marker 4-1BB (CD137) and to be able to detect secretion of IFNγ, both these outputs are not produced at detectable levels before 6h [209][210]. In order to study the ability of T cells to discriminate between different peptides, we submitted the T cell to stimulation with three different affinity peptides. All three peptides are variants from the well-characterise NY-ESO peptide, with single amino acid mutations that yield peptide of various affinity for the 1G4 TCR. We tested the 9V (SLLMWITQV, KD = 8μM), 3Y (SLYMWITQV, KD = 47μM) and 6T (SLLMWTTQV, KD = 162μM) peptides [115].

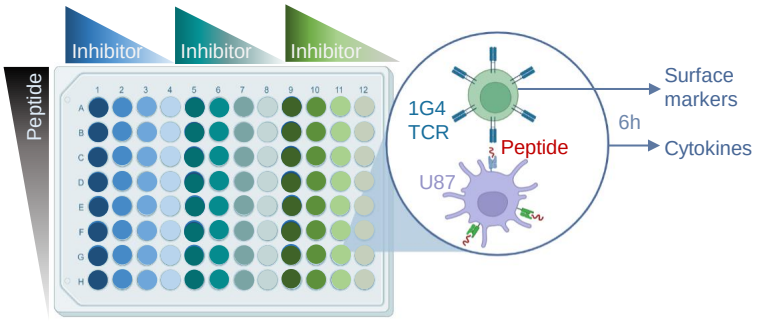


Figure 13: Studying antigen discrimination on pulsed APC: experimental set up. 1G4$^+$ T cells are incubated with a titration of inhibitor for one hour, then activated for 6h by co-culture with U87 pulsed with high (9V), intermediate (3Y) and low (6T) affinities peptides at titrating doses. The impact of inhibitor on T cell functions is studied by staining of T cell for activation markers and measure of cytokine secretion.

To study the impact of inhibition of individual signalling molecules on the ability of T cell to discriminate between antigens, T cell were pre-treated with different inhibitor concentrations (3 concentrations and an untreated control) before being co-cultured with the U87 target cells pulsed with different concentrations of each peptide antigen (figure 13). If the decrease in antigen sensitivity is similar between different antigens, we can conclude that they are not involved in discrimination. However, if the decrease

in antigen sensitivity is larger (or smaller) for lower affinity antigens, we can conclude that the inhibited molecule is selectively acting on low affinity antigens and therefore impacting antigen discrimination.

The measure of discrimination requires a measure of antigen sensitivity. In this work, because we observe a broad variability upon treatment with different inhibitors and between different donors, we defined antigen sensitivity as the concentration of antigen required to reach a threshold level of activation. This threshold level was decided by visual inspection, in order to intersect with the dose-curves across as many inhibitor concentrations and peptide affinities as possible. This threshold was common to all conditions within one experiment but it varied between experiments. The reason for the variation is related to the variation in the level of activation between experiments. We excluded the value of the intersect if:

- The intersect occurred in the plateau phase of the dose-response curve, rather than in the raising phase.
- There was not a minimum of 2 data points located higher than the intersect.

We tested the impact of six signalling molecules on antigen discrimination. In a similar approach as to sensitivity measure, we studied some molecules proximal to the TCR (Lck and PLCγ1). We also tested effectors involved in the different divergent signalling pathways: PI3K and PKCθ from the NFκB signalling cascade, MEK involved in the AP-1 pathway and Calcineurin, a direct regulator of the NFAT transcription factor (figure 14 and appendix figure 40).

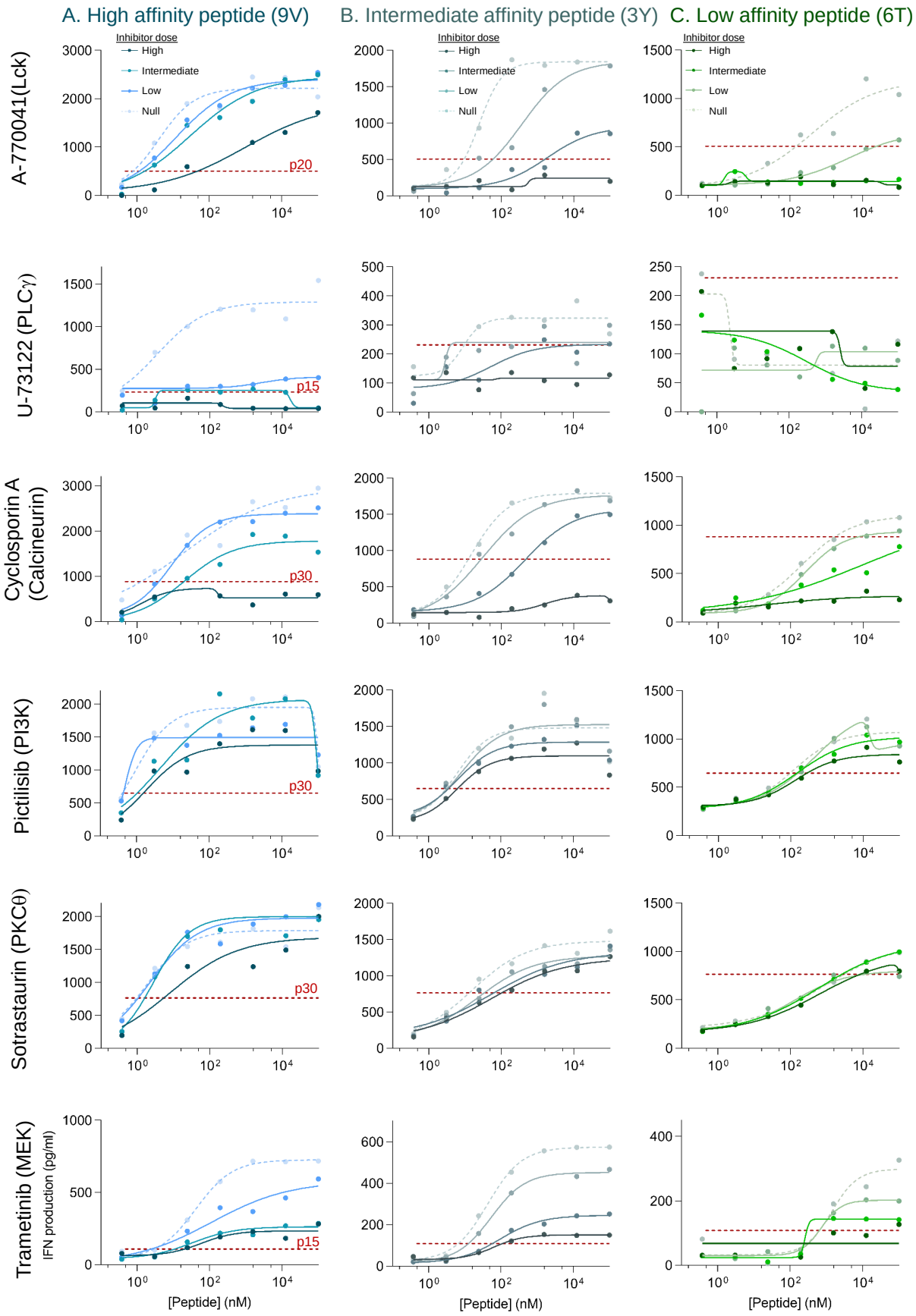


Figure 14: Impact of inhibition of signalling molecules on T cell discrimination. Production of IFNγ upon stimulation of 1G4$^+$ T cells on APC pulsed with peptides of high (A. column), intermediate (B. column) and low (C. column) affinities upon inhibitor treatment (one representative donor).

As actin demonstrated a role in T cell sensitivity, we investigated a potential role in the ability of T cells to discriminate between antigens. We made use of small-molecule inhibitors against the proximal regulator Nck and its substrate the Arp2/3 complex, but we also tested the impact of a direct inhibition of actin polymerisation by actin monomer sequestration (figure 15).

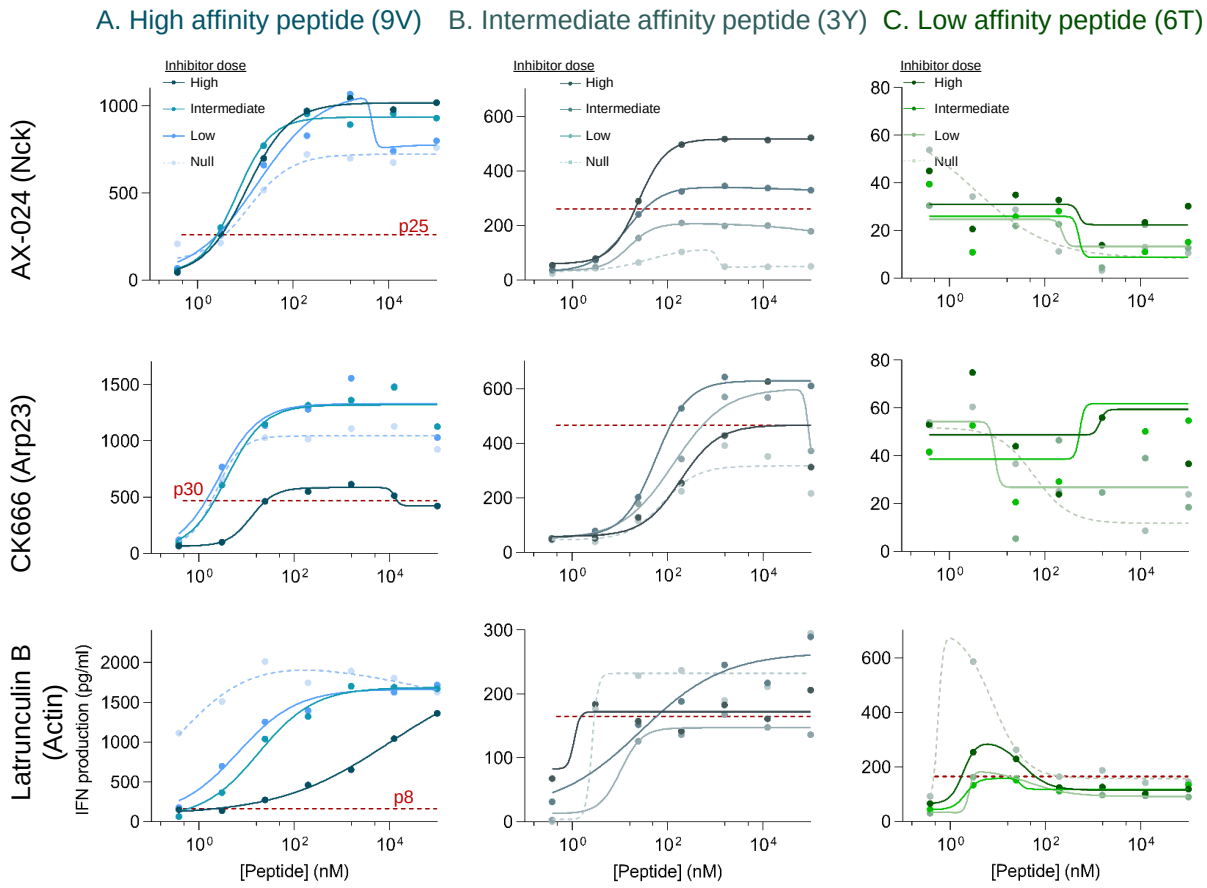


Figure 15: Impact of inhibition of actin-modulatory molecules on T cell discrimination. Production of IFNγ upon stimulation of 1G4$^+$ T cells on APC pulsed with peptides of high (A. column), intermediate (B. column) and low (C. column) affinities upon inhibitor treatment (one representative donor).

From the value of antigen sensitivity we extracted from the dose-response graphs, we we plotted the logarithm of the sensitivity against the logarithm of the dissociation constant (K_D) of each antigen. We often observed a linear relationship between these variables (on logarithmic axes) and the slope of this line has previously been termed the discrimination power and used as a quantitative measure of discrimination [115]. A larger slope corresponds to a higher discriminatory power. These data present some significant slopes variations when compared between different donors and different inhibitors. However, this data representation allows a comparison of the discriminatory power within each donor and inhibitor.

Inhibition of Lck alone induced a change in the slope of the discrimination lines, for both outputs tested (figure 16 and appendix figures 41 and 42). All other molecules tested presented lines with identical slopes (parallel lines) upon increasing doses of inhibitor.

In the case of molecules involved in the actin regulatory pathway, the data we obtained were insufficient to proceed to further analysis. Indeed while a given dose of inhibitor exerts a weak to small effect on high activation, they completely abrogated activation on weak stimulus. We hoped that our titration approach would offer us a panel of doses broad enough for a successful interrogation; however, this was still insufficient in the case of these very responsive molecules. This illustrates the challenge of working with highly sensitive molecules.

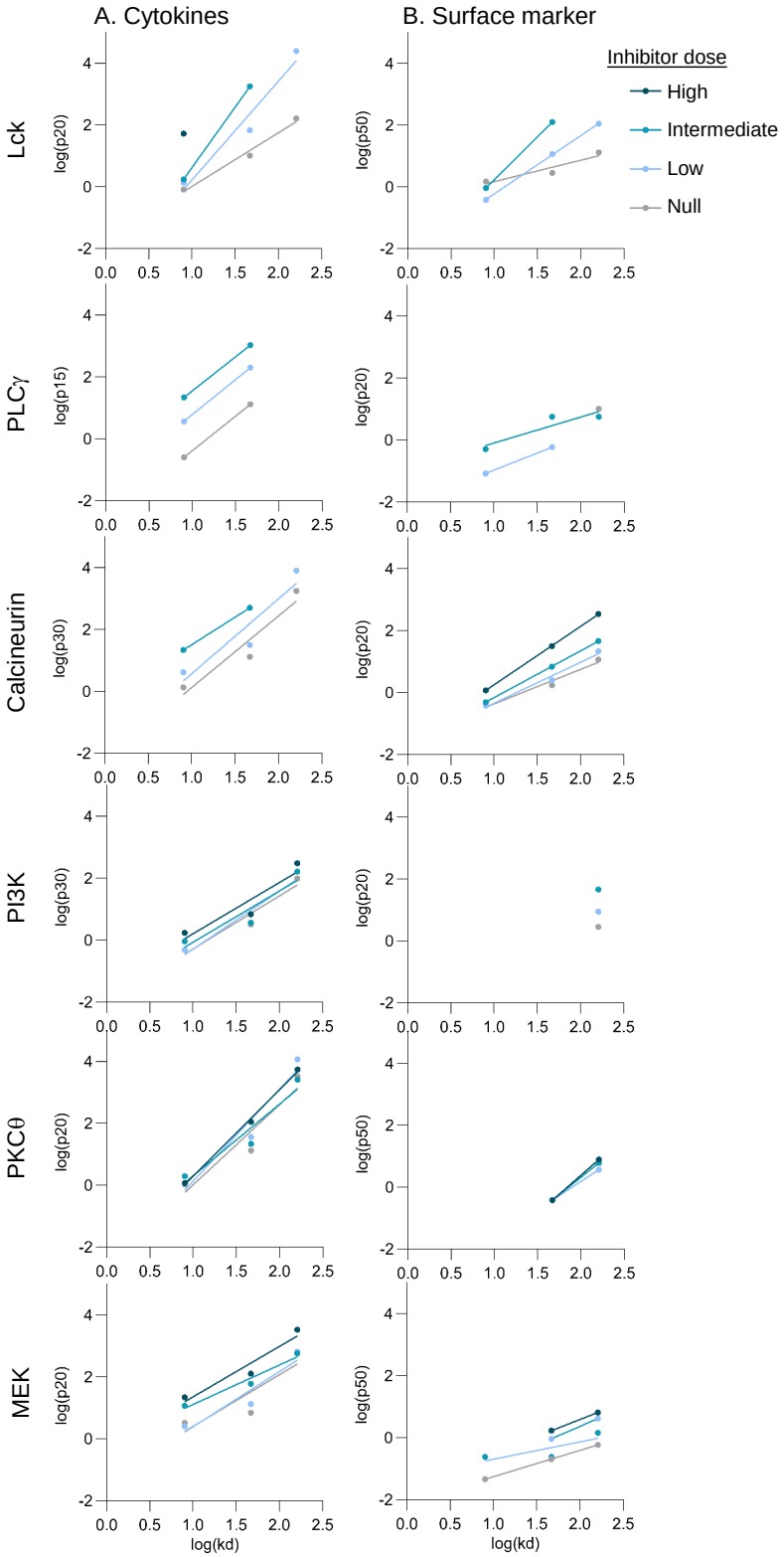


Figure 16: Impact of titrating doses of inhibitor on the T cell discriminatory power. Potency is defined as the dose of ligand required to reach 15% (p15) to 50% (p50) of activation measured by cytokines secretion (A. column) and surface marker upregulation (B. column). Potency is plotted against peptide affinity and a simple linear regression is fitted to the points. When expressing log of potency vs log of affinity, the slope of the line correspond to the discriminatory power. This representation allows the study of the impact of increasing inhibitor doses on the discrimination power (One representative donor per inhibitor).

The variations we observed between donors does not allow direct comparison of slopes values across donors. However, when the change in slopes is compared to the slopes of the untreated data, the impact of individual molecules can be evaluated across inhibitors and donors. Across both outputs (cytokine secretion and surface marker expression), Lck is the only molecule to impact the discriminatory power of T cells (figure 17).

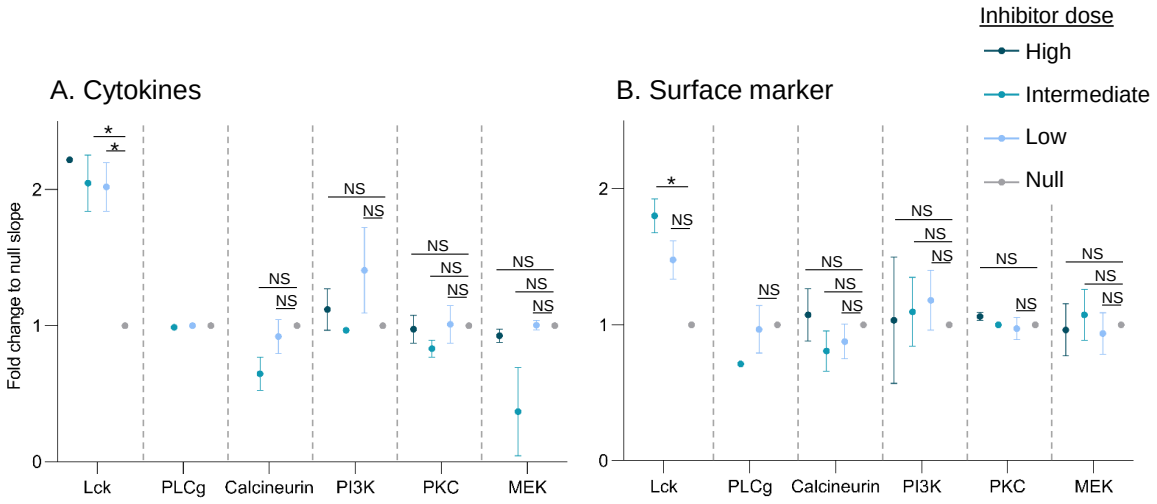


Figure 17: Lck controls T cell antigen discrimination. Discriminatory power is calculated from the slopes of the lines extracted from the (potency) vs (KD) graphs in figure 16) and in appendix figures 41 and 42. The impact of increasing doses of inhibitor is measured by calculating the fold change of the inhibitor-treated slopes versus no-inhibitor lines. The fold change of each inhibitor dose was compared to the null inhibitor-dose slope by unpaired t-test (NS (Not Significant) p = >0.05, * = p ≤ 0.05.). Data presented satisfied the non exclusion criteria of figure 16, error bars = SEM, for n= 2 or 3

2.3 Discussion

We made the choice of a phenotypic model to predict the impact of modulation of signalling effectors on the T cell output, the disadvantage of this model is that it does not offer a detailed view of each signalling effector and each intermediate interaction. The threshold switch for example is a parameter that could comprise one or several molecules and their interactions. However, it is sufficient to answer our question and decipher if a signalling molecule is involved in T cell sensitivity or not. And the minimal number of parameters allows us to calibrate the few free parameters to experimental data. This allows quick and easy prediction and experimental validations.

We used two different experimental set ups for our systematic study (plate-based assay and co-culture-

based assay) and could reproduce our observations in both. They led us to the same conclusion from a qualitative point of view: Lck is involved in T cell sensitivity; however, we observed quantitative differences between the systems. The EC50 shift induced by the inhibition of Lck is greater in our plate based assay. Several factors can explain this exacerbated effect on plate. The plate system is a minimalist environment displaying only chosen molecules on a flat, immobile surface. *In vivo*, however, the interaction between T cells and APCs is a event involving multiple accessory receptors ensuring increased adhesion for example. The interaction of the CD2 adhesion receptor with its ligand CD58 have been shown to play a key role in antigen sensitivity by improving TCR-pMHC interaction [128]. In our plate system, CD58 is immobile on the plate and can not be recruited to the vicinity of the TCR-pMHC interaction [211]. Moreover, the U87 cell line expresses several adhesive ligands while only CD58 is present on the plate. U87 cells expresses several ligands for LFA-1, another essential adhesion receptor (human protein atlas)[128]. Our plate system artificially increases the phenotype of Lck as, in this set up, the sensitivity process is restricted to TCR-activated pathways; our co-culture system allows a more physiological set up to evaluate the involvement of signalling molecules with inputs from accessory pathways. However, both system proved robust to identify sensitivity-involved or independent molecules.

Our approach allowed us to show that proximal signalling molecules play a role in antigen sensitivity and discrimination, while downstream effectors only impact the amplitude of the response. We observed that Lck and PLCγ1 were involved in antigen sensitivity while Lck alone was involved in antigen discrimination. This is in agreement with the work of several groups. Manz *et al.* [134] proposed that Lck was involved in antigen sensitivity and discrimination by modulating its regulator, Csk. However, their conclusion relied on indirect modulation of Lck. Lo *et al.* [137] proposed that the slow phopshorylation of LAT Y132 is a key step of T cell discrimination, and the last step allowing discrimination before the dissociation of the TCR complex. This is in close agreement with our data demonstrating the involvement of Lck but not PLCγ1, which is directly downstream of LAT activation. However, both Lo and our studies lack informative data about ZAP70, the intermediate effector located downstream of the TCR but upstream of LAT. Validation of its involvement in antigen sensitivity and discrimination would be interesting, but the lack of specific inhibitor makes its study challenging. As mentioned above, the Weiss lab developed an analogue mutant of ZAP70 that is targetable by a small-molecule inhibitor. However,

their work is restricted to the Jurkat T cell line, they never performed systematic studies in primary T cells with variation of peptide concentrations and affinities. Therefore their data does not allow us to conclude about the involvement of ZAP70 in antigen sensitivity and discrimination [212]. Britain and Weiner performed interesting research on ZAP70 using an optogenic-based CAR system. Their light-controlled system allowing a fine control of binding half-life of the CAR to its ligand. They demonstrated that ZAP70 recruitment correlates with ligand binding half-life, indicating that ZAP70 presents an analogue behaviour and would therefore be located before the switch and involved in antigen sensitivity [187]. However, they did not vary the concentrations or affinity of the ligand, so their study is insufficient to evaluate the involvement of ZAP70 in antigen discrimination.

Our system showed no evidence of involvement of signalling effectors located after PLCγ1. However, downstream effectors such as Erk and Calcineurin have been proposed to play direct feedback role on proximal molecules. The kinase Erk - downstream of the MAPK chain of phosphorylation - was proposed to play a central role in T cell activation by protecting Lck from SHP1 dephosphorylation [52]. In our system, we could show that MEK, located just upstream of Erk, does not impact antigen sensitivity. This is in agreement with Paster *et al.* [154] who showed that preventing binding of Erk to Lck through a mutation of Erk phosphorylation site on Lck (S59A) in mice, does not decrease T cell sensitivity, but rather slightly improves it. Dutta *at al.* suggest that Calcineurin affect sensitivity by regulating LFA-1 activation and therefore the ability of T cells to form cell/cell contact. In our hands, inhibition of Calcineurin does not impact T cell sensitivity, however, the experimental systems and timing we used differ from the ones chosen by Dutta *et al.* [50]. We will address these caveats in chapter 3.

Inhibition of actin polymerisation through the use of the Latrunculin B and Cytochalasin D inhibitors impacted T cell antigen sensitivity. However inhibiting the early molecules involved in the actin remodelling pathway, Nck and Arp2/3, respectively enhanced and did not affect T cell antigen sensitivity. The surprising results obtained with the AX-024 (Nck inhibitor) molecule will be discussed in chapter 3. The lack of effect of CK666 (Arp2/3 inhibitor) could be explained by redundancy in the pathway or insufficient inhibitor concentrations. In addition to the Arp2/3 complex, formins and tandem-monomer binding nucleators can also remodel actin [213], and actin-modulatory proteins such as cofilins can be

regulated by accessory receptors, independently from TCR signalling [214]. However Arp2/3 is the only molecule responsible for branched polymerisation of actin filaments. Because of this essential role however, the choice of inhibitor dose concentration was challenging. Indeed a concentration of 500μM induced a complete abrogation of cytokine production and surface markers upregulation (appendix figure 37). We decided to use a maximal concentration of 200μM to allow the generation of a dose-response curve, however this concentration only induces a 50% decrease of the E_{max} compared to the untreated sample, this relatively weak inhibition may prevent us from observing the impact on the EC50 with higher inhibitor concentrations.

In this study, we made the choice of a systematic approach using chemical inhibitors; they come with advantages compared to alternative modulation strategies such as genetic modification, but also limitations.

In the context of primary cells, genetic modifications are challenging as cells only have a short lifespan *in vitro*. In addition, when implementing genetic modifications that require selection and time to be effective, cells are at risk of adapting and developing compensatory mechanisms. Chemical inhibitors allow instant modifications and therefore reduce the risk of adaptation, especially since we only treated our T cells for short times (5-7h). Another advantage of small-molecule inhibitors is that it allows us to work with titration of the inhibition. This allows us to observe a systematic trend relative to a baseline; which is past the scope of a binary comparison of one dose to a control often performed in the literature [215].

The main limitations of small-molecule inhibitors are their specificity, appropriate dosage and toxicity.

The lack of specificity and therefore the risk of off-target effect is a concern when using commercial small-molecule inhibitors. We researched the literature before making our choices.

Several specific Lck inhibitors are available as inhibition of Lck is commonly performed *in vivo*, in the context of many anti-rejection strategies and anti-leukemia therapies [216]. In this study, we used the

molecule A-770041 which functions by blocking the ATP-binding site of Lck [198]. A-770041 is known to also target the Lyn, Src and Fyn kinases, however its affinity for Lck is respectively 8-fold, 60-fold and 300-fold superior to theirs [198] and Lyn and Scr are only expressed at very low level in $CD8^+$ T cells. As validation, Zepecki *and al.* used this inhibitor at similar doses as ours and observed no modification in the phosphorylation of these 3 kinases; however their data were obtained in human glioma cells [217].

The U73122 inhibitor we used against PLC also inhibits Phospholipase D (PLD) [202] and affect 5-lipoxygenase (5-LOX) [218]. However inhibition of 5-LOX should not have an impact in T cells as its metabolite is not present in T cells [219]. PLD1 and 2 are expressed in T cells where they play a similar role to PLCγ. They are involved in lipid metabolism, producing phosphatidic acid (PA) from phosphatidylcholine. PA can then be converted into DAG [220] therefore generating the same product as PLCγ and integrating at the same point in the signalling cascade. In line with this hypothesis, PLD deficiency does not affect early T cell signalling as calcium flux is unaffected [220]. U-73122 is a pan phospholipase C inhibitor, therefore it doesn't only affect PLCγ, but also other members of the phospholipase C family. In conclusion, this inhibitor therefore does not offer good specificity, but its alternative targets have redundant roles to PLCγ so the main risk posed by this lack of specificity is a dilution of the effect observed.

The Cyclosporin A inhibitor we used against Calcineurin is a well-characterised and widely used inhibitor. It only has 2 alternative targets identified: the cytochrome P450-3A4 [221], involved in drugs and toxins clearance but it is not expressed in T cells; and the P-glycoprotein, involved in multidrug resistance but it is only expressed at very low level in T cells and does not play any known role [222].

The Pictilisib inhibitor we used against PI3K is specific for the PI3 kinase but targets all of its 4 isoforms with higher affinities for the alpha and gamma isoforms (MedChem).

The Sotrastaurin inhibitor used to inhibit PKCθ is specific for the protein kinase C; but inhibits all the members of the PKC family [223]. However PKCη - the only other PKC expressed as similar level as PKCθ in T cells - is 10-fold less sensitive to the inhibitor (Human Protein Atlas). The role of PKCη

is however poorly characterised in $CD8^+$ T cells.

The Trametinib inhibitor we used against MEK is highly specific for the MEK1/2 heterodimer. Its specificity has been validated against a panel of 180 kinases including its closest homologue MEK5 [204][205].

The rapamycin inhibitor we used against mTorc is highly specific. This specificity is due to the unique interaction of rapamycin with the FRB domain of mTorc. This interaction prevents mTorc interaction with phosphatidic acid and therefore the formation of the mTorc1 complex [185].

Regarding the inhibitor of the actin regulatory pathway, we mainly used broadly validated inhibitors, with the exception of the AX-024 inhibitor we used against Nck which is still a matter of debate. Borroto *et al.* [207] described this small-molecule as a specific inhibitor of Nck. They argue that it has the ability to decrease T cell proliferation and TCR-proximal signalling events, therefore they recommend its use in the context of autoimmune disease. However, subsequent studies of the molecule were unable to confirm its binding to Nck, through SPR or NMR, or to reproduce its inhibitory effects on T cell functions [208]. Given this state of controversy, we will characterise the effects of this molecule further in chapter 3. The CK666 inhibitor we used against the Arp2/3 complex is a specific inhibitor of Arp2/3, which blocks Arp2/3 movement and therefore prevents conformational change into the active form of the complex. Its only known binding target is the Arp23 complex, with different affinities depending on the conformation of the complex [224]. The Latrunculin B inhibitor specifically binds actin monomers with a 1:1 stoichiometry, preventing the incorporation of the monomer blocks into actin polymers [225]. The Cytochalasin D inhibitor we used against actin monomers and polymers is able to bind glomerular actin, but also to the barbed end of actin polymers, preventing polymerisation [226].

Actin regulation plays a key role in many T cell effector functions, including T cell division and proliferation, formation of lamellipodia and filopodia allowing T cell migration and sensing of their environment, T cells formation of contacts with their target cells. Its inhibition has therefore broader implications that signalling inhibition. In our experimental system, neither cell division is relevant as

the experiment is carried over short time points (5h), nor cell migration, as T cells are spun down to facilitate interaction with APCs in high ratio (1:1). Therefore, we hypothesise that inhibition of actin polymerisation through treatment with agents such as Cytochalasin D and Latrunculin B will mainly impact the ability of T cells to establish stable conjugates with their target APC, as described by Rivas *et al.* [227]. We also envision signalling to be perturbed from the first steps, as Cytochalasin D has been showed to prevent formation of functional microclusters and recruitment of Lck to the TCR-CD3 complexes [156][228].

We also made sure to work within the concentration regimen in which the specificity of these small chemical inhibitors have been described and employed in the literature [229][217][202][230] [231][232][233][207][208][157][227 We based our top concentration to be within 10-fold of the concentration value previously described when this information was available for T cell treatment *in vitro*, alternatively, the concentrations were inferred from other cell types. As only exception, as discussed below in this section, the Arp2/3 inhibitor had to be used at lower concentrations than described in the literature [234].

The specificity limitation not only applies to the T cells but also to the U87 cells we used as APCs. As the small-molecule inhibitors we used are present in the culture media for the whole duration of the co-culture (4 to 6h), they could affect signalling molecules in the U87 antigen presenting cells. We attempted to control for effect of the inhibitors on immediate activation events by pre-treated the T cells, but not the APCs, with the inhibitor for one hour, before starting the co-culture. This pre-treatment allows the small chemical inhibitors to reach their target molecules and induce their inhibition before the TCR-mediated activation of these molecules. In the case of the APC, the addition of the inhibitor coincide with the start of the co-culture, limiting the impact of the inhibitor on the early stages of activation. There is very little information available about the half-life of small molecule inhibitors when used *in vitro* and it is difficult to infer it from *in vivo* data as the metabolization processes vary. However, it is reasonable to assume that after pre-treatment of the T cells, the concentration of inhibitor added in the culture media, to the APC, will be lower than the starting concentration. We have to keep in mind still that this remaining concentration can impact the APC, as Wojewodzka reports decreased expression of the integrin CD49d on the dendritic cells they use as APCs following treatment with cyclosporin A [235].

A strength of our approach is the consistency of the results we obtained on the APCs and on the plate systems, indicating that the potential impact of the drug on the APC is insufficient to affect the impact on T cell functions. However, not all results were reproduced in both systems; it might be interesting to extend the scope of the molecule inhibition tested on plate.

The use of small chemical molecule inhibitors comes with the challenge of appropriate dosage. The main challenge we encountered was the broad range of effects a given dose of inhibitor induces in different donors. Each of our experiments were repeated in three different biological donors. This approach strengthen our conclusions as we observed similar qualitative impact on the EC50 of the dose-response curves for all donors. However, the biological variability we observed between donors was too large to allow generalization of the data from a quantitative point of view.
Another challenge we described above was the identification of an appropriate window of doses that allowed us the production of titrating dose-response curve without reaching toxicity. From two extremes of the spectrum, high concentrations of rapamycin (mTorc inhibitor) only allowed a small impact on the amplitude of the response, while small concentrations of CK666 (Arp23 inhibitor) had dramatic impact on T cell response.

Another limitations of small-molecule inhibitors and their dosage is cell toxicity. With this in mind, we have included viability staining to assess cell survival at the end of our assays. Most inhibitors have very little impact on viability, as over 90% of the T cells are still healthy at the end of the functional assays. The only inhibitor inducing concerning level of cell death is the U-73122 inhibitor against PLCγ. At concentrations above 2.5μM, the inhibitor induces 95% cell death within 5h of treatment. Therefore, we used a maximum dose of 1.5μM, which ensures that a minimum of 60% of cells are viable (figure 43). We also performed the analysis on the cells alive at the end of the experiment only.

Chapter 3

Application of the system to intracellular molecules

3 Application of the system to intracellular molecules

3.1 Introduction

In the previous chapter, we have established an experimental assay to identify whether a given T cell signalling molecule impacts antigen sensitivity and/or discrimination. We showed that molecules whose inhibition induced a change in the antigen concentration required to achieve a given response (e.g. EC50) are involved in the peptide antigen sensitivity property of T cells. We showed that molecules integrating proximally to the TCR, such as Lck and PLCγ1, are controlling the antigen sensitivity process of T cells, whereas molecules previously established to be distal to the TCR did not control antigen sensitivity.

However, recent studies have provided evidence that several of these TCR distal molecules, including Calcineurin [50], Nck [207] and SHP1 [52], play a feedback role by directly modifying the TCR or TCR-proximal molecules. This raises the question of whether these distal molecules may impact T cell sensitivity and/or discrimination.

3.1.1 Calcineurin

Calcineurin is a serine/threonine phosphatase. In T cells, it is mainly known to play a role in the calcium-signalling cascade. Upon activating phosphorylation by Calmodulin [236], Calcineurin is responsible for dephosphorylation of NFAT molecules, allowing them to migrate into the nucleus where they regulate gene expression [237][48].

In their 2017 paper, Dutta *et al.* [50] proposed another, unexpected role for Calcineurin. They proposed that while a pool of Calcineurin is responsible for the well-characterised dephosphorylation of NFAT molecules, another pool of Calcineurin molecules exerts a positive impact on TCR proximal events. They suggested that Calcineurin is recruited to the TCR as it is co-immunoprecipitated with CD247 (the CD3 zeta chain of the TCR) upon TCR activation. This recruitment leads to dephosphorylation of Lck on its inhibitory serine 59 (s59) resulting in an increase in Lck activity. The use of Cyclosporin A (Calcineurin inhibitor) prevented Calcineurin-mediated dephosphorylation of Lck s59, which led to a decrease in phosphorylation of ZAP70, LAT, SLP76. It also reduced phosphorylation of the intracellular tail of

LFA-1 which is responsible for the conformational change of its extracellular domain, enhancing binding to ICAM-1. On the one hand, the lower phosphorylation of signalling molecules can directly lower T cell activation. On the other hand, the lower phosphorylation of LFA-1 can reduce the ability of T cells to sustain adhesion to target cells and, in this way, reduce the duration of TCR/pMHC interactions, which in turn reduces T cell activation [50].

Taken together, the work of Dutta *et al.* [50] suggests that Calcineurin, which was long considered a TCR distal molecule, has an important TCR-proximal role involving regulation of TCR-proximal signalling and T cell adhesion via LFA-1. However, Zeyda *et al.* [230] studied the impact of Cyclosporin A on the formation of the immune synapse (IS) and recruitment of its essential actors. They showed that while TCR translocation to the IS was reduced by Cyclosporin A, this inhibitor induced minimal impact on LFA-1 recruitment and did not affect T cell/APC conjugate formation [230]. Similarly, using canine T cells, Wojewodzka *et al.* showed that treatment with Cyclosporin A did not affect conjugates formation. They report however, a negative impact on the expression of another integrin, CD49d, on both T cells and APC (Dentritic Cells) [235].

3.1.2 Nck

Nck is well characterised as an adapter molecule involved in TCR-mediated actin remodelling, as discussed in section 1.4.2 [238][239], but Nck is also proposed to interact directly with the CD3 epsilon chain of the TCR [34].

Nck is a cytosolic adaptor, containing 3 SH3 domains and a SH2 domain. Upon activation, the TCR conformational change theory proposes that the proline-rich sequence (PRS) of the cytoplasmic tail of the TCR CD3epsilon chain become exposed and forms a binding site for Nck, through its SH3.1 domain. The role that Nck plays upon this binding is still not elucidated but it is suggested to impact interaction with target APCs, maturation of the immunological synapse and cytokine secretion [34].

Because of this suggested proximal role, Nck represents an interesting target for inhibition of TCR-

induced signalling. Specifically, it has been proposed that inhibition of Nck may allow T cells to continue recognising higher-affinity foreign antigens whilst reducing T cell responses to lower-affinity antigens [207]. This can be particularly useful in the context of autoimmune diseases where therapies are sought that limit T cells responses to self-antigens without impacting their ability to recognise higher-affinity pathogenic antigens (i.e. without leaving patients immuno-compromised).

Borroto *et al.* [207] propose to target the immediate TCR signal by inhibiting the interaction between the protein Nck and the TCR chains. In order to prevent Nck binding, Borroto *et al.* [207] developed a small chemical compound with a high affinity for the Nck-binding pocket. This compound - called AX-024 - is proposed to act by competition, docking into the binding cavity of the SH3.1 domain of Nck. That inhibition results in inhibition of ZAP70 phosphorylation (Y319) and cytokines production by T cells. However, it doesn't affect TCR-independent housekeeping processes or downstream signalling as it leaves T cells proliferation and activation by IL2 or Phorbol Myristate Acetate (PMA)-Ionomycin unaffected [207]. In mice, prophylactic administration of AX-024 is effective against autoimmune pathologies such as induced psoriasis, asthma and experimental autoimmune encephalitis, but does not prevent effective memory response against a pathogen (Ectromelia virus) [207].
The central role of the Nck - CD3 interaction is however questioned by Richer *et al.* [208], as they show that Jurkats lacking the Nck binding sequence on the CD3 chains do not display functional impairments (normal level of proliferation and ZAP70 phosphorylation). Moreover, they could not detect interaction between the AX-024 molecule and Nck-SH3.1 domain through NMR or SPR measurements. They suggest therefore that AX-024 exerts its effect on T cell functions independently from interaction with Nck, and that its target(s) remain unknown.

3.1.3 SHP1

SHP1, or PTPN6, is a tyrosine phosphatase described as playing a key regulatory role in T cells. This function is suggested because its knock-out in murine T cell results in hyper-proliferation, enhanced cytokine production and increased phosphorylation and activation of signalling effectors [240]. SHP1 is also proposed to be the main mediator of the inhibitory function of the receptor BTLA [241] and mediate PD-1 inhibition to some extend [242]. As these inhibitory receptors are targets for immunotherapy, iden-

tification of its inhibitory pathway and targets is essential. Although several studies have suggested that TCR signalling can regulate the activity of SHP1 through feedback mechanisms (i.e. without invoking inhibitory receptors) using biochemical assays, functional data demonstrating this regulation is still missing.

Lorenz *et al.* [240] suggested that phosphorylation of the kinases Lck and Fyn is controlled by SHP1 as SHP1 KO mice show increased phosphorylation and activation of the kinases. In line with these observations, Stefanova *et al.* proposed a negative feedback mechanism in which SHP1 is recruited to Lck to mediate its inactivating dephosphorylation (as described in 1.4). Plas *et al.* [243] proposed that ZAP70 is directly regulated by SHP1 as co-expression of the two proteins in HeLa cells induces dephosphorylation of ZAP70. Brockdorff *et al.* [244] also proposed ZAP70 as a SHP1 target because they observed reduced ZAP70 phosphorylation in Jurkat cells expressing a constitutively active form of SHP1. Binstadt suggested SLP-76 as a SHP1 target as they identify it by binding assay.

Collectively, data suggesting an impact of SHP1 on all these TCR signalling effectors rely on inference [240] , immunoprecipitation [245][246], pull-downs [243][246][52] or phosphorylation assays *in vitro* [246] or in non-lymphoid cells [247][243]. Therefore, assessment of the impact of TCR signalling-induced SHP1 activity directly on T cell functional responses has yet to be established.

3.2 Results

To resolve the controversy surrounding these important T cell signalling molecules, we performed a detailed analysis of how the activity of Calcineurin, Nck and SHP1 impact antigen sensitivity and discrimination based on quantitative functional T cell responses.

3.2.1 Inhibition of Calcineurin does not impact antigen sensitivity independent of ligation of LFA-1

In the previous chapter, we found that inhibition of Calcineurin did not impact antigen sensitivity when T cells recognise antigen on the U87 target cell line. However, we did not investigate whether LFA-1 activity was important in the context of this recognition. Therefore, it can be argued that when T cells

recognise antigen in the context where LFA-1 adhesion is important, inhibition of Calcineurin may impact antigen sensitivity. Therefore, we performed experiments to examine the role of Calcineurin in the presence and absence of LFA-1 ligation, by one of its ligand, ICAM-1.

As described previously, we isolated $CD8^+$ T cells from healthy donors and transduced them with the well-characterised 1G4 TCR. We pre-incubated T cells with different concentrations of the Calcineurin inhibitor for one hour after which T cells were activated for 4h on streptavidin plates, coated with purified 9V pMHC in presence or absence of a constant concentration of ICAM-1 (figure 18).

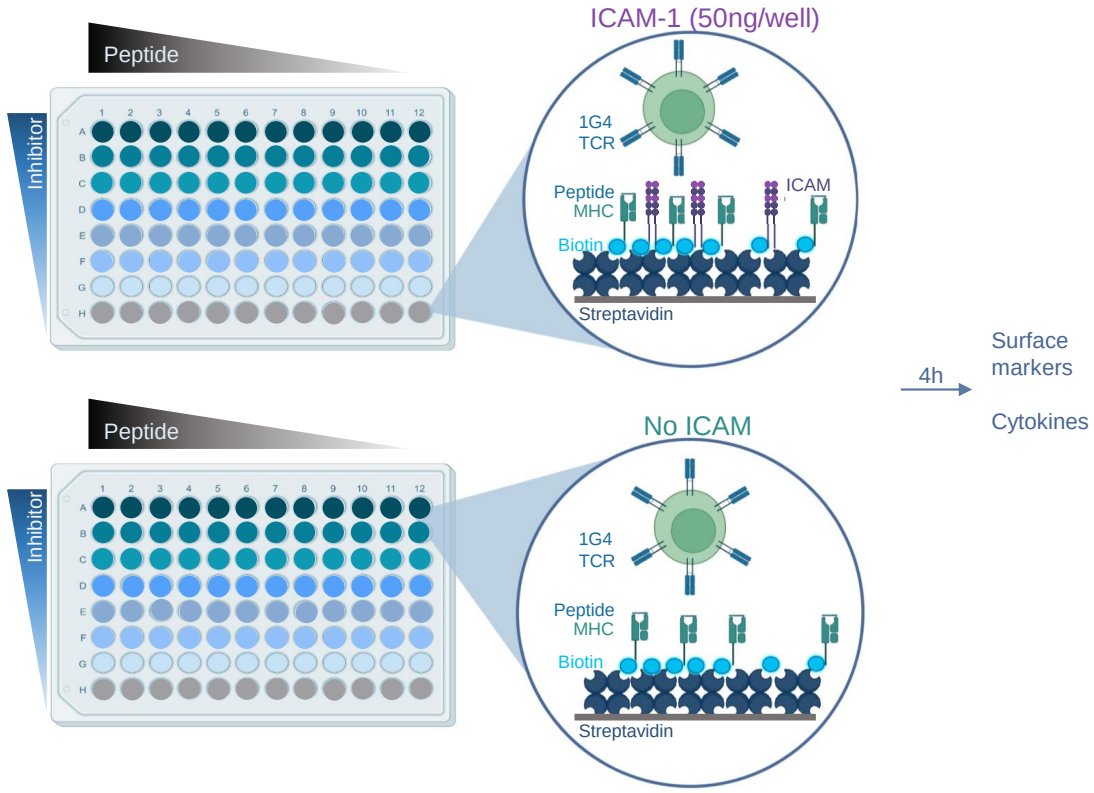


Figure 18: Experimental protocol for assessing the impact of small-molecule inhibition on antigen sensitivity to a titration of purified pMHC alone or in combination with purified ICAM-1. $1G4^+$ T cells are incubated with a titration of inhibitor for one hour followed by activation for 4h on streptavidin-coated plate presenting either purified 9V peptide on biotinylated MHC alone, or with a constant concentration of ICAM-1 (50ng/well) in presence of the inhibitor. The impact of inhibitor on T cell functions is studied by staining of T cell for activation markers and measure of cytokine secretion.

We hypothesised that if Calcineurin inhibition plays a central role on the ability of T cells to interact with APCs, titrating concentrations of Cyclosporin A (Calcineurin inhibitor) will decrease T cell binding ability; this should appear in our model as a proximal impact on k_{on} decreasing antigen sensitivity (figure 19 A). In the absence of ICAM-1, however, we expect inhibition of Calcineurin to play a role on NFAT

dephosphorylation alone. We have shown that this effect on k_{prod} in chapter 2 acts distally from the TCR kinetic proofreading cascade and does not affect T cell sensitivity.

The interaction of LFA-1 with its ligand, ICAM-1, on APCs increased the binding ability of T cells to their targets. We showed that we can reproduce the benefit of this interaction in our plate system, as the presence of purified ICAM-1 coated on the plate induced T cell response at lower pMHC concentrations compared to MHC alone (no ICAM-1) (figure 19 B). Therefore, ligation of LFA-1 by ICAM-1 increased antigen sensitivity as previously described. In our model, this can be reproduced by an increase in the k_{on} between TCR and pMHC.

In the presence of ICAM-1, increasing concentrations of Cyclosporin A (Calcineurin inhibitor) induced a decrease of the amplitude of the response (Emax) but did not change the concentration of peptide at which T cell response occurs (no shift of EC50) (figure 19 C-E and appendix figure 44 dataset 2 A-C and dataset 3 A-C). Therefore, the impact of inhibition of Calcineurin was the same in presence or absence of ICAM-1. As a control, inhibition of Lck in the presence of ICAM-1 in this system reproduced our previous observations; increasing concentrations of A-770041 (Lck inhibitor) induced an increase of the EC50 of the dose-response curves and a decrease of the amplitude of the response (E_{max}) (figure 19 F-H and appendix figure 44 dataset 2 D-F and dataset 3 D-F).

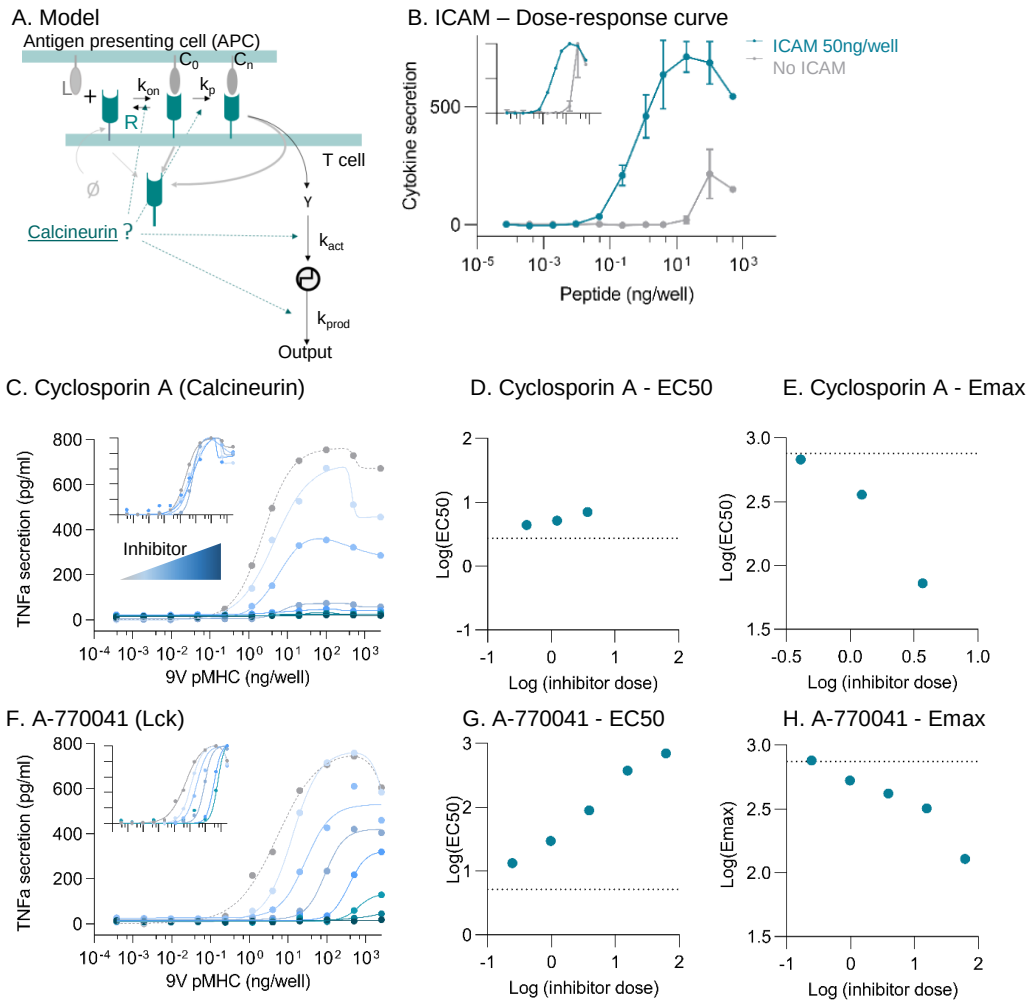


Figure 19: Lck, but not Calcineurin, controls the sensitivity of T cells to purified antigen in the presence of purified ICAM-1. A. Phenotypic model showing different possible integration points of Calcineurin in the signalling cascade. B. Impact of the presence of ICAM-1 on the plate on T cell response. C-H. Cytokine secretion upon stimulation of $1G4^+$ T cells on streptavidin-coated plate presenting a titration of 9V peptide on biotinylated MHC and a constant concentration of ICAM-1 (50ng/well) under increasing concentration of the inhibitors. C. Dose-response curves and their normalisation (inset graph) under titrating concentrations of Cyclosporin A (Calcineurin inhibitor), one representative donor from three independent repeats. D. Impact of titrating concentrations of Cyclosporin A on the EC50 of the curves. E. Impact of titrating concentrations of Cyclosporin A on the maximum of the curves (E_{max}). F. Dose-response curves and their normalisation (inset graph) under titrating concentrations of A-770041 (Lck inhibitor), one representative donor from three independent repeats. G. Impact of titrating concentrations of the A-770041 inhibitor on the EC50 of the curves. H. Impact of titrating concentrations of the A-770041 inhibitor on the maximum of the curves (E_{max}).
The EC50 and E_{max} values are extracted from sigmoid or bell-shaped curves (best fit) fitted to the raw data. The EC50 and E_{max} of the no inhibitor concentration are represented by the dotted lines.

In order to study the impact of the LFA-1 – ICAM-1 pair in a system that allows ligand mobility, we made use of the previously described U87 cell line as antigen presenting cells. We took advantage of the ICAM-1 knocked-out U87 cell line generated in the lab [128] (figure 21 B) to compare T cell activation in presence and absence of ICAM-1 in a cellular-based system. $1G4^+$ transduced T cells were pre-incubated

for one hour with titrating concentrations of the Calcineurin inhibitor before co-culture with U87 WT or ICAM-1 knocked out for four hours (figure 20). T cell functions were measured by cytokine secretion and surface marker expression.

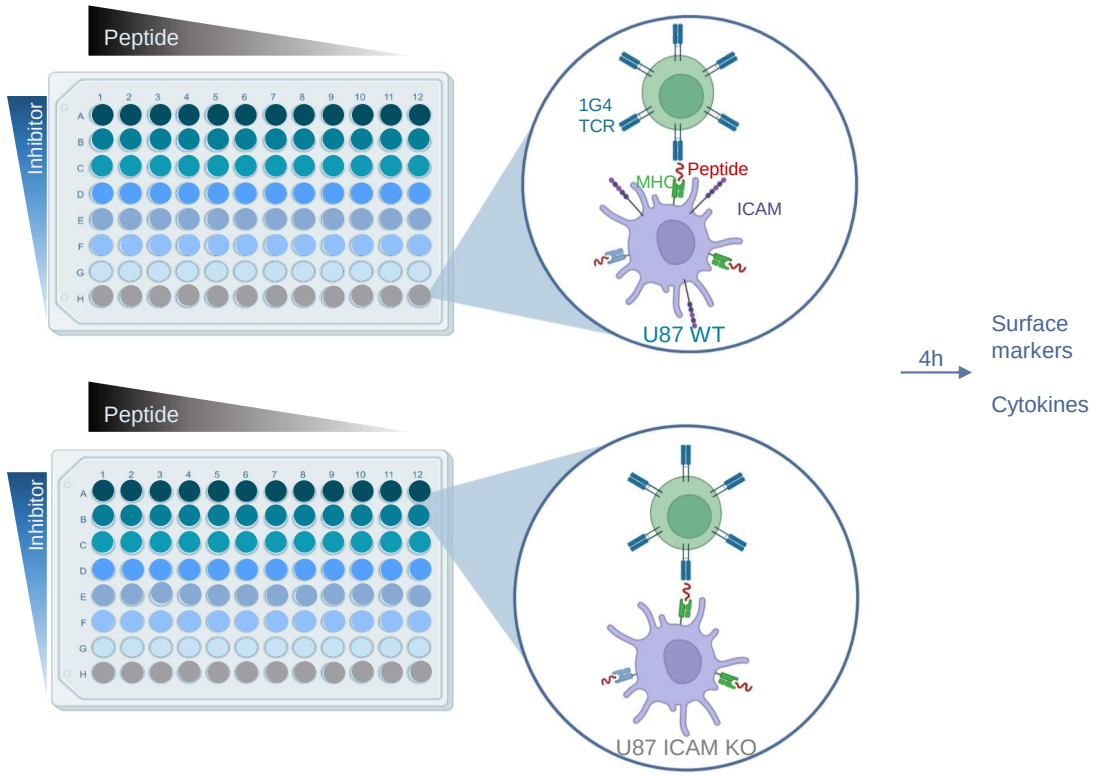


Figure 20: Experimental protocol for assessing the impact of small-molecule inhibition on antigen sensitivity to a titration of peptide on APCs with and without ICAM-1. $1G4^+$ T cells are incubated with a titration of inhibitor for one hour followed by activation for 4h by co-culture with U87 cells pulsed with the 9V peptide at titrating concentrations in presence of the inhibitor. T cells are co-cultured either with U87 WT cells expressing ICAM-1 on their surface or U87 cells in which ICAM-1 has been knocked-out. The impact of inhibitor on T cell functions is studied by staining of T cell for activation markers and measure of cytokine secretion.

Titrating concentrations of the Calcineurin inhibitor induced a decrease of the amplitude of the response (E_{max}) in presence or absence of the LFA-1 binding partner, ICAM-1 but did not change the peptide concentration at which T cells respond (figure 21 C-E and appendix figure 45 dataset 2 A-C, dataset 3 A-C). As a control, inhibition of the proximal molecule Lck reproduced our previous observations showing reduced antigen sensitivity in the wild-type and the ICAM-1 knockout U87 target cells (figure 21 F-H and appendix figure 45 dataset 2 D-F).

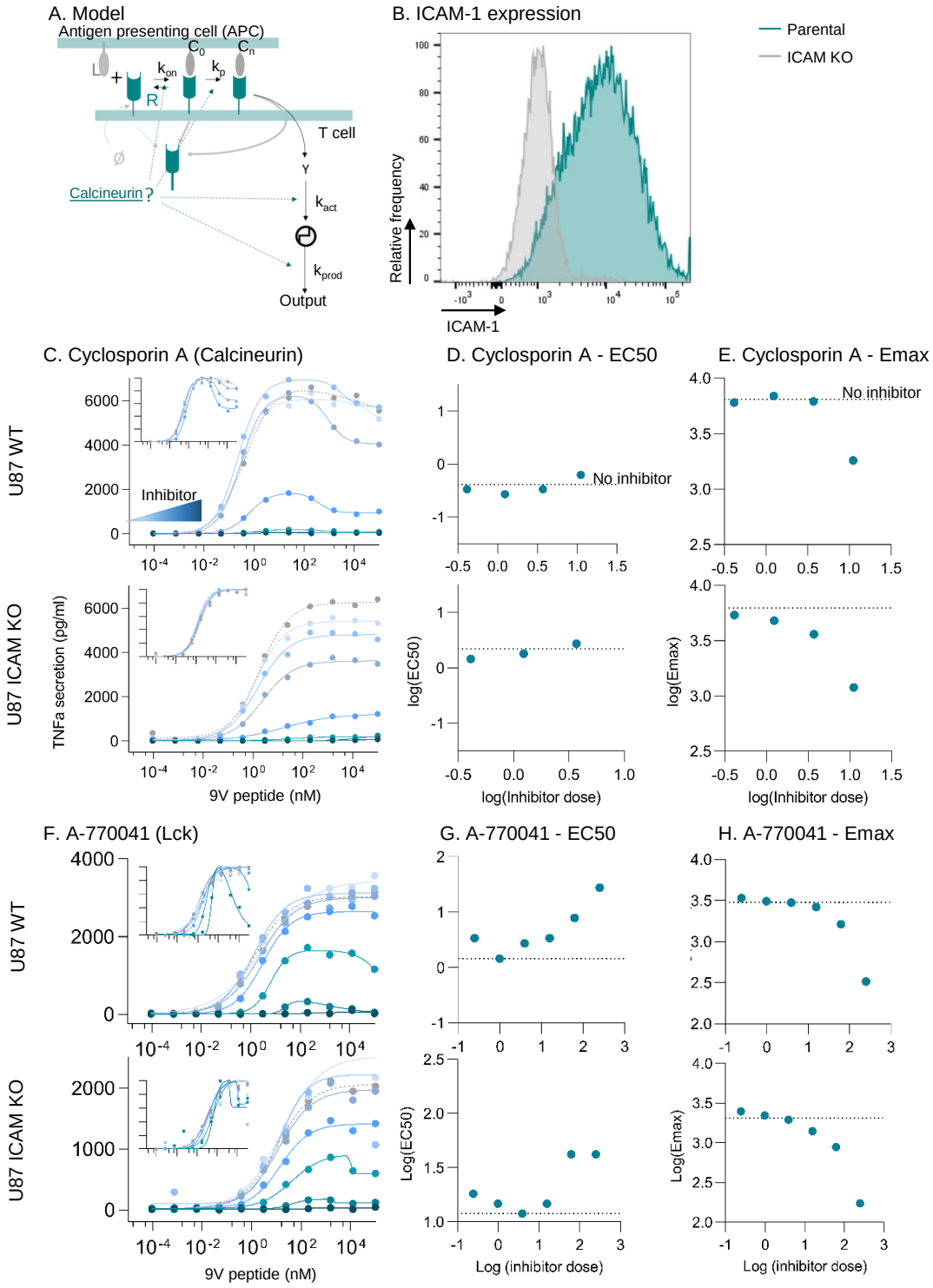


Figure 21: Lck, but not Calcineurin, controls the sensitivity of T cells to antigens on APCs presenting or no surface ICAM-1. A. Phenotypic model showing different possible integration points of Calcineurin in the signalling cascade. B. Validation of the knock-out of ICAM-1 on U87 cells. Knocked-out and characterisation have been performed by Johannes Pettmann. C. Dose-response curves and their normalisation (inset graph) under titrating concentrations of Cyclosporin A (Calcineurin inhibitor), one representative donor from three independent repeats. D. Impact of titrating concentrations of Cyclosporin A on the EC50 of the curves. E. Impact of titrating concentrations of Cyclosporin A on the maximum of the curves (E_{max}). F. Dose-response curves and their normalisation (inset graph) under titrating concentrations of A-770041 (Lck inhibitor), one representative donor from three independent repeats. G. Impact of titrating concentrations of the A-770041 inhibitor on the EC50 of the curves. H. Impact of titrating concentrations of the A-770041 inhibitor on the maximum of the curves (E_{max}). The EC50 and E_{max} values are extracted from sigmoid or bell-shaped curves (best fit) fitted to the raw data. The EC50 and E_{max} of the no inhibitor concentration are represented by the dotted lines.

The experiment was repeated across three independent donors and the average EC50 values revealed that inhibition of Calcineurin did not impact the EC50 whereas inhibition of Lck increased the EC50 (figure 22 A-B). There was no significant difference in the EC50 values between wild-type or ICAM-1 KO U87 cells. Therefore, we found no evidence that Calcineurin has a qualitatively different role in antigen sensitivity when the ligand for LFA-1 (ICAM-1) is presented.

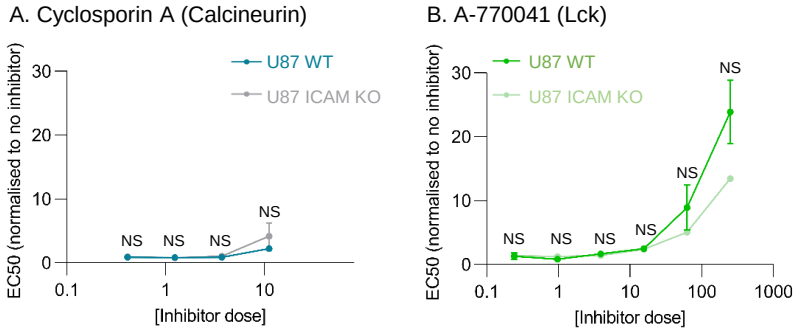


Figure 22: Lck, but not Calcineurin, impacts antigen sensitivity. A. Impact of increasing concentrations of Cyclosporin A (Calcineurin inhibitor) on the EC50s in presence and absence of ICAM-1 on the antigen presenting cell. B. Impact of increasing concentrations of A-770041 (Lck inhibitor) on the EC50s in presence and absence of ICAM-1 on the antigen presenting cells.
The EC50 values are extracted from sigmoid or bell-shaped curves fitted to the raw values as shown in figure 21 and normalised to the EC50 value of the no inhibitor concentration. Mean and SEM from 3 independent donors

3.2.2 The compound AX-024 increases T cell antigen sensitivity and decreases cytokine secretion

The data presented by Borroto *et al.* [207] implicate Nck at the very proximal stages of TCR signalling, by direct interaction with the CD3 chains. According to their hypothesis, the integration point of Nck in our model would occur within the kinetic proofreading stage, effectively modifying the proofreading rate constant (figure 23 A). In this scenario, a specific inhibitor of Nck would be predicted to increase the EC50 and decrease the E_{max} and hence have a similar phenotype to the inhibition of Lck.

As described above, we made use of $CD8^+$ T cells isolated from healthy donors and transduced with the 1G4 TCR. T cells were pre-incubated with titrating concentrations of AX-024 (Nck inhibitor) for one hour before co-culture for four hours with antigen presenting cells (U87 cell line) pulsed with titrating concentrations of the 9V peptide. We measured the T cells response by their ability to secrete TNFα and express the 4-1BB surface marker. Increasing concentrations of inhibitor had no effect on the magnitude

of the response for both outputs measured (figure 23 B-D and E-G). The lack of effect on the E_{max} suggests that the inhibitor does not affect the signalling cascade downstream of TCR and the effect on the EC50 is consistent with a TCR-proximal increase of the proofreading rate (k_p). AX-024 did not affect the EC50 of the dose-response curves, apart from one donor showing a shift to the left of the EC50 of the TNFα dose-response curves. This shift, resulting in lower EC50 values would indicate an increased sensitivity, however it was only observed in one donor and was not observed using other output measures such as surface marker (no impact on 4-1BB expression).

It is worth noting however that this experiment was performed with a high affinity peptide generating a strong stimulus. The lack of efficacy of the molecule under strong stimulus is in line with the data from Borroto *et al.* [207], therefore we set out to investigate its impact when using lower affinity peptides.

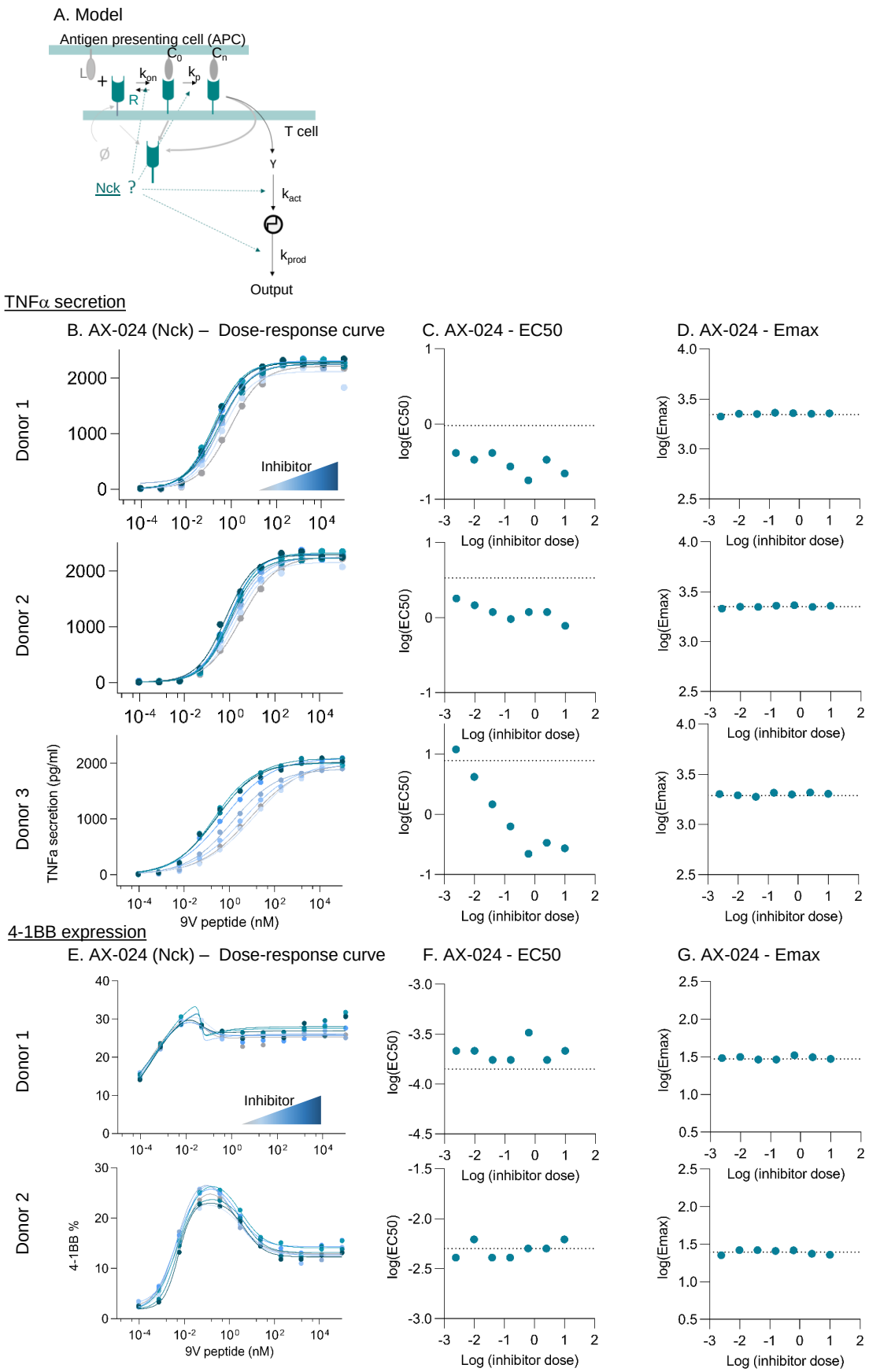

A. Model
Antigen presenting cell (APC)
L
R
T cell
Nck ?
Output
TNFα secretion
B. AX-024 (Nck) – Dose-response curve
C. AX-024 - EC50
D. AX-024 - Emax
Donor 1
Donor 2
Donor 3
Inhibitor
TNFa secretion (pg/ml)
9V peptide (nM)
log(EC50)
log(Emax)
Log (inhibitor dose)
4-1BB expression
E. AX-024 (Nck) – Dose-response curve
F. AX-024 - EC50
G. AX-024 - Emax
4-1BB %

Figure 23

Figure 23: Inhibition of Nck using the compound AX-024 increases antigen sensitivity. A. Phenotypic model showing different possible integration points of Nck in the signalling cascade. B. Dose-response curves showing cytokine secretion upon stimulation of $1G4^+$ T cells by U87 cells pulsed with the 9V peptide under increasing concentration of AX-024 (Nck inhibitor). TNFα in the media is measured by ELISA. C. Impact of titrating concentrations of the AX-024 molecule on the EC50 of the curves. D. Impact of titrating concentrations of the AX-024 molecule on the maximum of the curves (E_{max}). The EC50 and E_{max} values are extracted from sigmoid curves fitted to the raw data. The EC50 and E_{max} of the no inhibitor concentration are represented by the dotted lines. E. Dose-response curves showing 4-1BB expression upon stimulation of $1G4^+$ T cells by U87 cells pulsed with the 9V peptide under increasing concentration of AX-024 (Nck inhibitor). Surface marker expression is measured by flow cytometry. F. Impact of titrating concentrations of the AX-024 molecule on the EC50 of the curves. G. Impact of titrating concentrations of the AX-024 molecule on the maximum of the curves (E_{max}). The EC50 and E_{max} values are extracted from bell-shaped curves fitted to the raw data. The EC50 and E_{max} of the no inhibitor concentration are represented by the dotted lines.

We repeated the assay with intermediate (3Y, $K_D = 47\mu M$) and low (6T, $K_D = 162\mu M$) affinity peptides as described in 2.2.3. When stimulated by a titration of intermediate affinity peptide (3Y), AX-024 (Nck inhibitor) induced an increase in the T cell response (figure 24 A). In the context of low affinity peptide stimulation (6T), the inhibitor did not induce a clear impact on the magnitude of the response, but the measure is made challenging given the low amount of cytokine produced under such low affinity stimulus (figure 24 A and appendix figures 46 A and 47 A). In intermediate and low affinity context, the concentration of AX-024 did not affect antigen sensitivity (as highlighted by inset graphs in figure 24 A and appendix figures 46 A and 47 A). Given that part of the function of Nck is to regulate actin polymerisation, we sought to determine whether inhibition of this pathway using other well-established inhibitors would produce a similar phenotype. Interestingly, inhibition of the actin branching protein Arp2/3 using CK666 produced a similar phenotype to Nck whereby responses was increased to intermediate and low affinity peptides but only a modest impact was observed to the high affinity peptide (figure 24 B and appendix figures 46 B and 47 B). In contrast, inhibition of actin polymerisation using Latrunculin B reduced T cell response (figure 24 C and appendix figures 46 C and 47 C). These phenotypes could be reproduced across multiple independent donors (figure 25.

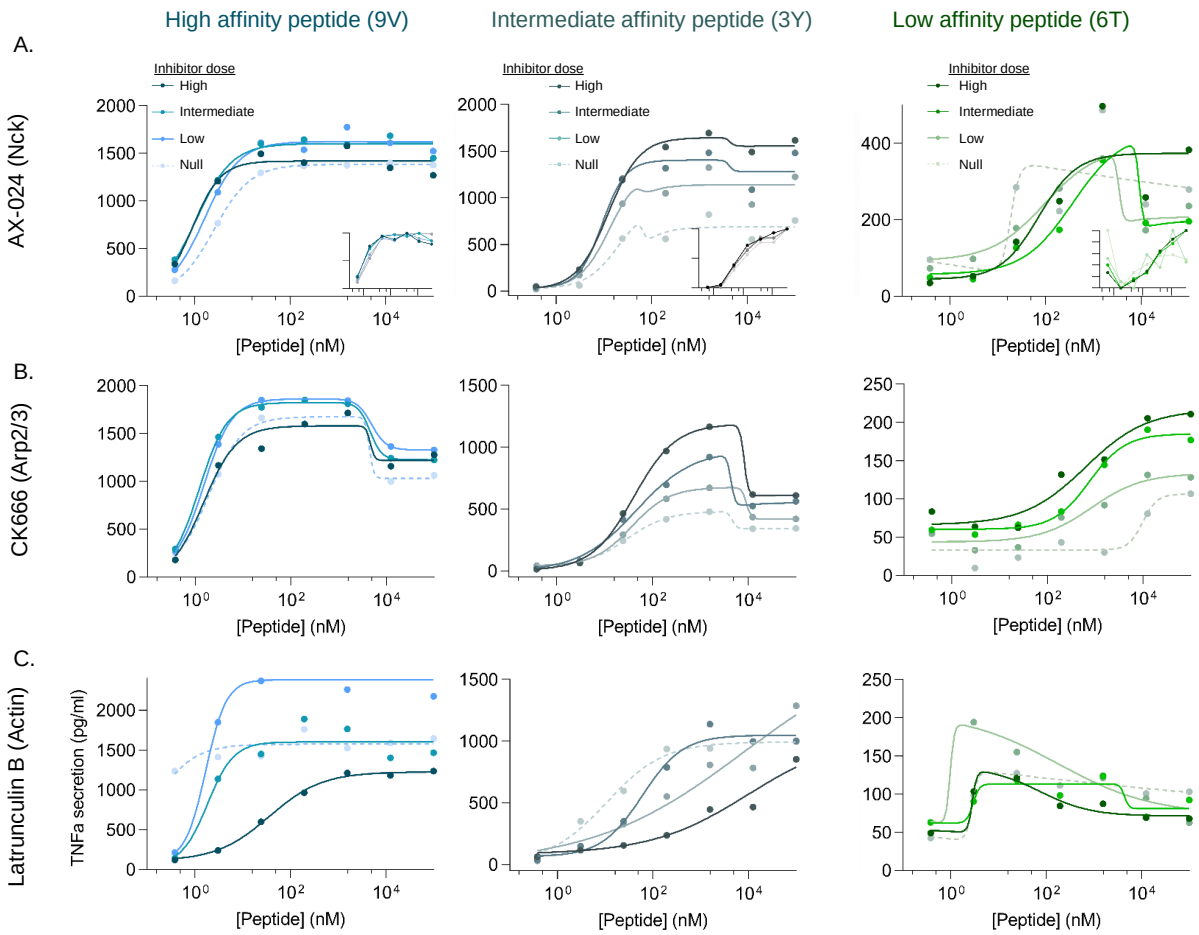


Figure 24: Impact of inhibition of actin-modulatory molecules on the magnitude of T cell response. Production of TNFα upon stimulation of 1G4$^+$ T cells on APC pulsed with peptides of high (A. column), intermediate (B. column) and low (C. column) affinities upon inhibitor treatment. One representative donor from three independent repeats.

Taken together, we observe that inhibition of Nck (AX-024) and Arp2/3 (CK666) resulted in increased TNFα concentration in the culture media, while direct inhibition of actin polymerisation (Latrunculin B treatment) induced a decrease of TNFα detected in the media (figure 25).

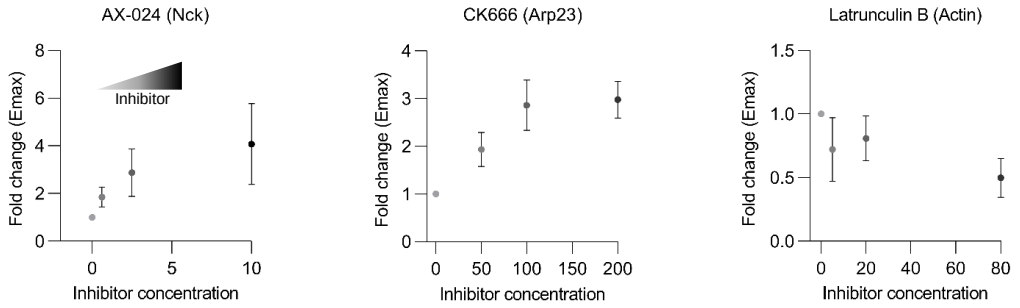


Figure 25: Inhibition of Nck and actin polymerization can increase supernatant cytokine levels. 1G4$^+$ T cells are stimulated on U87 APC pulsed with the intermediate affinity 3Y peptide (k_D=47μM) under inhibitor treatment. TNFα in the media is measured by ELISA. E_{max} is extracted from sigmoid or bell-shaped curves fitted to the raw data as shown in figure 24. Fold-change in the E_{max} under titrating concentrations of inhibitor compared to the no inhibitor concentration. Average of three independent donors, mean with SEM.

Given that supernatant cytokine levels are determined not only by cytokine production/secretion, but also by degradation and uptake, we sought to measure TNFα directly on the surface of T cells. We treated T cells with an inhibitor of the enzyme responsible for TNFα cleavage from the surface (TNFα converting enzyme, TACE) (figure 26 A) and measured the percentage of cells presenting TNFα on their surface after stimulation by the 3Y peptide. T cells treatment with a titration of the small-molecule inhibitors targeting Nck and Arp2/3 induced a decrease of the percent of cells displaying TNFα on their surface (figure 26 B and appendix figure 48). This decreased secretion upon inhibitor treatment was also observed when cells were treated with inhibitor of actin polymerisation (Latrunculin B) or early T cell signalling (A-770041, Lck inhibitor) (figure 26 and appendix figure 48) as controls. This decreased secretion was consistent across multiple donors (figure 26 C plotted from data extracted from figures 26 and 48).

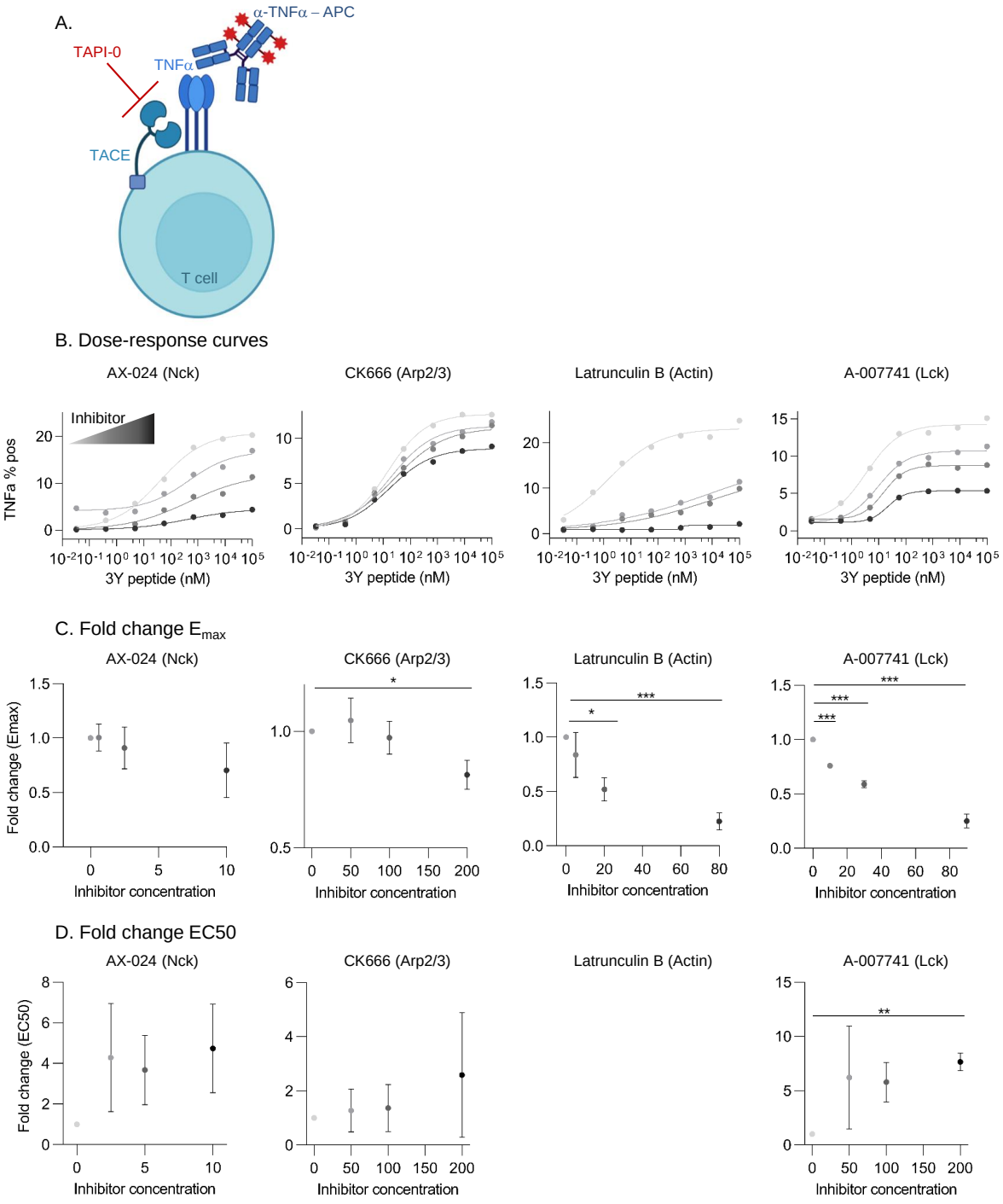


Figure 26: Inhibition of Nck and actin polymerisation reduces cytokine production at the single cell level. A. Detection of surface TNFα. TNFα is retained on the surface by inhibition of the TACE enzyme responsible for its cleavage. TNFα is detected on the surface via an anti-TNFα antibody coupled to the APC fluorophore. B. 1G4$^+$ T cells are stimulated on U87 APC pulsed with peptides of an intermediate affinity (3Y, K_D = 47μM) under inhibitor treatment. TNFα on the surface of T cells is measured by surface staining. C. E_{max} is extracted from sigmoid or bell-shaped curves fitted to the raw data as shown in figure 24. Fold-change in the E_{max} under titrating concentrations of inhibitor compared to the no inhibitor concentration. Average of three independent donors, mean with SEM. The fold change of each inhibitor dose was compared to the null inhibitor-dose slope by unpaired t-test, if no significance is indicated, comparison is Non Significant (NS) (NS (Not Significant) p = >0.05, * = p $\leq$ 0.05, ** = p $\leq$ 0.01, *** = p $\leq$ 0.001

3.2.3 SHP1 reconstitution in jurkat cells

Study of the SHP1 phosphatase is made challenging as a systemic knock-out is lethal [240]. As discussed above (3.1.3), the targets of the SHP1 phosphatase are still a matter of debate. In order to identify if the SHP1 phosphatase targets molecules involved in T cell sensitivity, we sought to measure antigen sensitivity directly by modulating the activity of SHP1. As there is no specific inhibitor of SHP1, we decided to work with Jurkat cells knock-out for SHP1 (figure 51), in which we would directly electroporate various concentrations of the purified SHP1 protein. We obtained SHP1 KO cells from the Hui lab (UCSD) and transduced the cells to express the $1G4^+$ TCR in order to be able to use them in our systematic study system.

In order to study the impact of incremental concentrations of the phosphatase, we electroporated SHP1 KO jurkat cells with increasing concentrations of full-length human purified SHP1 protein. We confirmed the introduction of the phosphatase intra-cellularly by Western Blot and compared the detected amount to the amount detected in parental control jurkat cells (figure 27 A). Electroporation of the jurkat cells with the highest amount of 1μg of SHP1 protein provided the jurkat with a comparable amount of phosphatase as the parental control. Electroporation amounts of SHP1 were detectable down to 0.1ug by Western Blot, with lower amounts undetectable (figure 27 A). However, electroporation with a 1μg of SHP1 lead to 40 percent lethality (figure 27 B). Electroporation of titrating amounts of SHP1 had no impact on antigen sensitivity measured by activation markers or cytokine secretion (figure 27 C and D). All electroporated cells displayed higher expressions of the activation marker CD69 at low antigen concentrations, but cytokine secretion remained minimal at these antigen concentrations. This lack of effect on cytokine secretion suggests that the basal level of activation of surface markers is due to electroporation-induced activation, rather than caused by the presence of SHP1. SHP1 KO jurkat cells all showed low level of IL-2 secretion, as opposed to WT jurkat cells. This could come from selective pressure when selecting for a KO clone, or from culture drift. Anyhow, the low production by the KO cell line prevents us from using this output as a measure of T cell response. Taken together, our data suggest that this electroporation method is not adequate to study of the impact of SHP1 on jurkats functional response.

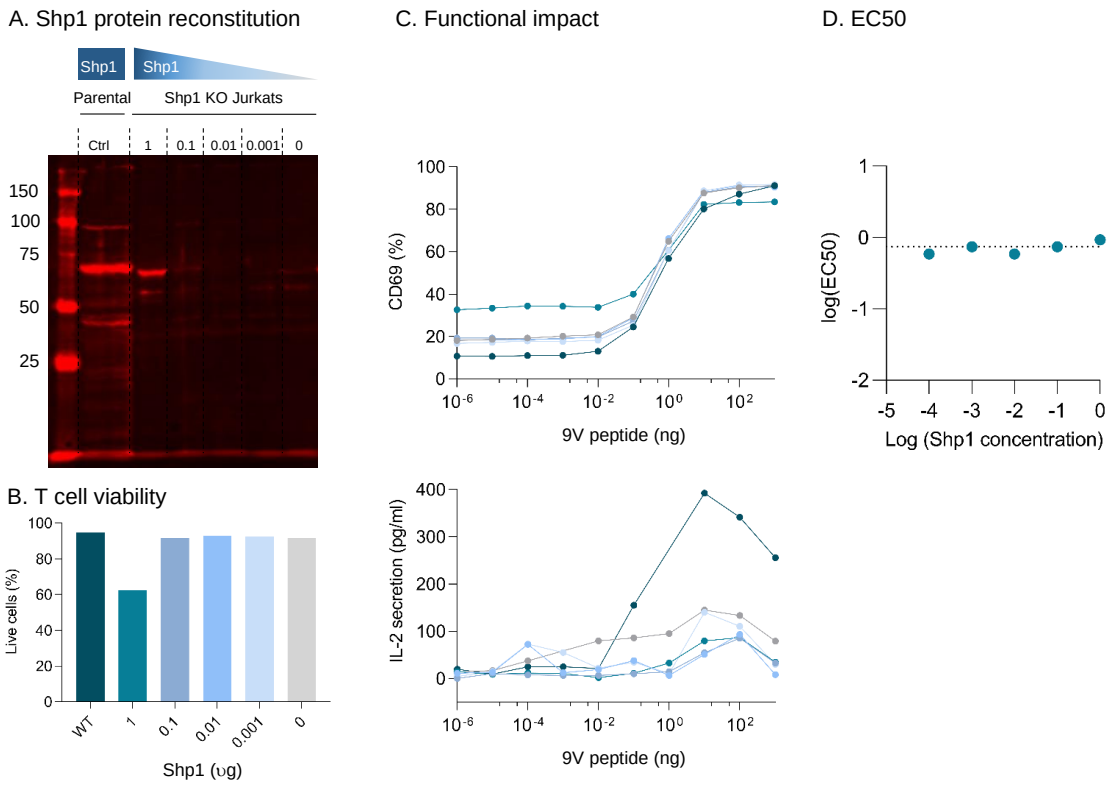


Figure 27: Impact of titrating re-constitutive concentrations of SHP1 protein on Jurkat functions. SHP1 knocked-out jurkats are reconstituted with titrating concentration of SHP1 protein. A. SHP1 KO jurkats are electroporated with titrating concentrations of the SHP1 protein (electroporation 200msec at 300V). Intracellular level of SHP1 after electroporation is visualised by Western Blot (Western Blot performed by Mikhail Kutuzov). B-D. Reconstituted Jurkat cells are stimulated by 4h co-culture with APC pulsed with titrating concentrations of the 9V peptide. B. Viability of the reconstituted cells is measured by flow cytometry (Free amines stain). C-D. Ability of the cells to upregulated the activation marker CD69 is measured by flow cytometry, cytokine production is measured by ELISA. D. Impact of titrating concentrations of SHP1 protein on the EC50 of the curves. The EC50 values are extracted from sigmoid curves fitted to the raw data. The EC50 of the no inhibitor concentration is represented by the dotted lines.

3.3 Discussion

Our systematic approach systems have the advantage of providing us with functional data over a range of peptide concentrations and affinities. In chapter 3, we were able to validate the use of both plate and co-culture-based assays to study the impact of modulation of signalling effectors on T cell antigen sensitivity. The plate-based assay has the advantage of being a very controlled environment, in which T cells are only presented with chosen types and amounts of ligands. We could validate that it allows detection of an impact on T cells adhesion (impact on k_{on}) as addition of ICAM-1 on the plate leads to a shift in the EC50 (figure 19 B). Therefore, we used this experimental set up to verify if we could reproduce the impact of Cyclosporin A on T cell adhesion observed by Dutta *et al.* [50]. They showed

that upon treatment with Cyclopsorin A (Calcineurin inhibitor) T cells binding to ICAM on plate is reduced. However, they do not complement this binding observation with evidence of impact on T cells functions. They also only study this impact at an early time point of activation (30 minutes) and using a single concentration of stimulus (anti-CD3 antibody coated on the plate). Therefore their data are not sufficient to conclude on an effect on T cell antigen sensitivity. In our hand, Cyclosporin A treatment of T cells stimulated by pMHC on ICAM-1 coated plates does not affect antigen sensitivity after 5 hours of activation (figure 19 C-E).

However a caveat of both our studies is that the plate environment is not representative of the interaction T cells would have with antigen presenting cells. On plate, ICAM-1 (LFA-1 ligand) is presented on an artificial plane surface, on which it is unable to move. Therefore, by interaction with ICAM-1, LFA-1 is prevented to be recruited to the p-SMAC of the immunological synapse and form clusters. This immobilisation effect could prevent LFA-1 to play its role in adhesion and stabilisation of the immunological synapse, therefore hiding the impact of Calcineurin on early signalling steps. However, both Dutta *et al.* [50] and us reproduced our experiments by exposing T cells to antigen presenting cells on which ICAM-1 is able to move freely, creating no hindrance to LFA-1 recruitment and clustering. Dutta *et al.* [50] made use of the DCEK fibroblast cell line as antigen presenting cells. In a co-culture-based assay, they reproduced their observation of decreased adhesion upon treatment of the T cells with Cyclosporin A, but they did not show functional consequence on T cells response. Again they measured adhesion at 30 minutes post stimulation, this early time point could exacerbate an impact LFA-1/ICAM-1 interaction, that is less relevant for the long-term activation of the T cells. In our assay, we were unable to detect an impact of Calcineurin inhibition on T cells function at 5h post stimulation (figure 22). This is in agreement with the work of Zeyda *et al.* [230] and Wojewodzka *et al.* [235] who did not detect impact of Calcineurin inhibition on T cells adhesion at 2h and 6 days post stimulation respectively.

In this assay, Dutta *et al.* [50] measured T cell response using a single concentration of antigen, therefore their system does not allow a quantitative measure of sensitivity. We made use of the U87 glioblastoma cell line as antigen presenting cells to present a range of peptide concentrations to T cells. In this assay, we were unable to detect an impact of Calcineurin inhibition on T cells sensitivity. One

could suggest that the ICAM-1 knock-out on U87 and subsequent selection could impact their ability to stimulate T cells. However, we treated T cells with the Lck inhibitor (A-770041) used in chapter 3 and we could reproduce our previous observations with this inhibitor both in the context of U87 parental and ICAM KO cells (figure 21 F-H). A discrepancy between our work and the data from Dutta *et al.* is the choice of antigen presenting cells, we made use of the U87 glioblastoma cell line, while they chose the DCEK cell line. A key aspect of this DCEK cell line, is that it only expresses CD80 and ICAM-1 [248] as adhesion-receptor ligands. The U87 cell line we used as APC expresses a broader range of adhesion-receptor ligands including CD58, the ligand for CD2, and ICAM-3, ICAM-5 and JAM-A, ligands for LFA-1 as characterised by Burton *et al.* [128]. Similarly, in their studies, Zeyda *et al.* [230] and Wojewodzka *et al.* [235] both use mature Dentritic Cells (DCs) as their target cells for conjugate assays. Mature DCs also express a broader range of adhesion receptors such as CD58. As ligation of CD2 by CD58 has been shown to play a key role in adhesion [249], it could play a compensatory role in the absence of ICAM. This is another factor that could explain that the marked effect of ICAM-1 in Dutta's system is not reproduced in our assays.

In conclusion, the data obtained by Dutta *et al.* [50] were insufficient to demonstrate an impact of Calcineurin inhibition on T cell antigen sensitivity. And, at a single antigen concentration, the discrepancies between the work from Dutta *et al.* and the results we, and others [230] [235], obtained, could be explained by differences in the timing of the experiments and the cell type used as antigen presenting cells.

Borroto *et al.* [207], showed that treatment of T cells with the AX-024 small-molecule inhibitor prevents its interaction with the CD3 epsilon chains of the TCR [207]. According to this proposed mode of action, treatment of T cells with AX-024 should result in an impact on k_p in our model, displayed by a increased of the EC50 and decrease of the E_{max}. In our experimental system, increasing concentrations of the AX-024 molecule had no impact on the EC50 of the dose-response curves when T cells response was measured by surface markers. It induced a decreased of the EC50 of the dose-response curves measuring TNFα secretion in a single experiment that could not be repeated. Taken together, we conclude that AX-024 does not impact T cell sensitivity. This is in contradiction with the proposed inhibitory role of AX-024. Surprisingly, treatment of T cells with AX-024 did not affect the amplitude of the response as we would expect from an inhibition of Nck in the context of its role in the actin pathway. It is possible

however that the proposed binding site of AX-024 on Nck (SH3.1) does not affect Nck function in the actin pathway, as Nck interacts with LAT through its SH2 domain [250].

It is important to note however that the AX-024 molecule is proposed to have an inhibitory role on Nck in the context of sub-physiological stimulation, as those induced by self-peptides. To replicate these conditions in their assays, Borroto *et al.* [207] tested the effect of AX-024 of T cells stimulated with the low affinity Q4R7 (k_D=220μM) peptide, a peptide variant derived from the well-characterised OVA peptide. In our assay, we made use of the 3Y (k_D=47μM) and 6T (k_D=162μM) peptides. None of the two present an affinity as low as the Q4R7 but we made the choice to privilege a stimulus high enough to allow detection of functional output through the same techniques as previously used in our systematic measure of discrimination (cytokine detection by ELISA in figure 24).

Surprisingly, when presented with lower affinity peptides, treatment of T cells with the AX-024 (Nck inhibitor) had no impact on antigen sensitivity, but induced a small increase in the concentration of cytokines detected in the media (figure 24A). This increase is not significant, but the trend is consistent across donors (figure 25). Presented with this surprising result, we observed that inhibition of Arp2/3, located directly downstream of Nck, induced a more pronounced, significant, increase in TNFα in the culture media (figure 24B and figure 25). Direct inhibition of actin however, induced an expected decrease in the concentration of TNFα in the media (figure 24C and figure 25). Because this effect was the clearest upon T cell stimulation with the 3Y peptide, we made use of this intermediate stimulus going further.

In order to decipher if this increase was a result of an increased percentage of T cells producing TNFα, we measured the proportion of T cells presenting TNFα on their surface after preventing its cleavage. Surface staining demonstrated that treatment of T cells with AX-024 (Nck inhibitor) or CK666 (Arp2/3 inhibitor) induced a decrease of the proportion of T cells presenting TNFα on their surface. This suggests that cytokine production and secretion is inhibited by treatment with the inhibitors. As controls, the same inhibition was observed when inhibiting actin polymerisation (Latrunculin B) or an early effector of T cell signalling (A-770041, Lck inhibitor) (figure 26). T cells carry TNF receptors (TNFR1 and TNFR2)[251] and, while there is no study of TNFα consumption by T cells in the literature

to our knowledge, T cells have been shown to consume cytokines such as IL-2 from their environment [252]. We hypothesise that inhibition of the early modulator of actin (Nck and Arp2/3) could prevent efficient cytokine uptake by interfering with actin remodelling. This effect would be exacerbated in the context of sub-physiological stimulus, as the production of cytokines is minimal, therefore, the amount consumed could exceed the amount produced. In this scenario, inhibition of consumption could lead to an accumulation of cytosine in the media that exceed the concentration in the presence of non-inhibited consumption. This is however a proposed hypothesis without supporting experimental data, but this research was past the scope of this thesis, focused on the study of antigen sensitivity and discrimination.

Given the report of lethality of SHP1 knock-out in mouse, a former student in the lab studied the impact of the phosphatase through knocked-down. However, he showed that knocked-down of SHP1 is insufficient to impact jurkat functions. He performed a constitutive knock-down in jurkat cells which yield a 90% reduction in expression of the phosphatase (appendix figure 49A). This reduction had no effect on T cell antigen sensitivity. Surprisingly, it induced a decreased in the expression of activation surface markers at low antigen concentrations, and a decrease in cytokine secretion at high antigen concentrations (figure 49B). As deletion of the SHP1 phosphatase has been reported to increase cytokine secretion and induce a general boost of T cell functions [240], these observations were challenging to explain. He hypothesised that a constitutive knock-down obtained after cells selection was likely to introduce bias and adaptation in the selected cells. In order to prevent this adaptation, he performed an inducible knocked-down induced by addition of doxycyclin. This induced knock-down had no impact on antigen sensitivity or amplitude of the response, either measured by expression of activation markers or cytokine secretion (figure 50).

In light of these previous data, we decided to study the impact of the SHP1 phosphatase in cell knocked-out of its expression. As discussed before, genetic modifications in primary T cells are challenging. As SHP1 is an intracellular molecules, sort of KO cells can not be performed based on surface expression. And because primary T cells only have short lifespan, single clone sort was not conceivable. Faced with these difficulties, we decided to make use of the jurkat cell line. We obtained SHP1 KO cells from Enfu Hui's lab (UCSD)(SHP1 KO validated in [241] and verified by WB in appendix figure 51).

This immortalised cell line model is debatable to study physiological T cell signalling, however we were able to reproduce our previous observations with the inhibitors targeting Lck and Calcineurin in this cell line (appendix figure 52).

The lack of effect we observed when reconstituting SHP1 KO jurkats with purified SHP1 proteins could be explained by different factors. The experimental protocol has flaws as reconstitution of SHP1 to a physiological level leads to extensive cell death (appendix figure 27B). We hypothesise that this lethality could be due to exposure of the cells to high volume of the SHP1-containing buffer. This buffer contained ion-chelating EDTA and traces of detergent (Tween20) which are toxic to the cells. In the case of lower dilutions, the SHP1 containing buffer was diluted in media, the cells were therefore maintained in an environment with low concentration of these toxic components. It would be ideal to repeat the experiment with a more concentrated sample of SHP1 further diluted in media, but this was not available to us at the time of the experiment.

The main interest of SHP1 is its role in mediating the inhibitory function of the surface receptor BTLA. I, and previous students in the lab, found no evidence of SHP1 impacting TCR-induced signalling. However, we are lacking positive controls validating this negative result. It would be useful to show, for example, that electroporation of purified SHP1 protein can increase the ability of BTLA to inhibit TCR signalling, but has no functional impact in the absence of BTLA ligation. In this context, we performed some studies of the impact of inhibitory receptors on T cell functions, but they were unsuccessful by lack of an appropriate experimental platform as described in 4.2.3. However since, a student in the lab, Ashna Patel, has established a cellular-based system, allowing ligand mobility, that allows study of these receptors. We had paused further SHP1 experiment during the establishment of this experimental system. In the future, by using this system, we will be able to study the role of SHP1 in a more physiological environment including inhibitory receptors.

Chapter 4

Application of the system to surface molecules

4 Application of the system to surface molecules

4.1 Introduction

We have shown in the previous chapters that we can make use of a systematic assay to determine if a signalling molecule impacts T cell antigen sensitivity and/or discrimination.

We sought to apply this system to surface molecules which impact T cell functions through non elucidated mechanisms. We focus in this chapter on two molecules: programmed cell death 1 (PD-1) which is classified as an inhibitory receptor (IR) as its ligation impairs T cells function; and CD6 whose role on T cells function is still a matter of debate. Both these molecules are the target of immunotherapies. Blockade of PD-1 interaction with its ligand programmed cell death ligand 1 (PD-L1) is broadly used in the clinic to increase T cells function in the case of cancers [253][254]. On the other hand, blockade of CD6 through monoclonal antibodies is used to inhibit T cells activation in the context of multiple autoimmune diseases (i.e. rheumatoid arthritis [255], psoriasis [256]). However these therapies have side effects [257][258][259] and are only effective for a subset of patients [260][261][259]. Therefore, there is a need for a better understanding of the mechanisms through which these surface molecules mediate their impact on T cells functions.

4.1.1 The PD-1 inhibitory receptor

The inhibitory receptor programmed-death 1 (PD-1 or CD279) is a member of the CD28 immunoglobulin superfamily, it is expressed on the surface of activated T cells [262]. PD-1 has two known ligands : PD-L1 which is broadly expressed [263] and PD-L2 which expression is restricted to professional APCs.

The inhibitory impact of PD-1 is well-established and its blockade is a successful immuno-therapeutic strategy in a subset of patients [264][253][265]. However, the mechanism through which it carries out its inhibition in T cells is still a matter of debate. PD-1 contains Immunoreceptor Tyrosine-based Inhibitory Motif (ITIM) and Immunoreceptor Tyrosine-based Switch Motif (ITSM) in its intracellular tail that undergo phosphorylation upon ligand binding. The phosphorylated motifs are binding sites for the SHP2 phosphatase through its SH2 tandem domains [266][267]. The SHP2 phosphatase is proposed to

be the main mediator of PD-1 inhibition [241]. However, this model is probably incomplete as Rota *et al.* demonstrated that PD-1 blocking in mouse leads to tumour control in the absence of SHP2 (SHP2 KO background) [268] and Xu *et al.* showed that PD-1 exert inhibitory function in primary T cells lacking both SHP1 and SHP2 (decreased proliferation and cytokine secretion) [241].

Similarly to SHP1 discussed in chapter 3, the target(s) of the SHP2 phosphatase are still a matter of debate. Many TCR signalling molecules have been proposed as dephosphorylation targets : the CD3 chains of the TCR [267], the kinases Lck [247] and ZAP70 [243] and their downstream effector SLP76 [246]. These candidates however have been identified through immuno-precipitation assay or imaging, and their implications has not been validated functionally. More recent papers have proposed the accessory receptor CD28 as the main PD-1-mediated SHP2 dephosphorylation target *in vitro* [269] and an *in vivo* murine model [270]. However, while Hui *et al.* [269] showed faster dephosphorylation of CD28 by SHP2 compared to the TCR, they only performed their assay under short time points in the jurkat cell line and do not confirm the impact of their observations functionally (e.g. cytokine production or the upregulation of surface receptors). In Kamphorst *et al.* [270], the importance of CD28 signalling is shown to be essential for re-activation of PD-1^+ T cells, but no functional data was presented to establish a link with PD-1 inhibition. On the contrary, Bennet *et al.* show that CD28 co-stimulation rather plays a protective role against PD-1 mediated T cell inhibition [271] . In line with this observation, Mizuno *et al.* showed that PD-1 mediated inhibition is less efficient when combined with CD28 co-stimulation (measured by cytokine production) [272].

Therefore the mechanism mediating PD-1 inhibition and its target(s) in the TCR signalling pathway are not elucidated. We decided therefore to make use of our systematic system to help answer these questions.

4.1.2 The CD6 receptor

CD6 is a glycoprotein from the scavenger receptor cysteine-rich superfamily, expressed in mature T cells, B cells and NK cells. Its ligand, CD166 (also known as ALCAM) is expressed on various cell types in

different tissues, notably at high level on monocytes and low levels on T cells [273]. The interaction of CD6 with CD166 allows T cells to form close contacts with their target APCs [274] and localise to the immune synapse [275][276].

CD6 is composed of 3 scavenger-receptor extracellular domains, among which the membrane proximal, domain 3, is responsible for binding to CD166 [273]. It has a long intracellular tail (244 amino acids) containing 9 tyrosines of which 6 are known to be phosphorylated. These allow for binding with diverse partners. Binding of CD6 to its ligand CD166 induces tyrosines phosphorylation, phosphorylated tyrosines at position 662 (Y662) and 629 (Y629) allow for recruitment of SLP76 and Gads respectively, through their SH2 domains.
These two tyrosines have been proposed to play a positive role in T cell activity as their mutations decrease cytokine production [273]. Because of this ability to recruits SLP76 and Gads, CD6 has been proposed to act as a partial alternative to LAT as scaffold protein in T cells[277]. However, it cannot fully replace LAT because LAT knocked-out (KO) cells are severely blunted and fail to proliferate [277].

CD6 also carries an SDSDY motif, which is a binding site for the cytoskeleton-associated molecules ezrin, radixin and moesin. These interactions have been proposed to help bring CD6 within the immunological synapse upon T cell activation [278] and impact T cell migration [279]. This motif has been proposed to be inhibitory as mutations of the serines and tyrosine of the motif (where the SDSDY motif is mutated into the ADADF sequence) enhance T cell activation. However, this inhibitory phenotype is dependent on context and can be overridden by co-stimulation through CD28 or a high concentration of APCs [279].

Therefore, the activatory role of the tyrosines, and their binding molecules SLP76 and Gads, is believed to be the dominant mechanism upon CD6 ligation [279]. This is in line with *in vitro* experiments suggesting an activatory role: blocking of its interaction with its ligand CD166 reduces antigen-induced T cell activation [274][275][280] while antibody-mediated cross-linking of CD6 on the T cell surface enhances T cell proliferation [281].

In mouse, Li *et al.* showed a protective role of CD6 KO against experimental autoimmune encephalomyelitis (EAE)[282], however, Orta-Mascaro *et al.* described CD6 as a regulatory molecule as, in their hands, CD6 KO increased the risk of autoimmune reaction (upon Collagen-Induced Arthritis (CIA) test) [283]. It is important to note however that in the case of Li *et al.* [282], a complete deletion of CD6 was performed, while in experiments by Orta-Mascaro *et al.* [283] only the extracellular region of CD6 was deleted. The presence of the intracellular tail of CD6 could therefore play a role, explaining the discrepancies between the two studies. Moreover, the consequences of the auto-immune diseases models also differ as EAE induction in CD6 KO mice lead to decreased Th1 and Th17 T cell responses [282], while CIA induction resulted in dysfunctional T regulatory cells activity, the latter therefore did not provide direct evidence of effector T cell dysfunction [283].

In human, CD6 appears to be protective against autoimmunity. Mutations (SNP) in the CD6 gene leading to the production of a shorter CD6 form lacking the binding domain 3 is associated with the development of auto-immune diseases such as psoriasis [284], rheumatoid arthritis [285] and multiple sclerosis [286]. The Itolizumab (Alzumab^{TM}) antibody targeting domain 1 of CD6 is used in the clinic to inhibit cytokine production [284], however as this antibody does not bind the CD166 binding domain 3, it does not act by preventing CD6 interaction with CD166 but through an unknown mechanism [287].

There has been extensive work studying these receptors, many based on biochemical approaches including antibody-mediated CD6 receptor blocking [273] or ligand/receptor cross-linking [281], phosphorylation assay [269]. However, most of these assays have been performed in artificial systems such as Large Unilamellar Vesicules (LUV)-based reconstitution [269] or jurkat cell line based assays [241]. Despite this work, systematic experiments to examine how a titration of their ligands impacts on a titration of antigens of different affinity has yet to be performed. Therefore, we currently do not know how these receptors impact T cell antigen sensitivity and discrimination. Here, we aimed to use a reductionist system where T cells can be submitted to a titration of antigen and ligands to different accessory receptors. In this way, our objective was to determine whether PD-1 and CD6 can impact T cell antigen sensitivity and discrimination. However, we found that ligation of these accessory receptors had no impact on T cell responses in this experimental system. We conclude with a discussion of possible reasons for these

results.

4.2 Results

To study the impact of PD-1 and CD6 ligation on T cell responses, we made use of a reductionist system whereby purified ligands to surface receptors can be titrated. We have used this system in chapters 2 and 3 and this system has been used to study the impact of purified ligands to different co-stimulation receptors [209][115][128] .

4.2.1 Purified PD-L1 does not impact T cell responses in a solid-phase stimulation system

To assess the impact of PD-1 on antigen sensitivity, we produced purified biotinylated pMHC ligands on streptavidin-coated plates (figure 28 A-B). We used primary human $CD8^+$ T cells transduced with the c58c61 TCR which recognises the 4A8K pMHC ligand ($K_D = 7\mu M$ [197]). We used this TCR instead of the 1G4 TCR because we planned to make use of the wide range of pMHC affinities described in Lever *et al.* [197].

Following an 8 hours stimulation assay, we assessed cytokine production (IFNγ) and activation marker (surface levels of 4-1BB). Unexpectedly, we found that increasing the concentration of purified PD-L1 did not impact the T cell responses at any concentration of pMHC that we tested.

Given that previous work suggested that the primary target of PD-1 is the inhibition of CD28 [269][270], we reasoned that including ligands to CD28 may reveal a phenotype for PD-1. We therefore included a condition where a constant concentration of purified CD86 (ligand for CD28) was included at all conditions. As expected, CD86 clearly led to an increase in T cell response but as before, increasing the concentration of PD-L1 did not impact T cell responses (figure 28 C-D and appendix figure 53 A-B).

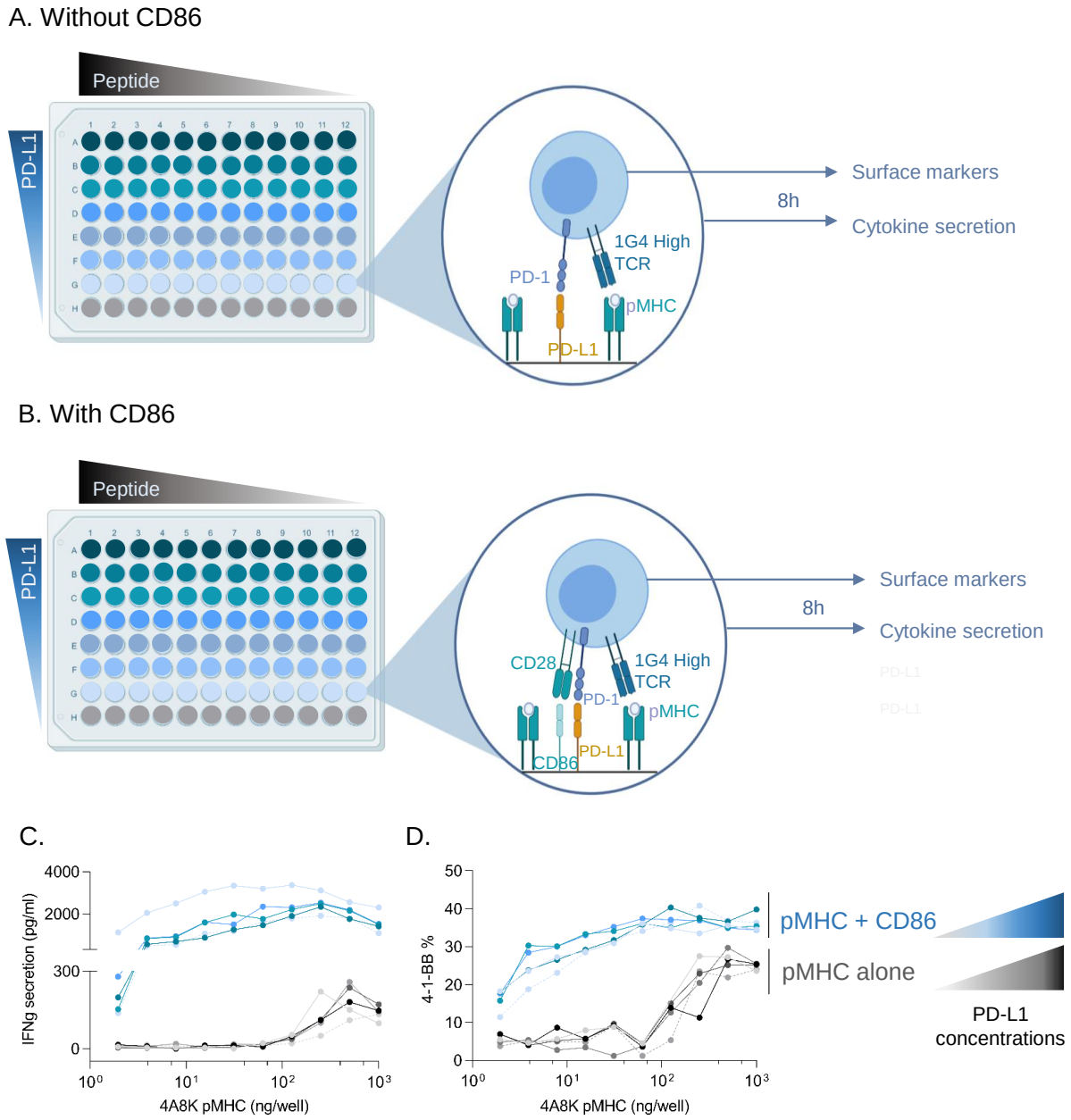


Figure 28: PD-L1 does not impact T cell activation to different concentrations of pMHC in the presence or absence of CD86. A-B. 1G4$^+$ T cells are incubated on streptavidin-coated plates presenting a titration of purified antigen and increasing concentrations of PD-L1 (PD-l ligand) in (A) absence or (B) presence of a constant concentration of CD86 (CD28 ligand). The impact on T cell functions is studied by staining T cells for activation markers and supernatant cytokine secretion after 8h of stimulation. C. Cytokine secretion and D. expression of the activation marker 4-1BB upon stimulation of 1G4$^+$ T cells on streptavidin coated plates presenting a titration of 4A8K peptide on biotinylated MHC and titrating concentrations of the purified PD-L1 molecule (PD-1 ligand) in presence or absence of a constant concentration of CD86 (CD28 ligand). Dose-response curves and their normalisation (inset graph), one representative donor of two independent repeats.

Although surface expression of PD-1 has been reported on CD8+ T cells, it is known to be further up-regulated on a time-scale longer than 8 hours with a maximum upregulation at 16 hours [288]. Indeed, we found that our *in vitro* expanded CD8$^+$ T cells expressed surface PD-1 at low level (4%, figure 29 A).

As PD-1 expression is induced upon T cell activation, we pre-stimulated CD8$^+$ T cells on streptavidin plates coated with a constant concentration of pMHC for 16 hours. After 16h of pre-stimulation, 21% of T cells express PD-1 on their surface (figure 29 A). The pre-stimulated T cells were stimulated on streptavidin plates coated with titrating concentrations of 4A8K peptide in presence or absence of PD-L1 and presence or absence of a constant concentration of CD86 for 8h. As before, CD86 increased T cell responses (29 B-C). Despite a higher expression of PD-1 on the T cells, the presence of PD-L1 on the plate had no impact on the T cell response, whether measured through cytokine secretion or surface marker expression (figure 29 B-C and appendix figure 54 A-B).

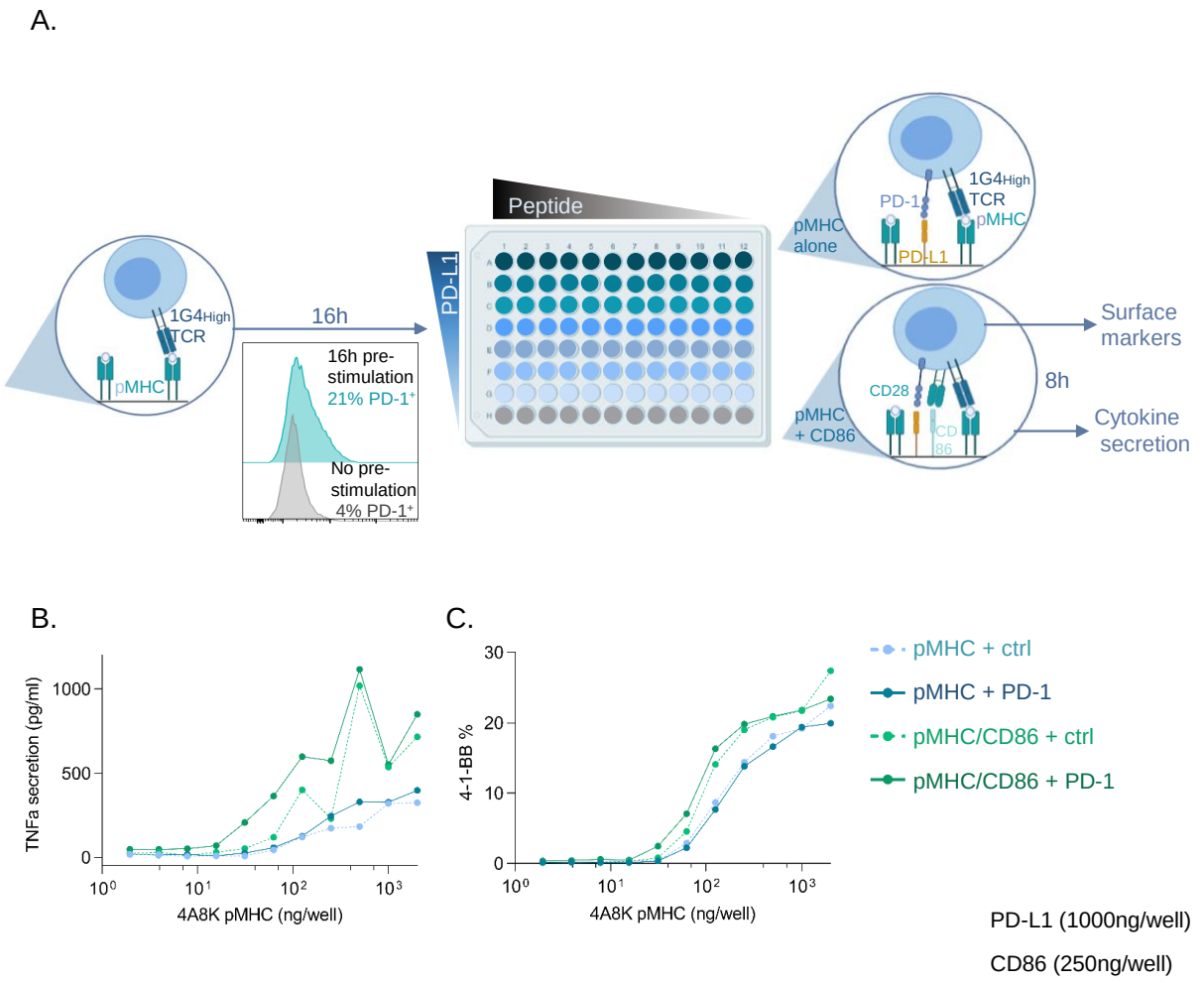


Figure 29: Pre-stimulated T cells with increased PD-1 expression remain inert to PD-L1 inhibition. A. 1G4$^+$ T cells are incubated on streptavidin-coated plate presenting a constant concentration of purified antigen for 16h to induce expression of PD-1. T cells are then incubated on streptavidin-coated plates presenting different concentrations of purified antigen and increasing concentrations of PD-L1 (PD-l ligand) in presence or absence of a constant concentration of CD86 (CD28 ligand). T cell functions are studied by staining of T cell for activation surface markers and measure of cytokine secretion after 8h of stimulation. B. Cytokine secretion and C. expression of the activation marker 4-1BB. Dose-response curves and their normalisation (inset graph), one representative donor of two independent repeats.

Taken together, we found no evidence that PD-1 can inhibit T cell responses in the presence or absence of ligands to CD28 in this experimental system.

4.2.2 Purified CD166 does not impact T cell responses in a solid-phase stimulation system

In parallel to the study of PD-1, we also initiated work to study the impact of CD6 on T cell responses.

We made use of $CD8^+$ T cells isolated from healthy donors and transduced them with the 1G4 TCR. T cells were incubated on streptavidin plates coated with titrating concentrations of 9V pMHC and a titration of biotinylated CD166 Wild-Type (WT) (the ligand for CD6) for 8h. In order to ensure that any observed effect was due to ligation of CD6, we used a mutant version of CD166 in which the lysine at position 55 has been mutated to an alanine in order to prevent binding (K55A). We also made use of a version of CD166 in which the membrane distal domain, which is responsible for binding CD6, has been deleted, producing a version of CD166 incapable of binding. Finally, we used biotinylated rat CD4, which does not interact with CD6, as a control protein (rCD4) (figure 30 A).

We observed that CD166 inhibited T cell responses and specifically led to an increase in the EC50 of the dose-response curve (figure 30 B-C and appendix figures 55 A-B and 56 A), suggesting that CD6 can reduce antigen sensitivity. However, a similar phenotype was observed with both the CD6 point mutation (figure 30 D-E and appendix figure 55 C-D) and the CD6 domain mutation (figure 30 F-G and appendix figures 55 E-F and 56 B). As expected, rCD4 had no impact on T cell responses (figure 30 H). This suggests that the inhibitory action of CD166 is independent of its ability to bind CD6.

In these experiments, we also measured the surface levels of CD6 (figure 30 I). We found that CD6 exhibited modest down-regulation with pMHC alone but that this was enhanced by CD166. Moreover, this enhancement appeared to be reduced in the CD166 point and domain mutant variants. This suggests that CD166 can bind CD6 on the surface of T cells.

Taken together, these results suggest that the inhibitory function of CD166 is independent of its ability to bind CD6. Given that CD166 is larger than rat CD4 [289], we speculate that the inhibitory function of CD166 in this experimental system is related to its ability to sterically prevent the TCR from binding pMHC.

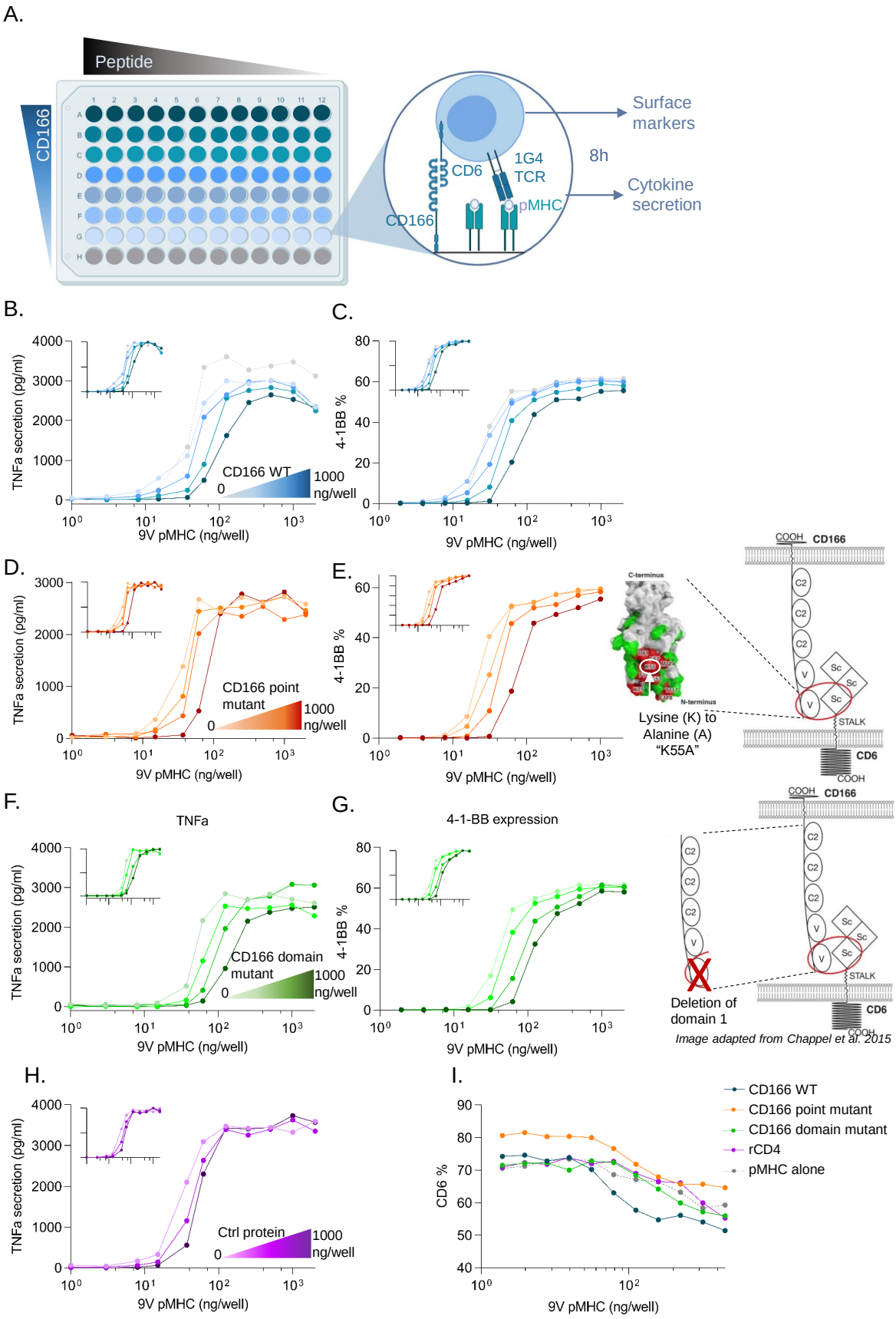

A.
Peptide
CD166
Surface markers
8h
Cytokine secretion
CD6
1G4 TCR
pMHC
CD166
B.
TNFa secretion (pg/ml)
CD166 WT
0
1000 ng/well
9V pMHC (ng/well)
C.
4-1BB %
9V pMHC (ng/well)
D.
TNFa secretion (pg/ml)
CD166 point mutant
0
1000 ng/well
9V pMHC (ng/well)
E.
4-1BB %
9V pMHC (ng/well)
C-terminus
N-terminus
Lysine (K) to Alanine (A) "K55A"
COOH
CD166
C2
V
Sc
STALK
CD6
F.
TNFa
TNFa secretion (pg/ml)
CD166 domain mutant
0
1000 ng/well
9V pMHC (ng/well)
G.
4-1-BB expression
4-1BB %
9V pMHC (ng/well)
Deletion of domain 1
Image adapted from Chappel et al. 2015
H.
TNFa secretion (pg/ml)
Ctrl protein
0
1000 ng/well
9V pMHC (ng/well)
I.
CD6 %
9V pMHC (ng/well)
CD166 WT
CD166 point mutant
CD166 domain mutant
rCD4
pMHC alone

Figure 30

Figure 30: CD166 reduces T cell antigen sensitivity independently of its ability to bind CD6. A. $1G4^+$ T cells are incubated on streptavidin-coated plates presenting different concentrations of purified 9V pMHC and increasing concentrations of CD166 (CD6 ligand or CD166 with a point mutation to abolish binding). The impact of surface molecule ligation on T cell functions are studied by staining of T cells for activation markers and measure of cytokine secretion after 8h of stimulation. B. Cytokine secretion and C. expression of the activation marker 4-1BB. Dose-response curves and their normalisation (inset graph), one representative donor out of two independent repeats. D. Cytokine secretion and E. expression of the activation marker 4-1BB upon stimulation of $1G4^+$ T cells on streptavidin-coated plates presenting a titration of 9V pMHC and titrating concentrations of the purified CD166 molecule carrying a mutation preventing binding to CD6 (K55A, binding mutant). Dose-response curves and their normalisation (inset graph), one representative donor out of two independent repeats. F Cytokine secretion and G. expression of the activation marker 4-1BB upon stimulation of $1G4^+$ T cells on streptavidin-coated plates presenting a titration of 9V peptide on biotinylated MHC and titrating concentrations of the purified CD166 molecule lacking domain 3 to prevent binding to CD6 (domain 3 mutant). Dose-response curves and their normalisation (inset graph), one representative donor of three independent repeats. H. Cytokine secretion upon stimulation of $1G4^+$ T cells on streptavidin-coated plates presenting a titration of 9V peptide on biotinylated MHC and titrating concentrations of the purified protein CD4 from rat (control protein). Dose-response curves and their normalisation (inset graph), one representative donor out of 3 independent repeats. I. Expression of CD6 on the surface measured by flow cytometry.

To test the hypothesis that the size of CD166 was involved in the inhibition, we generated a truncated version of CD166 containing only domains 1 and 2. We hypothesised that the reduced size of CD166 would not be able to sterically inhibit the ability of the TCR to bind pMHC. We repeated the previously described experiment but this time coating the plates with shorter (domains 1-2) versions of WT CD166 or the shorter version with the K55A point mutant to prevent binding to CD6. As before, we used rCD4 as control protein (figure 31 A).

When T cells were presented with short-length versions of CD166, we observed no impact of CD6 ligation on T cell response (figure 31 B-C and appendix figure 57 A). We observed a modest decrease in T cell responses with the short CD166 that contained the binding mutation (figure 31 D-E) and no impact when using the control rCD4 protein (31 F-G and appendix figure 57 C). In one independent experiment, we observed reduction in T cell responses when using the short version of CD166 point mutant (K55A) (appendix figure 57 B), but because this protein is unable to bind to CD6, we concluded in a non-specific phenotype.

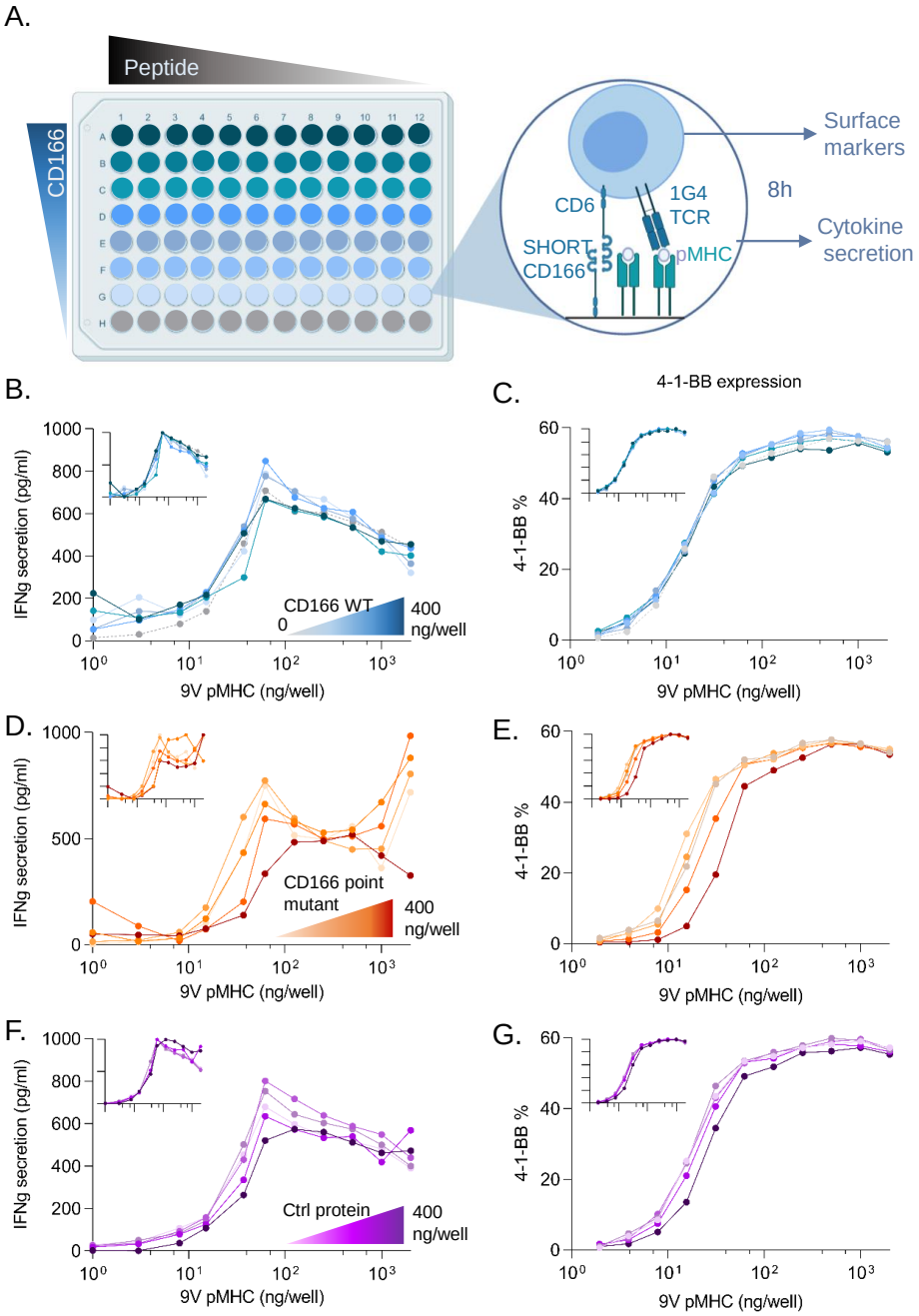


Figure 31: The short-length version of CD166 has no impact on antigen sensitivity to a titration of purified antigen in a plate-based system. A. 1G4$^+$ T cells are incubated on streptavidin-coated plates presenting titrating concentrations of purified antigen and increasing concentrations of CD166 (CD6 ligand). The impact of surface molecule ligation on T cell functions is studied by staining of T cell for activation markers and measure of cytokine secretion after 8h of stimulation. B. Cytokine secretion and C. expression of the activation marker 4-1BB upon stimulation of 1G4$^+$ T cells on streptavidin-coated plates presenting a titration of 9V peptide on biotinylated MHC and titrating concentrations of the purified CD166 molecule (CD6 ligand). Dose-response curves and their normalisation (inset graph), one representative donor of two independent repeats. D. Cytokine secretion and E. expression of the activation marker 4-1BB upon stimulation of 1G4$^+$ T cells on streptavidin-coated plates presenting a titration of 9V peptide on biotinylated MHC and titrating concentrations of the purified CD166 molecule carrying a mutation preventing binding to CD6 (K55A, binding mutant). Dose-response curves and their normalisation (inset graph), one representative donor of two independent repeats. F. Cytokine secretion and G. expression of the activation marker 4-1BB upon stimulation of 1G4$^+$ T cells on streptavidin-coated plates presenting a titration of peptide on biotinylated MHC and titrating concentrations of the purified protein CD4 from rat (control protein). Dose-response curves and their normalisation (inset graph), one donor of two independent repeats.

4.2.3 Establishment of a lipid bilayer-based assay system to study the impact of surface molecule on T cell antigen sensitivity

Using the plate-based stimulation system, we found that ligation of CD6 and PD-1 had no impact on T cell responses. Given that the plate-based system lacks ligand mobility and at least in the case of PD-1, its mechanism of action is dependent on close co-localisation with the TCR and/or CD28, we hypothesised that ligand mobility may be important to observe a functional phenotype.

Studies of molecules involved in the immunological synapse are often performed on supported lipid bilayer (SLB) [86][117], which replicate the fluidity of cellular membranes, while offering a well-controlled environment. Because we hypothesised that essential properties offered by membrane, such as mobility, are essential for the study of some surface molecules, we set out to establish a system of lipid bilayers that would allow us to reproduce plate-base experiments.

Lipid bilayers require glass surfaces to be produced. Because we wanted to reproduce systematic quantitative experiments, we made use of 96-well glass-bottom plates, in which we produced 96 independent bilayers. For that, the plates were cleaned using a solution of 1% Hellmanex^{TM} in 50% Isopropanol overnight, followed by a wash in sodium hydroxyde. Once the surface had been dried, we prepared lipid bilayers composed of a mix of DOPC lipids, in which we added a fraction of fluorescently labelled lipids (0.2%) and a fraction of biotinylated lipids (10%). This mix allowed us to couple the biotinylated lipids to proteins of interest on the one hand, and to visualise the fluorescent lipids by microscopy on the other hand (figure 32 A).

We made use of the presence of fluorescent lipids in the bilayer to visualise it and check its integrity by microscopy. We also verified its diffusion ability using the Fluorescence Recovery After Photobleaching (FRAP) technique. This technique consists in briefly (one second) subjecting a small area of the bilayer (10-20μm diameter circle) to high intensity light from a laser. Due to the high intensity light, fluorophores in this area are bleached, so unable to generate fluorescence. We could confirm the mobility of our bilayer as fluorescent lipids were able to rapidly diffuse in the bleached zone and 80% of the initial fluorescence was recovered after 30 seconds (figure 32 B).

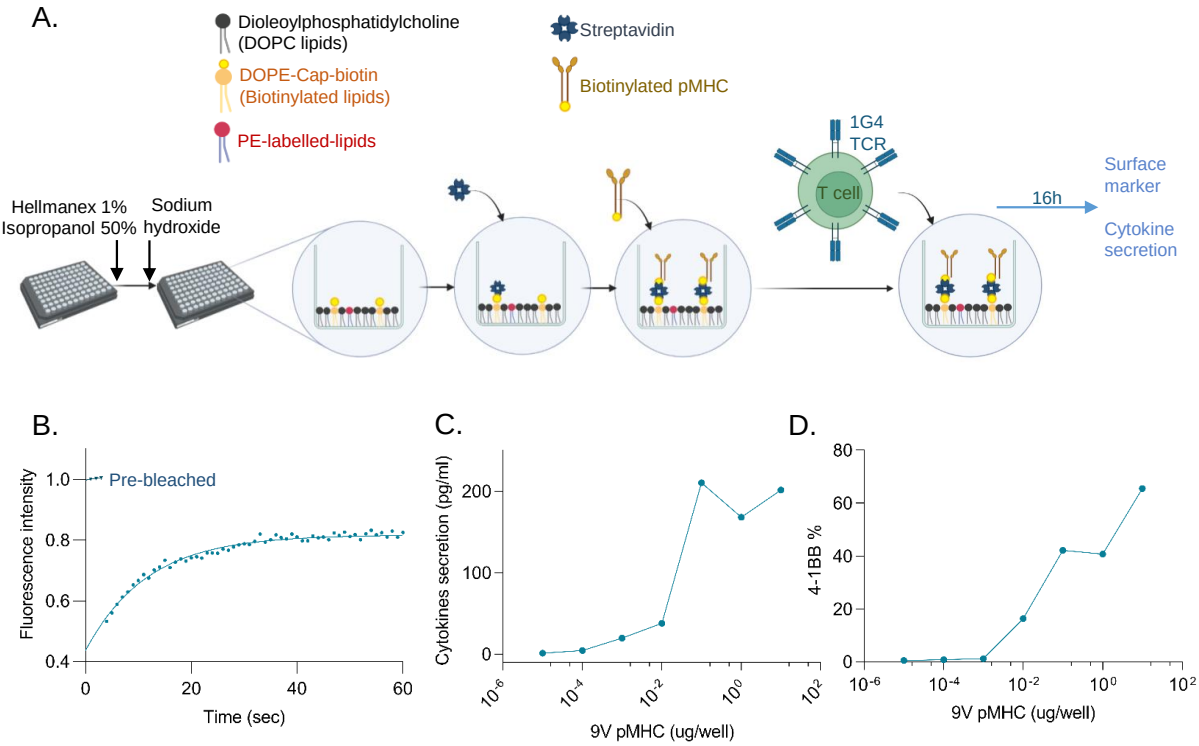


Figure 32: Lipid bilayer-based assay to study the impact of surface molecules on antigen sensitivity. A. Multi-well glass plates are cleaned with a solution of Hellmanex and Isopropanol, followed by a wash with Sodium hydroxide. The plate is coated with a mixture of DOPE-Cap-biotin, PE-lipids in DOPC lipids. Streptavidin is added to the well. Purified biotinylated MHC loaded with peptide is added to the well at titrating concentrations. $1G4^+$ T cells are incubated on the pMHC presenting bilayer for 16h. The impact of surface molecule ligation on T cell functions is studied by staining of T cell for activation markers and measure of cytokine secretion after 8h of stimulation. B. Fluorescence Recovery After Photobleaching (FRAP) of the fluorescently-labelled lipids of the bilayer. A small section of the bilayer is hit by high intensity light (100% laser intensity) for one second, diffusion of the neighbouring fluorescent lipids back into the zone is measured over 60 seconds. C. Cytokine secretion and D. expression of the activation marker 4-1BB upon stimulation of $1G4^+$ T cells on streptavidin-coated plate presenting a titration of 9V peptide on biotinylated MHC. Dose-response curves, one donor.

With the integrity and mobility of the bilayers confirmed, we coated the bilayer with streptavidin molecules that bind to the biotinylated lipids. Because of their multi-valency, these streptavidin molecules constitute anchors on which we can bind our biotinylated protein of choice. We coated the bilayer with a titration of biotinylated pMHC presenting the 9V peptide. As before, primary human $CD8^+$ T cells transduced with the 1G4 TCR were the incubated for 16 hours on these functionalised bilayers. We measured T cell activation by cytokine secretion and 4-1BB expression. We were able to demonstrate that, in this experiment system, both cytokine production and surface marker could readily be detected (figure 32 C-D).

Although it was feasible to generate bilayers in several wells of the 96-well plate, we found it difficult to produce functional bilayers in all 96 wells of the plate. This was partly a result of the manual pipetting required, including multiple manual washing of the plates to avoid disturbing the bilayers. Therefore, additional optimisation would be required for high throughput production of bilayers in the 96-well format.

4.3 Discussion

In the previous chapters of this thesis, we could demonstrate that a plate-based system was adequate to study intracellular signalling molecules. We showed that results obtained on plate could be reproduced in a cell-based system as the phenotypes caused by inhibition of multiple intracellular molecules (Lck, Calcineurin, PI3K and PKCθ) were similar whether obtained in a plate-based system or in a cellular co-culture setting (Chapter 2). When studying accessory receptors, previous work has demonstrated that the plate-based system can be used to observe an impact of co-stimulation receptors on T cell responses, including the ability of CD2, LFA-1, CD28, CD27, and 4-1BB ligation [115][290][128][209]. In the case of PD-1 and CD6 however, this system is insufficient as these molecules did not generate any phenotype while their impact on T cell functions is well described [241][274][273]. We propose that this lack of phenotype is due to the plate environment not providing mobility for proper surface molecules functions. As both CD6 and PD-1 have been shown to be recruited to the immunological synapse [291][276], we hypothesised that the lack of mobility imposed by their plate-bound ligands could prevent their recruitment and interaction with their targets.

We also speculate that the lack of mobility can potentially introduce steric inhibition. When studying the impact of full-length CD166 (ligand for CD6) in our plate-based system, we observed a decrease in T cell antigen sensitivity with increasing concentrations of CD166 in its WT form, but also in presence of the mutated, non-binding, forms of CD166. Because the presence of CD166 only induces an impact of the EC50 of the dose-response curves and not on the E_{max}, this indicates an impact on the binding ability of TCR to pMHC (k_{on}). From this observation we hypothesised that the inhibitory effect could be due to steric hindrance caused by the size of the CD166 molecule effectively masking the pMHC on the plate so that the effective on-rate of TCR binding to pMHC is reduced. Indeed, we evaluate the size

of CD166 based on the structure from Chappel *et al.* to be about 23nm (while pMHC is about 7nm [292]). Chappel *et al.* paper gives us insight on the size of the domains 1-2 of CD166 therefore the size we estimated is a result of an extrapolation of the size of full-length CD166 (composed of 5 domains), from the size of its first two domains. In the absence of more accurate measure and structural information, this size estimate is only a hypothesis. However, we could confirm in the same experiment that the presence of a shorter molecule such as our control protein rCD4 (estimated length 7nm, as its extracellular region is composed of 4 immunoglubulin superfamily domains [293]) did not induce this phenotype.

When reproducing these experiments with short versions of CD166, we observed no phenotype induced by the ligation of CD6, except for one independent repeat that showed a decrease of T cell antigen sensitivity in the presence of the point mutant version of CD166. Validation of the non-binding mutant is made challenging by the fact that CD6 ligation only partially induce its down-regulation, ligation of the TCR by pMHC playing the dominant role in CD6 downregulation. However, we could show that the wild-type version CD166 (CD166 WT) alone was able to induce additional CD6 down-regulation when compared with pMHC-induced alone (figure 30 I). This suggests that CD166 WT alone is able to bind to CD6. This isolated effect of the mutant version of CD166 in appendix figure 57 B could be due to competition of CD166 for streptavidin binding site on the plate. We make sure to avoid competition for the binding sites by keeping protein concentrations under the saturation capacity of the plate, however this isolated phenotype could be due to an calculation error.

Taken together, the negative data obtained when studying PD-1 and CD6 prompt us to reproduce our experiments in a more physiological settings that would allow ligand mobility. Because previous data reported T cell inhibition (decreased cytokine secretion) by PD-1 when assayed on supported lipid bilayers [267], we set out to reproduce our assay in this system. We could show that the system could be set up and was able to induce titrable T cell activation. However, we also showed that prior to experimentation, the set up requires stringent validations to ensure the integrity of the bilayer and the mobility of its lipids. Validation of the mobility of the pMHC and accessory protein anchored would be important and a measure of their diffusion coefficient too. While these controls can be routinely performed on a small number of bilayers, validation of the 96 individual bilayers necessary in our set up prior to each

experiment is time-consuming. These controls, in addition to the lengthy procedure required for the production of the 96 bilayers, can not be performed manually. We conclude that this system would be a good alternative to our set up, providing a more physiological experimental environment, however it requires automation.

Chapter 5

Discussion and future directions

5 Discussion and future directions

In this thesis, we have systematically inhibited intracellular molecules in T cells in order to identify molecules that impact antigen sensitivity and antigen discrimination. These two key properties of T cells have been objects of intense research but identification of the signalling molecules controlling them is still not elucidated.

Using systematic *in vitro* assays, we could show that Lck and PLCγ are involved in T cell antigen sensitivity, as their inhibition directly increased the concentration of antigen required to elicit T cell responses (i.e. EC50). Within the set of signalling molecules we investigated, we found that only Lck was involved in antigen discrimination.

Through the use of our systematic approach, we also focused on molecules whose role in antigen sensitivity and/or discrimination is controversial. We tested the impact of calcineurin, Nck and SHP1, three molecules located distally in the signalling cascade but that had been proposed to play feedback role on the TCR or TCR-proximal molecules [50][207][240][243][244]. In line with previous work, we did not find any evidence for calcineurin [154] or Nck [208] in T cell antigen sensitivity or discrimination. Our experimental assay proved insufficient for the study of SHP1. We were also limited by our experimental assay for the study of the surface molecule PD-1 and CD6, that prompted the development of a new system allowing ligand mobility relying on the production of lipid bilayers. This new experimental assay promised more physiological experimental conditions, however its wide application was hindered by the inability to systematically generate bilayers in high throughput 96-well plate format. Study of the intracellular molecule SHP1 and the surface molecules PD-1 and CD6 will therefore be the object of future research in the lab.

5.1 Strengths and limitations of our set up

The approach we used to study T cell sensitivity and discrimination is different from many methods used in the literature, as it relies on functional data rather than biochemical data. This strategy relies on directly measuring antigen sensitivity or discrimination when inhibiting different molecules instead of association data where the impact on sensitivity and discrimination is inferred from biochemistry (e.g. Co-IP). Functional response was measured through various outputs. In the context of this thesis, we focused on five outputs from T cell activation : the three main cytokines produced by $CD8^+$ T cells :

TNFα, IFNγ and IL-2 and two activation markers: CD69 and 4-1BB (CD137). In the introduction, we provide a review of their regulation by transcription factors showing that induction of the production of IFNγ and IL-2 is shared between the three main transcription factors (NFAT, NFκB and AP-1). This indicates that all three divergent signalling cascades downstream of the TCR are involved in their modulation, while TNFα appears to be mainly dependent on induction by the NFAT transcription factor [77]. In terms of activation markers, both CD69 and 4-1BB are mainly induced by activation of the transcription factors NFκB and AP-1 [78][79]. We made the choice of measuring multiple cytokines (at least 2) together with one or more surface markers in each experiment; while this is not a fully comprehensive measure of T cell functions, it ensured that we had a reporter for the activation of each main pathway. Our work also benefited from recent improvements in measure of peptide affinity through enhanced SPR techniques [115]. These allow the accurate measure of the kd of low affinity non-self peptides, which, in combination with our systematic functional assays, provide us with an enhance measure of T cell discrimination. These enhancements also open the way to the measure of very low affinity peptides such as self-peptides. These would provide us with information on the fold difference of affinity that a TCR must discriminate between, in order to avoid autoimmune response.

As we discussed in chapter 2, the experimental assay we chose to study discrimination was not ideal. We made the decision to measure T cell activation exposed to peptides of 3 different affinities, under 3 concentrations of each inhibitor. However, while these conditions would allow the extraction of large amount of data under fixed conditions, the many variables in our system resulted in some results being non usable. The cellular material we used differed for each repeat as we isolated $CD8^+$ T cells from different donors. As it is well-described in pharmacology, different individuals show different level of response to a same drug, at a given concentration [294]. This can be due to different factors such as cell metabolism [294]. Because of this variability our set up lost its main advantage : providing titration data. In light of these observations, we believe that a set up where T cells would be exposed to more peptides affinities (up to 8 different affinities), but a single inhibitor concentration (unique inhibitor concentration coupled to a no inhibitor control) would be more productive.

5.2 Future directions and applications

In this thesis we present the first systematic analysis of the implication of intracellular signalling molecules in T cell antigen sensitivity and discrimination. This study allowed the identification of Lck and PLCγ as essential actors of T cell sensitivity to antigen and identified Lck as a key actor in T cell discrimination. These findings are in agreement with previous data from the literature suggesting that the level of active-Lck directly impact T cell sensitivity and discrimination [133][134]. As discussed in section 2, *in vitro* assays [136][137], *ex vivo* murine experiments [295] and clinical patients observations [135] point to an implication of ZAP70 and LAT in antigen sensitivity and discrimination. These findings motivate the expansion of our study to these additional signalling molecules, which are signalling intermediates between activation of Lck and PLCγ. In the context of this thesis, we have been limited by the lack of specific inhibitor against ZAP70 and LAT. We have considered alternative approaches:

In the case of ZAP70, an analogue mutant that is sensitive to the small-molecule inhibitor 3MB-PP1 has been designed by the Weiss lab [212]. T cells expressing this analogue in place of the WT version of ZAP70 could be used in the same experimental assays we used to evaluate the role of other signalling molecules in T cell sensitivity and discrimination. This approach comes with the challenge of performing the complete knock-out of an essential signalling molecule in primary T cells. However, ZAP70 is an intracellular protein which add to the challenge of its knock-out because it is not possible to sort T cells based on ZAP70 expression.

In the case of LAT, to our knowledge, no drug-sensitive analogue have been designed. Its inhibition must therefore be carried out through an alternative approach. One possibility is to use the recently described RIPR system [296]. This system relies on the use of a diabody bridging the CD45 phosphatase on one hand, to a candidate molecule on the other hand. It would be interesting to test if such a system, bridging CD45 to LAT could induce LAT de-phosphorylation and/or its exclusion from the immune synapse. If such a technique was to be successful, titration of the RIPR diabody would allow us to produce a inhibitory titration of LAT activity in set-ups similar to the one we used for the study of sensitivity and discrimination.

As we discussed in the introduction, several surface molecules have been identified as playing a role in T cell antigen sensitivity and/or discrimination. The role of multiple accessory receptors (CD2, LFA-1,

CD27, 4-1BB and CD28) have been demonstrated by our lab and others [115][290][116][119][124][126][127]. A role for the co-receptor CD8 has also been proposed [109][110] but is still a matter of debate [27]. Understanding the impact of inhibitory accessory receptors such as PD-1 is key given the wide use of PD-1 blockade in immunotherapy. We discussed the challenges for its study in our original set-up but we believe that research into its mechanism of action and its impact on T cell sensitivity and discrimination is key to optimise its therapeutic efficacy. As mentioned in 4.2.3, the establishment of a new set-up system allowing ligand mobility will allow the continuation of our research on inhibitory accessory receptors.

Sensitivity is an important parameter in the design of CAR T cells, indeed most CAR T cells are designed to target tumour-associated antigens, which are expressed at high level on tumour cells, but also at low levels on healthy tissues. Recognition of these low-expressed antigens on healthy tissues by CAR T cells lead to off-target toxicity [297][298][299]. In these cases, a lower T cell sensitivity, that would recognise the high level of antigens on infected cells but ignore the low-expressing healthy cells would be desirable. Strategies tuning CAR sensitivity to prevent off-target toxicities have been exploited with success in mice [300][301]. In our study, we have identified Lck and PLCγ as key actors in T cell antigens sensitivity, showing that their modulation can impact T cells ability to detect antigens, making them interesting targets for sensitivity modulation.

We also identified Lck as paying an important role in antigen discrimination, and could show that Lck inhibition increases T cells ability to discriminate antigen. As described above, the ability of CAR T cells to discriminate between infected cells and healthy tissue is key to avoid off-target toxicity. However, reproducing the level of discrimination displayed by primary T cells in artificially designed CAR T cells arose as a challenge. This is due to multiple factors, Burton *et al.* [128] showed that CAR T cells failed to capitalise on accessory receptors, consequently decreasing their sensitivity to antigen. Burton *et al.* did not test the impact on antigen discrimination but one could hypothesise that it would be decreased as ligation of accessory receptors have been shown to enhance primary T cell discrimination capacities [115][290][119][116]. Therefore, our research brings essential data regarding mechanisms of antigen sensitivity and discrimination and offers new perspectives for immunotherapy optimisation.

Chapter 6

Material and methods

6 Material and methods

6.1 Methods

6.1.1 Cell lines and maintenance

HEK293 T cells were maintained in DMEM + 10% FBS + 1%PenStrep at 37°c in 10% CO_2 incubator. Every 2-3 days, cells were detached using Trypsin then seeded at 1-2Mio in a 75cm^2 flask.
U87 cells were maintained in DMEM + 10% FBS + 1%PenStrep at 37°c in 10% CO_2 incubator. Every 2-3 days, cells were detached using Trypsin then seeded at 1-2Mio in a 75cm^2 flask.
E6.1 Jurkat cells were maintained in RPMI + 10% FBS + 1%PenStrep at 37°c in 5% CO_2 incubator. Every 2-3 days, cells, 90% of the cells were discarded and the remaining 10% were put back in culture in a 75cm^2 flask.

6.1.2 Lentivirus production

HEK 293 T cells were seeded in 6-well plates 24h before transfection. Transfection mix including packaging plasmids and the 1G4 lentivirus vector with transfection reagent X-treme HP (Table 16) was added to the cells in a total volume of 2ml. The medium was replaced 24h after transfection, the lentiviral supernatant was harvested 24h after medium exchange. The supernatant was filtered through a 0.45μm filter to retain detached cells. The 2ml supernatant produced from each well were used to transduced 1Mio T cells.

6.1.3 Isolation of CD8$^+$ T cells

Whole blood was obtained from healthy donors or leucocytes cones from the NHS (Blood and transplantation service, John Radcliffe Hospital). In the case of healthy donors, 50ml of blood was collected after informed consent has been given. The project is conform to the Medical Sciences Inter-Divisional Research Ethics Committee of the University of Oxford (R51997/RE001). The samples are anonymised according to the Data Protection Act.

CD8$^+$ T cells were isolated using the RosetteSep Human CD8 enrichment cocktail, adding 6μl/ml of whole blood and 150μl/ml of blood from leucocyte cones. The mix was incubated for 20min at room

temperature, then diluted 3.125-fold in PBS in the case of blood cones. The sample was layered on Ficoll Paque Plus (ratio 0.8 to 1 of Ficoll to sample) and centrifugated at 1200g for 20min at room temperature. The gradient allows separation of the buffy coat containing the $CD8^+$ cells from the rest of the leucocytes. The $CD8^+$ layer was harvested, washed in PBS, counted and re-suspended in complete RPMI with 50U/ml of IL-2 and CD3/CD28 Human T-activator dynabeads (ration 1 bead: 1 T cell).

After 24h of activation, $CD8^+$ T cells were seeded at 1Mio/ml in 12 well plates. T cells were transduced by incubation with 2ml of the lentivirus supernatant prepared as described above. The medium was exchanged after 2 and 4 days, replaced with fresh complete RPMI with 50U/ml of IL-2. The activator Dynabeads were magnetically removed after 5 days and the $CD8^+$ T cells were cultured at 1Mio/ml in complete RPMI with 50U/ml of IL-2, with medium exchange every 2 days. The T cells were used for functional experiments between days 10 and 16 post-transduction.

The expression of the 1G4 TCR was checked by staining with 1G4 specific tetramer for each T cell batch.

6.1.4 pMHC tetramer

Tetramers was prepared in-house from monomeric biotinylated peptide-MHC (NYE 9V), mixed with streptavidin-PE (1 in 4). Streptavidin was added to the biotinylated pMHC in 10 steps, every 10min on shaker, at room temperature. The mix was then briefly centrifuged at 13000g to remove insoluble proteins. The tetramers were kept at 4c in 0.1% azide.

6.1.5 Peptides

We used peptides derived from the NYE-$ESO_{157-165}$ peptide (sequence SLLMWITQC), but carrying a valine as 9^{th} residue at position 165 for a more efficient loading on HLA-A*02 as described by [302]. The NYE-ESO peptide variants binds the 1G4 TCR as described and characterised in [115] and [197].

Peptide	Sequence	Kd (υM)
9V	SLLMWITQV	8
4A8K	SLLAWTTKV	2
3Y	SLYMWITQV	47
6T	SLLMWTTQV	162

Table 1: Affinities of the NYE-ESO peptides variants for the 1G4 TCR

Peptides were obtained from Peptide Protein research, UK at purity >95%.

6.1.6 Functional assay : incubation of T cells on plate

Streptavidin-coated plates were washed with PBS. Biotinylated peptide MHC proteins were diluted in PBS to the chosen concentrations (Table 5). The solution was added to the plate in 50μl/well and incubated at room temperature for 30min. The plates were washed twice in PBS. When used, biotinylated accessory ligand(s) were diluted to the chosen concentration in PBS (Table 6). The solution was added to the plate and incubated for 30min at room temperature.

In the context of inhibitory experiment, the 1G4 TCR-expressing $CD8^+$ T cells were undergoing the chosen inhibitory method (described below) for 1h (Table 2).

In stimulation without inhibitor, we proceeded directly to the next step.

After 30min, the plates were washed twice in PBS. The $CD8^+$ T cells were resuspended at 250 000Mio/ml in complete RPMI for stimulation experiments, in RPMI+inhibitor in the context of inhibitor experiments, and added to the coated plates (at 50 000 cells/well). The plates were spun for 1min at 50g to facilitate cell contact with the ligands. The cells were incubated at 37°c for 4-24h depending on the experiment.

6.1.7 Functional assay : co-culture of T cells with U87

U87 cells were detached using Trypsin, counted and resuspended at 250 000/ml in complete DMEM. 25 000 cells/well (100μl) were seeded in flat-bottom 96-well plates overnight. On experiment day, the U87 medium was discarded. Peptides were diluted in complete DMEM to reach the chosen concentration (Table 5). The prepared solution was added to the U87 at 100μl/well and incubated at 37°c for 1-2h. While the peptide was incubating, the 1G4 TCR-expressing $CD8^+$ T cells were undergoing the chosen

inhibitory treatment (described below) for 1h (Tables 3 and 4). After peptide incubation and inhibitor treatment were complete, the peptide solution was discarded. Pre-treated $CD8^+$ T cells are added to the U87 plate at 50 000 cells/well in 200μl. Plates were spun for 1min at 50g to facilitate contact between T cells and U87. The co-culture was incubated for 4-6h at 37˚c. After the incubation time, 5mM EDTA was added to the mix to help detach the cells by pipetting. The mix was spun down at 520g for 5min to pellet the cells. The supernatant was harvested and used fresh in ELISA to detect cytokine secretion. Cells were stained and analysed by flow cytometry.

6.1.8 Inhibition by small-molecule chemical inhibitor

1G4 TCR expressing $CD8^+$ T cells were counted and re-suspended at 312 500 cells/ml in complete RPMI. T cells were distributed at 62 500 cells/well (200μl) in round-bottom 96 well plates. The inhibitor was diluted in complete RPMI to reach 5x final concentration. 50μl of the inhibitor solution was added to the T cells (to reach 1x final concentration). All inhibitor concentrations used are summarised in tables 2, 3 and 4. The T cells underwent inhibitor pre-treatment for 1h before being placed on streptavidin-coated plates or in co-culture with loaded U87 as described above.

6.1.9 Flow cytometry

Cells were washed once in PBS by centrifugation for 5min at 520g. When stained with a viability dye, they were incubated for 20min at room temperature with the viability marker (1:10000). They were then washed in PBS/1% BSA and stained by a mix of antibodies (1:200) and tetramer (1:500-1000) for 20min at 4˚c in the dark. The cells were washed in PBS/BSA and resuspended in PBS, and analysed by flow cytometry using the X20 or Cytoflex cytometer. The analysis obtained through these machines were analysed using FlowJo^{TM}. All antibodies and concentrations used are in table 11.

A jurkat cell line transduced with a Cyan Fluorescent Protein (CFP) reporter induced by the expression of the Nuclear Factor of Activated T-cells (NFAT-CFP) were used in some experiments. This reporter is excited at 405nm and emits around 480nm.

6.1.10 Surface staining of TNFα

The cytokine TNFα is produced as a membrane-integrated protein. Its release depends on its cleavage by the metalloprotease TNFα converting enzyme (TACE also known as ADAM17). In order to measure the amount of TNFα present on the cell surface prior to its cleavage, we treated T cells with an inhibitor of TACE (TAPI-0 at 100μM) after 2h of stimulation. This treatment makes TNFα a surface-bound molecule, it is therefore detectable by surface staining by flow cytometry.

6.1.11 Enzyme-linked immuno-assays

ELISA are performed using Uncoated IFNγ TNFα or IL2 Kit to measure cytokine secretion. Nunc Maxisorp 96-well plates were coated with capture IFNγ, TNFα or IL-2 antibodies overnight, according to manufacturers instructions. Plates were washed 3x with ELISA washing buffer. Plates were blocked for a minimum of one hour with diluent according to manufacturers instructions. Diluent was discarded and standard curve was established by 8 dilutions of the standard provided by the manufacturer. The samples to test were diluted in diluent 4-10x and incubated overnight at 4°c. The plates were washed 3x with ELISA washing buffer and incubated for 1h with IFNγ, TNFα or IL2 detection antibodies according to the manufacturers instructions. Plates were washed 3x in ELISA washing buffer and incubated for 20-30min with avidin or streptavidin coupled to HRP according to manufacturers instructions. The plates were washed 6x with ELISA washing buffer. The concentration of HRP was revealed by addition of TMB brought to room temperature. The reaction was stopped using sulfuric acid (1M). Absorbance was measured using a SpectraMax plate reader. A linear line was plotted to fit the standard curve. The concentration of the samples are intrapolated using the equation of this curve.

6.1.12 Re-constitution of SHP-1 KO jurkats cells by protein electroporation

Prior to electroporation, the cells were counted and resuspended at 2x the desired final amount to compensate for cell loss and death induced by the protocol. Cells were washed 3 times in optiMEM medium, and resuspended in 50μl final volume in the BTX BIG R cuvettes.

The SHP-1 purified protein was added to the cuvettes to reach the desired final concentration (Table 8). Cells underwent electroporation to internalise the SHP-1 protein for 2msec at 300V. Electoporated cells were divided in 2 fractions :

- One fraction was put in culture in warm RMPI media. This fraction will be used for functional experiments.

- One fraction was washed 3 times in PBS then frozen as cell pellet. This fraction will be used for Western Blot.

6.1.13 Preparation of the bilayer-based stimulation platform

Glass plates must be washed before addition of lipids. Glass-bottom multi-well plates were washed overnight with 100μl of a solution of 1 % Hellmanex III^{TM} with 50% isopropanol. The wells were washed 7 times with 200μl of ultrapure water then dried by centrifugation for 1min at 200rpm. The wells were incubated for 1h with 100μl of sodium hydroxide (3N), followed by 7 washes with 200 μl of ultrapure water then dried by centrifugation for 1min at 200rpm.

Lipids mix are made of :

- 0.2% of 488-labelled lipids
- 10% of biotinylated lipids (DOPE-Cap-biotin)
- 89.8% of DOPC lipids

Each well was filled with 100μl of lipids mix and incubated for 20min then washed 7 times with 200μl of PBS with 0,1% Bovine Serum Albumin (BSA). The bilayer was blocked using a solution of 2% BSA in PBS before addition of 200μl of streptavidin at 5μg/ml for 20min. Streptavidin-coated bilayer was washed 7 times with 200μl of 0,1% BSA in PBS before addition of the biotinylated MHC loaded with 9V peptide at titrating concentrations (see table) then washed 7 times with 200μl of 0,1% BSA in PBS.

6.1.14 Fluorescence Recover After Photo bleaching (FRAP) on bilayers

Bilayers were imaged using the Olympus FV1000 microscope. To ensure proper fluidity of the lipid bilayer, a small section (10-20μm) was briefly (1 second) exposed to high intensity light (100% laser intensity). Images were acquired every 0.6sec, with 3 frames acquired before bleaching. Images were then acquired for 60 seconds post-bleaching.

The average fluorescence was measured at the site of bleaching and at a control site outside of the bleached area. Because the bilayer might be affected by the surge in light intensity outside of the focus

area, variation of average intensity in the bleached area were normalised to the average fluorescence in the control area.

6.1.15 Concentrations tables

Inhibitor concentrations used in sensitivity experiments on plates

Inhibitor	Molecule	Top concentration (nM)	Dilution factor	Number of dilution
A-770041	Lck	1000	4	11+blank
Cyclosporin A	Calcineurin	300	3	11+blank
Pictilisib	PI3K	1000	4	11+blank
Sotrastaurin	PKC	1000	4	11+blank

Table 2: Inhibitor concentrations used in sensitivity experiments on plate

Inhibitor concentrations used in sensitivity experiments by co-culture

Inhibitor	Molecule	Top concentration (nM)	Dilution factor	Number of dilution
A-770041	Lck	1000	4	11+blank
U73-122	PLCg	1500	2	11+blank
Cyclosporin A	Calcineurin	1000	4	11+blank
Pictilisib	PI3K	1000	4	11+blank
Sotrastaurin	PKC	1000	4	11+blank
Trametinib	MEK	1000	4	11+blank
Rapamycin	mTorc1	1000	4	11+blank
AX-024	Nck	10 000	4	11+blank
CK666	Arp2/3	200	2	11+blank
Latrunculin B	Actin	10 000	4	11+blank
Cytochalasin D	Actin	10 000	2	11+blank

Table 3: Inhibitor concentrations used in sensitivity experiments by co-culture

Inhibitor concentrations used in discrimination experiments by co-culture

Inhibitor	Molecule	Top concentration (nM)	Dilution factor	Number of dilution
A-770041	Lck	90	3	3+blank
U73-122	PLCg	1500	5	3+blank
Cyclosporin A	Calcineurin	90	3	3+blank
Pictilisib	PI3K	90	3	3+blank
Sotrastaurin	PKC	90	3	3+blank
Trametinib	MEK	30	5	3+blank
AX-024	Nck	10 000	4	3+blank
CK666	Arp2/3	200	2	3+blank
Latrunculin B	Actin	800	4	3+blank

Table 4: Inhibitor concentrations used in sensitivity experiments by co-culture

Peptide concentrations used on plate

Peptide	Top concentration	Dilution factor	Number of dilution
4A8K	2000ng/well	5	11+blank
9V	2000ng/well	5	11+blank

Peptide concentrations used on sensitivity experiments by co-culture

Peptide	Top concentration	Dilution factor	Number of dilution
9V	100uM	8	11+blank

Peptide concentrations used on discrimination experiments by co-culture

Peptide	Top concentration	Dilution factor	Number of dilution
9V	100uM	12	7+blank

Table 5: Peptide concentrations used in experiments

Accessory receptor used in plates experiments

	Protein	Top concentration used (ng/well)	Diluation factor	Number of dilutions
Titrating proteins	PD-L1	1000	2	3 +blank
	CD166 long	1000	2	4+blank
	CD166 short	400	2	4+blank

	Protein	Constant concentration used (ng/well)
Constant concentration proteins	PD-L1	1000
	CD58	250
	ICAM	50
	CD86	250

Table 6: Concentrations of accessory proteins used

Proteins added to the bilayer			
Protein	Top concentration used (ng/well)	Dilution factor	Number of dilution
9V pMHC	10 000	10	7+blank

Table 7: Concentrations of proteins used on bilayer experiments

Proteins added to cells by electroporation			
Protein	Top concentration used (υM)	Dilution factor	Number of dilutions
SHP-1 purified protein	1	10	5+blank

Table 8: Concentrations of proteins used in electroporation experiments

6.2 Modeling

6.2.1 Model parameters and ODE

Parameters

Synthesis rates

ksyn = 1e-2 $(molecules/um^2/s)$

kbasal = 1e-4 $(1/s)$

kdown = 5e-3 $(1/s)$

Binding rates

kon = 0.1 (um^2/s)

koff = 1 $(1/s)$

Activation rates

kp = 1 $(1/s)$

Outputs

kprod = 1

ystar = 0.5

sigystar = 0.1

kremove = 1e-4*100

Ligand titration

25 values of ligand concentrations are modelled between concentrations of 10^{-3} and 10^{3}, on a logarithmic scale.

LT=logspace(-3,3,25)

Time points

12 time point values are modelled between 0 and 1 on a linear scale.

timepoints = linspace(0,1,12)

Model parameters

L	Available ligand for binding
LT	Total ligand
C0	Non-phosphorylated ligand/TCR complex
Cn	Ligand/TCR complex after n phoshorylation steps
ksyn	Synthesis rate of the TCR
kbasal	Basal rate of TCR downregulation
kon	on-rate of the ligand/TCR interaction
koff	off-rate of the ligand/TCR interaction
kdown	Rate of binding-induced TCR downregulation
kp	Phosphorylation rate
kact	Activation rate of effectors located before the switch
kprod	Production rate of activated effectors after the switch
kdeg	Degradation rate of previously activated effectors
erf	Error function
ystar	Threshold to be reached to trigger the switch
sig_ystar	Standard deviation of ystar (threshold)
kremove	Downregulation of surface marker
x(1)	Receptor on the surface
x(2)	Unphosphorylated receptor on the surface
x(3)	Phosphorylated receptor on the surface
x(4)	Activated TCR-signalling effectors before the switch
x(5)	Non saturating output such as cytokine
x(6)	Saturating output such as surface marker

Table 9: Definition of the parameters used in the model

We model T cell signalling using a set of 6 ordinary differential equations (ODE)

Free ligand (L) is defined as ligand that is not involved in an interaction with the receptor (R) alone or in a complex (C0 or CN).

L = LT - x(2) - x(3)

Available receptor is defined as receptors present on the surface of the T cells and not bound to a ligand. The amount of available receptor is provided by new receptor synthesis (ksyn) and removed from

the surface through basal degradation (kbasal). The amount of available receptor is the amount that is not involved in interaction with the ligand (L), and the receptors that have unbound from the complexes (C0 or CN).

dxdt(1,1) = ksyn - kbasal*x(1) - kon*L*x(1) + koff*(x(2) + x(3))

The formation of the immature complex C0 directly depends on the binding of available receptor to ligands. Formation of the immature complex C0 leads to unbinding of the receptor, phosphorylation of the complex and downregulation of the receptor.

dxdt(2,1) = kon*L*x(1) - (koff + kp + kdown)*x(2)

The formation of a mature complex CN directly depends on phosphorylation of the immature complex. It is limited by receptor unbinding and receptor downregulation.

dxdt(3,1) = kp*x(2) - (koff + kdown)*x(3)

Activation of intracellular effectors depends on signal provided by the mature complex CN. Activation is only possible for effector not yet activated and is limited by their degradation following their activation.

dxdt(4,1) = kact*x(3)*(1 - x(4)) - kdeg*x(4)

We observed two outputs as markers of T cell activation : the secretion of cytokines and the expression of surface marker. They both depends on the activation of effectors at the previous step to be sufficient to overcome a threshold ystar. Cytokines can accumulate over time without saturation.

dxdt(5,1) = kprod*(1/2 + (1/2)* erf((x(4) - ystar)/(sqrt(2)*sigystar)))

Surface markers upregulation however saturates overtime, once all T cells have upregulated the activation marker.

dxdt(6,1) = kprod*(1/2 + (1/2)* erf((x(4) - ystar)/(sqrt(2)*sigystar))) - kremove*x(6)

The ODE15 is used to solve our system of ODE.

6.2.2 Fitting dose-response curves

EC50 and Emax values for dose-response curves are obtained after fitting of the curves with a sigmoid or bell shape curve on MatLab.

Sigmoid fit

$y = p(1) + ((p(2) - p(1))./(1 + (p(3)./x).^{p}(4)))$

Where :

p(1) = Emin

p(2) = Emax

p(3) = EC50

p(4) = Hill number of inhibition - constrained as 2

Bell shaped curve

$y = p(1) + p(2).*Section1 - p(2).*p(3).*Section2$

Where

$Section1 = 1./(1 + (p(4)./x).^{p}(5))$

$Section2 = 1./(1 + (p(4).*p(6)./x).^{(}p(7)))$

p(1) = background

p(2) = maximum of activation

p(3) = maximum of inhibition (as a fraction of activation, <1)

p(4) = EC50 of activation

p(5) = Hill number of activation - constrained as 3

p(6) = EC50 of inhibition (as a fold of activation, >1)

p(7) = Hill number of inhibition - constrained as 1.5

Extraction of values from sigmoid and bell-shaped fitted curves:

Extract EC50 from sigmoid curve fit : $sEC50(i) = x_fit(find(sy_fit >= (sEmax(i) + sEmin(i)) * 0.5, 1))$

Extract Emax from sigmoid curve fit : $sEmax(i) = max(sy_fit)$

Extract Threshold value from sigmoid curve : $sP(i) = min([x_fit(find(sy_fit >= P_threshold, 1)), max(x_fit)])$

Extract EC50 from bell-shaped curve fit : $bEC50(i) = x_fit(find(by_fit >= (bEmax(i) + bEmin(i)) * 0.5, 1))$

Extract Emax from bell-shaped curve fit : $bEmax(i) = max(by_fit)$

Extract Threshold value from bell-shaped curve : $bP(i) = min([x_fit(find(by_fit >= P_threshold, 1)), max(x_fit)])$

Statistical tests were performed using GraphPad v 9.0. p values were represented by

NS (Not Significant) p = >0.05

* = p $\leq$ 0.05

** = p $\leq$ 0.01

*** = p $\leq$ 0.001

6.3 Reagents

Cell lines

Name	Source
HEK293T	Previously obtained
U87	Vincenzo Cerundolo
Jurkat E6.1 NFAT-CFP	John Nguyen

Table 10: Cell lines

Antibodies and cell staining solutions

Target/Clone	Conjugate	Supplier	Catalogue number
Zombie NIR Fixable Viability Kit	NIR	Biolegend	423106
Human CD137 (4B4-1)	BV421	Biolegend	309819
Human CD45 (TS2/9)	BV421	Biolegend	304032
Human CD69 (FN50)	AF647	Biolegend	310918
Human CD69 (FN50)	BV421	Biolegend	310930
Human TNFα (MAb11)	APC	Biolegend	502913

Table 11: Antibodies and cell staining reagents

Chemical inhibition reagents

Small molecule inhibitor	Supplier	Catalogue number
A-770041	Merck	SML2678-5MG
AX-024 (Hydrochloride)	Cambridge Bioscience	CAY27333-1 mg
C8273-1MG (Cytochalasin D)	Sigma-Aldrich	C8273-1MG
Cyclosporin A	Sigma-Aldrich	30024-25MG
GDC-0941 (Pictilisib)	Abcam	ab141352
Latrunculin B	Sigma-Aldrich	L5288-1MG
Rapamycin	Cambridge Bioscience	CAY13346-1 mg
Sotrastaurin	Cambridge Bioscience	CAY16726-1 mg
Trametinib	Cambridge Bioscience	CAY16292-1 mg
U-73122	Sigma-Aldrich	U6756-5MG

Table 12: Chemical inhibition reagents

Functional assay reagents

Item	Supplier	Catalogue number
Human IL-2 Uncoated ELISA Kit	Thermo Fisher Scientific	88-7025-77
Human TNFa Uncoated ELISA Kit	Thermo Fisher Scientific	88-7346-77
Human IFNg Uncoated ELISA Kit	Thermo Fisher Scientific	88-7316-88
PE-Streptavidin	Biolegend	405245
Sulfuric acid	Merck	339741
Tween 20	Merck	P1379

Table 13: Functional assay reagents

Cell culture reagents

Reagent	Supplier	Catalogue number
BSA	Merck	A7906
DMEM	Merck	D6429
DMSO	Merck	D8418
DPBS	Merck	D8537
Dynabeads Human T-Activator CD3/CD28	Thermo Fisher Scientific	11132D
EDTA 0.5M, pH8	Thermo Fisher Scientific	15-575-020
FBS	Merck	F9665
Ficoll Paque Plus	Amersham Biosciences	17-1440-02
Opti-MEM with GlutaMAX	Thermo Fisher Scientific	51985034
Penicillin-streptomycin (10 000U/ml and 10ug/ml)	Thermo Fisher Scientific	15140122
Recombinant human IL-2	PeproTech	200-02
RosetteSep Human CD8+ T Cell Enrichement Cocktail	Stemcell Technologies	15063
RPMI 1640 Medium	Merck	R8758
Solution 13	Chemometec	910-3013
TrypLE Express	Thermo Fisher Scientific	12604013

Table 14: Cell culture reagents

Buffers and media

Buffer	Composition
ELISA washing buffer	PBS 0.05% Tween 20
Flow cytometry fixing buffer	PBS 1%BSA 4% Formaldehyde
Flow cytometry staining buffer	PBS 1%BSA
Complete RPMI	RPMI 10% FCS 1%Penicillin/Streptomycin
Complete DMEM	DMEM 10%FCS Penicillin/Streptomycin

Table 15: Buffers and media

Transfection mix

Plasmid/Reagent	Supplier	Catalogue number	Amount/well
pRSV-Rev	Addgene	12253	0.95ug
pVSV-G (pMD2.G)	Addgene	12259	0.37ug
pGAG (pMDLg/pRRE)	Addgene	12251	0.95ug
pHR-1G4	Adaptimmune (gift)	N/A	0.8ug
X-tremeGENE HP Transfection Reagent	Merck	6366546001	9ul

Table 16: Transfection mix

Lipid bilayer reagents

Reagent	Supplier	Catalogue number
Hellamex™ III	Sigma-Aldrich	9-307-011-4-507
DOPC Lipids	Gift from Dustin lab	N/A
DOPE-Cap-Biotin	Previously obtained from Dustin lab	N/A
ATTO 488 DOPE	Avanti Polar Lipids	AD-488-161

Table 17: Lipid bilayer reagents

Consumables

Item	Supplier	Catalogue number
6-well tissue culture plates	Corning	3516
12-well tissue culture plates	Greiner	665180
96-well Maxisorp plates	Thermo Fisher Scientific	442404
96-well tissue culture plates, flat bottom	Corning	3596
96-well tissue culture plates, round bottom	Corning	3799
96-well plates tissue culture plates, conical bottom	Corning	3898
Syringe end filters 0.22um	Sartorius	16534-K
Syringe end filters 0.45um	Sartorius	16555-K
T25 flasks	Corning	430639
T75 flasks	Corning	430641U
T175 flasks	Corning	431080
Cuvettes Plus™ Electroporation Cuvettes, BTX™	Harvard Apparatus	45-0125
Nunc MaxiSorp 96-well plates	Thermo Fisher Scientific	442404
Pierce™ Streptavidin Coated High Capacity Plates, 96-Well	Life Technologies	15500

Table 18: Consumables

Equipment

Equipment	Supplier
Allegra X-15 centrifuge	Beckman Coulter
BD X-20 flow cutometer	BD Biocsciences
Cytoflex flow cytometer	Beckman Coulter
ECM 830 Square Wave Electroporator	BTX
ELx405 microplate washer	BioTek
Nucleocounter NC-3000 cell counter	Chemometec
SpectraMax M5 Gemini plate reader	Molecular Devices

Table 19: Equipment

Software and package

Software	Version	Supplier
FlowJo	v10	BD Biosciences
GraphPad Prism	v7-9	GraphPad Software
MatLab	R2019A	MathWorks
Excell	2016	Windows
LaTeX	5.1.3 (2020)	TexWorks

Table 20: Softwares and packages

7 Appendix

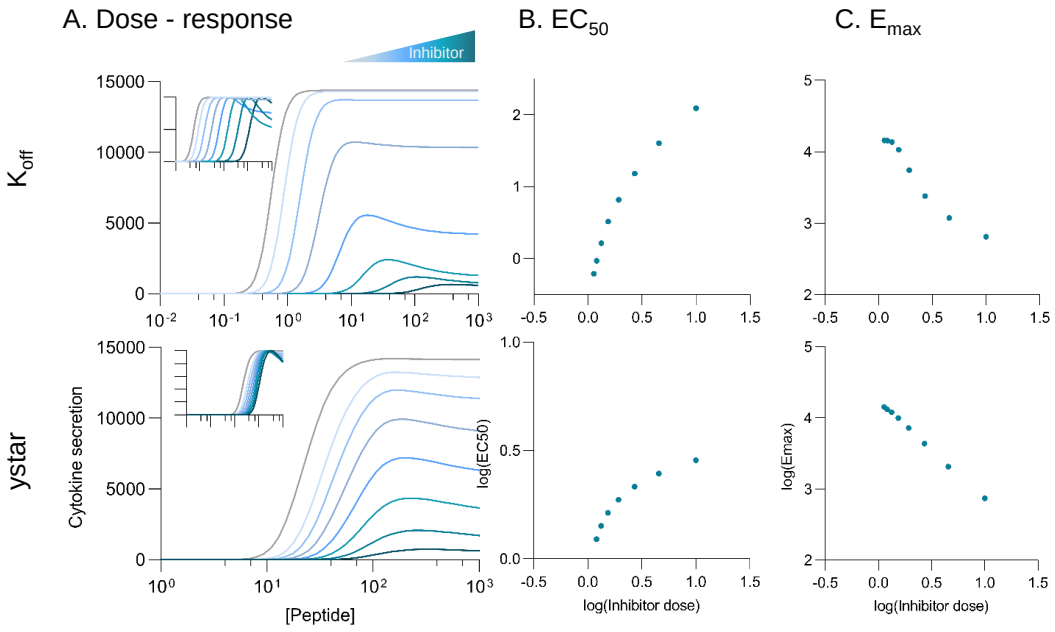


Figure 33: Phenotypic model as described in figure 6. Simulated degrees of inhibition on the reaction rates (koff and ystar) predict the impact on the E_{max} and EC50 of the dose-response curves. (B. column) The value of EC50 determined from the dose-response curves in (A) over the degree of inhibition of the indicated parameter. (C. column) The value of E_{max} determined from the dose-response curves in (A) over the degree of inhibition of the indicated parameter.

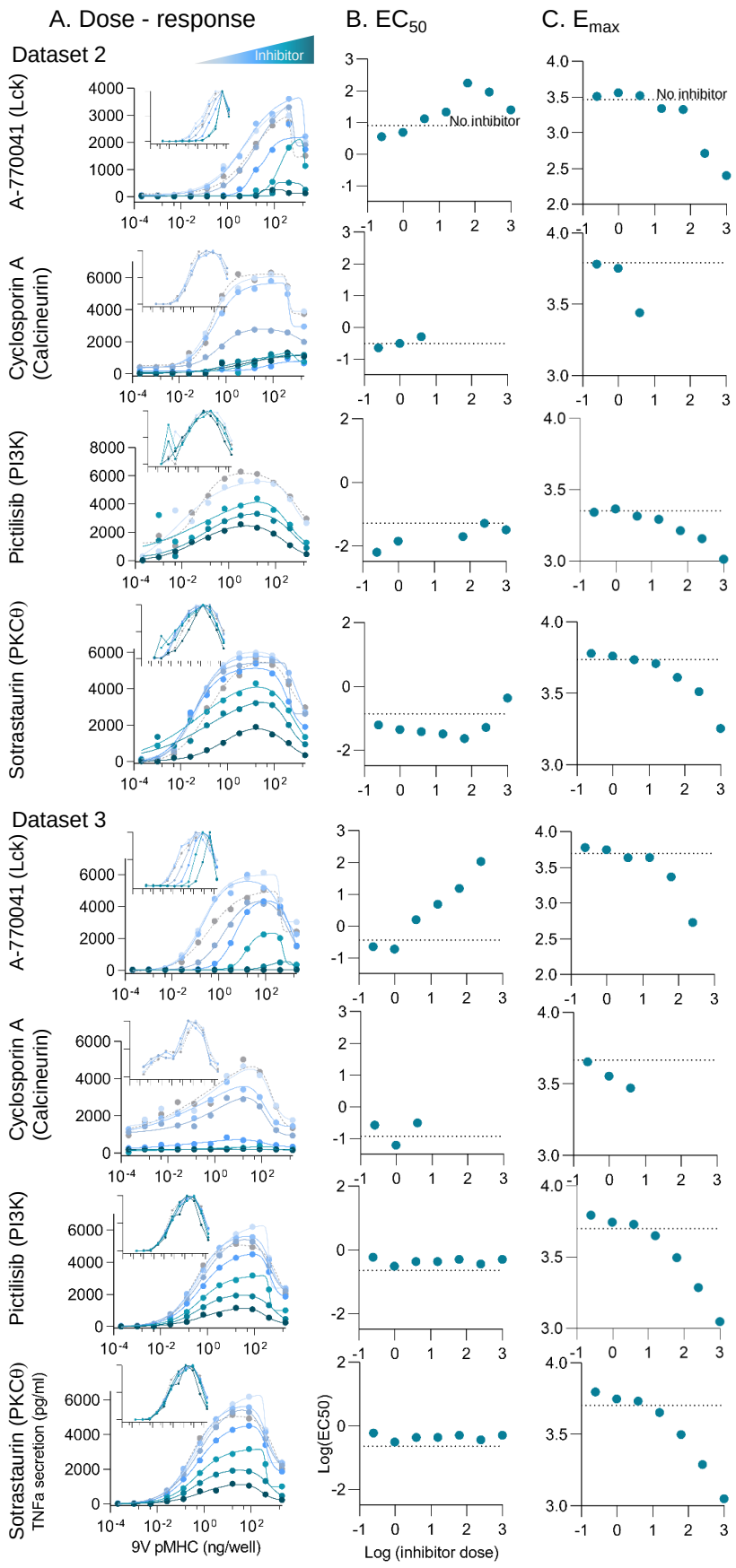


Figure 34: Independent repeat as described in figure 9.

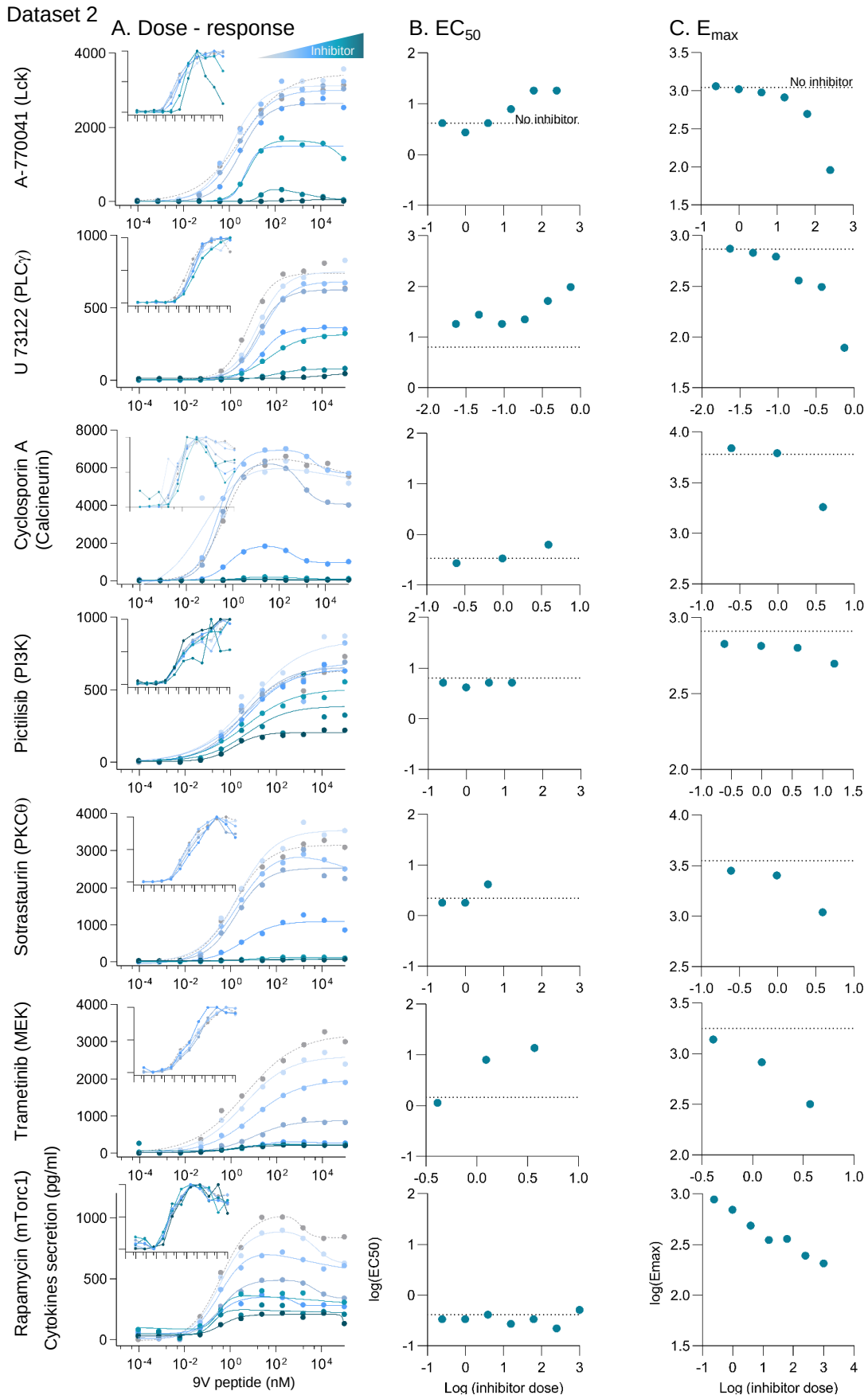


Figure 35: Independent repeat as described in figure 11.

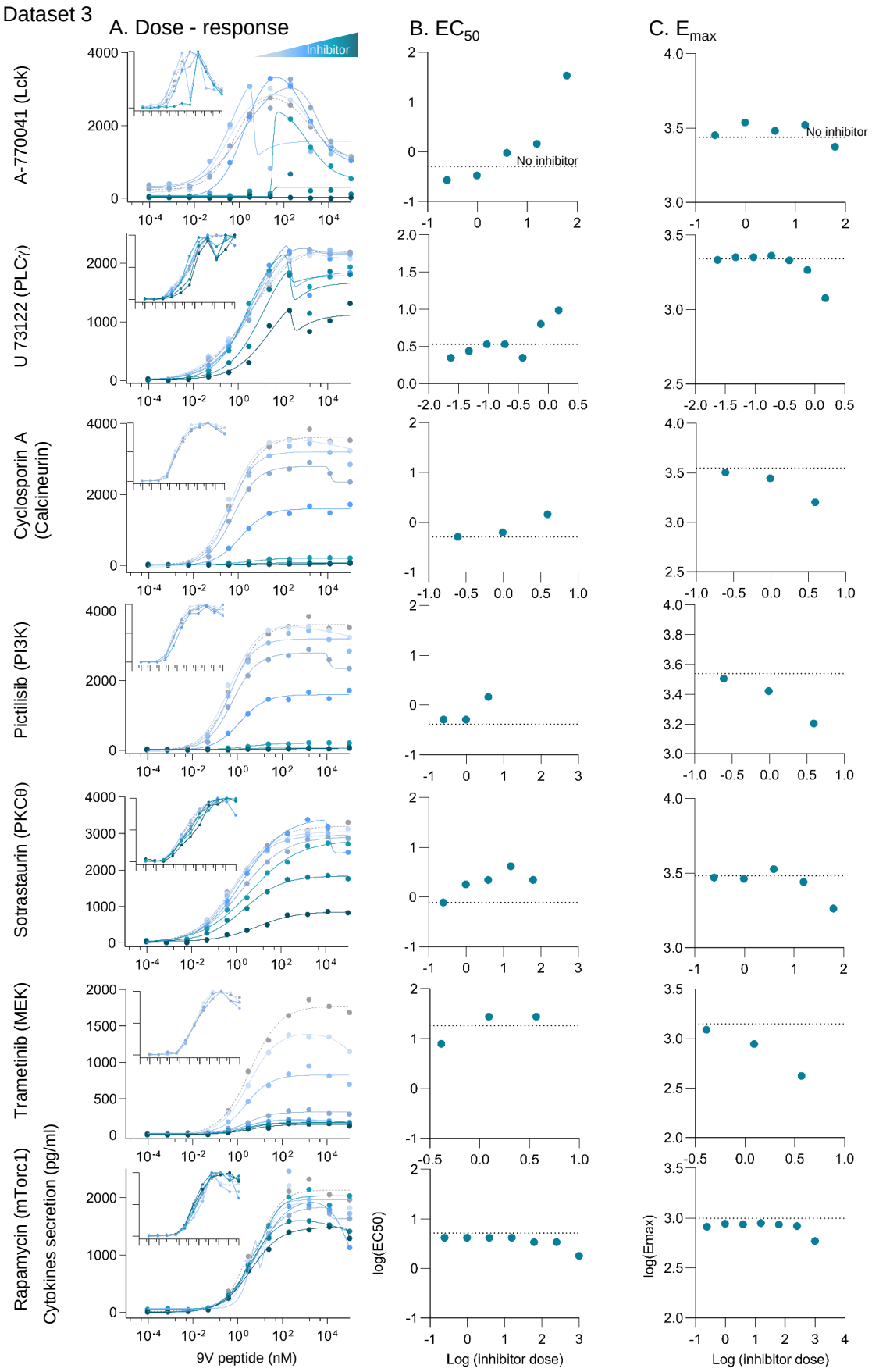


Figure 36: Independent repeat as described in figure 11.

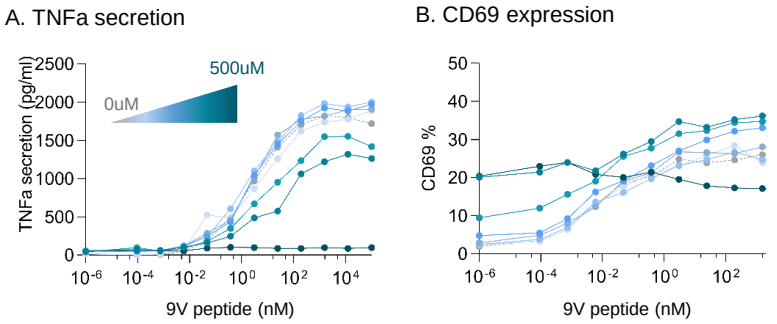


Figure 37: Optimisation of the CK666 (Arp2/3 inhibitor) concentrations range measured by impact on cytokine production and surface marker expression in an APC co-culture assay. (A. column) Dose-response curves under titrating concentrations of the CK666 inhibitor, one representative donor.

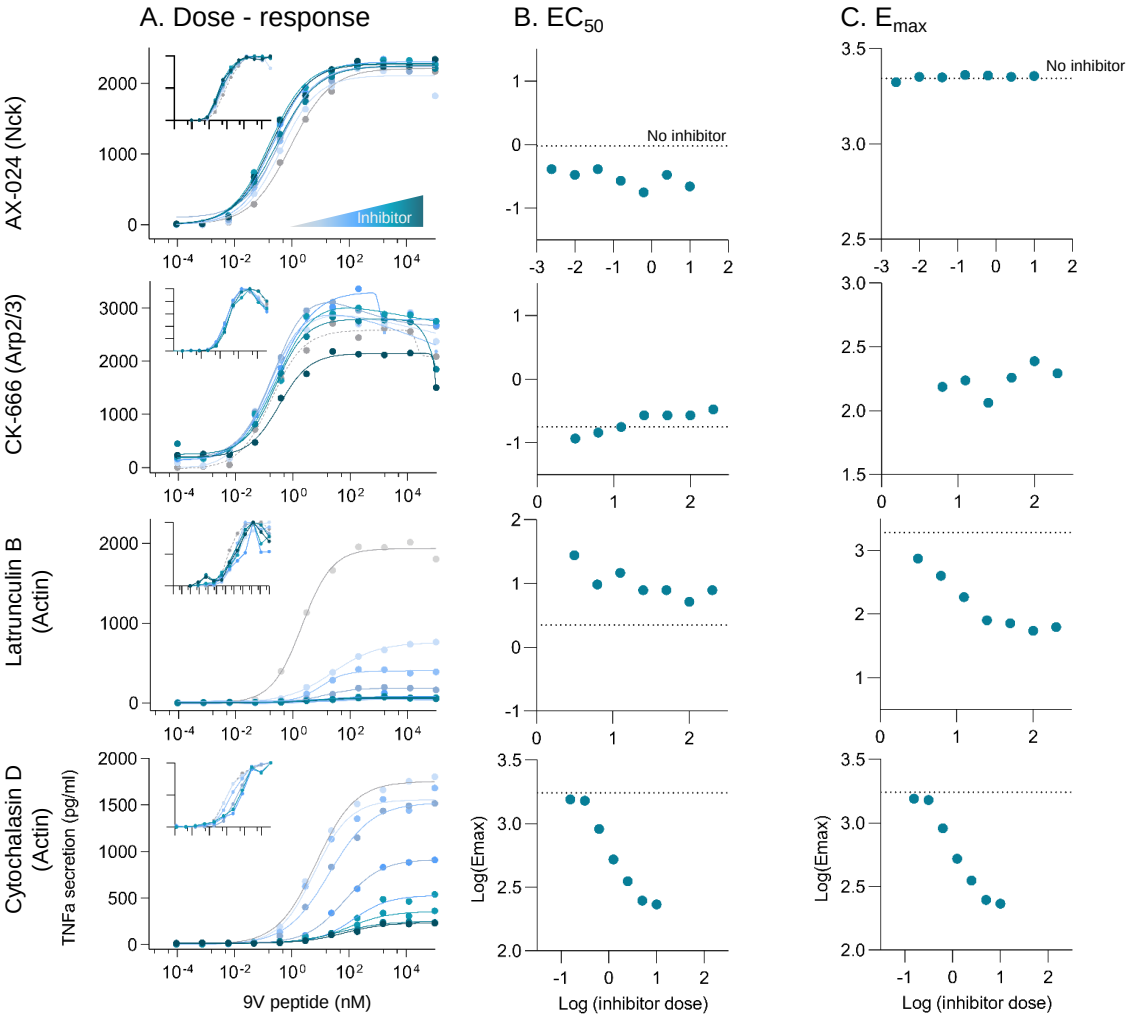


Figure 38: Independent repeat as described in figure 12.

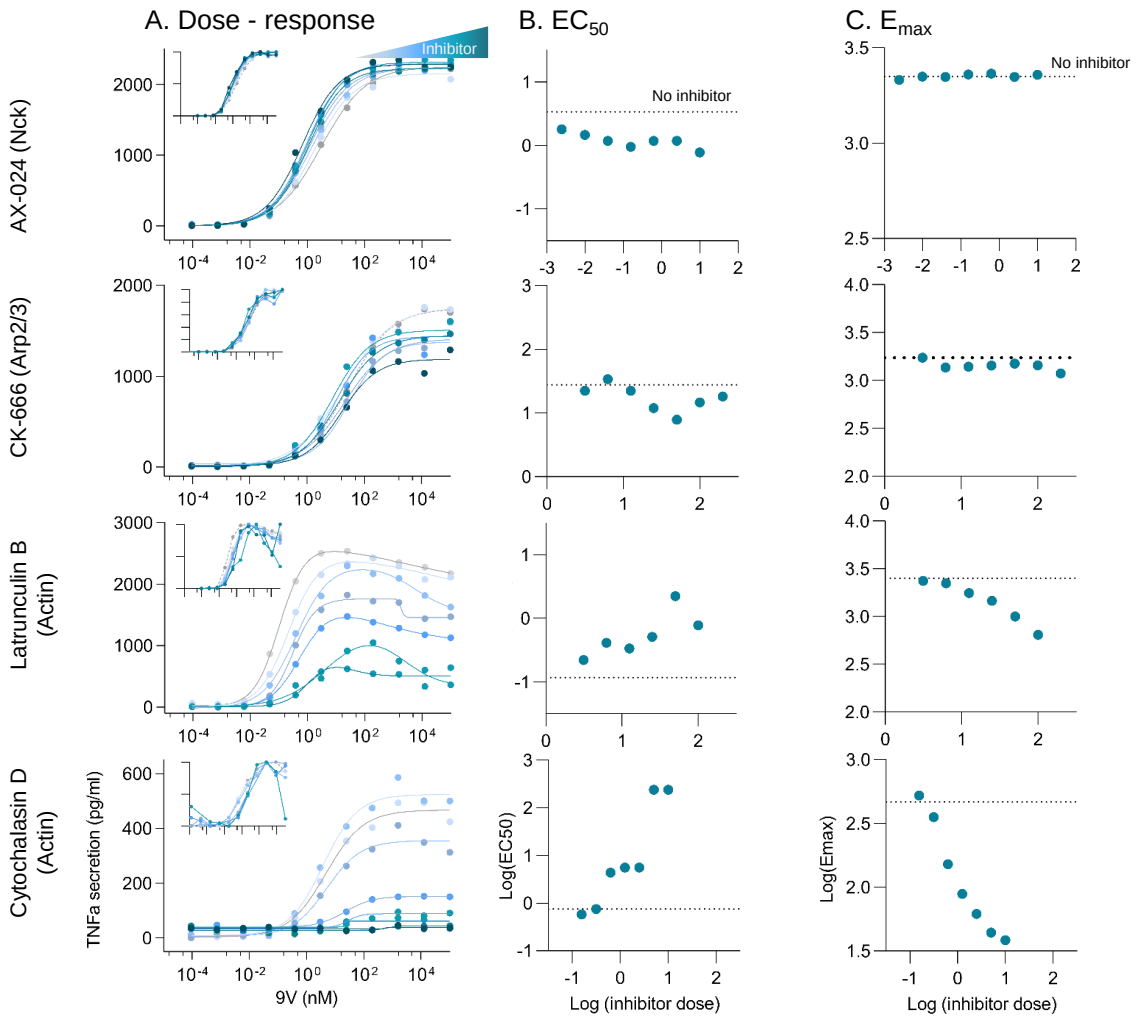


Figure 39: Independent repeat as described in figure 12.

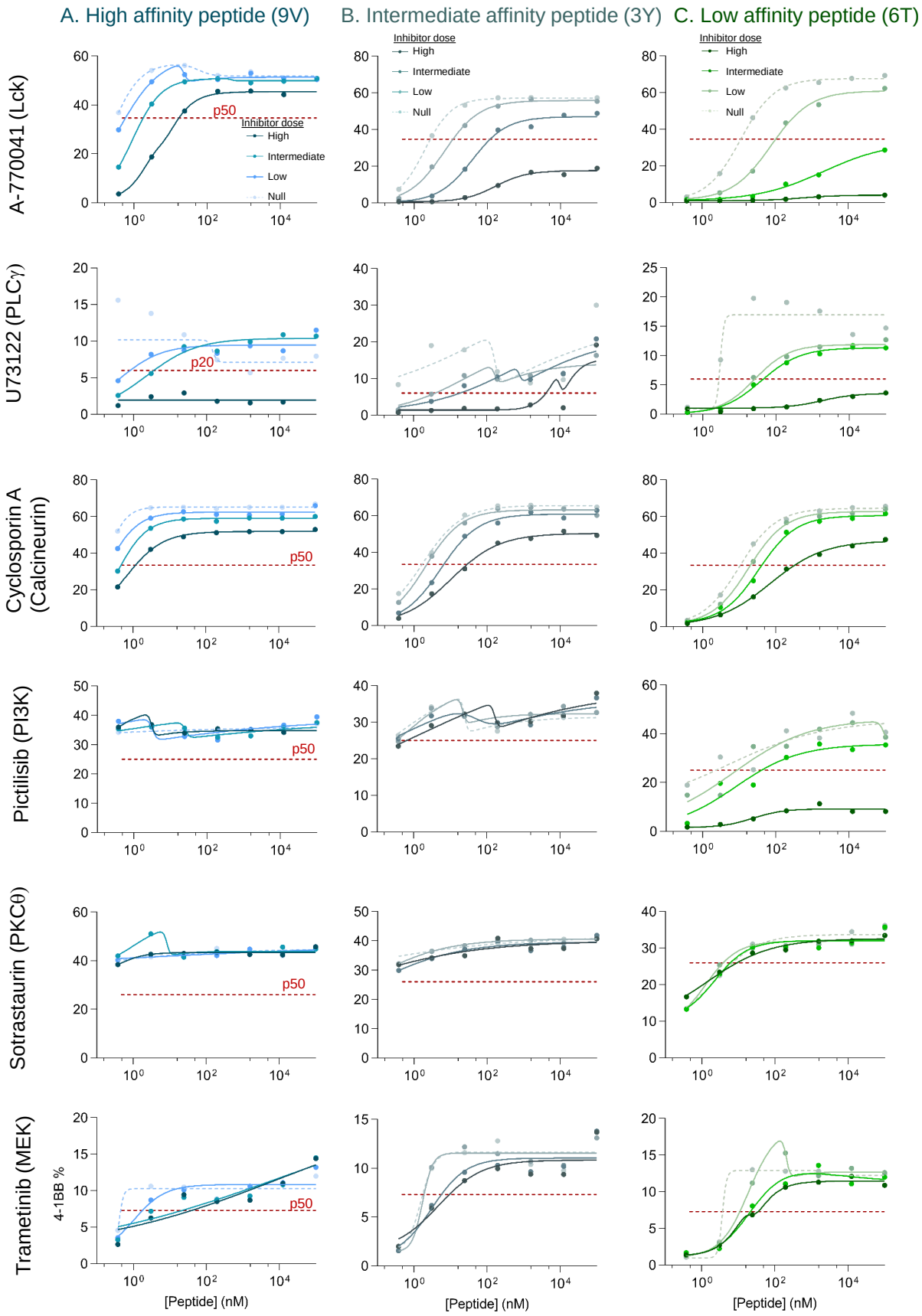


Figure 40: Impact of inhibition of signalling molecules on T cell discrimination - surface markers output. Co-culture assay as described in figure 14. Upregulation of the surface marker 4-1BB.

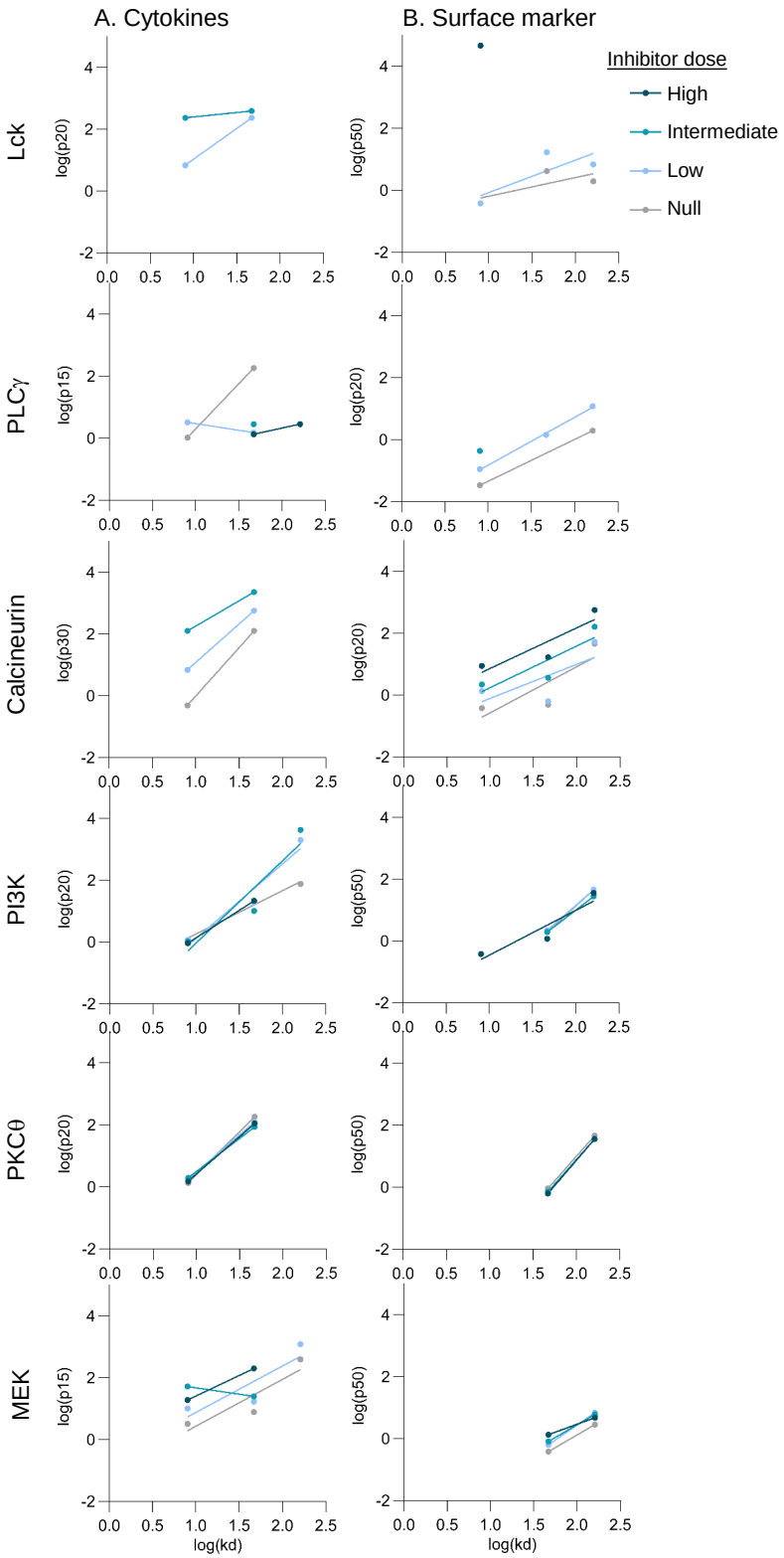


Figure 41: Independent dataset as described in figure 16.

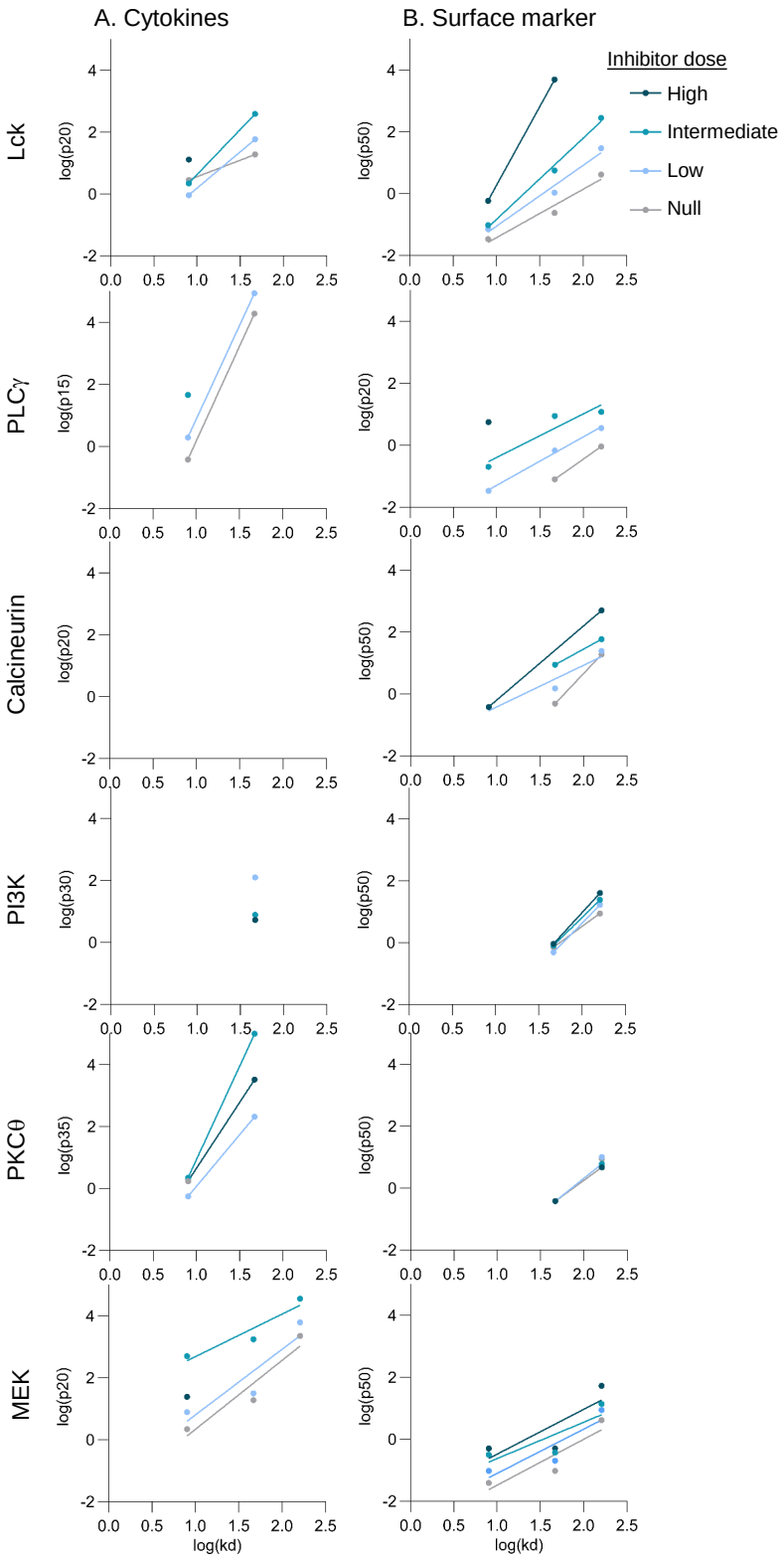


Figure 42: Independent dataset as described in figure 16.

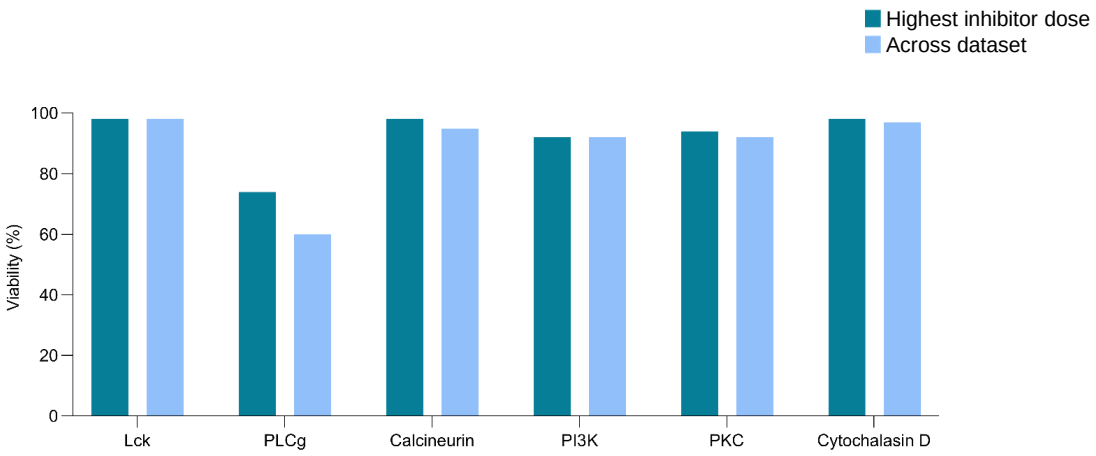


Figure 43: Impact of inhibitor treatment on cell viability. T cell viability is measured at the end of the stimulation experiment. Viability is assessed for each doses. Viability upon highest dose treatment and lowest viability observed across all datasets are plotted. Most inhibitor have no effect on T cells viability, only the PLCγ inhibitor induces mortality.

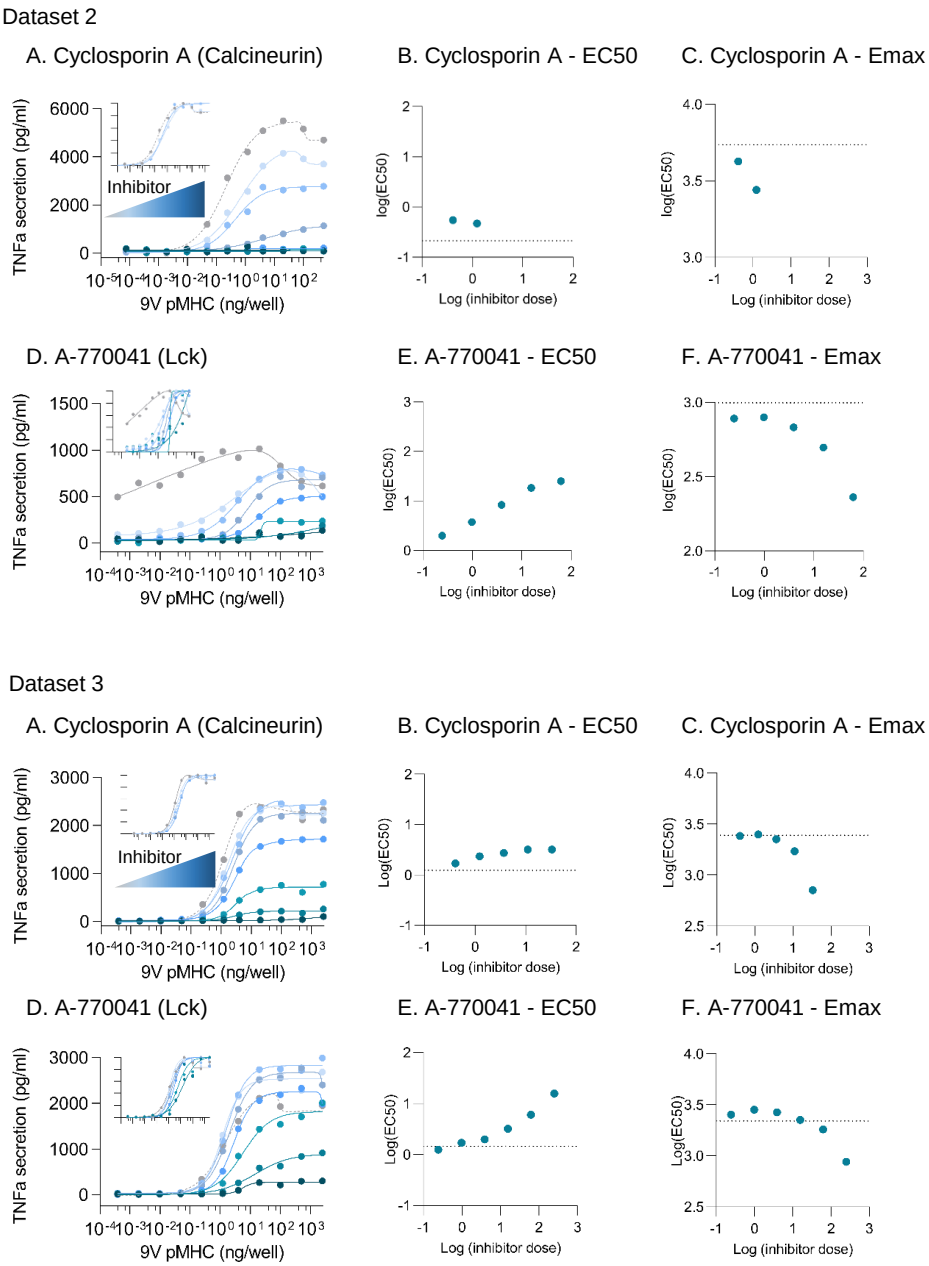


Figure 44: Independent repeat as described in figure 19.

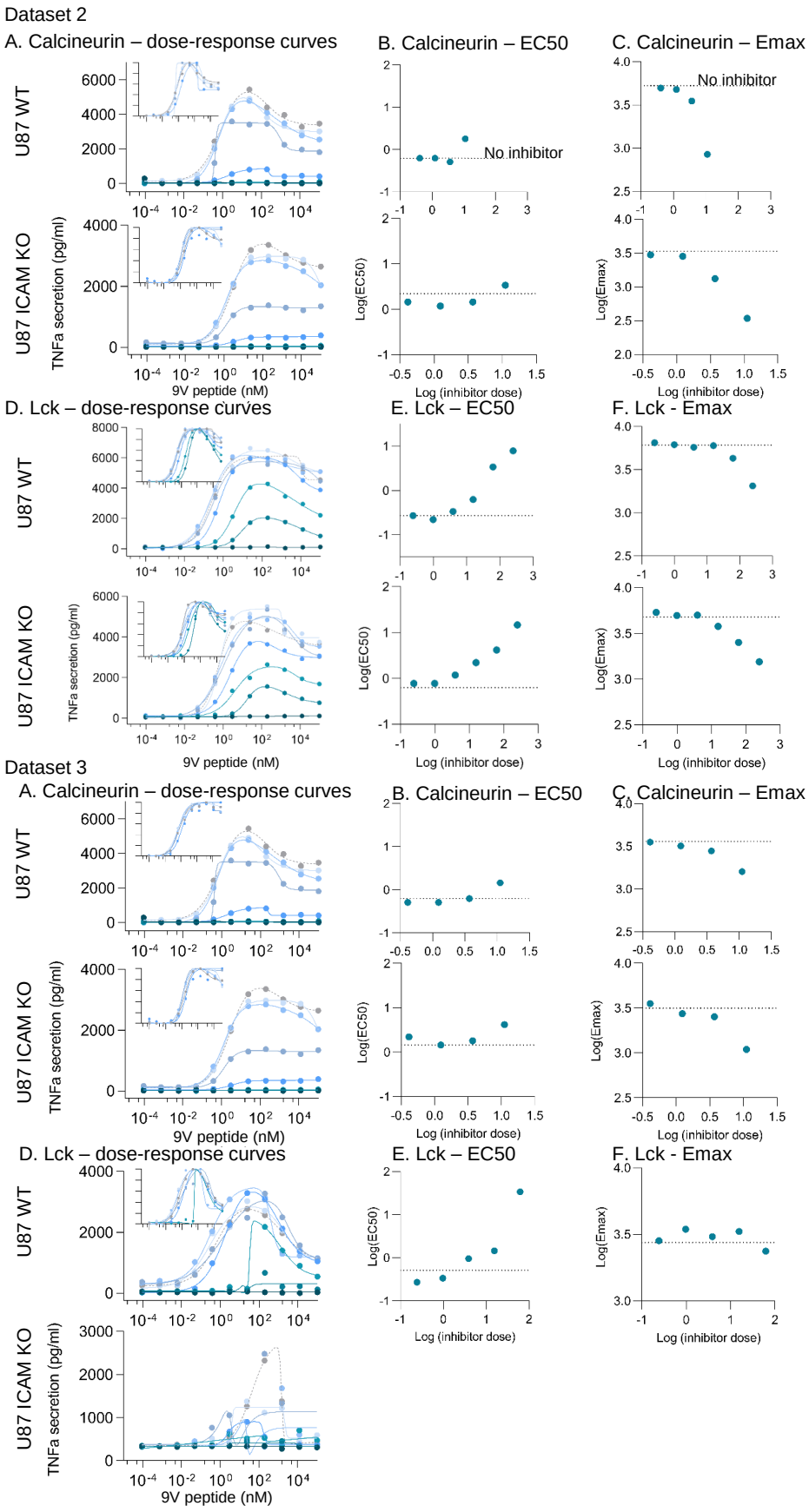


Figure 45: Independent repeat as described in figure 21.

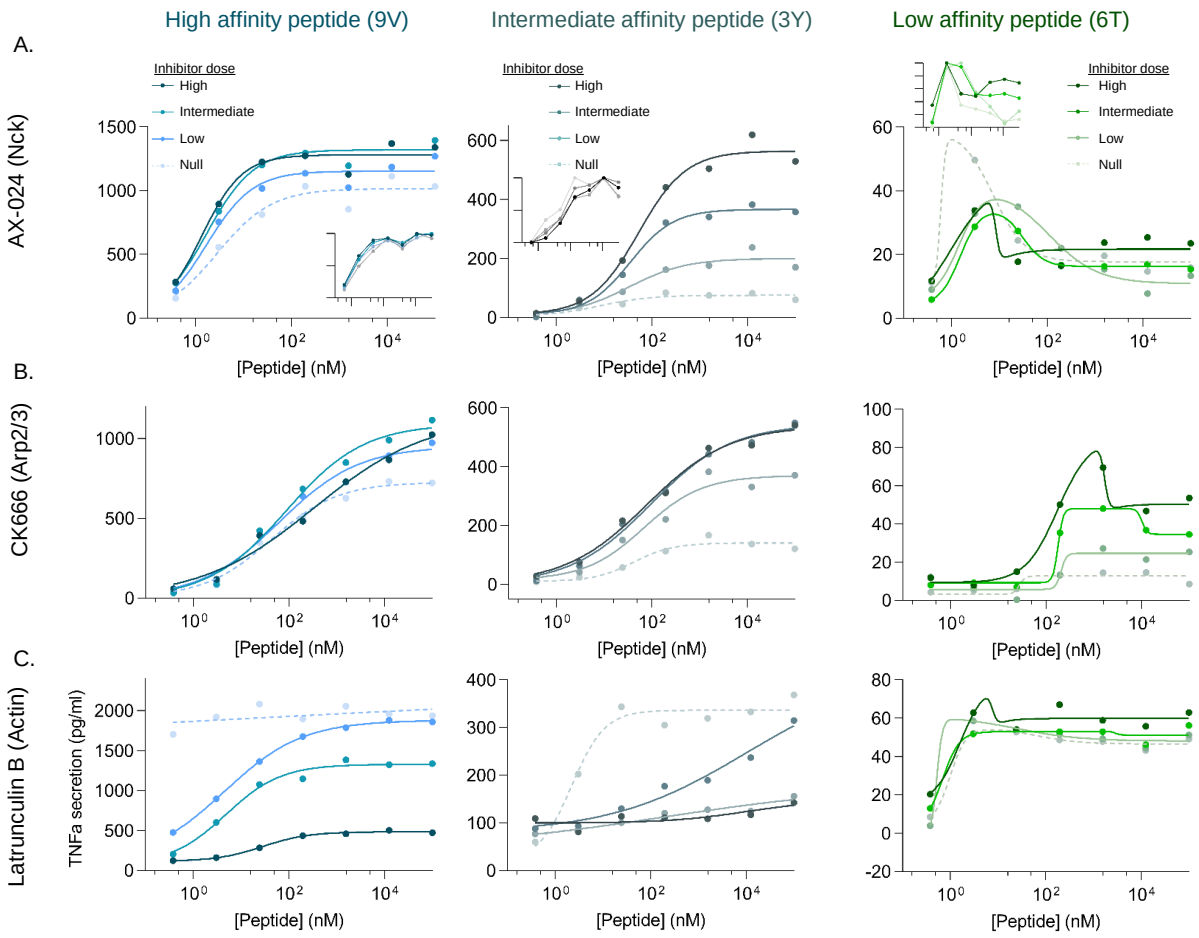


Figure 46: Independent repeat as described in figure 24.

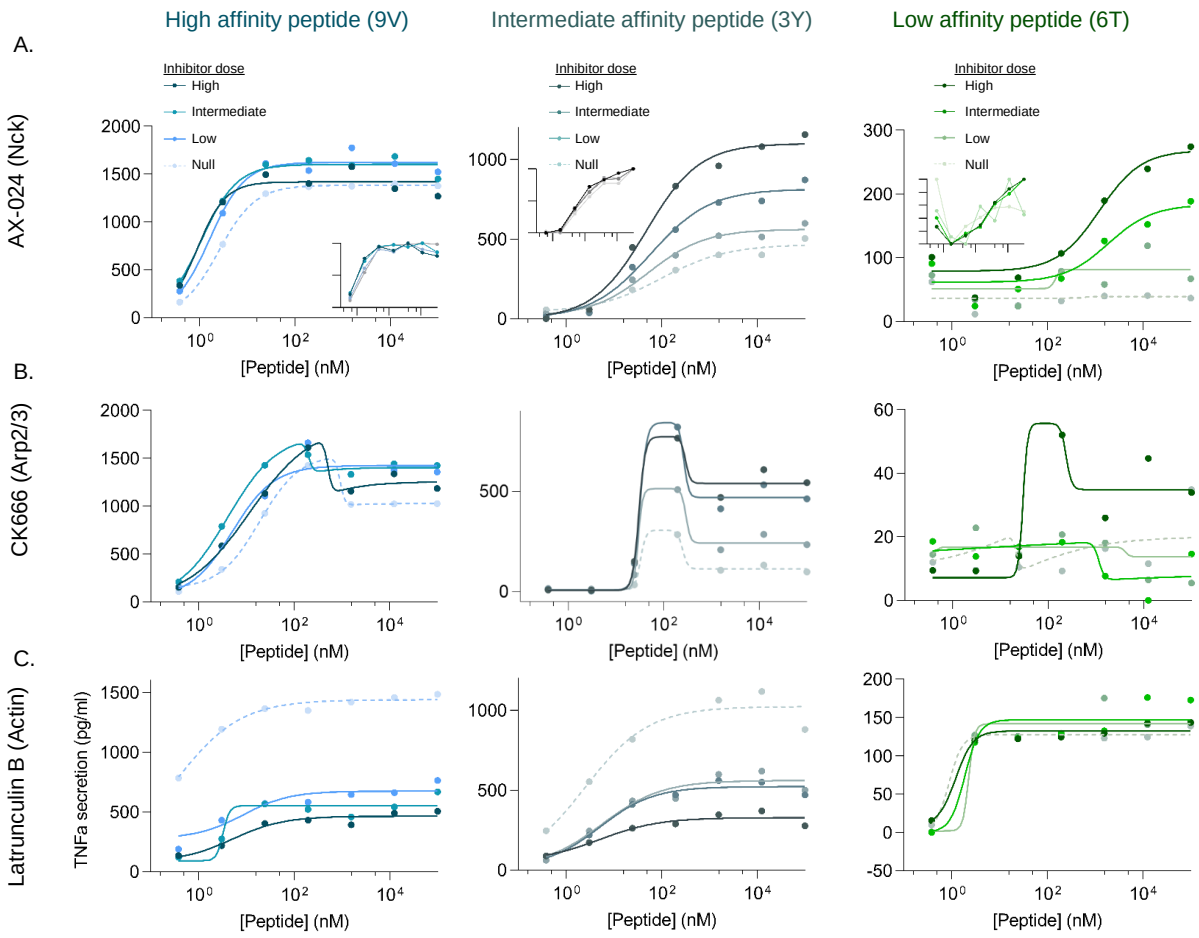


Figure 47: Independent repeat as described in figure 24.

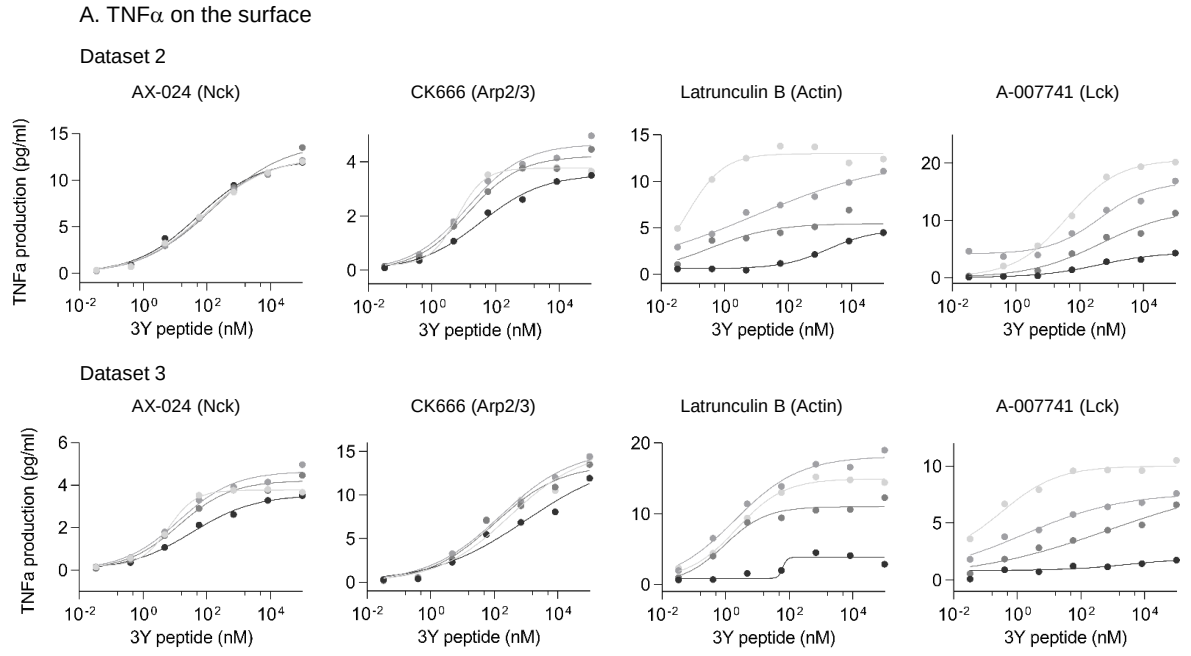


Figure 48: Independent repeats as described in figure 25.

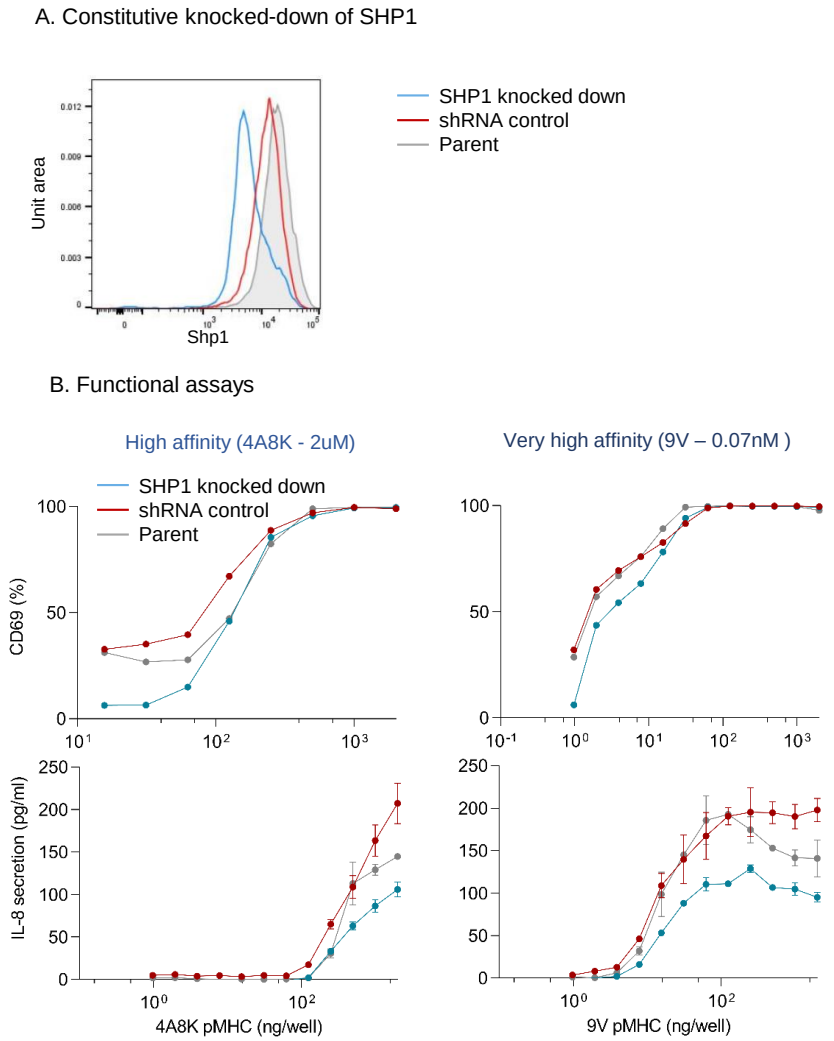


Figure 49: Constitutive knock-down of SHP1 in Jurkat cells. A. Validation of the knocked-down of SHP1 in Jurkat cells, expression measured by flow cytometry. B. Dose-response curves of WT, knocked-down and control Jurkat cells stimulated with the 4A8K and 9V peptides. Jurkat cell functions are measured by up regulation of the surface marker CD69 (one representative experiment) and secretion of cytokine IL-8 (technical triplicate). All these data have been produced and analysed by John Nguyen (former PhD student in the lab).

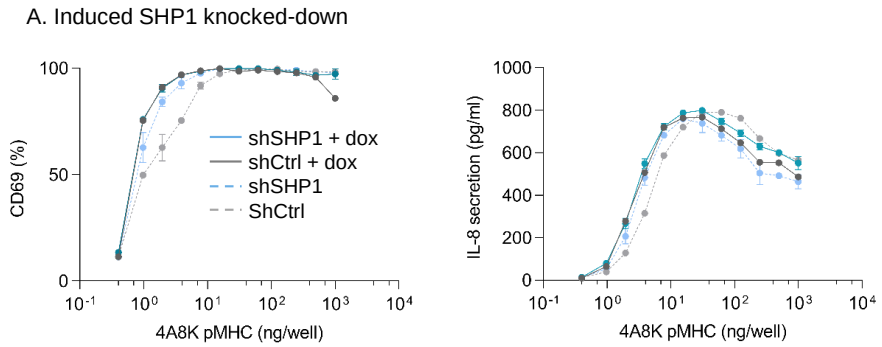


Figure 50: Induced knock-down of SHP1 in Jurkat cells. A. Dose-response curves of knocked-down and control Jurkat cells, with and without doxycycline induction, stimulated with the 4A8K peptide. Jurkat cell functions are measured by up regulation of the surface marker CD69 (one representative experiment) and secretion of cytokine IL-8 (technical triplicate). All these data have been produced and analysed by John Nguyen (former PhD student in the lab).

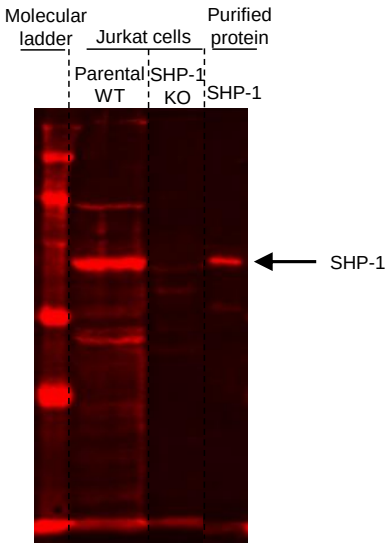


Figure 51: Validation of SHP1 KO in jurkat. Intracellular level of SHP1 after electroporation is visualised by Western Blot in Parental WT jurkat and SHP1 KO jurkats. SHP1 protein as a control.

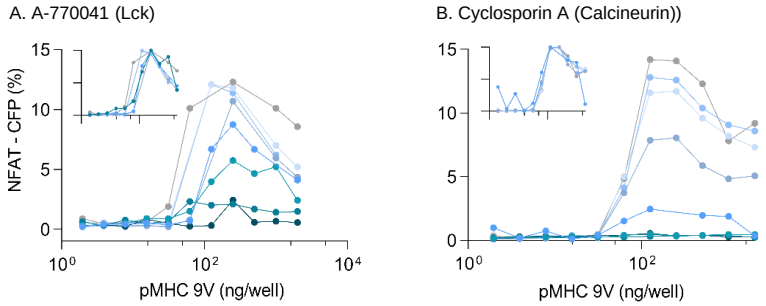


Figure 52: Lck, but not Calcineurin, controls the sensitivity to purified antigen in jurkat cells. A. Dose-response curves and their normalisation (inset graph) under titrating concentrations of A-770041 (Lck inhibitor), one representative experiment. B. Dose-response curves and their normalisation (inset graph) under titrating concentrations of Cyclosporin A (Calcineurin inhibitor), one representative experiment.

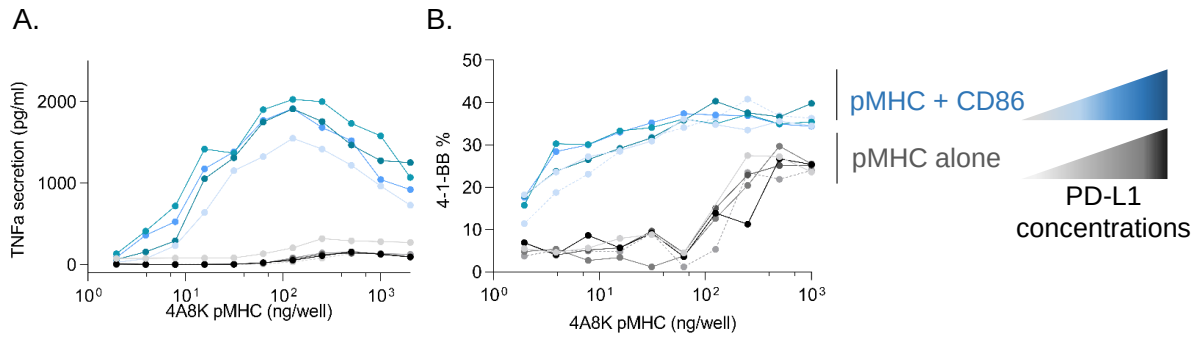


Figure 53: Independent repeat as described in figure 28.

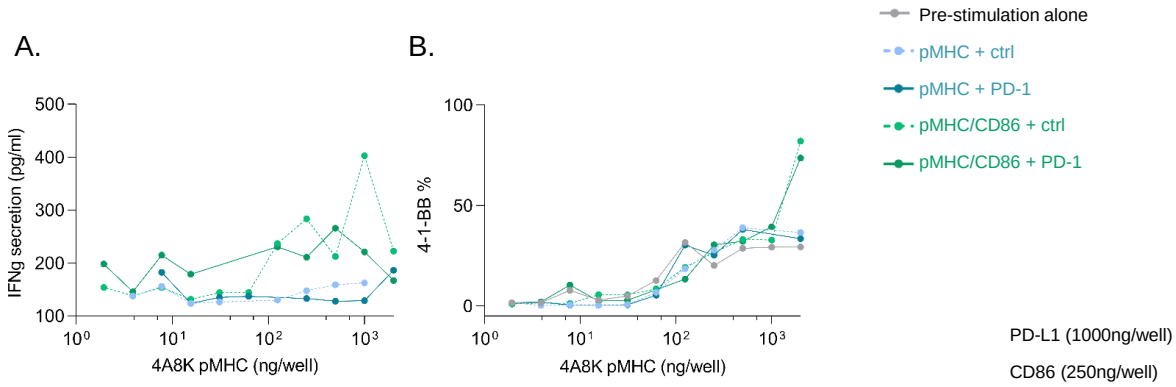


Figure 54: Independent repeat as described in figure 29.

Dataset 2

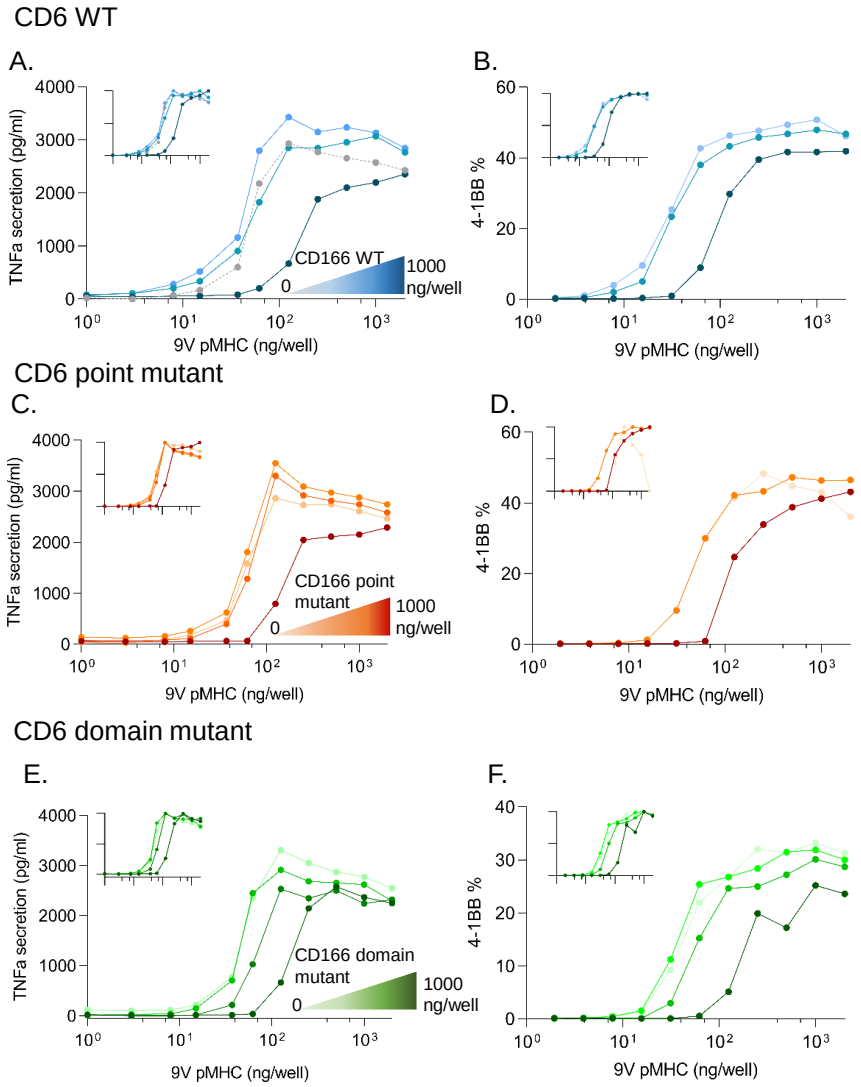


Figure 55: Independent repeat as described in figure 30.

Dataset 3

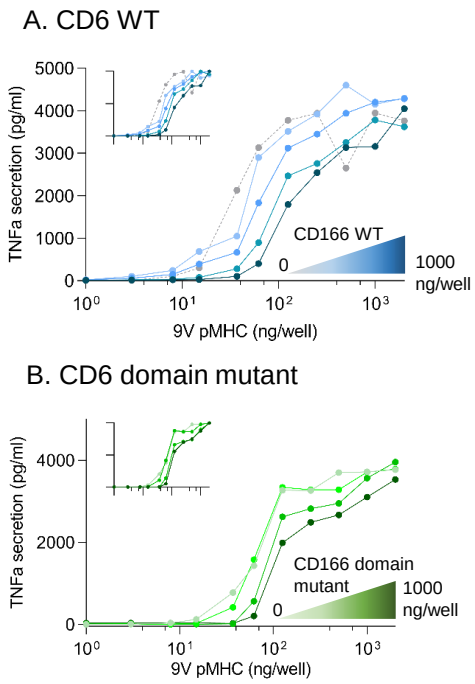
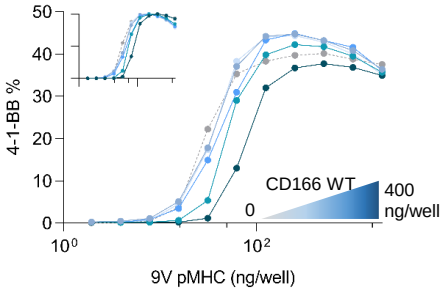


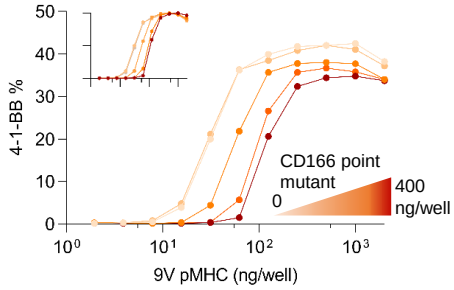
Figure 56: Independent repeat as described in figure 30.

Dataset 2

A. CD6 WT



B. CD6 point mutant



C. Ctrl protein

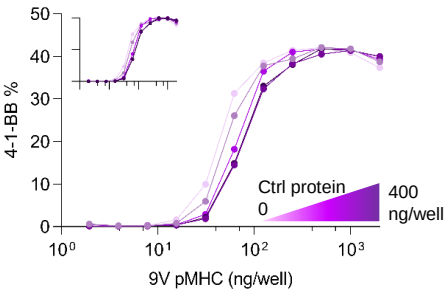


Figure 57: Independent repeat as described in figure 31.

References

1. Fritz, J. H., Le Bourhis, L., Magalhaes, J. G. & Philpott, D. J. Innate immune recognition at the epithelial barrier drives adaptive immunity: APCs take the back seat. *Trends Immunol.* **29,** 41–49 (2008).

2. Abreu, M. T., Fukata, M. & Arditi, M. TLR Signaling in the Gut in Health and Disease. *J. Immunol.* **174,** 4453–4460 (2005).

3. Et al Alberts B, J. A. L. J. *Molecular Biology of the Cell. 4th edition.* (2002).

4. Iwasaki, A. & Medzhitov, R. Control of adaptive immunity by the innate immune system. *Nat. Immunol.* **16,** 343–353 (2015).

5. Ramshaw, I. A. *et al.* Cytokines and immunity to viral infections. *Immunol. Rev.* **159,** 119–135 (1997).

6. Imanishi, J. Expression of cytokines in bacterial and viral infections and their biochemical aspects. *J. Biochem.* **127,** 525–530 (2000).

7. Parkin, J. & Cohen, B. An Overview of the Immune System. *Lancet* **357,** 1777–89 (2001).

8. MacConmara, M. & Lederer, J. A. B cells. *Crit. Care Med.* **33,** 514–516 (2005).

9. Reimann, J. & Schirmbeck, R. Alternative pathways for processing exogenous and endogenous antigens that can generate peptides for MHC class I-restricted presentation. *Immunol. Rev.* **172,** 131–152 (1999).

10. Otten, G. Antigen processing and presentation. *Curr. Opin. Immunol.* **2,** 204–209 (1989).

11. Zhu, J. & Paul, W. E. CD4 T cells: Fates, functions, and faults. *Blood* **112,** 1557–1569 (2008).

12. Hewitt, E. The MHC class I antigen presentation pathway: strategies for viral immune evasion. *Immunology* **110,** 163–169 (2003).

13. Rock, K. L., Reits, E. & Neefjes, J. Present Yourself! By MHC Class I and MHC Class II Molecules. *Trends Immunol.* **35,** 1252–1260. arXiv: 15334406 (2016).

14. Bevan, M. J. Brief Definitive Report. *J. Exp. Med.* **143,** 1283–1288 (1976).

15. Kurts, C. Cross-presentation: Inducing CD8 T cell immunity and tolerance. *J. Mol. Med.* **78,** 326–332 (2000).

16. Joffre, O. P., Segura, E., Savina, A. & Amigorena, S. Cross-presentation by dendritic cells. *Nat. Rev. Immunol.* **12,** 557–569 (2012).

17. Fehres, C. M., Unger, W. W., Garcia-Vallejo, J. J. & van Kooyk, Y. Understanding the biology of antigen cross-presentation for the design of vaccines against cancer. *Front. Immunol.* **5,** 1–10 (2014).

18. Oltz, E. M. Regulation of Antigen Receptor Gene Assembly In Lymphocytes. *Immunol. Res.,* 121–133 (2001).

19. Bonati, A. *et al.* T-cell receptor β-chain gene rearrangement and expression during human thymic ontogenesis. *Blood* **79,** 1472–1483 (1992).

20. Zarnitsyna, V. I., Evavold, B. D., Schoettle, L. N., Blattman, J. N. & Antia, R. Estimating the diversity, completeness, and cross-reactivity of the T cell repertoire. *Front. Immunol.* **4,** 1–11 (2013).

21. Alcover, A., Alarcón, B. & Di Bartolo, V. Cell Biology of T Cell Receptor Expression and Regulation. *Annu. Rev. Immunol.* **36,** 103–125 (2018).

22. Starr, T. K., Jameson, S. C. & Hogquist, K. A. Positive and negative selection of T cells. *Annu. Rev. Immunol.* **21,** 139–176 (2003).

23. Derbinski, J. & Kyewski, B. Linking signalling pathways, thymic stroma integrity and autoimmunity. *Trends Immunol.* **26,** 503–506 (2005).

24. Castellino, F. & Germain, R. N. Cooperation between CD4+ and CD8+ T cells: When, where, and how. *Annu. Rev. Immunol.* **24,** 519–540 (2006).

25. Cai, E. *et al.* Visualizing dynamic microvillar search and stabilization during ligand detection by T cells. *Science (80-.).* **356** (2017).

26. Trautmann, A. & Randriamampita, C. Initiation of TCR signalling revisited. *Trends Immunol.* **24,** 425–428 (2003).

27. Wei, Q. *et al.* Lck bound to coreceptor is less active than free Lck (2020).

28. Courtney, A. H., Lo, W. L. & Weiss, A. TCR Signaling: Mechanisms of Initiation and Propagation. *Trends Biochem. Sci.* **43,** 108–123 (2018).

29. Park, P. S.-H., Lodowski, D. & Palczewski, K. Activation of G Protein–Coupled Receptors: Beyond Two-State Models and Tertiary Conformational Changes. *Annu. Rev. Pharm. Toxicol.,* 107–141 (2008).

30. Garcia, K. C., Teyton, L. & Wilson, I. A. Structural basis of T cell recognition. *Annu. Rev. Immunol.* **17,** 369–97 (1999).

31. Boulter, J. M. *et al.* Potent T cell agonism mediated by a very rapid TCR/pMHC interaction. *Eur. J. Immunol.* **37,** 798–806 (2007).

32. Krogsgaard, M. *et al.* Evidence that Structural Rearrangements and / or Flexibility during TCR Binding Can Contribute to T Cell Activation. *Mol. Cell* **12,** 1367–1378 (2003).

33. Dong, D. *et al.* Structural basis of assembly of the human TCR–CD3 complex. *Nature* **3** (2019).

34. Gil, D., Schamel, W. W. A., Sa, F. & Alarco, B. Recruitment of Nck by CD3 Reveals a Ligand- Induced Conformational Change Essential for T Cell Receptor Signaling and Synapse Formation. *Cell* **109,** 901–912 (2002).

35. Sušac, L. *et al.* Structure of a fully assembled tumor-specific T cell receptor ligated by pMHC. *Cell* **185,** 3201–3213.e19 (2022).

36. Davis, S. J. & van der Merwe, P. A. The kinetic-segregation model: TCR triggering and beyond. *Nat. Immunol.* **7,** 803–809 (2006).

37. Courtney, A. H. *et al.* CD45 functions as a signaling gatekeeper in T cells. *Sci. Signal.* **12** (2019).

38. Fernandes, R. A. *et al.* A cell topography-based mechanism for ligand discrimination by the T cell receptor. *Proc. Natl. Acad. Sci. U. S. A.* **116,** 14002–14010 (2019).

39. Davis, M. M. & Bjorkman, P. J. The T cell receptor genes and T-cell recognition. *Nature* **334,** 395–402 (1988).

40. Chen, K. Y. *et al.* Trapping or slowing the diffusion of T cell receptors at close contacts initiates T cell signaling. *Proc. Natl. Acad. Sci. U. S. A.* **118** (2021).

41. Kim, P. W., Sun, Z. Y. J., Blacklow, S. C., Wagner, G. & Eck, M. J. A zinc clasp structure tethers Lck to T cell coreceptors CD4 and CD8. *Science (80-.).* **301,** 1725–1728 (2003).

42. Veillette, A., Bookman, M. A., Horak, E. M. & Bolen, J. B. The CD4 and CD8 T cell surface antigens are associated with the internal membrane tyrosine-protein kinase p56lck. *Cell* **55,** 301–308 (1988).

43. Van Laethem, F. *et al.* Deletion of CD4 and CD8 Coreceptors Permits Generation of $\alpha\beta$T Cells that Recognize Antigens Independently of the MHC. *Immunity* **27,** 735–750 (2007).

44. Straus, D. B., Chan, A. C., Patai, B. & Weiss, A. SH2 domain function is essential for the role of the Lck tyrosine kinase in T cell receptor signal transduction. *J. Biol. Chem.* **271,** 9976–9981 (1996).

45. Morch, A. *et al.* The kinase occupancy of T-cell coreceptors reconsidered. *bioRxiv* (2022).

46. Philipsen, L. *et al.* De novo phosphorylation and conformational opening of the tyrosine kinase Lck act in concert to initiate T cell receptor signaling. *Sci. Signal.* **10** (2017).

47. Liaunardy-Jopeace, A., Murton, B. L., Mahesh, M., Chin, J. W. & James, J. R. Encoding optical control in LCK kinase to quantitatively investigate its activity in live cells. *Nat. Struct. Mol. Biol.* **24,** 1155–1163 (2017).

48. Smith-Garvin, J. E., Koretzky, G. A. & Jordan, M. S. T cell activation. *Annu. Rev. Immunol.* **29,** 591–619. arXiv: NIHMS150003 (2009).

49. Winkler, D. G. *et al.* Phosphorylation of Ser-42 and Ser-59 in the N-terminal region of the tyrosine kinase p56(lck). *Proc. Natl. Acad. Sci. U. S. A.* **90,** 5176–5180 (1993).

50. Dutta, D. *et al.* Recruitment of calcineurin to the TCR positively regulates T cell activation. *Nat. Immunol.* **18,** 196–204 (2017).

51. Watts, J. D., Sanghera, J. S., Pelech, S. L. & Aebersold, R. Phosphorylation of serine 59 of p56(lck) in activated T cells. *J. Biol. Chem.* **268,** 23275–23282 (1993).

52. Štefanová, I. *et al.* TCR ligand discrimination is enforced by competing ERK positive and SHP-I negative feedback pathways. *Nat. Immunol.* **4,** 248–254 (2003).

53. Yan, Q. *et al.* Structural Basis for Activation of ZAP-70 by Phosphorylation of the SH2-Kinase Linker. *Mol. Cell. Biol.* **33,** 2188–2201 (2013).

54. Wang, H. *et al.* ZAP-70: an essential kinase in T-cell signaling. *Cold Spring Harb. Perspect. Biol.* **2** (2010).

55. Lo, W. *et al.* Lck promotes Zap70-dependent LAT phosphorylation by bridging Zap70 to LAT. *Nat. Immunol.* **19,** 733–741 (2018).

56. Ganti, R. S. *et al.* How the T cell signaling network processes information to discriminate between self and agonist ligands. *Proc. Natl. Acad. Sci. U. S. A.* **117,** 26020–26030 (2020).

57. Wange, R. L. LAT, the linker for activation of T cells: a bridge between T cell-specific and general signaling pathways. *Sci. STKE* **2000,** 1–14 (2000).

58. Ragab, A. *et al.* Roles of the C-terminal tyrosine residues of LAT in GPVI-induced platelet activation: Insights into the mechanism of PLCγ2 activation. *Blood* **110,** 2466–2474 (2007).

59. Su, X. *et al.* Phase separation of signaling molecules promotes T cell receptor signal transduction. *Science (80-.).* **352,** 595–600 (2016).

60. Brownlie, R. J. & Zamoyska, R. T cell receptor signalling networks: Branched, diversified and bounded. *Nat. Rev. Immunol.* **13,** 257–269 (2013).

61. Bartok, A. *et al.* IP3 receptor isoforms differently regulate ER-mitochondrial contacts and local calcium transfer. *Nat. Commun.* **10,** 1–14 (2019).

62. Macian, F. NFAT proteins: Key regulators of T-cell development and function. *Nat. Rev. Immunol.* **5,** 472–484 (2005).

63. Huse, M. The T-cell-receptor signalling network. *J. Cell Sci.* **122,** 1269–1273 (2009).

64. Okamura, H. *et al.* Concerted dephosphorylation of the transcription factor NFAT1 induces a conformational switch that regulates transcriptional activity. *Mol. Cell* **6,** 539–550 (2000).

65. Limnander, A. & Weiss, A. Ca2+-dependent Ras/Erk signaling mediates negative selection of autoreactive B cells. *Small GTPases* **2,** 282–288 (2011).

66. Isakov, N. & Altman, A. PKC-theta-mediated signal delivery from the TCR/CD28 surface receptors. *Front. Immunol.* **3,** 1–12 (2012).

67. Genot, E. & Cantrell, D. A. Genot_CurrOpinImmunol_2000 Ras in lymphocytes (2000).

68. Matsumoto, R. *et al.* Phosphorylation of CARMA1 plays a critical role in T cell receptor-mediated NF-κB activation. *Immunity* **23,** 575–585 (2005).

69. David, L. *et al.* Assembly mechanism of the CARMA1–BCL10–MALT1–TRAF6 signalosome. *Proc. Natl. Acad. Sci. U. S. A.* **115,** 1499–1504 (2018).

70. Zhou, H. *et al.* Bcl10 activates the NF-κB pathway through ubiquitination of NEMO. *Nature* **427,** 167–171 (2004).

71. Vallabhapurapu, S. & Karin, M. Regulation and function of NF-κB transcription factors in the immune system. *Annu. Rev. Immunol.* **27,** 693–733 (2009).

72. Macián, F. *et al.* Transcriptional mechanisms underlying lymphocyte tolerance. *Cell* **109,** 719–731 (2002).

73. Fehr, T. *et al.* A CD8 T cell-intrinsic role for the calcineurin-NFAT pathway for tolerance induction in vivo. *Blood* **115,** 1280–1287 (2010).

74. Macián, F., López-Rodríguez, C. & Rao, A. Partners in transcription: NFAT and AP-1. *Oncogene* **20,** 2476–2489 (2001).

75. Gaffen, S. L. & Liu, K. D. Overview of interleukin-2 function , production and clinical applications. *Cytokine* **28,** 109–123 (2004).

76. Schoenborn, J. R. & Wilson, C. B. Regulation of Interferon-γ During Innate and Adaptive Immune Responses. *Adv. Immunol.* **96,** 41–101 (2007).

77. Falvo, J. V., Tsytsykova, A. V. & Goldfeld, A. E. Transcriptional Control of the TNF Gene. *Curr. Dir. Autoimmun.* **11,** 27–60 (2010).

78. Laguna, T. *et al.* New insights on the transcriptional regulation of CD69 gene through a potent enhancer located in the conserved non-coding sequence 2. *Mol. Immunol.* **66,** 171–179 (2015).

79. Pichler, K. *et al.* Strong induction of 4-1BB, a growth and survival promoting costimulatory receptor, in HTLV-1-infected cultured and patients' T cells by the viral Tax oncoprotein. *Blood* **111,** 4741–4751 (2008).

80. Ziegler, S. F., Ramsdell, F. & Alderson, M. R. The activation antigen CD69. *Stem Cells* **12,** 456–465 (1994).

81. Castellanos, M. C. *et al.* Expression of the leukocyte early activation antigen CD69 is regulated by the transcription factor AP-1. *J. Immunol.* **159,** 5463–73 (1997).

82. Kim, J. O., Kim, H. W., Baek, K. M. & Kang, C. Y. NF-κB and AP-1 regulate activation-dependent CD137 (4-1BB) expression in T cells. *FEBS Lett.* **541,** 163–170 (2003).

83. Barnes, P. J. & Adcock, I. M. Transcription factors and asthma. *Eur. Respir. J.* **12,** 221–234 (1998).

84. Spolski, R., Li, P. & Leonard, W. J. Biology and regulation of IL-2: from molecular mechanisms to human therapy. *Nat. Rev. Immunol.* **18,** 648–659 (2018).

85. Murphy, K. M. *et al.* S Ignaling and T Ranscription in, 451–494 (2000).

86. Dustin, M. L. The immunological synapse. *Cancer Immunol. Res.* **2,** 1023–1033 (2014).

87. Sun, X., Wei, Y., Lee, P. P., Ren, B. & Liu, C. The role of WASp in T cells and B cells. *Cell. Immunol.* **341,** 103919 (2019).

88. Voskoboinik, I., Whisstock, J. C. & Trapani, J. A. Perforin and granzymes: Function, dysfunction and human pathology. *Nat. Rev. Immunol.* **15,** 388–400 (2015).

89. Allenspach, E. J. *et al.* ERM-dependent movement of CD43 defines a novel protein complex distal to the immunological synapse. *Immunity* **15,** 739–750 (2001).

90. Huse, M. Microtubule-organizing center polarity and the immunological synapse: Protein kinase C and beyond. *Front. Immunol.* **3,** 1–11 (2012).

91. Labno, C. *et al.* Itk Functions to Control Actin Polymerization at the Immune Synapse through Localized Activation od Cdc42 and WASP. *Curr. Biol.* **13,** 1619–1624. arXiv: `NIHMS150003` (2003).

92. LeClaire, L. L., Rana, M., Baumgartner, M. & Barber, D. L. The Nck-interacting kinase NIK increases Arp2/3 complex activity by phosphorylating the Arp2 subunit. *J. Cell Biol.* **208,** 161–170 (2015).

93. Sasahara, Y. *et al.* Mechanism of recruitment of WASP to the immunological synapse and of its activation following TCR ligation. *Mol. Cell* **10,** 1269–1281 (2002).

94. Song, K. H. *et al.* T cells sense biophysical cues using lamellipodia and filopodia to optimize intraluminal path finding. *Integr. Biol. (United Kingdom)* **6,** 450–459 (2014).

95. Le Clainche, C. & Carlier, M. F. Regulation of actin assembly associated with protrusion and adhesion in cell migration. *Physiol. Rev.* **88,** 489–513 (2008).

96. Hartzell, C. A., Jankowska, K. I., Burkhardt, J. K. & Lewis, R. S. Calcium influx through CRAC channels controls actin organization and dynamics at the immune synapse. *Elife* **5,** 1–28 (2016).

97. Nolz, J. C. *et al.* The WAVE2 complex regulates T cell receptor signaling to integrins via Abl- and CrkL-C3G-mediated activation of Rap1. *J. Cell Biol.* **182,** 1231–1244 (2008).

98. Nolz, J. C. *et al.* The WAVE2 Complex Regulates Actin Cytoskeletal Reorganization and CRAC-Mediated Calcium Entry during T Cell Activation. *Curr. Biol.* **16,** 24–34 (2006).

99. Gainey, M. D., Rivenbark, J. G., Cho, H., Yang, L. & Yokoyama, W. M. Viral MHC class I inhibition evades CD8+ T-cell effector responses in vivo but not CD8+ T-cell priming. *Proc. Natl. Acad. Sci. U. S. A.* **109** (2012).

100. Clancy-Thompson, E. *et al.* Altered binding of tumor antigenic peptides to MHC class I affects CD8+ T cell-effector responses Eleanor. *Cancer Immunol. Res.* **6,** 1524–1536 (2018).

101. Irvine, D. J., Purbhoo, M. A., Krogsgaard, M. & Davis, M. M. Direct observation of ligand recognition by T cells. *Nature* **419,** 845–849 (2002).

102. Huang, J. *et al.* A Single Peptide-Major Histocompatibility Complex Ligand Triggers Digital Cytokine Secretion in CD4(+) T Cells. *Immunity* **39** (2013).

103. Sykulev, Y., Joo, M., Vturina, I., Tsomides, T. J. & Eisen, H. N. Evidence that a single peptide-MHC complex on a target cell can elicit a cytolytic T cell response. *Immunity* **4,** 565–571 (1996).

104. Hellmeier, J. *et al.* DNA origami demonstrate the unique stimulatory power of single pMHCs as T cell antigens. *Proc. Natl. Acad. Sci.* **118,** e2016857118 (2021).

105. Zhong, S. *et al.* T-cell receptor affinity and avidity defines antitumor response and autoimmunity in T-cell immunotherapy. *Proc. Natl. Acad. Sci. U. S. A.* **110,** 6973–6978 (2013).

106. Stone, J. D., Chervin, A. S. & Kranz, D. M. T-cell receptor binding affinities and kinetics: impact on T-cell activity and specificity. *Immunology* **126,** 165–176 (2009).

107. Van Der Merwe, P. A. & Dushek, O. Mechanisms for T cell receptor triggering. *Nat. Rev. Immunol.* **11,** 47–55 (2011).

108. Kerry, S. *et al.* Interplay between TCR Affinity and Necessity of Coreceptor Ligation: High-Affinity Peptide-MHC/TCR Interaction Overcomes Lack of CD8 Engagement. *J Immunol* **171,** 4493–4503. arXiv: `NIHMS150003` (2003).

109. Artyomov, M. N., Lis, M., Devadas, S., Davis, M. M. & Chakraborty, A. K. CD4 and CD8 binding to MHC molecules primarily acts to enhance Lck delivery. *Proc. Natl. Acad. Sci. U. S. A.* **107,** 16916–16921 (2010).

110. Stepanek, O. *et al.* Coreceptor scanning by the T cell receptor provides a mechanism for T cell tolerance. *Cell* **159,** 333–345 (2014).

111. Sanchez-Madrid, F. *et al.* Three distinct antigens associated with human T-lymphocyte-mediated cytolysis: LFA-1, LFA-2, and LFA-3. *Proc. Natl. Acad. Sci. U. S. A.* **79,** 7489–7493 (1982).

112. Wang, B. *et al.* Combination cancer immunotherapy targeting PD-1 and GITR can rescue CD8+ T cell dysfunction and maintain memory phenotype. *Sci. Immunol.* **3,** 1–14 (2018).

113. Patel, S. J. *et al.* Identification of essential genes for cancer immunotherapy. *Nature* **548,** 537–542 (2017).

114. Koneru, M., Monu, N., Schaer, D., Barletta, J. & Frey, A. B. Defective Adhesion in Tumor Infiltrating CD8 + T Cells. *J. Immunol.* **176,** 6103–6111 (2006).

115. Pettmann, J. *et al.* The discriminatory power of the T cell receptor. *Elife,* 1–42 (2021).

116. Koyasu, S. *et al.* Role of interaction of CD2 molecules with lymphocyte function-associated antigen 3 in T-cell recognition of nominal antigen. *Proc. Natl. Acad. Sci. U. S. A.* **87,** 2603–2607 (1990).

117. Demetriou, P. *et al.* Author Correction: A dynamic CD2-rich compartment at the outer edge of the immunological synapse boosts and integrates signals. *Nat. Immunol.* **22,** 99–99 (2021).

118. Bachmann, M. F., Barner, M. & Kopf, M. CD2 sets quantitative thresholds in T cell activation. *J. Exp. Med.* **190,** 1383–1391 (1999).

119. Bachmann, M. F. *et al.* Distinct roles for LFA-1 and CD28 during activation of naive T cells: Adhesion versus costimulation. *Immunity* **7,** 549–557 (1997).

120. Walling, B. L. & Kim, M. LFA-1 in T cell migration and differentiation. *Front. Immunol.* **9** (2018).

121. Nordenfelt, P., Elliott, H. L. & Springer, T. A. Coordinated integrin activation by actin-dependent force during T-cell migration. *Nat. Commun.* **7,** 1–15 (2016).

122. Yron, I. *et al.* Integrin-dependent tyrosine phosphorylation and growth regulation by Vav. *Cell Adhes. Commun.* **7,** 1–11 (1999).

123. Baker, R. G. *et al.* The Adapter Protein SLP-76 Mediates "Outside-In" Integrin Signaling and Function in T Cells. *Mol. Cell. Biol.* **29,** 5578–5589 (2009).

124. Van Gisbergen, K. P. *et al.* The costimulatory molecule CD27 maintains clonally diverse CD8+ T cell responses of low antigen affinity to protect against viral variants. *Immunity* **35,** 97–108 (2011).

125. Akiba, H. *et al.* CD27, a member of the tumor necrosis factor receptor superfamily, activates NF-κB and stress-activated protein kinase/c-Jun N-terminal kinase via TRAF2, TRAF5, and NF-κB-inducing kinase. *J. Biol. Chem.* **273,** 13353–13358 (1998).

126. Viola, A. & Lanzavecchia, A. T cell activation determined by T cell receptor number and tunable thresholds. *Science (80-.).* **273,** 104–106 (1996).

127. Zhang, J. *et al.* Cutting Edge: Regulation of T Cell Activation Threshold by CD28 Costimulation Through Targeting Cbl-b for Ubiquitination. *J. Immunol.* **169,** 2236–2240 (2002).

128. Burton, J. *et al.* Inefficient exploitation of accessory receptors reduces the sensitivity of chimeric antigen receptors. *bioRxiv,* 2021.10.26.465853 (2021).

129. Burr, J. S. *et al.* Cutting Edge: Distinct Motifs Within CD28 Regulate T Cell Proliferation and Induction of Bcl-X L. *J. Immunol.* **166,** 5331–5335 (2001).

130. Dodson, L. F. *et al.* Targeted Knock-In Mice Expressing Mutations of CD28 Reveal an Essential Pathway for Costimulation. *Mol. Cell. Biol.* **29,** 3710–3721 (2009).

131. Friend, L. D. *et al.* A dose-dependent requirement for the proline motif of CD28 in cellular and humoral immunity revealed by a targeted knockin mutant. *J. Exp. Med.* **203,** 2121–2133 (2006).

132. Richter, M., Nolz, J. & Harty, J. Pathogen-specific inflammatory milieux tune the antigen sensitivity of CD8(+) T cells by enhancing T cell receptor signaling. Immunity. *Immunity* **38,** 140–152 (2013).

133. Moogk, D. *et al.* Constitutive Lck Activity Drives Sensitivity Differences between CD8+ Memory T Cell Subsets. *J. Immunol.* **197,** 644–654 (2016).

134. Manz, B. N. *et al.* Small molecule inhibition of Csk alters affinity recognition by T cells. *Elife* **4,** 1–12 (2015).

135. Shen, L., Matloubian, M., Kadlecek, T. A. & Weiss, A. A disease-associated mutation that weakens ZAP70 autoinhibition enhances responses to weak and self-ligands. *Sci. Signal.* **14,** eabc4479 (2021).

136. Katz, Z. B., Blount, A., Biophotonics, W. A. & Jolla, L. Amplifies and Disperses Antigenic Stimuli. **18,** 86–95 (2017).

137. Lo, W. L. *et al.* Slow phosphorylation of a tyrosine residue in LAT optimizes T cell ligand discrimination. *Nat. Immunol.* **20,** 1481–1493 (2019).

138. Hansburg, D., Fairwell, T., Schwartz, R. H. & Appella, E. The T lymphocyte response to cytochrome c. IV. Distinguishable sites on a peptide antigen which affect antigenic strength and memory. *J. Immunol.* **131,** 319–324 (1983).

139. Lever, M., Maini, P. K., Van Der Merwe, P. A. & Dushek, O. Phenotypic models of T cell activation. *Nat. Rev. Immunol.* **14,** 619–629 (2014).

140. Dushek, O. *et al.* Antigen potency and maximal efficacy reveal a mechanism of efficient T cell activation. *Sci. Signal.* **4** (2011).

141. McKeithan, T. W. Kinetic proofreading in T-cell receptor signal transduction. *Proc. Natl. Acad. Sci.* **92,** 5042–5046 (1995).

142. François, P., Voisinne, G., Siggia, E. D., Altan-bonnet, G. & Vergassola, M. Phenotypic model for early T-cell activation displaying sensitivity , speci fi city , and antagonism. *Proc. Natl. Acad. Sci. U. S. A.* **110,** E888–E897 (2013).

143. Dushek, O. & Van der Merwe, P. A. An induced rebinding model of antigen discrimination. *Trends Immunol.* **35,** 153–158 (2014).

144. Chakraborty, A. K. & Weiss, A. Insights into the initiation of TCR signaling. *Nat. Immunol.* **15,** 798–807 (2014).

145. Alam, S. M. *et al.* T cell-receptor affinity and thymocyte positive selection. *Nature* **381,** 616–620 (1996).

146. Alam, S. M. *et al.* Qualitative and quantitative differences in T cell receptor binding of agonist and antagonist ligands. *Immunity* **10,** 227–237 (1999).

147. Hogquist, K. A., Jameson, S. C. & Bevan, M. J. Strong agonist ligands for the T cell receptor do not mediate positive selection of functional CD8+ T cells. *Immunity* **3,** 79–86 (1995).

148. Kersh, G. J. & Allen, P. M. Structural basis for T cell recognition of altered peptide ligands: A single T cell receptor can productively recognize a large continuum of related ligands. *J. Exp. Med.* **184,** 1259–1268 (1996).

149. Kersh, G. J., Kersh, E. N., Fremont, D. H. & Allen, P. M. High- and Low-Potency Ligands with Similar Affinities for the TCR. *Immunity* **9,** 817–826 (1998).

150. Lyons, D. S. *et al.* A TCR binds to antagonist ligands with lower affinities and faster dissociation rates than to agonists. *Immunity* **5,** 53–61 (1996).

151. Altan-Bonnet, G. & Germain, R. N. Modeling T cell antigen discrimination based on feedback control of digital ERK responses. *PLoS Biol.* **3,** 1925–1938 (2005).

152. Štefanová, I. *et al.* TCR ligand discrimination is enforced by competing ERK positive and SHP-I negative feedback pathways. *Nat. Immunol.* **4,** 248–254 (2003).

153. Feinerman, O., Veiga, J., Dorfman, J. R., Germain, R. N. & Altan-Bonnet, G. Variability and robustness in T cell activation from regulated heterogeneity in protein levels. *Science (80-.).* **321,** 1081–1084 (2008).

154. Paster, W *et al.* A THEMIS:SHP1 complex promotes T-cell survival. *Embo J* **34,** 393–409 (2015).

155. Vogel, R. M., Erez, A. & Altan-Bonnet, G. Dichotomy of cellular inhibition by small-molecule inhibitors revealed by single-cell analysis. *Nat. Commun.* **7** (2016).

156. Yokosuka, T. *et al.* Newly generated T cell receptor microclusters initiate and sustain T cell activation by recruitment of Zap70 and SLP-76. *Nat. Immunol.* **6,** 1253–1262 (2005).

157. Campi, G., Varma, R. & Dustin, M. L. Actin and agonist MHC-peptide complex-dependent T cell receptor microclusters as scaffolds for signaling. *J. Exp. Med.* **202,** 1031–1036 (2005).

158. Yin, Y., Li, Y. & Mariuzza, R. A. Structural basis for self-recognition by autoimmune T-cell receptors. *Immunol. Rev.* **250,** 32–48 (2012).

159. Korem Kohanim, Y., Tendler, A., Mayo, A., Friedman, N. & Alon, U. Endocrine Autoimmune Disease as a Fragility of Immune Surveillance against Hypersecreting Mutants. *Immunity* **52,** 872–884.e5 (2020).

160. Cui, W. & Mehta, P. Identifying feasible operating regimes for early T-cell recognition: The speed, energy, accuracy trade-off in kinetic proofreading and adaptive sorting. *PLoS One* **13,** 1–16. arXiv: 1703.03398 (2018).

161. Huse, M. *et al.* Spatial and Temporal Dynamics of T Cell Receptor Signaling with a Photoactivatable Agonist. *Immunity* **27,** 76–88 (2007).

162. Tortorella, D, Gewurz, B., Furman, M., Schust, D. & Ploegh, H. Mechanisms of Tumor Cell–Intrinsic Immune Evasion. *Annu. Rev. Immunol.,* 861–926 (2000).

163. Spranger, S. & Gajewski, T. F. Mechanisms of Tumor Cell-Intrinsic Immune Evasion. *Annu. Rev. Cancer Biol.* **2,** 213–228 (2018).

164. Iezzi, G., Karjalainen, K. & Lanzavecchia, A. The duration of antigenic stimulation determines the fate of naive and effector T cells. *Immunity* **8,** 89–95 (1998).

165. Huppa, J. B., Gleimer, M., Sumen, C. & Davis, M. M. Continuous T cell receptor signaling required for synapse maintenance and full effector potential. *Nat. Immunol.* **4,** 749–755 (2003).

166. O'Donoghue, G. P., Pielak, R. M., Smoligovets, A. A., Lin, J. J. & Groves, J. T. Direct single molecule measurement of TCR triggering by agonist pMHC in living primary T cells. *Elife* **2013,** 1–16 (2013).

167. Dembic, Z. in *Cytokines Immune Syst.* 1–16 (2015).

168. Siller-Farfán, J. A. & Dushek, O. Molecular mechanisms of T cell sensitivity to antigen. *Immunol. Rev.* **285,** 194–205 (2018).

169. Strickland, S. & Loeb, J. N. Obligatory separation of hormone binding and biological response curves in systems dependent upon secondary mediators of hormone action. *Proc. Natl. Acad. Sci. U. S. A.* **78,** 1366–1370 (1981).

170. Huang, C. Y. F. & Ferrell, J. E. Ultrasensitivity in the mitogen-activated protein kinase cascade. *Proc. Natl. Acad. Sci. U. S. A.* **93,** 10078–10083 (1996).

171. Navarro, M. N., Feijoo-Carnero, C., Arandilla, A. G., Trost, M. & Cantrell, D. A. Protein kinase D2 is a digital amplifier of T cell receptor-stimulated diacylglycerol signaling in naïve CD8+ T cells. *Sci. Signal.* **7,** ra99 (2014).

172. Bagowski, C. P., Besser, J., Frey, C. R. & Ferrell, J. E. The JNK Cascade as a Biochemical Switch in Mammalian Cells : Ultrasensitive and All-or-None Responses. *Curr. Biol.* **13,** 315–320 (2003).

173. Das, J. *et al.* Digital signaling and hysteresis characterize Ras activation in lymphoid cells. *Cell* **136,** 337–351. arXiv: `NIHMS150003` (2009).

174. Podtschaske, M. *et al.* Digital NFATc2 Activation per Cell Transforms Graded T Cell Receptor Activation into an All-or-None IL-2 Expression. *plosOne* **e935** (2007).

175. Tay, S. *et al.* Single-cell NF-κB dynamics reveal digital activation and analog information processing in cells. *Nature* **466,** 267–271 (2010).

176. Kar, P., Nelson, C. & Parekh, A. B. CRAC channels drive digital activation and provide analog control and synergy to Ca 2+-dependent gene regulation. *Curr. Biol.* **22,** 242–247 (2012).

177. Wertek, F. & Xu, C. Digital response in T cells: To be or not to be. *Cell Res.* **24,** 265–266 (2014).

178. Tischer, D. K. & Weiner, O. D. Light-based tuning of ligand half-life supports kinetic proofreading model of T cell signaling. *Elife* **8,** 1–25 (2019).

179. Yousefi, O. S. *et al.* Optogenetic control shows that kinetic proofreading regulates the activity of the t cell receptor. *Elife* **8,** 1–33 (2019).

180. Taylor, M. J., Husain, K., Gartner, Z. J., Mayor, S. & Vale, R. D. A DNA-Based T Cell Receptor Reveals a Role for Receptor Clustering in Ligand Discrimination. *Cell* **169,** 108–119.e20 (2017).

181. Love, P. E. & Hayes, S. M. ITAM-mediated signaling by the T-cell antigen receptor. *Cold Spring Harb. Perspect. Biol.* **2,** 1–11 (2010).

182. Dushek, O., Goyette, J. & van der Merwe, P. A. Phosphorylated Receptors. *Immunol. Rev.* **250,** 258–276 (2012).

183. Mukhopadhyay, H., Cordoba, S. P., Maini, P. K., van der Merwe, P. A. & Dushek, O. Systems Model of T Cell Receptor Proximal Signaling Reveals Emergent Ultrasensitivity. *PLoS Comput. Biol.* **9** (2013).

184. James, J. R. Tuning ITAM multiplicity on T cell receptors can control potency and selectivity to ligand density. *Sci. Signal.* **11** (2018).

185. Mukhopadhyay, S., Frias, M., Chatterjee, A., Yellen, P. & Foster, D. The Enigma of Rapamycin Dosage. *Mol. cancer Ther.* **15,** 347–353 (2016).

186. Hui, E. *et al.* In vitro membrane reconstitution of the T-cell receptor proximal signaling network. *Nat. Struct. Mol. Biol.* **21,** 133–142 (2014).

187. Britain, D & Weiner, O. Progressive enhancement of kinetic proofreading in T cell antigen discrimination from receptor activation to DAG generation. *bioRxiv,* 1–49 (2021).

188. Voisinne, G. *et al.* Quantitative interactomics in primary T cells unveils TCR signal diversification extent and dynamics. *Nat. Immunol.* **20,** 1530–1541 (2019).

189. Dobbins, J. *et al.* Binding of the cytoplasmic domain of CD28 to the plasma membrane inhibits Lck recruitment and signaling. *Sci. Signal.* **9,** 1–13 (2016).

190. Yang, W. *et al.* Dynamic regulation of CD28 conformation and signaling by charged lipids and ions. *Nat. Struct. Mol. Biol.* **24,** 1081–1092 (2017).

191. Michel, F., Attal-Bonnefoy, G., Mangino, G., Mise-Omata, S. & Acuto, O. CD28 as a molecular amplifier extending TCR ligation and signaling capabilities. *Immunity* **15,** 935–945 (2001).

192. Casas, J. *et al.* Ligand-engaged TCR is triggered by Lck not associated with CD8 coreceptor. *Nat. Commun.* **5** (2014).

193. Aguado, E. & Arbulo-echevarria, M. M. Slow phosphor-Y-LAT-ion for TCR ligand discrimination. *Nat. Immunol.* **20,** 1420–1422 (2019).

194. Pettmann, J. *et al.* Mechanical forces impair antigen discrimination by reducing differences in T cell receptor off-rates. *bioRxiv,* 1–22 (2022).

195. Lee, K. H. *et al.* The Immunological Synapse Balances T Cell Receptor Signaling and Degradation. *Science (80-.).* **302,** 1218–1222 (2003).

196. Aleksic, M. *et al.* Dependence of T Cell Antigen Recognition on T Cell Receptor-Peptide MHC Confinement Time. *Immunity* **32,** 163–174 (2010).

197. Lever, M. *et al.* Architecture of a minimal signaling pathway explains the T-cell response to a 1 million-fold variation in antigen affinity and dose. *Proc. Natl. Acad. Sci. U. S. A.* **113,** E6630–E6638 (2016).

198. Stachlewitz, R. F. *et al.* A-770041 , a Novel and Selective Small-Molecule Inhibitor of Lck , Prevents Heart Allograft Rejection. *J. Pharmacol. Exp. Ther.* **315,** 36–41 (2005).

199. Holländer, G. A., Bierer, B. E. & Burakoff, S. J. Molecular and biological actions of cyclosporin A and FK506 on T cell development and function. *Transfus. Sci.* **15,** 207–220 (1994).

200. Yue, Q. *et al.* Absorption, metabolism and excretion of pictilisib, a potent pan-class I phosphatidylinositol-3-Kinase (PI3K) inhibitor, in rats, dogs, and humans. *Xenobiotica* **51,** 796–810 (2021).

201. Kovarik, J. M. & Slade, A. Overview of sotrastaurin clinical pharmacokinetics. *Ther. Drug Monit.* **32,** 540–543 (2010).

202. Burgdorf, C., Schäfer, U., Richardt, G. & Kurz, T. U73122, an aminosteroid phospholipase C inhibitor, is a potent inhibitor of cardiac phospholipase D by a PIP2-dependent mechanism. *J. Cardiovasc. Pharmacol.* **55,** 555–559 (2010).

203. Hou, C., Kirchner, T., Singer, M., Matheis, M. & Argentieri, D. In Vivo Activity of a Phospholipase C Inhibitor , 1- (6- ((17 -3- dione (U73122), in Acute and Chronic Inflammatory Reactions. *J. Pharmacol. Exp. Ther.* **309,** 697–704 (2004).

204. Lugowska, I., Koseła-Paterczyk, H., Kozak, K. & Rutkowski, P. Trametinib: A MEK inhibitor for management of metastatic melanoma. *Onco. Targets. Ther.* **8,** 2251–2259 (2015).

205. Yamaguchi, T., Kakefuda, R., Tajima, N., Sowa, Y. & Sakai, T. Antitumor activities of JTP-74057 (GSK1120212), a novel MEK1/2 inhibitor, on colorectal cancer cell lines in vitro and in vivo. *Int. J. Oncol.* **39,** 23–31 (2011).

206. Henney, C. S. & Eric, J. Antigen-T Lymphocyte Interactions : Inhibition by Cytochalasin B This information is current as practicing scientists. *J. Immunol.* **111,** 85–90 (1973).

207. Borroto, A. *et al.* First-in-class inhibitor of the T cell receptor for the treatment of autoimmune diseases. *Sci. Transl. Med.* **8** (2016).

208. Richter, K. *et al.* Small molecule AX-024 reduces T cell proliferation independently of CD3ϵ/Nck1 interaction, which is governed by a domain swap in the Nck1-SH3.1 domain. *J. Biol. Chem.* **295,** 7849–7864 (2020).

209. Nguyen, T. V., Ke, Y., Zhang, E. E. & Alerts, E. Conditional Deletion of Shp2 Tyrosine Phosphatase in Thymocytes Suppresses Both Pre-TCR and TCR Signals. *J. Immunol.* **177,** 5990–5996 (2021).

210. Leonard, D. *et al.* Activated T cells enhance interferon-α production by plasmacytoid dendritic cells stimulated with RNA-containing immune complexes. *Ann. Rheum. Dis.* **75,** 1728–1734 (2016).

211. Chan, P. Y. *et al.* Influence of receptor lateral mobility on adhesion strengthening between membranes containing LFA-3 and CD2. *J. Cell Biol.* **115,** 245–255 (1991).

212. Levin, S. E., Zhang, C., Kadlecek, T. A., Shokat, K. M. & Weiss, A. Inhibition of ZAP-70 kinase activity via an analog-sensitive allele blocks T cell receptor and CD28 superagonist signaling. *J. Biol. Chem.* **283,** 15419–15430 (2008).

213. Swaney, K. & Li, R. Function and regulation of the Arp2/3 complex during cell migration in diverse environments. *Curr. Opin. Cell Biol.* **42,** 63.72 (2016).

214. Huang, Y. & Burkhardt, J. K. T-cell-receptor-dependent actin regulatory mechanisms. *J. Cell Sci.* **120,** 723–730 (2007).

215. Mestermann, K. *et al.* The tyrosine kinase inhibitor dasatinib acts as a pharmacologic on/off switch for CAR-T cells. *Sci. Transl. Med.* **11** (2019).

216. Yamane, H. *et al.* Successful Treatment of Chronic Myeloid Leukemia With Dasatinib After Kidney Transplantation: A Case Report. *Transplant. Proc.* **52,** 600–603 (2020).

217. Zepecki, J. P. *et al.* Regulation of human glioma cell migration, tumor growth, and stemness gene expression using a Lck targeted inhibitor. *Oncogene* **38,** 1734–1750 (2019).

218. Hörnig, M. *et al.* Inhibition of 5-lipoxygenase by U73122 is due to covalent binding to cysteine 416. *Biochim. Biophys. Acta - Mol. Cell Biol. Lipids* **1821,** 279–286 (2012).

219. Cook-Moreau, J. M. *et al.* Expression of 5-lipoxygenase (5-LOX) in T lymphocytes. *Immunology* **122,** 157–166 (2007).

220. Zhu, M., Foreman, D., Brien, S. A. O., Jin, Y. & Zhang, W. activation. *J. Immunol.* **200,** 2165–2173 (2019).

221. Niwa, T., Yamamoto, S., Saito, M., Shiraga, T. & Takagi, A. Effect of cyclosporine and tacrolimus on cytochrome P450 activities in human liver microsomes. *Yakugaku Zasshi* **127,** 209–216 (2007).

222. Barbarino, J., Staatz, C., Venkataramanan, R., Klein, T. & Altman, R. PharmGKB summary: cyclosporine and tacrolimus pathways. *Pharmacogenetic Genomics* **23,** 563–585 (2013).

223. Wojciechowski, D. & Vincenti, F. *Novel Immunosuppressive Drugs* Third Edit, 1332–1342 (Elsevier Inc., 2015).

224. Hetrick, B., Suk Han, M. & Nolen, B. Small Molecules CK-666 and CK-869 Block an Activating Conformational Change to Inhibit Arp2/3 Complex. *Biophys. J.* **102,** 46a (2012).

225. Helal, M. A., Khalifa, S. & Ahmed, S. Differential binding of latrunculins to G-actin: A molecular dynamics study. *J. Chem. Inf. Model.* **53,** 2369–2375 (2013).

226. Shoji, K., Ohashi, K., Sampei, K., Oikawa, M. & Mizuno, K. Cytochalasin D acts as an inhibitor of the actin-cofilin interaction. *Biochem. Biophys. Res. Commun.* **424,** 52–57 (2012).

227. Rivas, F. V., O'Keefe, J. P., Alegre, M.-L. & Gajewski, T. F. Actin Cytoskeleton Regulates Calcium Dynamics and NFAT Nuclear Duration. *Mol. Cell. Biol.* **24,** 1628–1639 (2004).

228. Ike, H. *et al.* Mechanism of Lck recruitment to the T-cell receptor cluster as studied by single-molecule-fluorescence video imaging. *ChemPhysChem* **4,** 620–626 (2003).

229. Duan, Z. *et al.* A-770041 reverses paclitaxel and doxorubicin resistance in osteosarcoma cells. *BMC Cancer* **14,** 1–11 (2014).

230. Zeyda, M. *et al.* Impairment of T cell interactions with antigen-presenting cells by immunosuppressive drugs reveals involvement of calcineurin and NF-κB in immunological synapse formation. *J. Leukoc. Biol.* **81,** 319–327 (2007).

231. Nguyen, L. X. T. *et al.* Regulation of ribosomal RNA synthesis in T cells: Requirement for GTP and Ebp1. *Blood* **125,** 2519–2529 (2015).

232. Xu, H. *et al.* MEK nuclear localization promotes YAP stability via sequestering β-TrCP in KRAS mutant cancer cells. *Cell Death Differ.* **26,** 2400–2415 (2019).

233. Ogino, H. *et al.* Regulatory T cells expanded by rapamycin in vitro suppress colitis in an experimental mouse model. *J. Gastroenterol.* **47,** 366–376 (2012).

234. Tamzalit, F. *et al.* Interfacial actin protrusions mechanically enhance killing by cytotoxic T cells. *Sci. Immunol.* **4,** 139 (2019).

235. Wojewodzka, J., Galkowska, H. & Olszewski, W. L. Inhibition of formation of synapses between dendritic cells and lymphocytes in skin lymph in an allogeneic reaction by cyclosporine and tacrolimus. *Transplant. Proc.* **35,** 2376–2378 (2003).

236. Hayden-Martinez, K., Kane, L. P. & Hedrick, S. M. Effects of a Constitutively Active Form of Calcineurin on T Cell Activation and Thymic Selection. *J. Immunol.* **165,** 3713–3721 (2000).

237. Shibasaki, F., Price, E. R., Milan, D. & Mckeon, F. Role of kinases and the phosphatase calcineurin in the nuclear shuttling of transcription factor NF-AT4. *Lett. to Nat.* **382,** 370–373 (1996).

238. Wunderlich, L., Faragó, A., Downward, J. & Buday, L. Association of Nck with tyrosine-phosphorylated SLP-76 in activated T lymphocytes. *Eur. J. Immunol.* **29,** 1068–1075 (1999).

239. Buday, L. Membrane-targeting of signalling molecules by SH2/SH3 domain-containing adaptor proteins. *Biochim. Biophys. Acta - Rev. Biomembr.* **1422,** 187–204 (1999).

240. Lorenz, U, Ravichandran, K. S., Burakoff, S. J. & Neel, B. G. Lack of SHPTP1 results in src-family kinase hyperactivation and thymocyte hyperresponsiveness. *Proc. Natl. Acad. Sci. U. S. A.* **93,** 9624–9 (1996).

241. Xu, X. *et al.* PD-1 and BTLA regulate T cell signaling differentially and only partially through SHP1 and SHP2. *J. Cell Biol.* **219** (2020).

242. Celis-Gutierrez, J. *et al.* Quantitative Interactomics in Primary T Cells Provides a Rationale for Concomitant PD-1 and BTLA Coinhibitor Blockade in Cancer Immunotherapy. *Cell Rep.* **27,** 3315–3330.e7 (2019).

243. Plas, D. R. *et al.* Direct regulation of ZAP-70 by SHP-1 in T cell antigen receptor signaling. *Science (80-.).* **272,** 1173–1176. arXiv: `arXiv:1002.2562v1` (1996).

244. Brockdorff, J., Williams, S., Couture, C. & Mustelin, T. Dephosphorylation of ZAP-70 and inhibition of T cell activation by activated SHP1. *Eur. J. Immunol.* **29,** 2539–2550 (1999).

245. Ormonde, J. V. S., Li, Z., Stegen, C. & Madrenas, J. TAOK3 Regulates Canonical TCR Signaling by Preventing Early SHP-1–Mediated Inactivation of LCK. *J. Immunol.* **201,** 3431–3442 (2018).

246. Binstadt, B. A. *et al.* SLP-76 is a direct substrate of SHP-1 recruited to killer cell inhibitory receptors. *J. Biol. Chem.* **273,** 27518–27523 (1998).

247. Chiang, G. G. & Sefton, B. M. Specific Dephosphorylation of the Lck Tyrosine Protein Kinase at Tyr-394 by the SHP-1 Protein-tyrosine Phosphatase. *J. Biol. Chem.* **276,** 23173–23178 (2001).

248. Dubey, C, Croft, M & Swain, S. L. Costimulatory requirements of naive CD4+ T cells. ICAM-1 or B7-1 can costimulate naive CD4 T cell activation but both are required for optimum response. *J. Immunol.* **155,** 45–57 (1995).

249. Binder, C. *et al.* CD2 Immunobiology. *Front. Immunol.* **11,** 1–14 (2020).

250. Lettau, M., Pieper, J. & Janssen, O. Nck adapter proteins: Functional versatility in T cells. *Cell Commun. Signal.* **7,** 1–13 (2009).

251. Mehta, A. K., Gracias, D. T. & Croft, M. TNF activity and T cells. *Cytokine* **101,** 14–18 (2018).

252. Feinerman, O. *et al.* Single-cell quantification of IL-2 response by effector and regulatory T cells reveals critical plasticity in immune response. *Mol. Syst. Biol.* **6,** 1–16 (2010).

253. Baitsch, L. *et al.* Exhaustion of tumor-specific CD8+ T cells in metastases from melanoma patients. *J. Clin. Invest.* **121,** 2350–2360 (2011).

254. Johnson, D. B., Peng, C. & Sosman, J. A. Nivolumab in melanoma: Latest evidence and clinical potential. *Ther. Adv. Med. Oncol.* **7,** 97–106 (2015).

255. Viada, C. *et al.* Immunological evaluation of rheumatoid arthritis patients treated with itolizumab. *MAbs* **8,** 187–195 (2015).

256. Pai, G. & Pai, A. H. Itolizumab – A New Biologic for Management of Psoriasis and Psoriatic Arthritis. *Case Rep. Dermatol.,* 141–145 (2017).

257. Patnaik, A. *et al.* Phase i study of pembrolizumab (MK-3475; Anti-PD-1 monoclonal antibody) in patients with advanced solid tumors. *Clin. Cancer Res.* **21,** 4286–4293 (2015).

258. Boutros, C. *et al.* Safety profiles of anti-CTLA-4 and anti-PD-1 antibodies alone and in combination. *Nat. Rev. Clin. Oncol.* **13,** 473–486 (2016).

259. Menon, R. & David, B. G. Itolizumab – A humanized anti-CD6 monoclonal antibody with a better side effects profile for the treatment of psoriasis. *Clin. Cosmet. Investig. Dermatol.* **8,** 215–222 (2015).

260. Zhao, B., Zhao, H. & Zhao, J. Efficacy of PD-1/PD-L1 blockade monotherapy in clinical trials. *Ther. Adv. Med. Oncol.* **12,** 1–22 (2020).

261. Kumagai, S. *et al.* The PD-1 expression balance between effector and regulatory T cells predicts the clinical efficacy of PD-1 blockade therapies. *Nat. Immunol.* **21,** 1346–1358 (2020).

262. Simon, S. & Labarriere, N. PD-1 expression on tumor-specific T cells: Friend or foe for immunotherapy? *Oncoimmunology* **7,** 1–7 (2018).

263. Freeman, G. J. *et al.* Engagement of the Pd-1 Immunoinhibitory Receptor by a Novel B7 Family Member Leads to Negative Regulation of Lymphocyte Activation. *J. Exp. Med.* **192,** 1027–1034 (2000).

264. Pauken, K. E. & Wherry, E. J. Overcoming T cell exhaustion in infection and cancer. *Trends Immunol.* **36,** 265–276 (2015).

265. Topalian, S. L., Hodi, F., Brahmer, J., Gettinger, S. & Smith, D. Re: Safety, activity, and immune correlates of anti-PD-1 antibody in cancer. *N. Engl. J. Med.* **366,** 2443–2454 (2012).

266. Chemnitz, J. M., Lanfranco, A. R., Braunstein, I. & Riley, J. L. B and T Lymphocyte Attenuator-Mediated Signal Transduction Provides a Potent Inhibitory Signal to Primary Human CD4 T Cells That Can Be Initiated by Multiple Phosphotyrosine Motifs. *J. Immunol.* **176,** 6603–6614 (2006).

267. Yokosuka, T. *et al.* Programmed cell death 1 forms negative costimulatory microclusters that directly inhibit T cell receptor signaling by recruiting phosphatase SHP2. *J. Exp. Med.* **209,** 1201–1217 (2012).

268. Rota, G. *et al.* Shp-2 Is Dispensable for Establishing T Cell Exhaustion and for PD-1 Signaling In Vivo. *Cell Rep.* **23,** 39–49 (2018).

269. Hui, E. *et al.* The T cell costimulatory receptor CD28 is a primary target of PD-1 mediated inhibition. *Science (80-.).* **4,** 1–14 (2016).

270. Kamphorst, A. O. *et al.* Rescue of exhausted CD8 T cells by PD-1 targeted therapies is CD28-dependent. *Science (80-.).* **355,** 1423–1427 (2017).

271. Bennett, F. *et al.* Program Death-1 Engagement Upon TCR Activation Has Distinct Effects on Costimulation and Cytokine-Driven Proliferation: Attenuation of ICOS, IL-4, and IL-21, But Not CD28, IL-7, and IL-15 Responses. *J. Immunol.* **170,** 711–718 (2003).

272. Mizuno, R. *et al.* PD-1 Primarily Targets TCR Signal in the Inhibition of Functional T Cell Activation. *Front. Immunol.* **10,** 630 (2019).

273. Hassan, N. J. *et al.* CD6 Regulates T-Cell Responses through Activation-Dependent Recruitment of the Positive Regulator SLP-76. *Mol. Cell. Biol.* **26,** 6727–6738 (2006).

274. Zimmerman, A. W. *et al.* Long-term engagement of CD6 and ALCAM is essential for T-cell proliferation induced by dendritic cells. *Blood* **107,** 3212–3220 (2006).

275. Gimferrer, I. *et al.* Relevance of CD6-Mediated Interactions in T Cell Activation and Proliferation. *J. Immunol.* **173,** 2262–2270 (2004).

276. Castro, M. A. A. *et al.* Extracellular Isoforms of CD6 Generated by Alternative Splicing Regulate Targeting of CD6 to the Immunological Synapse. *J. Immunol.* **178,** 4351–4361 (2007).

277. Roncagalli, R. *et al.* Quantitative proteomics analysis of signalosome dynamics in primary T cells identifies the surface receptor CD6 as a Lat adaptor-independent TCR signaling hub. *Nat. Immunol.* **15,** 384–392 (2014).

278. Kupfer, A., Monks, C. R. F., Freiberg, B. A., Kupfer, H. & Sciaky, N. Pillars Article : Three-Dimensional Segregation of Supramolecular Activation. *Science (80-.).* **285,** 221–227 (1998).

279. Breuning, J. & Brown, M. H. A sequence conserved between <scp>CD</scp> 5 and <scp>CD</scp> 6 binds an <scp>FERM</scp> domain and exerts a restraint on T-cell activation. *Immunology,* imm.13025 (2018).

280. Hassan, N. J., Barclay, A. N. & Brown, M. H. Frontline: Optimal T cell activation requires the engagement of CD6 and CD166. *Eur. J. Immunol.* **34,** 930–940 (2004).

281. C.Chow, L. M. A. The Anti-CD6 mAb, IOR-T1, Defined a New Epitope on the Human CD6 Molecule That Induces Greater Responsiveness in T Cell Receptor/CD3-Mediated T Cell Proliferation. *Cell. Immunol.* **154,** 123–133 (1994).

282. Li, Y. *et al.* CD6 as a potential target for treating multiple sclerosis. *PNAS* **114,** 1687–1692. arXiv: `arXiv:1408.1149` (2017).

283. Orta-Mascaró, M. *et al.* CD6 modulates thymocyte selection and peripheral T cell homeostasis. *J. Exp. Med.* **213,** 1387–1397 (2016).

284. Alonso-Ramirez, R. *et al.* Rationale for Targeting CD6 as a Treatment for Autoimmune Diseases. *Arthritis* **2010,** 1–9 (2010).

285. Kofler, D. M., Severson, C. A., Mousissian, N., De Jager, P. L. & Hafler, D. A. The CD6 Multiple Sclerosis Susceptibility Allele Is Associated with Alterations in CD4+ T Cell Proliferation. *J. Immunol.* **187,** 3286–3291 (2011).

286. Swaminathan, B. *et al.* Fine Mapping and Functional Analysis of the Multiple Sclerosis Risk Gene CD6. *PLoS One* **8,** 1–10 (2013).

287. Bughani, U. *et al.* T cell activation and differentiation is modulated by a CD6 domain 1 antibody Itolizumab. *PLoS One* **12,** 1–29 (2017).

288. Legat, A., Speiser, D. E., Pircher, H., Zehn, D. & Fuertes Marraco, S. A. Inhibitory receptor expression depends more dominantly on differentiation and activation than "exhaustion" of human CD8 T cells. *Front. Immunol.* **4,** 1–15 (2013).

289. Chappell, P. E. *et al.* Structures of CD6 and Its Ligand CD166 Give Insight into Their Interaction. *Structure* **23,** 1426–1436 (2015).

290. Abu-shah, E. *et al.* Human CD8 + T Cells Exhibit a Shared Antigen Threshold for Different Effector Responses. *J. Immunol.* **205,** 1503–1512 (2020).

291. Pentcheva-Hoang, T., Chen, L., Pardoll, D. M. & Allison, J. P. Programmed death-1 concentration at the immunological synapse is determined by ligand affinity and availability. *Proc. Natl. Acad. Sci. U. S. A.* **104,** 17765–17770 (2007).

292. Choudhuri, K., Wiseman, D., Brown, M. H., Gould, K. & Van Der Merwe, P. A. T-cell receptor triggering is critically dependent on the dimensions of its peptide-MHC ligand. *Nature* **436,** 578–582 (2005).

293. Lange, G. *et al.* Crystal structure of an extracellular fragment of the rat CD4 receptor containing domains 3 and 4. *Structure* **2,** 469–481 (1994).

294. Nagar, S., Argikar, U. & Tweedie, D. *Enzyme Kinetics in Drug Metabolism Fundamentals and Applications Methods in Molecular Biology 1113* 149–166 (2014).

295. Voisinne, G. *et al.* Kinetic proofreading through the multi-step activation of the ZAP70 kinase underlies early T cell ligand discrimination. *Nat. Immunol.* (2022).

296. Fernandes, R. A. *et al.* Immune receptor inhibition through enforced phosphatase recruitment. *Nature* **586,** 779–784 (2020).

297. Parkhurst, M. R. *et al.* T cells targeting carcinoembryonic antigen can mediate regression of metastatic colorectal cancer but induce severe transient colitis. *Mol. Ther.* **19,** 620–626 (2011).

298. Morgan, R. A. *et al.* Case report of a serious adverse event following the administration of t cells transduced with a chimeric antigen receptor recognizing ERBB2. *Mol. Ther.* **18,** 843–851 (2010).

299. Lamers, C. H. *et al.* Treatment of metastatic renal cell carcinoma with CAIX CAR-engineered T cells: Clinical evaluation and management of on-target toxicity. *Mol. Ther.* **21,** 904–912 (2013).

300. Drent, E. *et al.* A Rational Strategy for Reducing On-Target Off-Tumor Effects of CD38-Chimeric Antigen Receptors by Affinity Optimization. *Mol. Ther.* **25,** 1946–1958 (2017).

301. Liu, X. *et al.* Affinity-Tuned ErbB2 or EGFR Chimeric Antigen Receptor T Cells Exhibit an Increased Therapeutic Index against Tumors in Mice. *Cancer Res.* **75,** 3596–3607 (2015).

302. Chen, J. L. *et al.* Structural and kinetic basis for heightened immunogenicity of T cell vaccines. *J. Exp. Med.* **201,** 1243–1255 (2005).